AD —

8200

UNCLASSIFIED

BLANK PAGES
IN THIS
DOCUMENT
WERE NOT
FILMED

GAMMA-RAY TRANSMISSION THROUGH FINITE SLABS

G. H. PEEBLES

December 1, 1952

R-240

The RAND Corporation
1700 MAIN ST • SANTA MONICA • CALIFORNIA

GAMMA-RAY TRANSMISSION THROUGH FINITE SLABS

G. H. PEEBLES

December 1, 1952

R-240

The RAND Corporation
1700 MAIN ST • SANTA MONICA • CALIFORNIA

ACKNOWLEDGMENT

The writer found it necessary to seek advice on a number of items, large and small, in connection with this work. He is indebted to, and wishes to thank, Prof. Milton S. Plesset for technical advice, helpful suggestions, and excellent counsel.

SUMMARY

The quantity which is considered in this report to be of first importance is the build-up factor for a monoenergetic, monoangular beam of photons incident on a slab of finite thickness but infinite extent. This quantity is obtained for a set of discrete values of slab thickness, of incident energy, and of incident angle. Slab thickness, in mean free paths, spans the interval (0, 20); incident energy, in units of mc^2, the interval (1, 20); and incident angle, in degrees, the interval (0, 90). Two materials are used for the slab—lead and iron.

The processes used to obtain the set of "build-up" factors and to establish their accuracy within reasonable limits are such that a considerable amount of supplementary information is produced. This information is also presented. The supplementary results consist in the probabilities and expected energies corresponding to the transmission of photons with exactly one, two, or three scatterings; distributions of the transmitted photons over energy and angle; some results for slabs of air and of the pure Compton scatterer; some build-up factors in an energy range just below that stated above; photon and energy densities for three source configurations; and other quantities which on occasion might prove interesting or useful. Also, a discussion of the effect of variation of the total absorption coefficient on transmission probabilities is given which leads to estimates of build-up factors for a material of arbitrary atomic number Z.

CONTENTS

FIGURES

TABLES

SYMBOLS

a = thickness of slab in cm

c = velocity of light

$e_s(\alpha', X)$ = distribution of the energy density in the scattered photons at the rear face of a slab of thickness X

$e_t(X)$ = energy density at the rear face of a slab of thickness X

E_b = expected energy of a photon reflected with one collision

E_f = expected energy of a photon transmitted with one collision

E_{bb} = expected energy of a photon reflected with exactly two backward scatterings

E_{bf} = expected energy of a photon transmitted with exactly two scatterings, the first backward, the second forward

E_{fb} = expected energy of a photon reflected with exactly two scatterings, the first forward, the second backward

E_{ff} = expected energy of a photon transmitted with exactly two forward scatterings

$E_i = \alpha_0 N_i$

$E_i' = \alpha_0 N_i'$

$E_j(\alpha', X)$ = distribution of the expected energy in the transmitted photons scattered j times by the last of a succession of elementai slabs, the thickness of the combined slabs being X

E_k = expected energy of a photon transmitted through a slab with exactly k scatterings

$E_s(\alpha', X)$ = distribution of the expected energy in the scattered photons transmitted through a slab of thickness X

$E_t(X)$ = total expected energy of the photons transmitted through a slab of thickness X

$F_k = k!N_k/(KX)^k e^{-X}$

$G_k = k!E_k/\alpha_0(KX)^k e^{-X}$

k = number of scatterings of a photon

$K = \nu r^2/\mu_0$

$n_s(\alpha', X)$ = distribution of the density of scattered photons at the rear face of a slab of thickness X

$n_t(X)$ = density of photons at the rear face of a slab of thickness X

N_b = probability that a photon will be reflected from a slab with only one scattering

N_f = probability that a photon will be transmitted through a slab with only one scattering

N_{bb} = probability that a photon will be reflected from a slab with exactly two backward scatterings

N_{bf} = probability that a photon will be transmitted through a slab with exactly two scatterings, the first backward, the second forward

N_{fb} = probability that a photon will be reflected from a slab with exactly two scatterings, the first forward, the second backward

N_{ff} = probability that a photon will be transmitted through a slab with exactly two forward scatterings

N_i = number of photons, from a point source, incident on a slab

N_i' = number of photons, from a plane of sources, incident per unit area per unit time on a slab

$N_j(\alpha', X)$ = distribution of the transmitted photons scattered j times by the last of a succession of elemental slabs, the thickness of the combined slabs being X

N_k = probability that a photon will be transmitted through a slab with exactly k scatterings

$N_s(\alpha', X)$ = distribution of the scattered photons transmitted through a slab of thickness X

$N_t(X)$ = total number of photons transmitted through a slab of thickness X

q_k = expected energy of a photon surviving its kth collision in an infinite homogeneous medium

r = classical electron radius

r_k = probability that a photon will survive its kth collision in an infinite homogeneous medium

s = distance traveled by a photon from the incident face to its first collision

$X = \mu_0 d$

Z = atomic number

α = photon energy in units of mc^2

α' = α for transmitted photons

α_0 = α for incident photons

$\beta = 1/\alpha$

$\beta_0 = 1/\alpha_0$

γ = cosine of the angle between the path of a photon and the normal to the slab

γ' = γ after transmission

γ_0 = γ before first collision

γ_1 = γ after first collision

$\zeta = (\mu_1\gamma_0/\mu_0\gamma_1) - 1$

λ = slope of μ/μ_0 when μ is a linear function of β

μ = total absorption coefficient

μ_0 = value of μ at the incident energy

μ_1 = value of μ after the first collision

ν = electron density

σ_{kn} = cross section per electron for Compton scattering

σ_{pe} = cross section per atom for the photoelectric effect

σ_{pp} = cross section per atom for pair production

$d\sigma$ = differential of the Klein-Nishina scattering formula for one electron

I. INTRODUCTION

The purpose of this report is to present data which, it is hoped, will be of use to those who work on practical problems in gamma-ray transmission. The conditions under which gamma-ray attenuation can be calculated are so idealized that the results cannot typically provide the engineer and designer with exact solutions to his problems. High accuracy, therefore, does not add greatly to the usefulness of the data. A characteristic more likely to increase usefulness is extensiveness, since in the practical problem an unexpected use for uncommon data is often found. The calculations presented here were made to obtain fairly complete and varied data with a degree of accuracy which, though low, is reasonably well established.

The first and most important calculation is for the transmission of monoenergetic, monoangular gamma rays through slabs of lead and of iron. The method used calculates successively the probability that a photon will be transmitted with zero, one, two, and three scatterings, estimates the probability that the photon will be transmitted with four, five, etc., scatterings, and then sums to find the total probability of transmission with any number of scatterings. To check the results of these calculations, a second method, which considers the transmission through a thick slab as a succession of transmissions through thin slabs, is applied to an incident distribution discrete in energy, but continuous over angle.

The results of the two methods, along with some results for the Compton scatterer, are the foundation for most of the developments given in this report. Build-up factors, distributions of transmitted photons, and similiar useful quantities are given for slabs of lead, iron, and the Compton scatterer. Other geometries and materials are considered, but briefly and only as far as the results for these three materials can be made to carry the discussion and furnish the answers.

* * *

II. TRANSMISSION OF PHOTONS OF 1 TO 20 mc^2 THROUGH SLABS OF LEAD AND OF IRON

The probability that a photon will be transmitted through a slab of finite thickness but infinite extent is the sum of the probabilities that it will be transmitted with no scattering, one scattering, two scatterings, etc. If the slab is sufficiently thin, the first few scatterings are enough to determine the total transmission accurately. Thick slabs require the calculation of the transmission for an excessive number of scatterings, but if errors of the order of 20 to 30 per cent are acceptable, estimates of the total transmission through thicknesses of 20 mean free paths (mfp) are possible from relatively few scatterings, particularly in the case of the heavy materials, where the absorption from the photoelectric effect and pair production is large.

Most practical transmission problems are such that contributions to their solution by idealized problems have an acceptable error of at least 20 to 30 per cent. In view of this, and in view of the considerable amount of information to be gained by a detailed approach, the first few scatterings have been calculated and estimates have been made of the total transmission for monoenergetic, monodirectional photons falling on slabs of lead and of iron.* Bremsstrahlung and polarization have been neglected. Back-scatter was not neglected at the outset, but it was found that back-scatter could be ignored, at least within the scope of these calculations.

Theory

A method, which is very simple in concept, exists for calculating transmission by successive scatterings. The probability that a photon will pass through a slab with exactly k collisions can be considered as the product of four probabilities: (1) $e^{-\mu_0 s}$, the probability that the photon will travel a distance s without collision (see Fig. 1), where μ_0 is the total absorption coefficient at the incident energy; (2) $\mu_0\, ds$, the probability that it will collide in ds at s; (3) $\nu\, d\sigma/\mu_0$, the probability that the photon will survive the collision and scatter into a new path, where ν is the electron density and $d\sigma$ is the differential Klein-Nishina scattering formula for one electron; and (4) N_{k-1}, the probability that the photon will pass on through the slab with exactly $k - 1$ collisions.

Let us now consider N_{k-1}, which is the probability that a photon *originating in the interior of a slab* of thickness a (see Fig. 1) will escape through a specified face with exactly $k - 1$ collisions. Except for the fact that the photon can scatter backwards into the forepart of the slab, it could be considered as the probability that a photon *will pass through a slab* of thickness b ($b \leq a$) with exactly $k - 1$ collisions. The probability of transmission with two scatterings is the first to require consideration of back-scatter, since

* For similar attacks on the problem of gamma-ray transmission, see Refs. 1 through 5, p. 185.

transmission with no collision or one collision does not allow the possibility of back-scatter. It was found, however, that those photons which are transmitted with a backward scatter after the first collision make a significant contribution to the twice-scattered beam only for slabs so thin that the transmission is composed mainly of unscattered and once-scattered photons. For example, a slab 1-mfp thick may typically be expected to have 10 to 15 per cent of the total transmission in twice-scattered photons, and of these twice-scattered photons, 10 to 15 per cent have suffered a backward scattering. Similarly, a slab thick enough to make thrice-scattered photons important is too thick for back-scatter to count heavily. It follows then that one can write, with a consequent error of only a few per cent, for small values of k:

$$dN_k = e^{-\mu_0 s} \cdot \mu_0 \, ds \cdot \frac{\nu \, d\sigma}{\mu_0} \cdot N_{k-1},$$

where N_k is now defined as the probability that a photon will be transmitted with exactly k collisions.

By beginning with

$$N_0 = e^{-X/\gamma_0},$$

where X is the slab thickness in mean free paths (calculated at the incident energy) and γ_0 is the cosine of the angle between the normal to the slab and the incident path, it is possible to calculate successively $N_1, N_2, \cdots$. At each step N_{k-1} must be known for a sufficiently wide range of three parameters—slab thickness, incident energy, and incident angle—so that a considerable amount of work is entailed. But by the same token, a considerable amount of information is gained.

Similar arguments hold for E_k, the expected energy transmitted in the beam of exactly k scatterings. Since back-scatter plays a role in the transmission of energy even smaller than it does in the transmission of photons, one can write, with less error than that for N_k:

$$dE_k = e^{-\mu_0 s} \cdot \mu_0 \, ds \cdot \frac{\nu \, d\sigma}{\mu_0} \cdot E_{k-1}.$$

The results of three successive operations with the preceding formulas are given in Tables 1 through 4. Tables 1 and 2, respectively, give N_k/e^{-X} for lead and for iron. Tables 3 and 4 show $E_k/\alpha_0 e^{-X}$, where α_0 is the incident energy.

The Accuracy of N_k and E_k

It can be seen that Tables 1 through 4 give values within a rectangle whose vertices lie at $(\gamma_0, X) = (1, 1), (1, 20), (0, 20), (0, 1)$. This rectangle may be divided roughly into three areas, each with its different computational requirements and accuracy. In the area near the vertex (0, 20), the values of N_k/e^{-X} and $E_k/\alpha_0 e^{-X}$ are very small and are difficult

to compute out of all proportion to their useful value. One is not likely to require accurate transmission values for photons grazing a slab 20-mfp thick. On the other hand, cases of this character do have some interest, and one hesitates to fix a boundary beyond which no results are given. The best means of meeting these considerations seemed to be by estimation based on a few supplementary calculations and on such pertinent information as was readily obtainable.

In the area near the vertex (1, 1), estimation was again used, though for different reasons. Here the values of N_k and E_k for large values of k contribute so little to the total transmission that there was no need to know them accurately. In particular, the transmission with three scatterings was almost negligible and was obtained largely by estimation.

The tabulated values, then, can be separated roughly into three classes: those values which were obtained by calculation, those which depended on calculation and on estimation in about equal proportions, and those which largely resulted from estimation. The class to which a result belongs is indicated in Tables 1 through 4 by the number of significant figures given; results of the first class named are tabulated with three figures, those of the second, with two figures, and those of the last, with one. The results of a class, however, are not necessarily sufficiently accurate to make the last figure significant in the usual sense. The third figure, when given for N_2, N_3, E_2, and E_3, is rarely significant, since the maximum error was set at about 2 per cent. It was not feasible to ensure attainment of this accuracy, and there is no doubt that this accuracy was not always reached. Nevertheless, three figures are given to indicate that calculation and not estimation played the major role. On the other hand, the third figure for N_1 and E_1 is usually significant, since the values of N_1 and E_1 were calculated in most instances with an error of ½ per cent or less. The values of N_0 and E_0, which represent trivial calculations, have a third significant figure. In the case of the two-figure and one-figure results, the magnitude of the error is not easily determined, but it is certainly never less (except coincidentally) than that indicated by the number of figures in the tabulated result, and in many instances is undoubtedly larger by a factor of 10 or more.

Accuracy of the Sums $\sum_{k=0}^{\infty} N_k/e^{-X}$ and $\sum_{k=0}^{\infty} E_k/\alpha_0 e^{-X}$

Estimates of the total transmission are conveniently expressed in the form of the so-called "build-up" factor. The build-up factor is defined here as $\sum_{k=0}^{\infty} N_k/e^{-X}$, in the case of the number of photons transmitted, and as $\sum_{k=0}^{\infty} E_k/\alpha_0 e^{-X}$, in the case of the energy transmitted. Tables 1 through 4 supply the first four terms of the build-up factor; the terms beyond $k = 3$ must be estimated in some way.

Figure 2 shows graphically the calculated and estimated values of N_k/e^{-X} for $\gamma_0 = 1$, $\alpha_0 = 5$. Calculated values of N_k/e^{-X} for a fixed value of X are connected by a solid line and estimated values are connected by a dashed line. The estimated values are reasonable enough, and it is clear that unless the point at which N_k/e^{-X} becomes negligibly small is moved out to a large value of k, the value of $\sum_{k=0}^{\infty} N_k/e^{-X}$ is not excessively in error by the standards of these calculations. To increase the value of the build-up factor for

$X = 20$ by 20 per cent, the point of negligibility must be moved from its present position at about $k = 10$ to about $k = 15$. This is, of course, possible, but it does not seem from the figure that the point could be moved much farther. Thus an accuracy of about 20 per cent for the total transmission is indicated.

The position taken in this respect can be made stronger. Suppose a photon originates within an infinite homogeneous medium of the same material as the slab. Let r_k be the probability that this photon will reach and survive its kth collision and let ρ_k be the corresponding probability that the same photon—i.e., a photon of the same energy—incident on the finite slab will also reach and survive its kth collision. After surviving each collision, the photon in the slab has a probability of avoiding the next collision by escaping through one of the faces. The photon in the infinite medium is certain to make the next collision; hence $r_k > \rho_k$. The probability ρ_k, in turn, exceeds N_k, since a photon must survive its kth collision in order to be transmitted with exactly k collisions. So for all slab thicknesses,

$$r_k > \rho_k > N_k.$$

It will be recognized that r_k satisfies a recurrent integral formula much like the one for N_k, but with the important difference that the integral for r_k is readily expressed in one variable. The recursive calculation of r_k, therefore, is rapid. Values of r_k and its energy counterpart, q_k—the expected energy of a photon after k collisions in the infinite medium —are given in Table 5 for the materials lead and iron.

Since r_k bounds N_k above, one can establish an upper limit on the remainder $\sum_{k=4}^{\infty} N_k/e^{-X}$. This bound, however is far too large to be of any use, at least for present purposes. To get a reasonable estimate of the remainder, rigor will have to be set aside and a persuasive argument built around r_k.

When one examines the mechanism of transmission, it seems likely that the sequences $\{N_k\}$ and $\{\rho_k\}$ should exhibit similar behavior. To put it more exactly, one expects the ratio N_k/ρ_k to vary more slowly as a function of k than either N_k or ρ_k. For N_k/ρ_k is that fraction of the photons surviving after k collisions which succeed in passing on through the slab. This fraction depends on the distribution of the photons with respect to position, energy, and direction immediately after collision. As the photons become disorganized—lose all "memory" of their initial state—during a succession of collisions, the character of the distribution function should tend to stabilize. If so, then N_k/ρ_k should tend toward a constant value as k increases.

The behavior of N_k/ρ_k for the first values of k can be easily determined for thick slabs from the data in Tables 1 through 5. For when the slab is sufficiently thick, ρ_k is nearly identical to r_k, so that N_k/r_k can be used instead of N_k/ρ_k. In the case under consideration above (lead, $\alpha_0 = 5$, $\gamma_0 = 1$, $X = 20$), one has

$$\frac{N_1}{r_1} = .657 \times 10^{-8}, \qquad \frac{N_2}{r_2} = 1.29 \times 10^{-8}, \qquad \frac{N_3}{r_3} = 2.31 \times 10^{-8}.$$

A reasonable extrapolation of this sequence gave the estimated values for $X = 20$ shown in Fig. 2. Only by assuming an extreme behavior for the sequence can the estimates of

N_4/e^{-X}, N_5/e^{-X}, etc., be increased so as to affect significantly the estimates of the build-up factor in accordance with the standards of these calculations. For example, to increase the build-up factor by 20 per cent by moving the point where N_k/e^{-X} becomes negligible from $k = 10$ to $k = 15$ requires that N_k/r_k be allowed to increase to a value of about 10^{-2} at $k = 15$. The first few values of N_k/r_k do not indicate the existence of the necessary rate of growth, and since the first values should show the greatest variation, it seems likely that the estimate of a 20 per cent error in the build-up factor will not turn out to be too small.

All the build-up factors were obtained by extrapolation of the ratio N_k/r_k. Whether or not the extrapolation of N_k/r_k is an improvement over the one for N_k, the former extrapolation had the unforeseen advantage of a procedure which could be made similar in all cases. One set of data, when suitably prepared, was remarkably like another for the first values of k. Therefore, a reasonable way of extrapolation in a particular case having been selected, it was possible to parallel the process in all cases. Although such parallelism does not signify a better estimate of the build-up factor, all estimates are expected to have comparable accuracy. This is a rather important point, because certain cases will be checked later by an entirely different calculation. A definite, consistent scheme of extrapolation gives some substance to the thought that the degree of accuracy found in the cases checked holds in all cases.

The build-up factors corresponding to the results of Tables 1 through 4 are shown on logarithmic scales as functions of X in Figs. 3*a* through 6*e*. Where the curves are solid, the accuracy is thought to be satisfactory. Where the curves are dashed, the estimates are open to large error. The accuracy of these estimates depends on the accuracy of the first four values, the proportion of the total contributed by the first four values, and the excellence of the method of estimating N_k (or E_k) for large k. In the region near $(\gamma_0, X) = (0, 20)$, the values of N_1, N_2, and N_3 are not accurately known and the evidence is that the sum of the first four values is but a small part of the total. These estimates, therefore, have a double source of error and must be regarded as guesses. The excuse for offering them here is that even the roughest guess may on occasion be useful, and it seemed only reasonable that such estimates should be included where nothing better was available.

All the build-up factors have the value of unity at $X = 0$, except when $\gamma_0 = 0$. For this exceptional case one must have recourse to the limit which depends on the order in which γ_0 and X are allowed to approach zero. The limit wanted is clearly that which is obtained when first γ_0 and then X tends toward zero. When $\gamma_0 = 0$, the photon must be considered as moving parallel to, and just in the surface of, the slab, so that a first collision is certain. As X tends toward zero, a state is approached in which one half of the photons surviving the first collision are transmitted and one half are reflected without further collisions. Hence the build-up factor at $X = 0$, $\gamma_0 = 0$ is $r_1/2$, in the case of the number of photons transmitted, and is $q_1/2\alpha_0$, in the case of the expected energy. Figures 3*a* through 6*e* show these values.

The error in the build-up factor is, of course, zero when $X = 0$ and is estimated to be more or less proportional to X, reaching about 20 per cent at $X = 20\gamma_0$, $\gamma_0 \neq 0$. For

$\gamma_0 = 0$, the value of X for 20 per cent error is small but not 0, perhaps 2. For $X > 20\gamma_0$, the estimates of the build-up factor, when given, rapidly lose accuracy and become, as noted above, very rough guesses in the neighborhood of $(\gamma_0, X) = (0, 20)$.

This simple representation of the error corresponds to the estimated potential accuracy of the method. It is probably a fair representation in the main, but needs some qualification in detail.

Examination of Tables 1 through 5 shows that the proportion of the total transmission made up by the calculated values is greater for lead than for iron and greater for energy than for number. Other things being equal, one expects, therefore, that the build-up factors for lead and for energy will be, respectively, more accurate than these for iron and for number. Iron also has other difficulties. Because of the limitations of the calculational procedure, the values for the second and third scatterings tend to be less accurate when $\alpha_0 = 1.0$. In the case of lead, this is not too important, since absorption reduces the contributions of the higher-ordered scatterings. But for iron, the absorption is so small, near $\alpha = 1.0$ (see Fig. 7), that errors in the second and third scatterings have an effect on the build-up factors. The same remarks apply to a lesser degree when $\alpha_0 = 2.5$. In addition to these known sources of likely error, there is, of course, the undetected inadvertent error which may enter at any point from the start of the calculations to the final placement of the results in a table or on a graph. Although many safeguards against error were used, it is estimated that errors of the order of 10 per cent in N_k and E_k, with the help of coincidence, might have escaped detection. Errors of this magnitude could decrease the accuracy of the build-up factor below that stated.

Supplementary calculations and consistency of results, both to be considered below, leads the writer to believe that the build-up factors can be used with confidence if the preceding remarks on accuracy in the region of the solid curves are kept well in mind and if it is remembered that the dashed curves reach into an area of rough guesses where an error of 1000 per cent is not unlikely. The factors should not be used for fine calculations, since absurd results would be obtained. For example, the factors are not satisfactory for calculating the average energy of the transmitted photons for large X and small γ_0. This is clear when one considers that an error of 1000 per cent may give an average energy greater than the incident energy. One should also guard against discerning interesting trends and behaviors which are solely the consequence of errors. As implied in the introductory remarks of this section, these results are intended to provide quick and rough estimates of gamma-ray transmission for a wide range of conditions. It is believed that for this purpose they will be satisfactory.

* * *

Table 1

N_k/e^{-X} FOR LEAD SLABS*

X	α_0	γ_0	N_0/e^{-X}	N_1/e^{-X}	N_2/e^{-X}	N_3/e^{-X}
1	20	1.0	1.000	.152	.0240	$.0^235$
		.8	.779	.147	.0272	$.0^244$
		.6	.513	.130	.0292	$.0^255$
		.4	.223	.0954	.0275	$.0^261$
		.2	.0183	.0494	.0205	$.0^256$
		0	0	.0168	.0118	$.0^242$
	10	1.0	1.000	.257	.0530	$.0^294$
		.8	.779	.241	.0578	.011
		.6	.513	.209	.0583	.013
		.4	.223	.148	.0524	.014
		.2	.0183	.0701	.0360	.012
		0	0	.0189	.0169	$.0^272$
	5	1.0	1.000	.340	.0786	.015
		.8	.779	.314	.0841	.018
		.6	.513	.271	.0877	.022
		.4	.223	.185	.0762	.023
		.2	.0183	.0853	.0500	.018
		0	0	.0198	.0194	$.0^289$
	2.5	1.0	1.000	.333	.0689	.011
		.8	.779	.309	.0721	.013
		.6	.513	.260	.0741	.016
		.4	.223	.170	.0632	.016
		.2	.0183	.0849	.0434	.013
		0	0	.0199	.0151	$.0^256$
	1.0	1.0	1.000	.175	.0200	$.0^220$
		.8	.779	.159	.0199	$.0^221$
		.6	.513	.141	.0205	$.0^223$
		.4	.223	.106	.0187	$.0^223$
		.2	.0183	.0514	.0123	$.0^217$
		0	0	.0142	$.0^2590$	$.0^296$
2	20	1.0	1.000	.302	.0803	.019
		.8	.607	.238	.0727	.019
		.6	.264	.153	.0592	.018
		.4	.0498	.0745	.0395	.015
		.2	$.0^3335$	.0250	.0209	$.0^296$
		0	0	$.0^2728$	.0114	$.0^265$

* X = slab thickness in mean free paths.

α_0 = energy of incident photon in units of mc^2.

γ_0 = cosine of the angle between the slab normal and the incident path.

N_k = probability that a photon will be transmitted with exactly k collisions.

Table 1—continued

X	α_0	γ_0	N_0/e^{-X}	N_1/e^{-X}	N_2/e^{-X}	N_3/e^{-X}
2	10	1.0	1.000	.459	.154	.040
		.8	.607	.347	.133	.040
		.6	.264	.215	.0996	.034
		.4	.0498	.0928	.0571	.024
		.2	$.0^3335$	0240	.0228	.012
		0	0	$.0^2486$	$.0^2857$	$.0^251$
	5	1.0	1.000	.570	.209	.056
		.8	.607	.420	.176	.053
		.6	.264	.255	.131	.045
		.4	.0498	.104	.0722	.031
		.2	$.0^3335$	.0224	.0260	.014
		0	0	$.0^2352$	$.0^2798$	$.0^253$
	2.5	1.0	1.000	.535	.166	.037
		.8	.607	.401	.139	.035
		.6	.264	.239	.103	.030
		.4	.0498	.0980	.0575	.020
		.2	$.0^3335$	.0209	.0190	$.0^280$
		0	0	$.0^2329$	$.0^2583$	$.0^231$
	1.0	1.0	1.000	.274	.0439	$.0^256$
		.8	.607	.202	.0362	$.0^249$
		.6	.264	.128	.0272	$.0^241$
		.4	.0498	.0543	.0158	$.0^227$
		.2	$.0^3335$	.0136	$.0^2623$	$.0^212$
		0	0	$.0^2269$	$.0^2224$	$.0^355$
4	20	1.0	1.000	.636	.289	.106
		.8	.368	.341	.192	.0815
		.6	.0695	.139	.101	.050
		.4	$.0^2248$	0423	.0426	.025
		.2	$.0^4113$	.0113	.0177	.013
		0	0	$.0^222$	$.0^265$	$.0^258$
	10	1.0	1.000	.812	.418	.164
		.8	.368	.399	.245	.111
		.6	.0695	.139	.111	.058
		.4	$.0^2248$	.0297	.0348	.022
		.2	$.0^4113$	0^2461	$.0^2918$	$.0^272$
		0	0	$.0^344$	$.0^220$	$.0^220$
	5	1.0	1.000	.910	.485	.192
		.8	.368	.431	.276	.121
		.6	.0695	.140	.117	.059
		.4	$.0^2248$	.0236	.0296	.018
		.2	$.0^4113$	$.0^2246$	$.0^2554$	$.0^243$
		0	0	$.0^318$	$.0^393$	$.0^210$

Table 1—continued

X	α_0	γ_0	N_0/e^{-X}	N_1/e^{-X}	N_2/e^{-X}	N_3/e^{-X}
4	2.5	1.0	1.000	.813	.368	.117
		.8	.368	.385	.209	.0755
		.6	.0695	.121	.0836	.035
		.4	$.0^2248$	.0200	.0207	.011
		.2	$.0^6113$	$.0^2197$	$.0^2349$	$.0^223$
		0	0	$.0^314$	$.0^369$	$.0^360$
	1.0	1.0	1.000	.406	.0914	.0150
		.8	.368	.197	.0524	$.0^2976$
		.6	.0695	.0657	.0232	$.0^250$
		.4	$.0^2248$	.0118	$.0^2600$	$.0^215$
		.2	$.0^6113$	$.0^2156$	$.0^2130$	$.0^339$
		0	0	$.0^314$	$.0^325$	$.0^310$
8	20	1.0	1.000	1.58	1.35	.767
		.8	.135	.483	.535	.343
		.6	$.0^2483$	.124	.181	.13
		.4	$.0^5614$	.0259	.0508	.045
		.2	$.0^{13}127$	$.0^238$	.011	.012
		0	0	$.0^33$	$.0^22$	$.0^23$
	10	1.0	1.000	1.40	1.11	.670
		.8	.135	.326	.340	.248
		.6	$.0^2483$	.0479	.0722	.063
		.4	$.0^5614$	$.0^2479$	.0121	.013
		.2	$.0^{13}127$	$.0^330$	$.0^214$	$.0^221$
		0	0	$.0^57$	$.0^31$	$.0^32$
	5	1.0	1.000	1.390	1.07	.596
		.8	.135	.282	.291	.186
		.6	$.0^2483$	.0292	.0443	.033
		.4	$.0^5614$	$.0^2159$	$.0^2419$	$.0^241$
		.2	$.0^{13}127$	$.0^445$	$.0^326$	$.0^336$
		0	0	$.0^66$	$.0^41$	$.0^43$
	2.5	1.0	1.000	1.18	.742	.316
		.8	.135	.233	.196	.100
		.6	$.0^2483$	.0227	.0267	.017
		.4	$.0^5614$	$.0^2106$	$.0^2220$	$.0^218$
		.2	$.0^{13}127$	$.0^426$	$.0^313$	$.0^315$
		0	0	$.0^63$	$.0^37$	$.0^31$
	1.0	1.0	1.000	.570	.171	.0361
		.8	.135	.119	.0475	.0124
		.6	$.0^2483$	.0125	$.0^2762$	$.0^225$
		.4	$.0^5614$	$.0^3751$	$.0^3767$	$.0^333$
		.2	$.0^{13}127$	$.0^427$	$.0^458$	$.0^433$
		0	0	$.0^66$	$.0^54$	$.0^53$

Table 1—continued

X	α_0	γ_0	N_0/e^{-X}	N_1/e^{-X}	N_2/e^{-X}	N_3/e^{-X}
12	20	1.0	1.000	3.14	4.14	3.13
		.8	.0498	.741	1.25	1.08
		.6	$.0^{3}335$	.148	.327	.33
		.4	$.0^{7}152$	.020	.061	.073
		.2	$.0^{20}143$	$.0^{2}2$	$.0^{2}8$	.01
		0	0	$.0^{4}5$	$.0^{3}7$	$.0^{2}1$
	10	1.0	1.000	1.95	1.94	1.40
		.8	.04[illegible]8	.234	.354	.341
		.6	$.0^{3}335$	.0185	.0457	.056
		.4	$.0^{7}152$	$.0^{3}93$	$.0^{2}40$	$.0^{2}67$
		.2	$.0^{20}143$	$.0^{4}2$	$.0^{3}2$	$.0^{3}5$
		0	0	$.0^{6}2$	$.0^{5}8$	$.0^{4}3$
	5	1.0	1.000	1.74	1.60	1.08
		.8	.0498	.157	.215	.177
		.6	$.0^{3}335$	$.0^{2}633$	.0142	.015
		.4	$.0^{7}152$	$.0^{3}14$	$.0^{3}64$	$.0^{3}93$
		.2	$.0^{20}143$	$.0^{5}1$	$.0^{4}2$	$.0^{4}4$
		0	0	$.0^{8}5$	$.0^{6}3$	$.0^{5}1$
	2.5	1.0	1.000	1.42	1.06	.540
		.8	.0498	.119	.131	.0839
		.6	$.0^{3}335$	$.0^{2}408$	$.0^{2}721$	$.0^{2}62$
		.4	$.0^{7}152$	$.0^{4}60$	$.0^{3}21$	$.0^{3}26$
		.2	$.0^{20}143$	$.0^{6}4$	$.0^{5}5$	$.0^{5}9$
		0	0	$.0^{9}9$	$.0^{7}9$	$.0^{6}3$
	1.0	1.0	1.000	.678	.242	.0595
		.8	.0498	.0615	.0321	.0102
		.6	$.0^{3}335$	$.0^{2}244$	$.0^{2}213$	$.0^{3}91$
		.4	$.0^{7}152$	$.0^{4}54$	$.0^{4}96$	$.0^{4}60$
		.2	$.0^{20}143$	$.0^{6}6$	$.0^{5}3$	$.0^{5}3$
		0	0	$.0^{8}3$	$.0^{7}9$	$.0^{6}1$
16	20	1.0	1.000	5.90	10.9	10.8
		.8	.0183	1.25	2.77	3.14
		.6	$.0^{4}233$	.20	.59	.76
		.4	$.0^{10}378$	.02	.08	.1
		.2	$.0^{27}160$	$.0^{3}8$	$.0^{2}7$	.01
		0	0	$.0^{4}1$	$.0^{3}3$	$.0^{2}1$
	10	.0	1.000	2.47	2.98	2.73
		.8	.0183	.169	.356	.415
		.6	$.0^{4}233$	$.0^{2}78$	.031	.049
		.4	$.0^{10}378$	$.0^{3}2$	$.0^{2}2$	$.0^{2}4$
		.2	$.0^{27}160$	$.0^{5}2$	$.0^{4}5$	$.0^{3}2$
		0	0	$.0^{8}5$	$.0^{6}8$	$.0^{5}4$

Table 1—continued

X	α_0	γ_0	N_0/e^{-X}	N_1/e^{-X}	N_2/e^{-X}	N_3/e^{-X}
16	5	1.0	1.000	2.02	2.11	1.60
		.8	.0183	.0819	.145	.142
		.6	$.0^{4}233$	$.0^{2}15$	$.0^{2}49$	$.0^{2}67$
		.4	$.0^{10}378$	$.0^{4}1$	$.0^{3}1$	$.0^{3}2$
		.2	$.0^{27}160$	$.0^{7}5$	$.0^{5}1$	$.0^{5}5$
		0	0	$.0^{10}2$	$.0^{8}9$	$.0^{7}6$
	2.5	1.0	1.000	1.60	1.34	783
		.8	.0183	.0586	.0786	.0583
		.6	$.0^{4}233$	$.0^{3}74$	$.0^{2}18$	$.0^{2}19$
		.4	$.0^{10}378$	$0^{5}4$	$.0^{4}2$	$.0^{4}4$
		.2	$.0^{27}160$	$.0^{8}8$	$.0^{6}2$	$.0^{6}6$
		0	0	$.0^{11}3$	$.0^{8}2$	$.0^{7}1$
	1.0	1.0	1.000	.759	.303	.0830
		.8	.0183	.0296	.0195	$.0^{2}736$
		.6	$.0^{4}233$	$.0^{3}48$	$.0^{3}58$	$.0^{3}32$
		.4	$.0^{10}378$	$.0^{5}4$	$.0^{4}1$	$.0^{4}1$
		.2	$.0^{27}160$	$.0^{7}2$	$.0^{6}2$	$.0^{6}3$
		0	0	$.0^{10}2$	$.0^{8}3$	$.0^{8}8$
20	20	1.0	1.000	10.8	25.3	31.3
		.8	$.0^{2}674$	2.2	6.2	8.8
		.6	$.0^{5}162$	.3	1.	2.
		.4	$.0^{13}936$	.02	.1	.2
		.2	$.0^{34}180$	$.0^{3}5$	$.0^{2}6$	.01
		0	0	$.0^{5}2$	$.0^{3}2$	$.0^{3}7$
	10	1.0	1.000	2.94	4.36	4.55
		.8	$.0^{2}674$	.12	.35	.50
		.6	$.0^{5}162$	$.0^{2}3$	.02	.04
		.4	$.0^{13}936$	$.0^{4}4$	$.0^{3}7$	$.0^{2}2$
		.2	$.0^{34}180$	$.0^{6}2$	$.0^{4}1$	$.0^{4}6$
		0	0	$.0^{9}2$	$.0^{6}1$	$.0^{6}9$
	5	1.0	1.000	2.24	2.59	2.12
		.8	$.0^{2}674$	.043	.095	.11
		.6	$.0^{5}162$	$.0^{3}4$	$.0^{2}2$	$.0^{2}3$
		.4	$.0^{13}936$	$.0^{5}2$	$.0^{4}2$	$0^{4}6$
		.2	$.0^{34}180$	$.0^{8}2$	$.0^{6}2$	$.0^{6}8$
		0	0	$.0^{12}1$	$.0^{9}5$	$.0^{8}6$
	2.5	1.0	1.000	1.71	1.57	.990
		.8	$.0^{2}674$	.029	.045	.039
		.6	$.0^{5}162$	$.0^{3}1$	$.0^{3}5$	$.0^{3}6$
		.4	$.0^{13}936$	$.0^{6}3$	$.0^{5}3$	$0^{5}6$
		.2	$.0^{34}180$	$.0^{9}2$	$.0^{7}1$	$.0^{7}6$
		0	0	$.0^{13}2$	$.0^{10}6$	$.0^{9}6$

Table 1—continued

X	α_0	γ_0	N_0/e^{-X}	N_1/e^{-X}	N_2/e^{-X}	N_3/e^{-X}
20	1.0	1.0	1.000	.822	.349	.103
		.8	$.0^{2}674$	.015	.012	$.0^{2}49$
		.6	$.0^{5}162$	$.0^{3}1$	$.0^{3}2$	$.0^{3}1$
		.4	$.0^{13}936$	$.0^{6}4$	$.0^{5}2$	$.0^{5}3$
		.2	$.0^{34}180$	$.0^{9}5$	$.0^{7}2$	$.0^{7}4$
		0	0	$.0^{12}2$	$.0^{9}1$	$.0^{9}6$

Table 2

N_k/e^{-X} FOR IRON SLABS*

X	α_0	γ_0	N_0/e^{-X}	N_1/e^{-X}	N_2/e^{-X}	N_3/e^{-X}
1	20	1.0	1.000	.278	.0793	.018
		.8	.779	.262	.0857	.024
		.6	.513	.221	.0931	.032
		.4	.223	.155	.0869	.038
		.2	.0183	.0660	.0561	.033
		0	0	.0146	.0230	.018
	10	1.0	1.000	.387	.129	.043
		.8	.779	.357	.140	.051
		.6	.513	.305	.142	.060
		.4	.223	.218	.139	.071
		.2	.0183	.0923	.0904	.057
		0	0	.0233	.0370	.030
	5	1.0	1.000	.462	.169	.056
		.8	.779	.436	.183	.070
		.6	.513	.370	.179	.080
		.4	.223	.265	.156	.083
		.2	.0183	.127	.107	.068
		0	0	.0401	.0623	.048
	2.5	1.0	1.000	.485	.181	.060
		.8	.779	.459	.196	.073
		.6	.513	.407	.211	.087
		.4	.223	.313	.198	.096
		.2	.0183	.161	.141	.081
		0	0	.0695	.0929	.066

* X = slab thickness in mean free paths.
α_0 = energy of incident photon in units of mc^2.
γ_0 = cosine of the angle between the slab normal and the incident path.
N_k = probability that a photon will be transmitted with exactly k collisions.

Table 2—continued

X	α_0	γ_0	N_0/e^{-X}	N_1/e^{-X}	N_2/e^{-X}	N_3/e^{-X}
1	1.0	1.0	1.000	.455	.169	.045
		.8	.779	.436	.181	.056
		.6	.513	.401	.199	.070
		.4	.223	.326	.202	.084
		.2	.0183	.187	.150	.073
		0	0	.104	.114	.066
2	20	1.0	1.000	.481	.201	.070
		.8	.607	.355	.162	.066
		.6	.264	.209	.128	.068
		.4	.0498	.0840	.0764	.054
		.2	$.0^3335$	.0153	.0241	.023
		0	0	$.0^2235$	$.0^2735$	$.0^298$
	10	1.0	1.000	.638	.294	.13
		.8	.607	.480	.268	.13
		.6	.264	.279	.193	.11
		.4	.0498	.112	.113	.078
		.2	$.0^3335$	.0212	.0370	.033
		0	0	$.0^2349$	.0112	.014
	5	1.0	1.000	.761	.430	.20
		.8	.607	.557	.347	.18
		.6	.264	.341	.258	.16
		.4	.0498	.149	.162	.12
		.2	$.0^3335$	.0353	.0626	.055
		0	0	$.0^2814$	.0271	.031
	2.5	1.0	1.000	.796	.449	.21
		.8	.607	.592	.397	.21
		.6	.264	.388	.309	.19
		.4	.0498	.190	.201	.14
		.2	$.0^3335$	.0625	.0947	.072
		0	0	.0268	.0612	.064
	1.0	1.0	1.000	.753	.425	.18
		.8	.607	.576	.381	.19
		.6	.264	.412	.325	.19
		.4	.0498	.230	.231	.15
		.2	$.0^3335$	.100	.140	.11
		0	0	.0488	.0972	.095
4	20	1.0	1.000	.807	.498	.269
		.8	.368	.385	.275	.174
		.6	.0695	.114	.107	.092
		.4	$.0^2248$	.0173	.0264	.031
		.2	$.0^6113$	$.0^2139$	$.0^2426$	$.0^271$
		0	0	$.0^310$	$.0^371$	$.0^217$

Table 2—continued

X	α_0	γ_0	N_0/e^{-X}	N_1/e^{-X}	N_2/e^{-X}	N_3/e^{-X}
4	10	1.0	1.000	1.02	.667	.387
		.8	.368	.500	.388	.257
		.6	.0695	.142	.151	.12
		.4	$.0^2248$	.0204	.0364	.038
		.2	$.0^6113$	$.0^2162$	$.0^2559$	$.0^281$
		0	0	$.0^316$	$.0^213$	$.0^227$
	5	1.0	1.000	1.17	.882	.564
		.8	.368	.556	.487	.347
		.6	.0695	.177	.216	.18
		.4	$.0^2248$	.0304	.0597	.061
		.2	$.0^6113$	$.0^2368$	.0138	.018
		0	0	$.0^359$	$.0^246$	$.0^276$
	2.5	1.0	1.000	1.21	.953	.660
		.8	.368	.614	.581	.458
		.6	.0695	.220	.276	.25
		.4	$.0^2248$	.0521	.0946	.10
		.2	$.0^6113$	.0128	.0342	.046
		0	0	$.0^248$	.020	.033
	1.0	1.0	1.000	1.17	.957	.619
		.8	.368	.635	.599	.449
		.6	.0695	.268	.327	.30
		.4	$.0^2248$	.0922	.152	.17
		.2	$.0^6113$	.0327	.0719	.10
		0	0	.014	.043	.075
8	20	1.0	1.000	1.34	1.16	.833
		.8	.135	.261	.282	.251
		.6	$.0^2483$	.0240	.0405	.053
		.4	$.0^5614$	$.0^3983$	$.0^2320$	$.0^262$
		.2	$.0^{13}127$	$.0^420$	$.0^316$	$.0^350$
		0	0	$.0^63$	$.0^58$	$.0^43$
	10	1.0	1.000	1.52	1.39	.952
		.8	.135	.293	.341	.298
		.6	$.0^2483$	.0240	.0441	.056
		.4	$.0^5614$	$.0^3796$	$.0^2308$	$.0^256$
		.2	$.0^{13}127$	$.0^415$	$.0^314$	$.0^339$
		0	0	$.0^65$	$.0^41$	$.0^45$
	5	1.0	1.000	1.70	1.61	1.32
		.8	.135	.335	.431	.418
		.6	$.0^2483$	.0316	.0668	.079
		.4	$.0^5614$	$.0^2157$	$.0^2639$	$.0^296$
		.2	$.0^{13}127$	$.0^465$	$.0^358$	$.0^212$
		0	0	$.0^35$	$.0^31$	$.0^33$

Table 2—continued

X	α_0	γ_0	N_0/e^{-X}	N_1/e^{-X}	N_2/e^{-X}	N_3/e^{-X}
8	2.5	1.0	1.000	1.77	1.87	1.68
		.8	.135	.394	.547	.605
		.6	$.0^{2}483$	.0504	.108	.15
		.4	$.0^{5}614$	$.0^{2}521$	.0199	.034
		.2	$.0^{13}127$	$.0^{3}75$	$.0^{2}53$	.012
		0	0	$.0^{3}2$	$.0^{2}2$	$.0^{2}6$
	1.0	1.0	1.000	1.71	1.90	1.68
		.8	.135	.456	.631	.709
		.6	$.0^{2}483$	.0939	.193	.28
		.4	$.0^{5}614$	.0210	.0621	.12
		.2	$.0^{13}127$	$.0^{2}53$	.023	.056
		0	0	$.0^{2}2$	.01	.04
12	20	1.0	1.000	1.79	1.86	1.51
		.8	.0498	.154	.223	.232
		.6	$.0^{3}335$	$.0^{2}515$	.0130	.022
		.4	$.0^{7}152$	$.0^{4}79$	$.0^{3}53$	$.0^{2}15$
		.2	$.0^{20}143$	$.0^{6}4$	$.0^{5}9$	$.0^{4}4$
		0	0	$.0^{8}1$	$.0^{6}1$	$.0^{6}9$
	10	1.0	1.000	1.90	2.09	1.59
		.8	.0498	.151	.233	.248
		.6	$.0^{3}335$	$.0^{2}397$	.0106	.017
		.4	$.0^{7}152$	$.0^{4}37$	$.0^{3}26$	$.0^{3}65$
		.2	$.0^{20}143$	$.0^{6}2$	$.0^{5}4$	$.0^{4}2$
		0	0	$.0^{8}1$	$.0^{6}1$	$.0^{6}8$
	5	1.0	1.000	2.05	2.31	2.05
		.8	.0498	.169	.273	.320
		.6	$.0^{3}335$	$.0^{2}560$	.0175	.027
		.4	$.0^{7}152$	$.0^{3}10$	$.0^{3}77$	$.0^{2}16$
		.2	$.0^{20}143$	$.0^{5}1$	$.0^{4}3$	$.0^{4}9$
		0	0	$.0^{7}5$	$.0^{5}3$	$.0^{4}1$
	2.5	1.0	1.000	2.15	2.70	2.69
		.8	.0498	.215	.378	.495
		.6	$.0^{3}335$	.0118	.0370	.065
		.4	$.0^{7}152$	$.0^{3}67$	$.0^{2}48$	.011
		.2	$.0^{20}143$	$.0^{4}5$	$.0^{2}1$	$.0^{3}3$
		0	0	$.0^{5}6$	$.0^{3}3$	$.0^{2}2$
	1.0	1.0	1.000	2.08	2.71	2.80
		.8	.0498	.284	.526	.716
		.6	$.0^{3}335$	.0359	.107	.19
		.4	$.0^{7}152$	$.0^{2}54$	.026	.062
		.2	$.0^{20}143$	$.0^{2}1$	$.0^{2}8$	.03
		0	0	$.0^{3}3$	$.0^{2}4$	02

Table 2—continued

X	α_0	γ_0	N_0/e^{-X}	N_1/e^{-X}	N_2/e^{-X}	N_3/e^{-X}
16	20	1.0	1.000	2.18	2.57	2.26
		.8	.0183	.0861	.165	.188
		.6	$.0^{4}233$	$.0^{2}12$	$.0^{2}45$	$.0^{2}90$
		.4	$.0^{10}378$	$.0^{5}7$	$.0^{4}9$	$.0^{5}3$
		.2	$.0^{27}160$	$.0^{8}7$	$.0^{6}5$	$.0^{6}4$
		0	0	$.0^{11}3$	$.0^{8}2$	$.0^{7}3$
	10	1.0	1.000	2.21	2.75	2.26
		.8	.0183	.0722	.142	.175
		.6	$.0^{4}233$	$.0^{3}68$	$.0^{2}28$	$.0^{2}55$
		.4	$.0^{10}378$	$.0^{5}2$	$.0^{4}3$	$.0^{4}9$
		.2	$.0^{27}160$	$.0^{8}2$	$.0^{6}1$	$.0^{6}8$
		0	0	$.0^{11}3$	$.0^{8}1$	$.0^{7}2$
	5	1.0	1.000	2.34	3.02	2.76
		.8	.0183	.0821	.155	.214
		.6	$.0^{4}233$	$.0^{2}10$	$.0^{2}45$	$.0^{2}93$
		.4	$.0^{10}378$	$.0^{5}7$	$.0^{3}1$	$.0^{3}3$
		.2	$.0^{27}160$	$.0^{7}3$	$.0^{5}2$	$.0^{5}8$
		0	0	$.0^{9}4$	$.0^{6}1$	$.0^{6}8$
	2.5	1.0	1.000	2.42	3.53	3.71
		.8	.0183	.110	.245	.378
		.6	$.0^{4}233$	$.0^{2}31$	.014	.032
		.4	$.0^{10}378$	$.0^{4}9$	$.0^{2}1$	$.0^{2}4$
		.2	$.0^{27}160$	$.0^{5}4$	$.0^{3}2$	$.0^{2}1$
		0	0	$.0^{6}2$	$.0^{4}7$	$.0^{3}5$
	1.0	1.0	1.000	2.37	3.61	4.06
		.8	.0183	.172	.443	.657
		.6	$.0^{4}233$	.014	.063	.12
		.4	$.0^{10}378$	$.0^{2}1$	.01	.03
		.2	$.0^{27}160$	$.0^{3}2$	$.0^{2}3$	.01
		0	0	$.0^{4}5$	$.0^{2}1$	$.0^{2}7$
20	20	1.0	1.000	2.53	3.29	3.02
		.8	$.0^{2}674$	.046	.11	.14
		.6	$.0^{5}162$	$.0^{3}3$	$.0^{2}2$	$.0^{2}4$
		.4	$.0^{13}936$	$.0^{6}5$	$.0^{4}2$	$.0^{4}9$
		.2	$.0^{34}180$	$.0^{9}1$	$.0^{7}3$	$.0^{6}4$
		0	0	$.0^{13}1$	$.0^{10}5$	$.0^{8}1$
	10	1.0	1.000	2.46	3.30	2.91
		.8	$.0^{2}674$	.035	.082	.12
		.6	$.0^{5}162$	$.0^{3}1$	$.0^{3}8$	$.0^{2}2$
		.4	$.0^{13}936$	$.0^{6}1$	$.0^{5}4$	$.0^{4}2$
		.2	$.0^{34}180$	$.0^{10}2$	$.0^{8}5$	$.0^{7}4$
		0	0	$.0^{14}7$	$.0^{10}3$	$.0^{9}4$

Table 2—continued

X	α_0	γ_0	N_0/e^{-X}	N_1/e^{-X}	N_2/e^{-X}	N_3/e^{-X}
20	5	1.0	1.000	2.59	3.81	3.69
		.8	$.0^{2}674$	.039	.087	.14
		.6	$.0^{5}162$	$.0^{3}2$	$.0^{2}1$	$.0^{2}3$
		.4	$.0^{13}936$	$.0^{6}5$	$.0^{5}1$	$.0^{4}6$
		.2	$.0^{34}180$	$.0^{9}5$	$.0^{7}8$	$.0^{6}7$
		0	0	$.0^{11}3$	$.0^{8}4$	$.0^{7}6$
	2.5	1.0	1.000	2.67	4.41	5.01
		.8	$.0^{2}674$	.055	.15	27
		.6	$.0^{5}162$	$.0^{3}9$	$.0^{2}6$	.02
		.4	$.0^{13}936$	$.0^{4}1$	$.0^{3}4$	$.0^{2}2$
		.2	$.0^{34}180$	$.0^{6}3$	$.0^{4}6$	$.0^{3}5$
		0	0	$.0^{8}8$	$.0^{5}2$	$.0^{4}2$
	1.0	1.0	1.000	2.58	4.44	5.43
		.8	$.0^{2}674$	.10	.35	.56
		.6	$.0^{5}162$	$.0^{2}5$	.04	.08
		.4	$.0^{13}936$	$.0^{3}3$	$.0^{2}5$	.01
		.2	$.0^{34}180$	$.0^{4}4$	$.0^{2}1$	$.0^{2}4$
		0	0	$.0^{4}1$	$0^{3}7$	$.0^{2}3$

Table 3

$E_k/\alpha_0 e^{-X}$ FOR LEAD SLABS*

X	α_0	γ_0	$E_0/\alpha_0 e^{-X}$	$E_1/\alpha_0 e^{-X}$	$E_2/\alpha_0 e^{-X}$	$E_3/\alpha_0 e^{-X}$
1	20	1.0	1.000	.0672	$.0^{2}450$	$.0^{3}36$
		.8	.779	.0650	$.0^{2}531$	$.0^{3}52$
		.6	.513	.0571	$.0^{2}582$	$.0^{3}72$
		.4	.223	.0390	$.0^{2}583$	$.0^{3}98$
		.2	.0183	.0157	$.0^{2}394$	$.0^{3}92$
		0	0	$.0^{2}337$	$.0^{2}167$	$.0^{3}57$
	10	1.0	1.000	.141	.0157	$.0^{2}18$
		.8	.779	.133	.0178	$.0^{2}23$
		.6	.513	.114	.0187	$.0^{2}29$
		.4	.223	.0770	.0165	$.0^{2}33$
		.2	.0183	.0307	.0104	$.0^{2}29$
		0	0	$.0^{2}610$	$.0^{2}421$	$.0^{2}21$

* X = slab thickness in mean free paths.
α_0 = energy of incident photon in units of mc^2.
γ_0 = cosine of the angle between the slab normal and the incident path.
E_k = expected energy of a photon transmitted with exactly k collisions.

Table 3—continued

X	α_0	γ_0	$E_0/\alpha_0 e^{-X}$	$E_1/\alpha_0 e^{-X}$	$E_2/\alpha_0 e^{-X}$	$F_3/\alpha_0 e^{-X}$
1	5	1.0	1.000	.223	.0340	$.0^{2}45$
		.8	.779	.206	.0370	$.0^{2}56$
		.6	.513	.176	.0370	$.0^{2}65$
		.4	.223	.116	.0306	$.0^{2}66$
		.2	.0183	.0482	.0198	$.0^{2}58$
		0	0	$.0^{2}920$	$.0^{2}758$	$.0^{2}30$
	2.5	1.0	1.000	.248	.0380	$.0^{2}43$
		.8	.779	.230	.0430	$.0^{2}57$
		.6	.513	.193	.0440	$.0^{2}70$
		.4	.223	132	.0366	$.0^{2}71$
		.2	.0183	.0570	.0227	$.0^{2}58$
		0	0	.0120	$.0^{2}860$	$.0^{2}34$
	1.0	1.0	1.000	.148	.0132	$.0^{3}88$
		.8	.779	.136	.0135	$.0^{3}99$
		.6	.513	.115	.0136	$.0^{2}11$
		.4	.223	.0805	.0114	$.0^{2}11$
		.2	.0183	.0405	$.0^{2}772$	$.0^{3}90$
		0	0	.0107	$.0^{2}357$	$.0^{3}61$
2	20	1.0	1.000	.140	.0166	$.0^{2}23$
		.8	.607	.106	.0155	$.0^{2}26$
		.6	.264	.0680	.0133	$.0^{2}29$
		.4	.0498	.0279	$.0^{2}843$	$.0^{2}26$
		.2	$.0^{3}335$	$.0^{2}660$	$.0^{2}355$	$.0^{2}15$
		0	0	$.0^{2}133$	$.0^{2}148$	$.0^{2}10$
	10	1.0	1.000	.268	.0530	$.0^{2}91$
		.8	.607	.198	.0452	$.0^{2}88$
		.6	.264	.121	.0336	$.0^{2}80$
		.4	.0498	.0476	.0192	$.0^{2}63$
		.2	$.0^{3}335$	$.0^{2}980$	$.0^{2}722$	$.0^{2}37$
		0	0	$.0^{2}149$	$.0^{2}243$	$.0^{2}23$
	5	1.0	1.000	.394	.0970	.020
		.8	.607	.283	.0840	.020
		.6	.264	.174	.0610	.017
		.4	.0498	.0667	.0327	.012
		.2	$.0^{3}335$	.0126	.0110	$.0^{2}54$
		0	0	$.0^{2}162$	$.0^{2}287$	$.0^{2}20$
	2.5	1.0	1.000	.420	.105	.020
		.8	.607	.304	.0880	.020
		.6	.264	.182	.0618	.016
		.4	.0498	.0723	.0326	.010
		.2	$.0^{3}335$	.0143	.0106	$.0^{2}46$
		0	0	$.0^{2}198$	$.0^{2}299$	$.0^{2}22$

Table 3—continued

X	α_0	γ_0	$E_0/\alpha_0 e^{-X}$	$E_1/\alpha_0 e^{-X}$	$E_2/\alpha_0 e^{-X}$	$E_3/\alpha_0 e^{-X}$
2	1.0	1.0	1.000	.239	.0320	$.0^231$
		.8	.607	.175	.0263	$.0^228$
		.6	.264	.108	.0194	$.0^224$
		.4	.0498	.0449	.0111	$.0^217$
		.2	$.0^3335$	.0110	$.0^2442$	$.0^385$
		0	0	$.0^2203$	$.0^2164$	$.0^349$
4	20	1.0	1.000	.308	.0690	.0156
		.8	.368	.157	.0450	.0127
		.6	.0695	.0563	.0238	$.0^290$
		.4	$.0^2248$	.0131	$.0^2936$	$.0^252$
		.2	$.0^6113$	$.0^2236$	$.0^2311$	$.0^226$
		0	0	$.0^337$	$.0^396$	$.0^213$
	10	1.0	1.000	.503	.162	.0443
		.8	.368	.243	.0930	.0300
		.6	.0695	.0786	.0434	.019
		.4	$.0^2248$	.0143	.0128	$.0^287$
		.2	$.0^6113$	$.0^2173$	$.0^2284$	$.0^332$
		0	0	$.0^315$	$.0^354$	$.0^211$
	5	1.0	1.000	.669	.257	.0794
		.8	.368	.313	.150	.0539
		.6	.0695	.0960	.0590	.027
		.4	$.0^2248$	.0152	.0151	$.0^295$
		.2	$.0^6113$	$.0^2136$	$.0^2252$	$.0^222$
		0	0	$.0^166$	$.0^227$	$.0^342$
	2.5	1.0	1.000	.665	.248	.0712
		.8	.368	.310	.140	.0460
		.6	.0695	.0948	.0526	.020
		.4	$.0^2248$	.0152	.0133	$.0^268$
		.2	$.0^6113$	$.0^2136$	$.0^2231$	$.0^217$
		0	0	$.0^148$	$.0^319$	$.0^128$
	1.0	1.0	1.000	.364	.0730	.0104
		.8	.368	.174	.0412	$.0^2668$
		.6	.0695	.0566	.0176	$.0^235$
		.4	$.0^2248$	.0100	$.0^2464$	$.0^212$
		.2	$.0^6113$	$.0^2118$	$.0^3950$	$.0^333$
		0	0	$.0^192$	$.0^322$	$.0^313$
8	20	1.0	1.000	.785	.374	.136
		.8	.135	.209	.138	.0646
		.6	$.0^2483$	.0419	.0430	.028
		.4	$.0^5614$	$.0^2680$	.0122	.012
		.2	$.0^{13}127$	$.0^384$	$.0^229$	$.0^246$
		0	0	$.0^45$	$.0^34$	$.0^21$

Table 3—continued

X	α_0	γ_0	$E_0/\alpha_0 e^{-X}$	$E_1/\alpha_0 e^{-X}$	$E_2/\alpha_0 e^{-X}$	$E_3/\alpha_0 e^{-X}$
8	10	1.0	1.000	.936	.482	.213
		.8	.135	.202	.138	.0796
		.6	$.0^2483$	.0258	.0295	.026
		.4	$.0^3614$	$.0^2208$	$.0^2458$	$.0^267$
		.2	$.0^{13}127$	$.0^496$	$.0^343$	$.0^211$
		0	0	$.0^52$	$.0^13$	$.0^32$
	5	1.0	1.000	1.06	.648	.286
		.8	.135	.213	.168	.0964
		.6	$.0^2483$	.0209	.0239	.019
		.4	$.0^3614$	$.0^2101$	$.0^2236$	$.0^228$
		.2	$.0^{13}127$	$.0^423$	$.0^313$	$.0^326$
		0	0	$.0^62$	$.0^35$	$.0^42$
	2.5	1.0	1.000	.986	.549	.210
		.8	.135	.194	.137	.0645
		.6	$.0^2483$	.0176	.0177	.010
		.4	$.0^3614$	$.0^3811$	$.0^2145$	$.0^212$
		.2	$.0^{13}127$	$.0^421$	$.0^194$	$.0^313$
		0	0	$.0^79$	$.0^33$	$.0^58$
	1.0	1.0	1.000	.518	.150	.0295
		.8	.135	.108	.0374	$.0^2923$
		.6	$.0^2483$	.0106	$.0^2599$	$.0^220$
		.4	$.0^3614$	$.0^3654$	$.0^3628$	$.0^328$
		.2	$.0^{13}127$	$.0^426$	$.0^453$	$.0^436$
		0	0	$.0^64$	$.0^55$	$.0^57$
12	20	1.0	1.000	1.58	1.25	.625
		.8	.0498	.275	.311	.193
		.6	$.0^3335$	.0449	.0807	.069
		.4	$.0^7152$	$.0^263$	.022	.030
		.2	$.0^{20}143$	$.0^346$	$.0^23$	$.0^28$
		0	0	$.0^59$	$.0^32$	$.0^38$
	10	1.0	1.000	1.34	.941	.546
		.8	.0498	.142	.152	.123
		.6	$.0^3335$	$.0^2970$	.0179	.023
		.4	$.0^7152$	$.0^339$	$.0^215$	$.0^235$
		.2	$.0^{20}143$	$.0^58$	$.0^17$	$.0^33$
		0	0	$.0^75$	$.0^52$	$.0^43$
	5	1.0	1.000	1.37	1.05	.575
		.8	.0498	.118	.132	.102
		.6	$.0^3335$	$.0^2457$	$.0^2828$	$.0^297$
		.4	$.0^7152$	$.0^488$	$.0^337$	$.0^371$
		.2	$.0^{20}143$	$.0^66$	$.0^41$	$.0^44$
		0	0	$.0^81$	$.0^62$	$.0^51$

Table 3—continued

X	α_0	γ_0	$E_0/\alpha_0 e^{-X}$	$E_1/\alpha_0 e^{-X}$	$E_2/\alpha_0 e^{-X}$	$E_3/\alpha_0 e^{-X}$
12	2.5	1.0	1.000	1.21	.819	.373
		.8	.0498	.0990	.0910	.0532
		.6	$.0^{4}335$	$.0^{2}337$	$.0^{2}479$	$.0^{2}36$
		.4	$.0^{7}152$	$.0^{4}68$	$.0^{3}19$	$.0^{3}21$
		.2	$.0^{20}143$	$.0^{6}5$	$.0^{5}5$	$.0^{4}1$
		0	0	$.0^{9}3$	$.0^{7}7$	$.0^{6}4$
	1.0	1.0	1.000	.621	.215	.0500
		.8	.0498	.0545	.0260	$.0^{2}801$
		.6	$.0^{4}335$	$.0^{2}221$	$.0^{2}173$	$.0^{3}75$
		.4	$.0^{7}152$	$.0^{4}65$	$.0^{4}98$	$.0^{4}62$
		.2	$.0^{20}143$	$.0^{6}9$	$.0^{5}4$	$.0^{5}4$
		0	0	$.0^{8}2$	$.0^{6}2$	$.0^{6}4$
16	20	1.0	1.000	2.93	3.53	2.22
		.8	.0183	.457	.833	.641
		.6	$.0^{4}233$	.069	.21	.23
		.4	$.0^{10}378$	$.0^{2}7$	.05	.09
		.2	$.0^{27}160$	$.0^{3}3$	$.0^{2}5$	.02
		0	0	$.0^{5}2$	$.0^{3}1$	$.0^{2}1$
	10	1.0	1.000	1.72	1.58	1.06
		.8	.0183	.105	.166	.162
		.6	$.0^{4}233$	$.0^{2}44$	.012	.021
		.4	$.0^{10}378$	$.0^{3}1$	$.0^{3}6$	$.0^{2}2$
		.2	$.0^{27}160$	$.0^{6}8$	$.0^{4}2$	$.0^{3}1$
		0	0	$.0^{8}1$	$.0^{6}3$	$.0^{5}5$
	5	1.0	1.000	1.63	1.40	.893
		.8	.0183	.0645	.0948	.0923
		.6	$.0^{4}233$	$.0^{2}12$	$.0^{2}31$	$.0^{2}49$
		.4	$.0^{10}378$	$.0^{5}9$	$.0^{4}6$	$.0^{3}2$
		.2	$.0^{27}160$	$.0^{7}2$	$.0^{6}8$	$.0^{5}5$
		0	0	$.0^{11}8$	$.0^{8}8$	$.0^{6}2$
	2.5	1.0	1.000	1.40	1.06	.533
		.8	.0183	.0503	.0567	.0374
		.6	$.0^{4}233$	$.0^{3}82$	$.0^{2}16$	$.0^{2}14$
		.4	$.0^{10}378$	$.0^{5}7$	$.0^{4}3$	$.0^{4}4$
		.2	$.0^{27}160$	$.0^{7}1$	$.0^{6}3$	$.0^{6}8$
		0	0	$.0^{11}2$	$.0^{8}3$	$.0^{7}3$
	1.0	1.0	1.000	.708	.265	.0709
		.8	.0183	.0274	.0150	$.0^{2}542$
		.6	$.0^{4}233$	$.0^{3}55$	$.0^{3}53$	$.0^{3}28$
		.4	$.0^{10}378$	$.0^{5}8$	$.0^{4}2$	$.0^{4}1$
		.2	$.0^{27}160$	$.0^{7}3$	$.0^{6}3$	$.0^{6}5$
		0	0	$.0^{10}2$	$.0^{8}7$	$.0^{7}2$

Table 3—continued

X	α_0	γ_0	$E_0/\alpha_0 e^{-X}$	$E_1/\alpha_0 e^{-X}$	$E_2/\alpha_0 e^{-X}$	$E_3/\alpha_0 e^{-X}$
20	20	1.0	1.000	5 34	9.25	6.82
		.8	$.0^{2}674$	.96	2.7	2.5
		.6	$.0^{5}162$	.1	.8	1.
		.4	$.0^{13}936$	.01	.1	.3
		.2	$.0^{34}180$	$.0^{3}2$	.01	.05
		0	0	$.0^{6}4$	$.0^{4}7$	$.0^{2}1$
	10	1.0	1.000	2.11	2.43	1.80
		.8	$.0^{2}674$	.089	.20	.23
		.6	$.0^{5}162$	$.0^{2}2$	.01	.02
		.4	$.0^{13}936$	$.0^{4}3$	$.0^{3}3$	$.0^{2}1$
		.2	$.0^{34}180$	$.0^{6}1$	$.0^{5}4$	$.0^{4}4$
		0	0	$.0^{10}5$	$.0^{7}3$	$.0^{5}1$
	5	1.0	1.000	1.83	1.73	1.26
		.8	$.0^{2}674$	.038	.073	.087
		.6	$.0^{5}162$	$0^{3}4$	$.0^{2}1$	$.0^{2}3$
		4	$.0^{13}936$	$.0^{6}9$	$.0^{4}1$	$.0^{4}5$
		.2	$.0^{34}180$	$.0^{9}6$	$.0^{7}9$	$.0^{6}9$
		0	0	$.0^{13}6$	$.0^{9}4$	$.0^{7}2$
	2.5	1.0	1.000	1.53	1.26	.682
		.8	$.0^{2}674$	.028	.036	.026
		.6	$.0^{5}162$	$.0^{3}2$	$.0^{3}6$	$.0^{3}6$
		4	$.0^{13}936$	$.0^{6}8$	$.0^{5}5$	$.0^{5}8$
		.2	$.0^{34}180$	$.0^{9}3$	$.0^{7}2$	$.0^{7}7$
		0	0	$.0^{13}1$	$.0^{9}1$	$.0^{8}3$
	1.0	1.0	1.000	.761	.308	.0929
		.8	$.0^{2}674$	.015	$.0^{2}90$	$.0^{2}37$
		.6	$.0^{5}162$	$.0^{3}2$	$.0^{3}2$	$.0^{3}1$
		.4	$.0^{13}936$	$.0^{5}1$	$.0^{5}3$	$.0^{5}3$
		.2	$.0^{34}180$	$.0^{8}2$	$.0^{7}3$	$.0^{7}6$
		0	0	$.0^{12}2$	$.0^{9}3$	$.0^{8}1$

Table 4

$E_k/\alpha_0 e^{-X}$ FOR IRON SLABS*

X	α_0	γ_0	$E_0/\alpha_0 e^{-X}$	$E_1/\alpha_0 e^{-X}$	$E_2/\alpha_0 e^{-X}$	$E_3/\alpha_0 e^{-X}$
1	20	1.0	1.00	.133	.0165	$.0^220$
		.8	.779	.125	.0178	$.0^225$
		.6	.513	.107	.0190	$.0^233$
		.4	.223	.0698	.0178	$.0^241$
		.2	.0183	.0181	$.0^2829$	$.0^228$
		0	0	$.0^2289$	$.0^2296$	$.0^216$
	10	1.0	1.00	.218	.0396	$.0^265$
		.8	.779	.204	.0428	$.0^282$
		.6	.513	.173	.0447	.010
		.4	.223	.115	.0391	.011
		.2	.0183	.0329	.0188	$.0^270$
		0	0	$.0^2639$	$.0^2758$	$.0^244$
	5	1.0	1.00	.298	.0671	.015
		.8	.779	.275	.0727	.018
		.6	.513	.234	.0756	.021
		.4	.223	.160	.0682	.023
		.2	.0183	.0662	.0421	.017
		0	0	.0148	.0173	.010
	2.5	1.0	1.00	.352	.0955	.025
		.8	.779	.322	.0981	.028
		.6	.513	.283	.0978	.030
		.4	.223	.202	.0860	.030
		.2	.0183	.0945	.0577	.023
		0	0	.0322	.0347	.018
	1.0	1.0	1.00	.379	.102	.026
		.8	.779	.384	.118	.034
		.6	.513	.318	.121	.039
		.4	.223	.232	.111	.041
		.2	.0183	.132	.0848	.037
		0	0	.0664	.0610	.031
2	20	1.0	1.00	.249	.0518	.010
		.8	.607	.183	.0447	.010
		.6	.264	.106	.0375	$.0^287$
		.4	.0498	.0378	.0175	$.0^263$
		.2	$.0^33335$	$.0^2463$	$.0^2417$	$.0^222$
		0	0	$.0^3394$	$.0^3908$	$.0^378$

* X = slab thickness in mean free paths.
α_0 = energy of incident photon in units of mc^2.
γ_0 = cosine of the angle between the slab normal and the incident path.
E_k = expected energy of a photon transmitted with exactly k collisions.

Table 4—continued

X	α_0	γ_0	$E_0/\alpha_0 e^{-X}$	$E_1/\alpha_0 e^{-X}$	$E_2/\alpha_0 e^{-X}$	$E_3/\alpha_0 e^{-X}$
2	10	1.0	1.00	.379	.114	.029
		.8	.607	.282	.0952	.028
		.6	.264	.166	.0694	.025
		.4	.0498	.0593	.0354	.016
		.2	$.0^3335$	$.0^2849$	$.0^2904$	$.0^256$
		0	0	$.0^3916$	$.0^2216$	$.0^222$
	5	1.0	1.00	.510	.184	.061
		.8	.607	.375	.162	.061
		.6	.264	.225	.121	.054
		.4	.0498	.0880	.0653	.035
		.2	$.0^3335$	.0168	0207	.014
		0	0	$.0^2309$	$.0^2783$	$.0^280$
	2.5	1.0	1.00	.587	.260	.095
		.8	.607	.436	.219	.088
		.6	.264	.285	.167	.073
		.4	.0498	.124	.0975	.049
		.2	$.0^3335$	.0350	.0463	.027
		0	0	$.0^2940$	.0224	.019
	1.0	1.0	1.00	.636	.278	.1[illegible]
		.8	.607	.514	.268	.11
		.6	.264	.330	.210	.099
		.4	.0498	.174	143	.078
		.2	$.0^3335$	.0691	[illegible]810	.052
		0	0	.0301	541	.044
4	20	1.0	1.00	.456	.148	.0439
		.8	.368	.215	.0855	.0296
		.6	.0695	.0594	.0316	.013
		.4	$.0^2248$	$.0^2755$	$.0^2672$	$.0^240$
		.2	$.0^6113$	$.0^3421$	$.0^3853$	$.0^378$
		0	0	$.0^416$	$.0^310$	$.0^316$
	10	1.0	1.00	.657	.300	.108
		.8	.368	.308	.162	.0680
		.6	.0695	.0869	.0594	.031
		.4	$.0^2248$	.0109	.0117	$.0^283$
		.2	$.0^6113$	$.0^3750$	$.0^2160$	0^217
		0	0	$.0^444$	$.0^322$	$.0^340$
	5	1.0	1.00	.840	.443	.210
		.8	.368	.396	.261	.149
		.6	.0695	.118	.106	.074
		.4	$.0^2248$	.0183	.0252	.022
		.2	$.0^6113$	$.0^2201$	$.0^2485$	$.0^257$
		0	0	$.0^321$	$.0^211$	$.0^219$

Table 4—continued

X	α_0	γ_0	$E_0/\alpha_0 e^{-X}$	$E_1/\alpha_0 e^{-X}$	$E_2/\alpha_0 e^{-X}$	$E_3/\alpha_0 e^{-X}$
4	2.5	1.0	1.00	.960	.623	.311
		.8	.368	.470	.354	.205
		.6	.0695	.158	.158	.11
		.4	$.0^2248$	.0339	.0522	.044
		.2	$.0^6113$	$.0^2659$	.0182	.020
		0	0	$.0^214$	$.0^284$	.013
	1.0	1.0	1.00	1.01	.656	.349
		.8	.368	.537	.445	.278
		.6	.0695	.218	.243	.18
		.4	$.0^2248$	.0692	.107	.097
		.2	$.0^6113$	.0237	.0513	.057
		0	0	$.0^285$	.028	.038
8	20	1.0	1.00	.828	.413	.170
		.8	.135	.157	.101	.0534
		.6	$.0^2483$	.0127	.0130	$.0^293$
		.4	$.0^5614$	$.0^3397$	$.0^3800$	$.0^389$
		.2	$.0^{13}127$	$.0^554$	$.0^429$	$.0^455$
		0	0	$.0^74$	$.0^69$	$.0^53$
	10	1.0	1.00	1.09	.737	.344
		.8	.135	.201	.170	.0983
		.6	$.0^2483$	.0155	.0196	.015
		.4	$.0^5614$	$.0^3425$	$.0^2102$	$.0^212$
		.2	$.0^{13}127$	$.0^581$	$.0^445$	$.0^483$
		0	0	$.0^61$	$.0^52$	$.0^56$
	5	1.0	1.00	1.31	1.02	.623
		.8	.135	.252	.251	.196
		.6	$.0^2483$	.0229	.0343	.035
		.4	$.0^5614$	$.0^3944$	$.0^2249$	$.0^234$
		.2	$.0^{13}127$	$.0^436$	$.0^319$	$.0^338$
		0	0	$.0^51$	$.0^42$	$.0^46$
	2.5	1.0	1.00	1.47	1.30	.869
		.8	.135	.314	.356	.301
		.6	$.0^2483$	.0375	.0663	.071
		.4	$.0^5614$	$.0^2336$	.0103	.015
		.2	$.0^{13}127$	$.0^339$	$.0^220$	$.0^239$
		0	0	$.0^45$	$.0^38$	$.0^23$
	1.0	1.0	1.00	1.52	1.36	1.02
		.8	.135	.393	.501	.455
		.6	$.0^2483$	.0772	.142	.16
		.4	$.0^5614$	.0157	.0420	.060
		.2	$.0^{13}127$	$.0^238$	.015	.027
		0	0	$.0^21$	$.0^26$	.01

Table 4—continued

X	α_0	γ_0	$\Sigma_0/\alpha_0 e^{-X}$	$E_1/\alpha_0 e^{-X}$	$E_2/\alpha_0 e^{-X}$	$E_3/\alpha_0 e^{-X}$
12	20	1.0	1.00	1.15	.768	.387
		.8	.0498	.0928	.0894	.0589
		.6	$.0^{3}3335$	$.0^{2}2275$	$.0^{2}443$	$.0^{2}46$
		.4	$.0^{7}152$	$.0^{4}29$	$.0^{3}11$	$.0^{3}20$
		.2	$.0^{20}143$	$.0^{7}9$	$.0^{5}1$	$.0^{5}5$
		0	0	$.0^{9}1$	$.0^{7}2$	$.0^{6}1$
	10	1.0	1.00	1.40	1.12	.609
		.8	.0498	.106	.119	.0874
		.6	$.0^{3}3335$	$.0^{2}262$	$.0^{2}506$	$.0^{2}52$
		.4	$.0^{7}152$	$.0^{4}21$	$.0^{4}95$	$.0^{3}15$
		.2	$.0^{20}143$	$.0^{6}1$	$.0^{5}1$	$.0^{5}4$
		0	0	$.0^{9}3$	$.0^{7}2$	$.0^{6}1$
	5	1.0	1.00	1.63	1.59	1.10
		.8	.0498	.131	.181	.163
		.6	$.0^{3}3335$	$.0^{2}405$	$.0^{2}927$	.011
		.4	$.0^{7}152$	$.0^{4}64$	$.0^{3}29$	$.0^{3}54$
		.2	$.0^{20}143$	$.0^{6}9$	$.0^{4}1$	$.0^{4}3$
		0	0	$.0^{7}1$	$.0^{6}4$	$.0^{5}2$
	2.5	1.0	1.00	1.79	1.98	1.56
		.8	.0493	.175	.274	.277
		.6	$.0^{3}3335$	$.0^{2}893$	.0230	.031
		.4	$.0^{7}152$	$.0^{3}40$	$.0^{2}20$	$.0^{2}39$
		.2	$.0^{20}143$	$.0^{4}3$	$.0^{3}3$	$.0^{3}8$
		0	0	$.0^{5}2$	$.0^{4}8$	$.0^{3}4$
	1.0	1.0	1.00	1.85	2.12	1.90
		.8	.0498	.244	.423	.470
		.6	$.0^{3}3335$	.0293	.0772	.11
		.4	$.0^{7}152$	$.0^{2}42$	.018	.033
		.2	$.0^{20}143$	$.0^{3}7$	$.0^{2}5$	.01
		0	0	$.0^{3}2$	$.0^{2}2$	$.0^{2}7$
16	20	1.0	1.00	1.46	1.16	.645
		.8	.0183	.0538	.0677	.0537
		.6	$.0^{4}233$	$.0^{3}61$	$.0^{2}15$	$.0^{2}22$
		.4	$.0^{10}378$	$.0^{5}2$	$.0^{4}2$	$.0^{4}5$
		.2	$.0^{27}160$	$.0^{8}2$	$.0^{7}5$	$.0^{6}5$
		0	0	$.0^{12}5$	$.0^{9}3$	$.0^{7}1$
	10	1.0	1.00	1.66	1.52	.931
		.8	.0183	.0528	.0783	.0669
		.6	$.0^{4}233$	$.0^{3}42$	$.0^{2}13$	$.0^{2}17$
		.4	$.0^{10}378$	$.0^{5}1$	$.0^{4}1$	$.0^{4}2$
		.2	$.0^{27}160$	$.0^{8}1$	$.0^{7}5$	$.0^{6}2$
		0	0	$.0^{12}7$	$.0^{9}3$	$.0^{8}3$

Table 4—continued

X	α_0	γ_0	$E_0/\alpha_0\epsilon^{-X}$	$E_1/\alpha_0\epsilon^{-X}$	$E_2/\alpha_0\epsilon^{-X}$	$E_3/\alpha_0\epsilon^{-X}$
16	5	1.0	1.00	1.88	2.11	1.55
		.8	.0183	.0645	.113	.116
		.6	$.0^{4}233$	$.0^{3}69$	$.0^{2}23$	$.0^{2}35$
		.4	$.0^{10}378$	$.0^{3}5$	$.0^{4}4$	$.0^{4}$
		.2	$.0^{27}160$	$.0^{7}2$	$.0^{6}6$	$.0^{5}3$
		0	0	$.0^{9}1$	$.0^{7}1$	$.0^{7}9$
	2.5	1.0	1.00	2.04	2.61	2.27
		.8	.0183	.0908	.184	.225
		.6	$.0^{4}233$	$.0^{2}21$	$.0^{2}74$	.013
		.4	$.0^{10}378$	$.0^{4}5$	$.0^{3}4$	$.0^{2}1$
		.2	$.0^{27}160$	$.0^{5}2$	$.0^{4}4$	$.0^{3}2$
		0	0	$.0^{7}9$	$.0^{4}1$	$.0^{4}8$
	1.0	1.0	1.00	2.11	2.91	2.77
		.8	.0183	.151	.343	.420
		.6	$.0^{4}233$	.012	.045	.075
		.4	$.0^{10}378$	$.0^{2}1$	$.0^{2}8$	.02
		.2	$.0^{27}160$	$.0^{3}2$	$.0^{2}2$	$.0^{2}7$
		0	0	$.0^{4}3$	$.0^{3}7$	$.0^{2}4$
20	20	1.0	1.00	1.74	1.57	.957
		.8	$.0^{2}674$	.032	.049	.046
		.6	$.0^{5}162$	$.0^{3}1$	$.0^{3}5$	$.0^{2}1$
		.4	$.0^{13}936$	$.0^{6}2$	$.0^{5}2$	$.0^{4}1$
		.2	$.0^{34}180$	$.0^{10}3$	$.0^{8}3$	$.0^{7}5$
		0	0	$.0^{14}2$	$.0^{11}8$	$.0^{9}9$
	10	1.0	1.00	1.89	2.00	1.35
		.8	$.0^{2}674$	.025	.048	.047
		.6	$.0^{5}162$	$.0^{4}6$	$.0^{3}3$	$.0^{3}5$
		.4	$.0^{13}936$	$.0^{7}6$	$.0^{5}1$	$.0^{5}3$
		.2	$.0^{34}180$	$.0^{10}2$	$.0^{8}2$	$.0^{8}9$
		0	0	$.0^{14}1$	$.0^{11}4$	$.0^{10}6$
	5	1.0	1.00	2.13	2.59	2.05
		.8	$.0^{2}674$	.031	.067	.078
		.6	$.0^{5}162$	$.0^{3}1$	$.0^{3}5$	$.0^{2}1$
		.4	$.0^{13}936$	$.0^{6}3$	$.0^{5}5$	$.0^{4}1$
		.2	$.0^{34}180$	$.0^{9}6$	$.0^{7}4$	$.0^{6}2$
		0	0	$.0^{12}8$	$.0^{9}4$	$.0^{8}5$
	2.5	1.0	1.00	2.29	3.32	3.20
		.8	$.0^{2}674$	.045	.11	.16
		.6	$.0^{5}162$	$.0^{3}5$	$.0^{2}3$	$.0^{2}5$
		.4	$.0^{13}936$	$.0^{5}7$	$.0^{4}9$	$.0^{3}3$
		.2	$.0^{34}180$	$.0^{8}1$	$.0^{5}8$	$.0^{4}4$
		0	0	$.0^{8}3$	$.0^{5}1$	$.0^{4}2$

Table 4—continued

X	α_0	γ_0	$E_0/\alpha_0 e^{-X}$	$E_1/\alpha_0 e^{-X}$	$E_2/\alpha_0 e^{-X}$	$E_3/\alpha_0 e^{-X}$
20	1.0	1.0	1.00	2.36	3.71	3.74
		.8	$.0^{2}674$	.093	.27	.36
		.6	$.0^{5}162$	$.0^{2}5$	.03	.05
		.4	$.0^{13}936$	$.0^{3}4$	$.0^{2}4$	.01
		.2	$.0^{34}180$	$.0^{4}4$	$.0^{3}8$	$.0^{2}4$
		0	0	$.0^{5}6$	$.0^{3}3$	$.0^{2}3$

Table 5

VALUES OF r_k AND q_k FOR LEAD AND FOR IRON*

		Lead		Iron	
α_0	k	r_k	q_k	r_k	q_k
20	0	1.00	20.00	1.00	20.00
	1	.216	1.36	.475	2.99
	2	.109	.233	.404	.842
	3	.0524	.0661	.370	.371
	4	.0212	.0203	.315	.201
	5	$.0^{2}739$	$.0^{2}594$	.243	.115
	6	$.0^{2}223$	$.0^{2}162$	.170	.0662
	7	$.0^{3}604$	$.0^{3}429$	.107	.0369
	8	$.0^{3}157$	$.0^{3}107$	.0621	.0196
	9	$.0^{4}372$	$.0^{4}262$	.0331	.0100
	10	$.0^{5}877$	$.0^{5}622$	.0163	$.0^{2}470$
	11	$.0^{5}199$	$.0^{5}142$	$.0^{2}756$	$.0^{2}218$
	12	$.0^{6}453$	$.0^{6}310$	$.0^{2}328$	$.0^{2}100$
10	0	1.00	10.00	1.00	10.00
	1	.446	1.65	.741	2.74
	2	.254	.445	.690	1.10
	3	.122	.142	.635	.557
	4	.0487	.0443	.534	.316
	5	.0165	.0128	.408	.184
	6	$.0^{2}488$	$.0^{2}341$	.281	.106
	7	$.0^{2}128$	$.0^{3}882$	.175	.0586
	8	$.0^{3}314$	$.0^{3}208$	.0990	.0308
	9	$.0^{4}720$	$.0^{4}480$	.0518	.0152
	10	$.0^{4}162$	$.0^{4}106$	.0252	$.0^{2}730$
	11	$.0^{5}353$	$.0^{5}211$	.0114	$.0^{2}320$
	12	$.0^{6}770$	$.0^{6}402$	$.0^{2}487$	$.0^{2}138$

* r_k = the probability that a photon will survive its kth collision in an infinite homogeneous medium.

q_k = the expected energy of a photon surviving its kth collision in an infinite homogeneous medium.

α_0 = energy of incident photon in units of mc^2.

Table 5—continued

α_0	k	Lead		Iron	
		r_k	q_k	r_k	q_k
3	0	1.00	5.00	1.00	5.00
	1	.703	1.55	.934	2.06
	2	.414	.548	.908	1.04
	3	.189	.184	.830	.593
	4	.0697	.0556	.683	.350
	5	.0216	.0152	.505	.205
	6	$.0^2582$	$.0^2377$	.334	.117
	7	$.0^2138$	$.0^3910$	.200	.0635
	8	$.0^3297$	$.0^3198$	.109	.0326
	9	$.0^4580$	$.0^4420$	.0549	.0153
	10	$.0^4109$	$.0^5852$	.0255	$.0^2700$
	11	$.0^5194$	$.0^5167$	.0111	$.0^2280$
	12	$.0^6338$	$.0^6300$	$.0^2454$	$.0^2109$
2.5	0	1.00	2.50	1.00	2.50
	1	.776	1.02	1.00	1.32
	2	.393	.366	.971	.775
	3	.146	.108	.856	.470
	4	.0432	.0278	.667	.281
	5	.0109	$.0^2636$	.461	.162
	6	$.0^2222$	$.0^2122$	.282	.0899
	7	$.0^3399$	$.0^3202$	.150	.0471
	8	$.0^4663$	$.0^4300$	.0801	.0228
	9	$.0^4109$	$.0^5415$	.0376	.0102
	10	$.0^5174$	$.0^6532$	.0161	$.0^2410$
	11	$.0^6271$	$.0^7620$	$.0^2650$	$.0^2160$
	12	$.0^7424$	$.0^8722$	$.0^2242$	$.0^3600$
1.0	0	1.00	1.00	1.00	1.00
	1	.458	.300	.981	.643
	2	.119	.0618	.900	.405
	3	.0221	$.0^2972$	.675	.243
	4	$.0^2313$	$.0^2119$	.450	.138
	5	$.0^3336$	$.0^3122$	.251	.0753
	6	$.0^4344$	$.0^4114$	.131	.0373
	7	$.0^5305$	$.0^6850$	.0604	.0169
	8	$.0^6250$	$.0^7533$	.0256	$.0^2695$
	9	$.0^7198$	$.0^8268$	$.0^2923$	$.0^2265$
	10	$.0^8149$	$.0^9108$	$.0^2321$	$.0^3910$
	11	$.0^9107$	$.0^{11}301$	$.0^3973$	$.0^3261$
	12	$.0^{11}738$	$.0^{13}837$	$.0^3268$	$.0^4670$

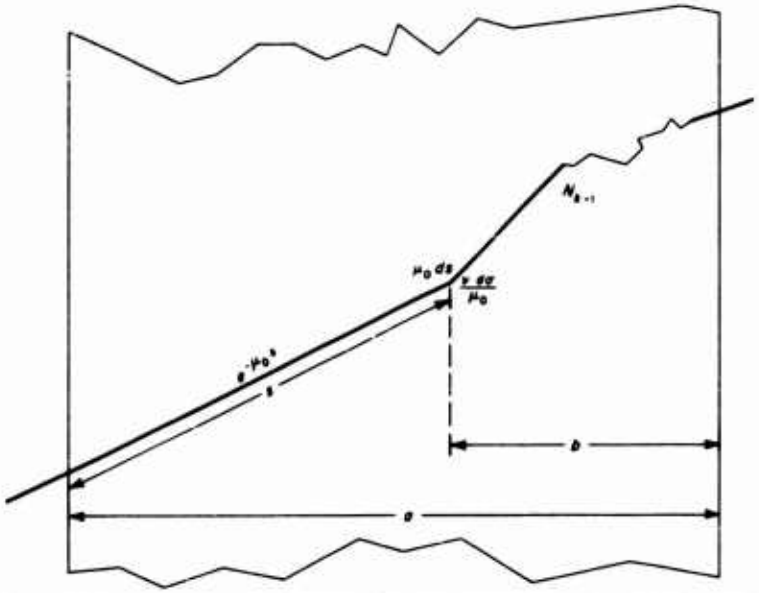

Fig. 1—A diagram showing the probabilities associated with the transmission of a photon and clarifying the derivation of the formula

$$dN_k = e^{-\mu_0 s} \cdot \mu_0\, ds \cdot \frac{\nu\, d\sigma}{\mu_0} \cdot N_{k-1}$$

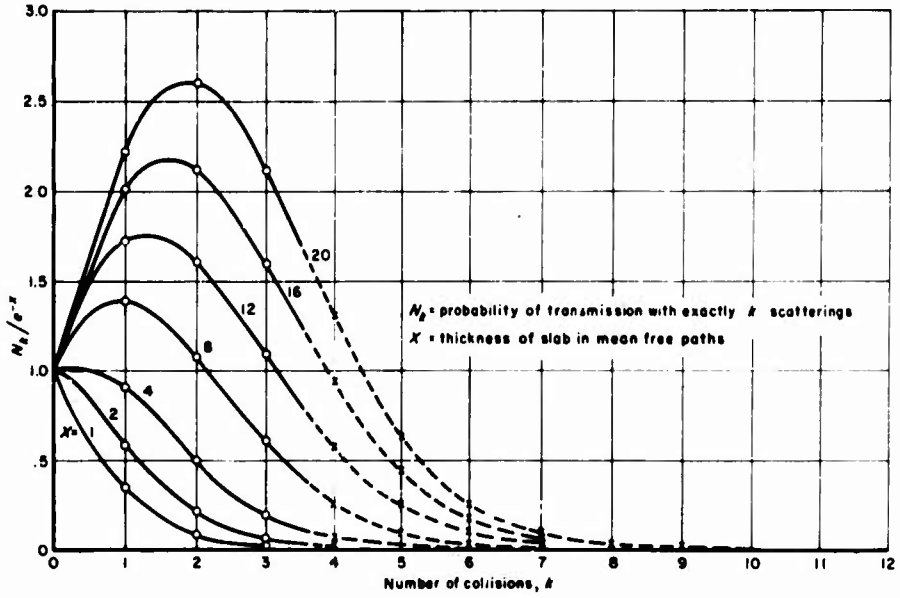

Fig. 2—Graphical representation of the calculated and estimated behavior of N_k/e^{-X} with respect to k in the case of a photon of energy 5 mc² normally incident on a lead slab

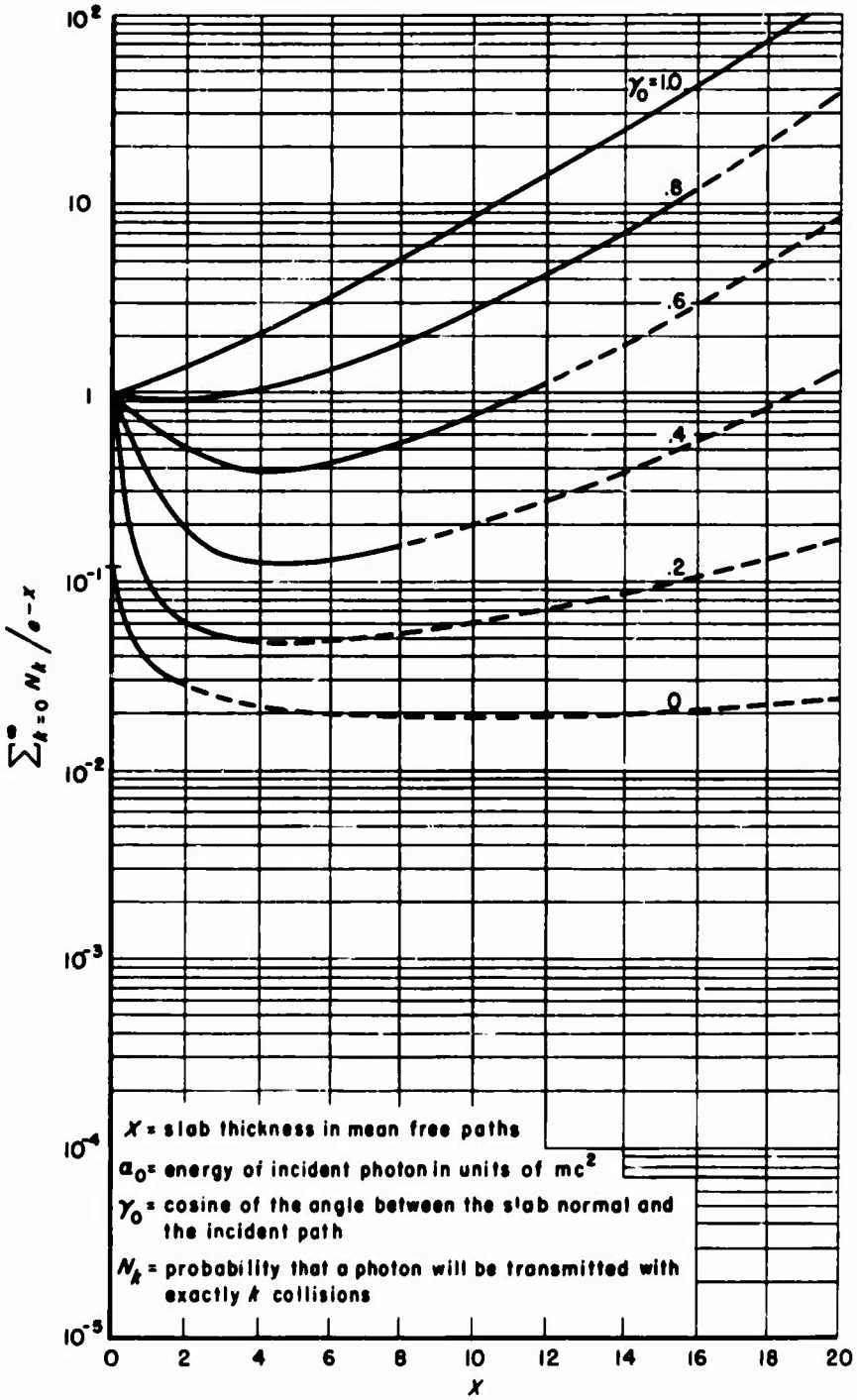

Fig. 3a—Number build-up factors for lead slabs, $\alpha_0 = 20$

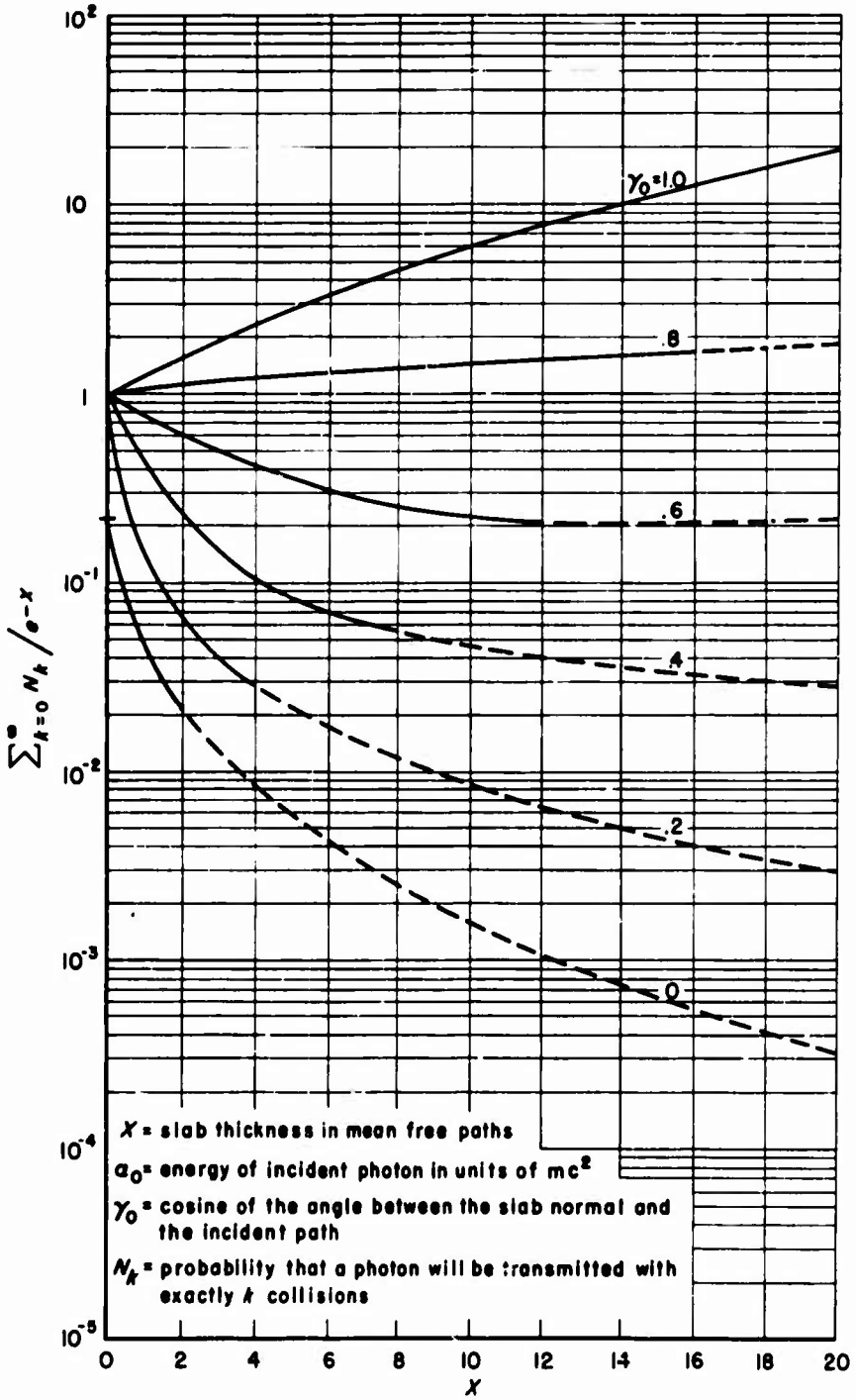

Fig. 3b—Number build-up factors for lead slabs, $\alpha_0 = 10$

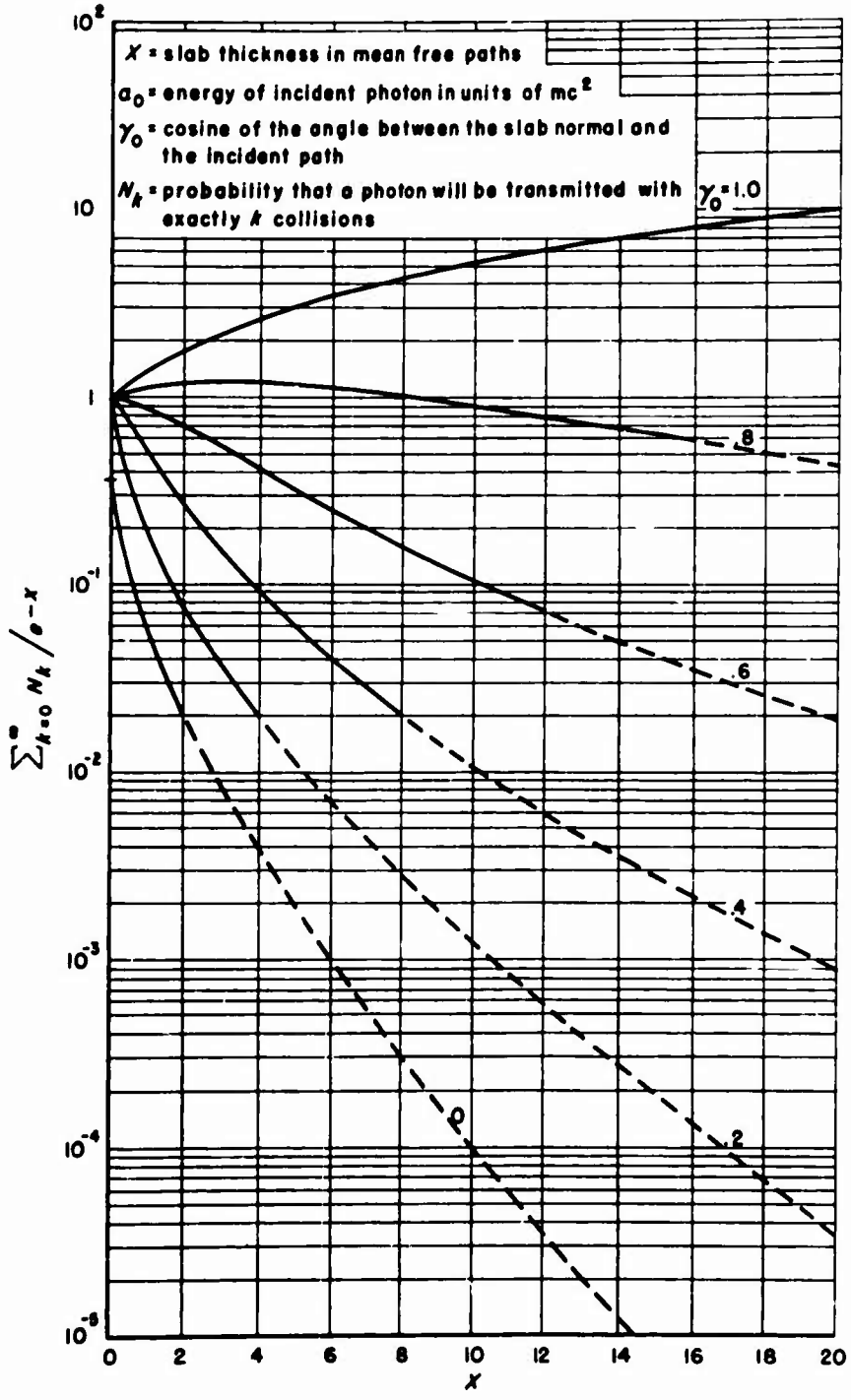

Fig. 3c—Number build-up factors for lead slabs, $\alpha_0 = 5$

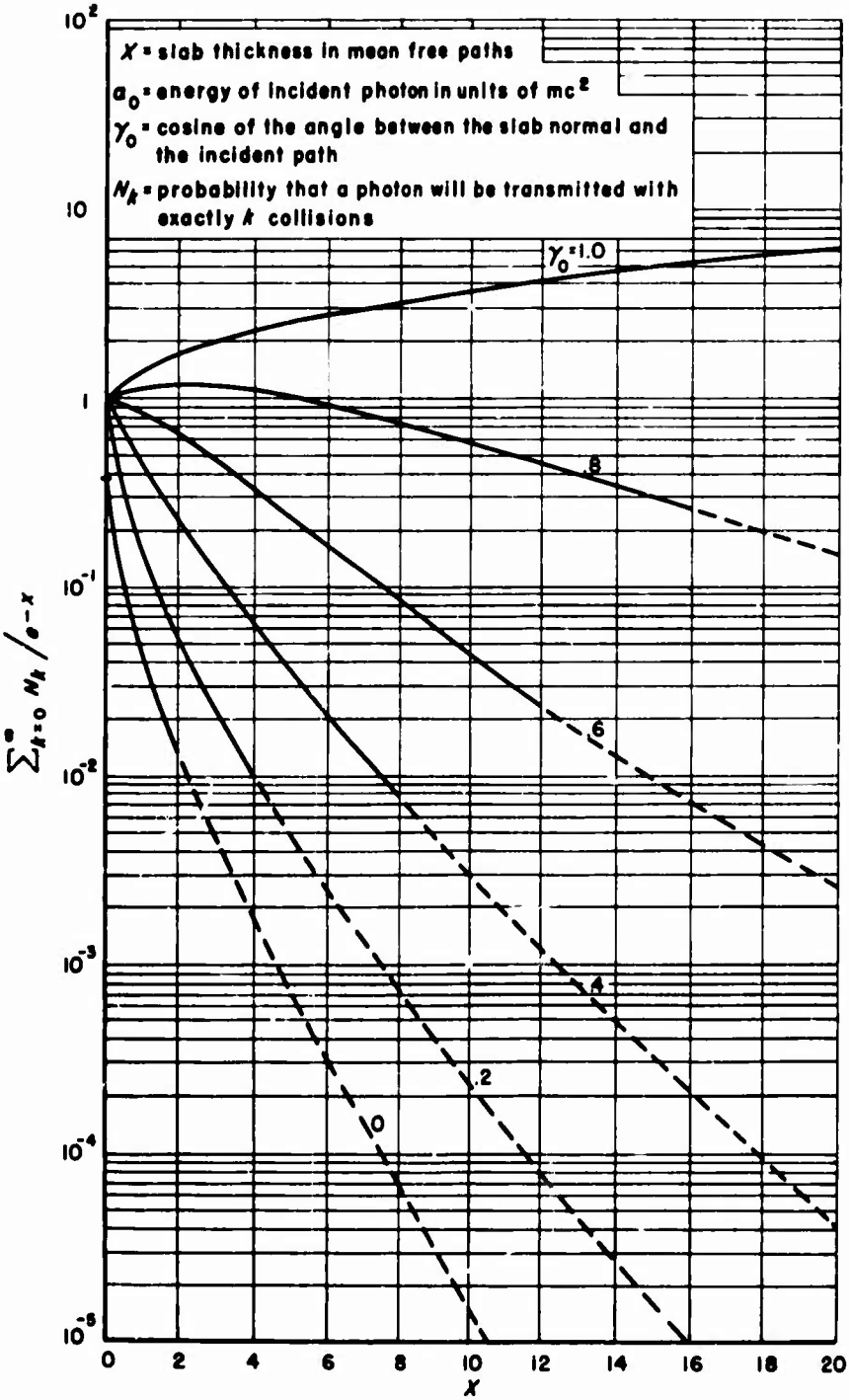

Fig. 3*d*—Number build-up factors for lead slabs, $\alpha_0 = 2.5$

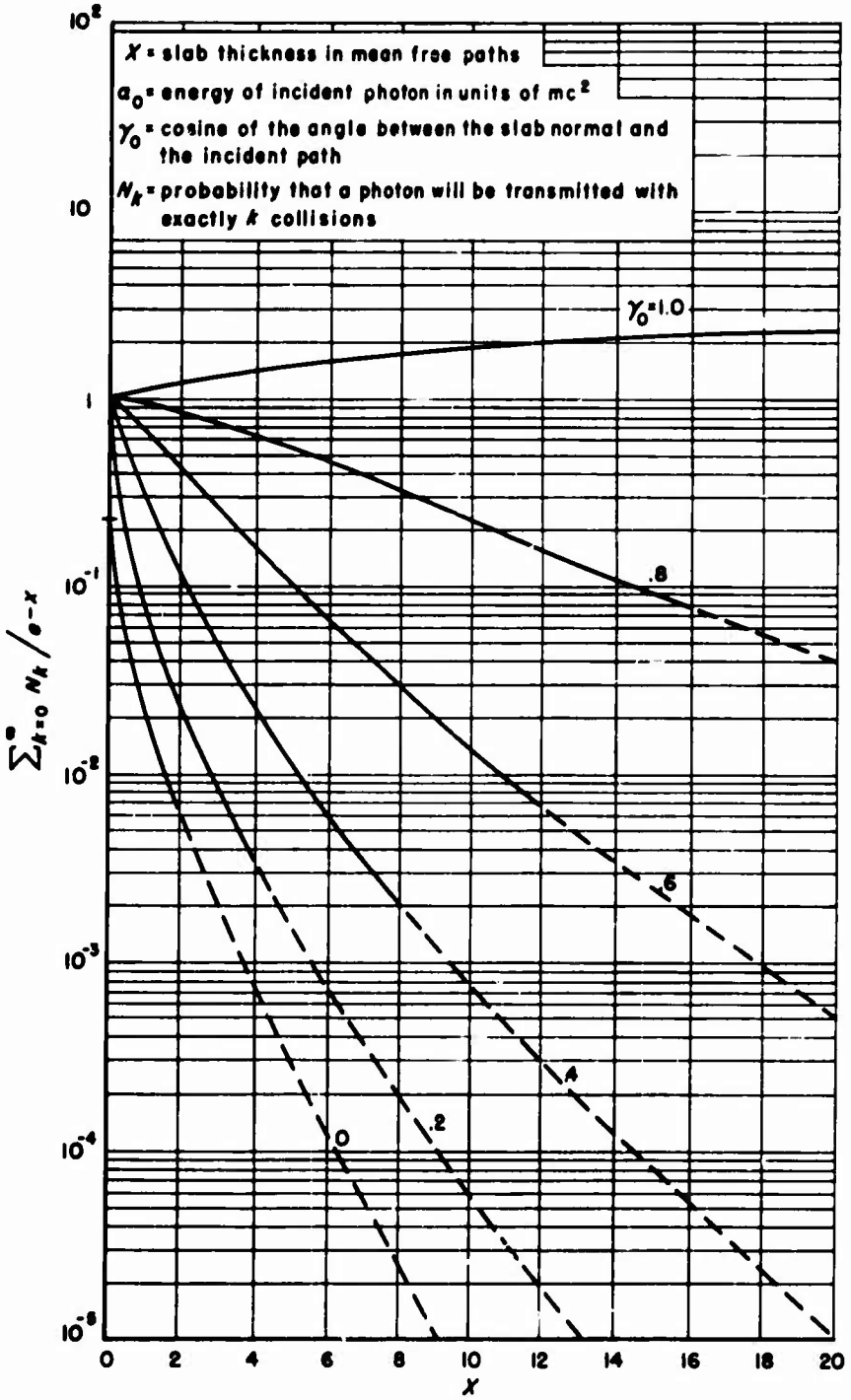

Fig. 3e—Number build-up factors for lead slabs, $\alpha_0 = 1$

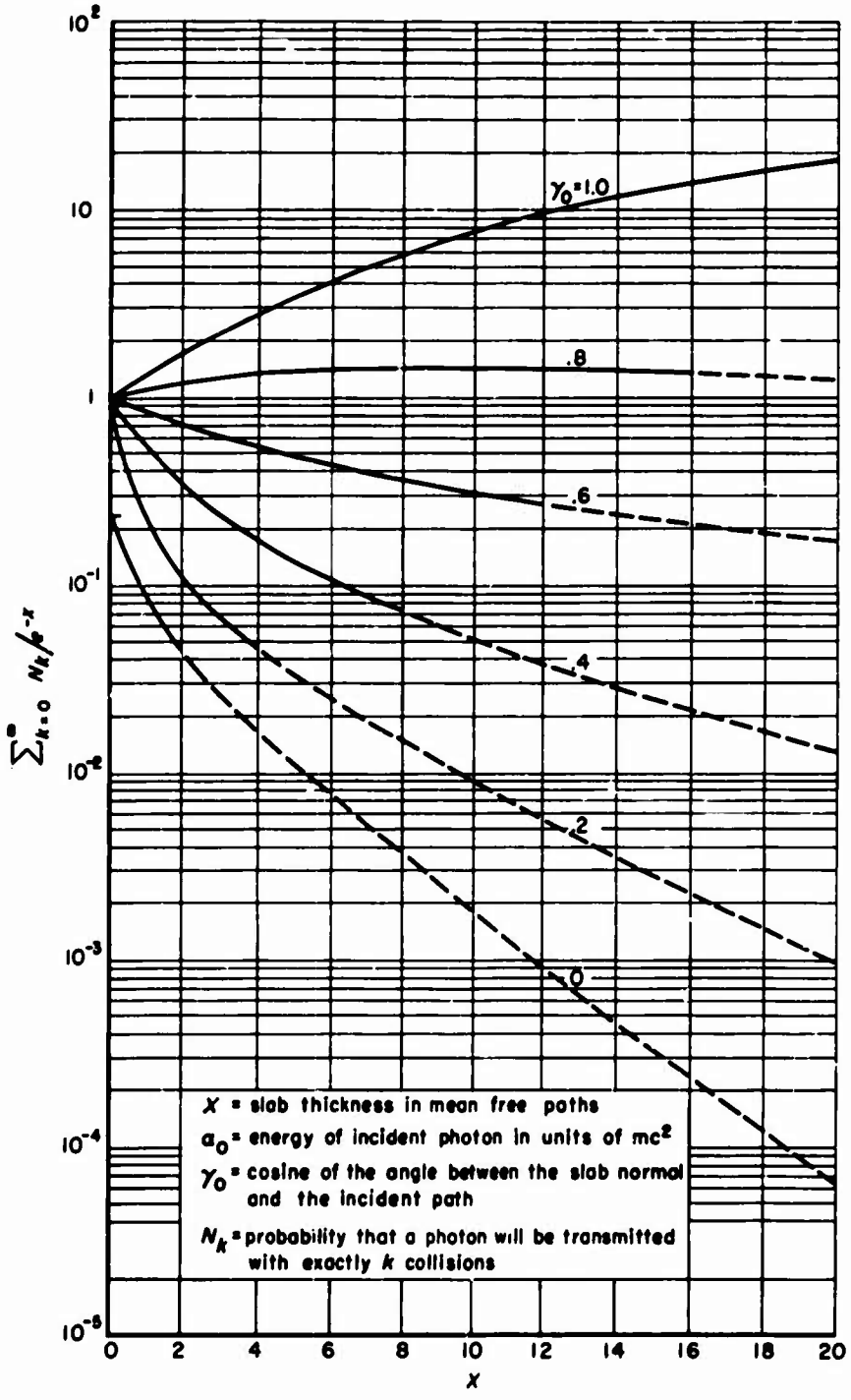

Fig. 4a—Number build-up factors for iron slabs, $\alpha_0 = 20$

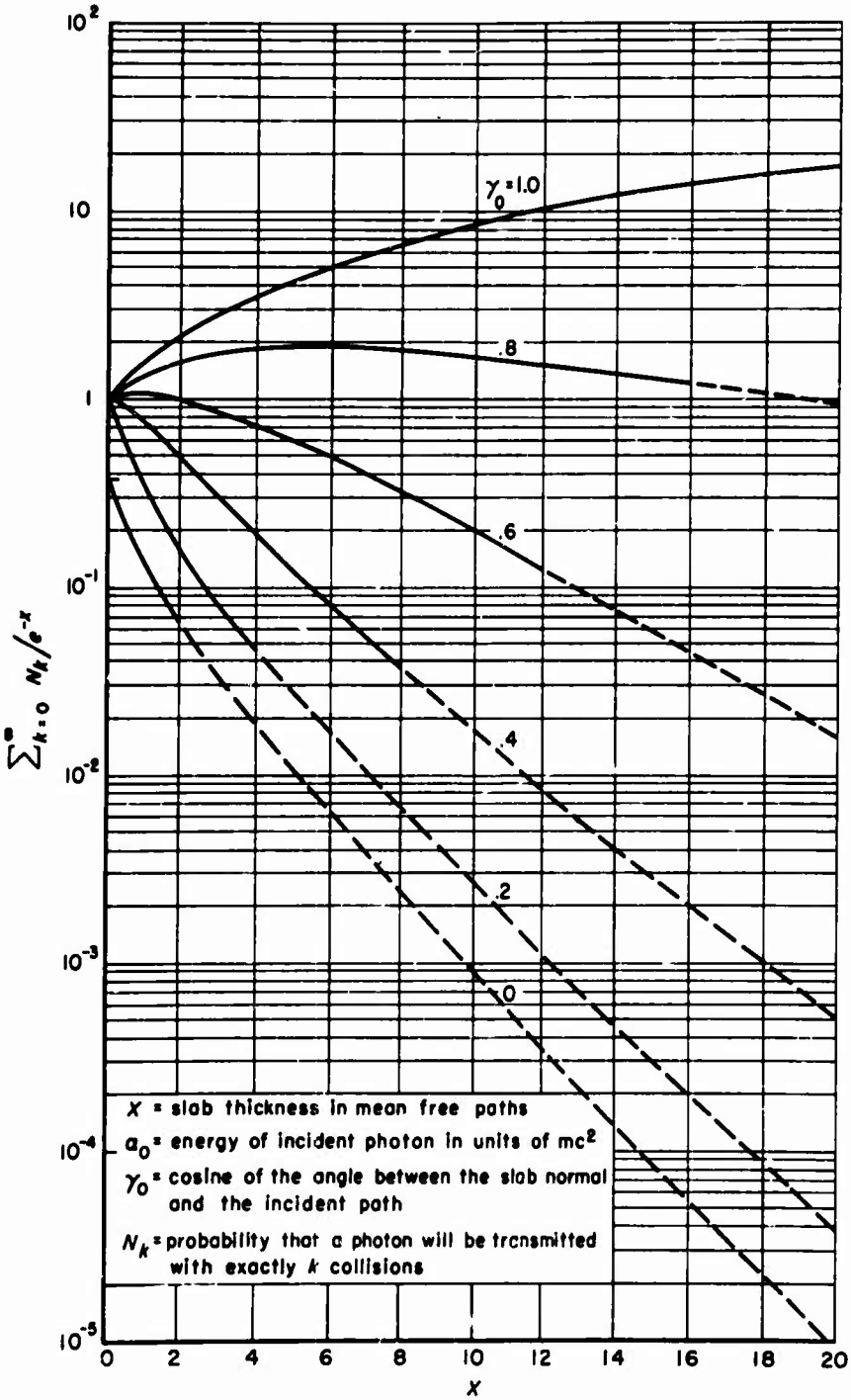

Fig. 4b—Number build-up factors for iron slabs, $\alpha_0 = 10$

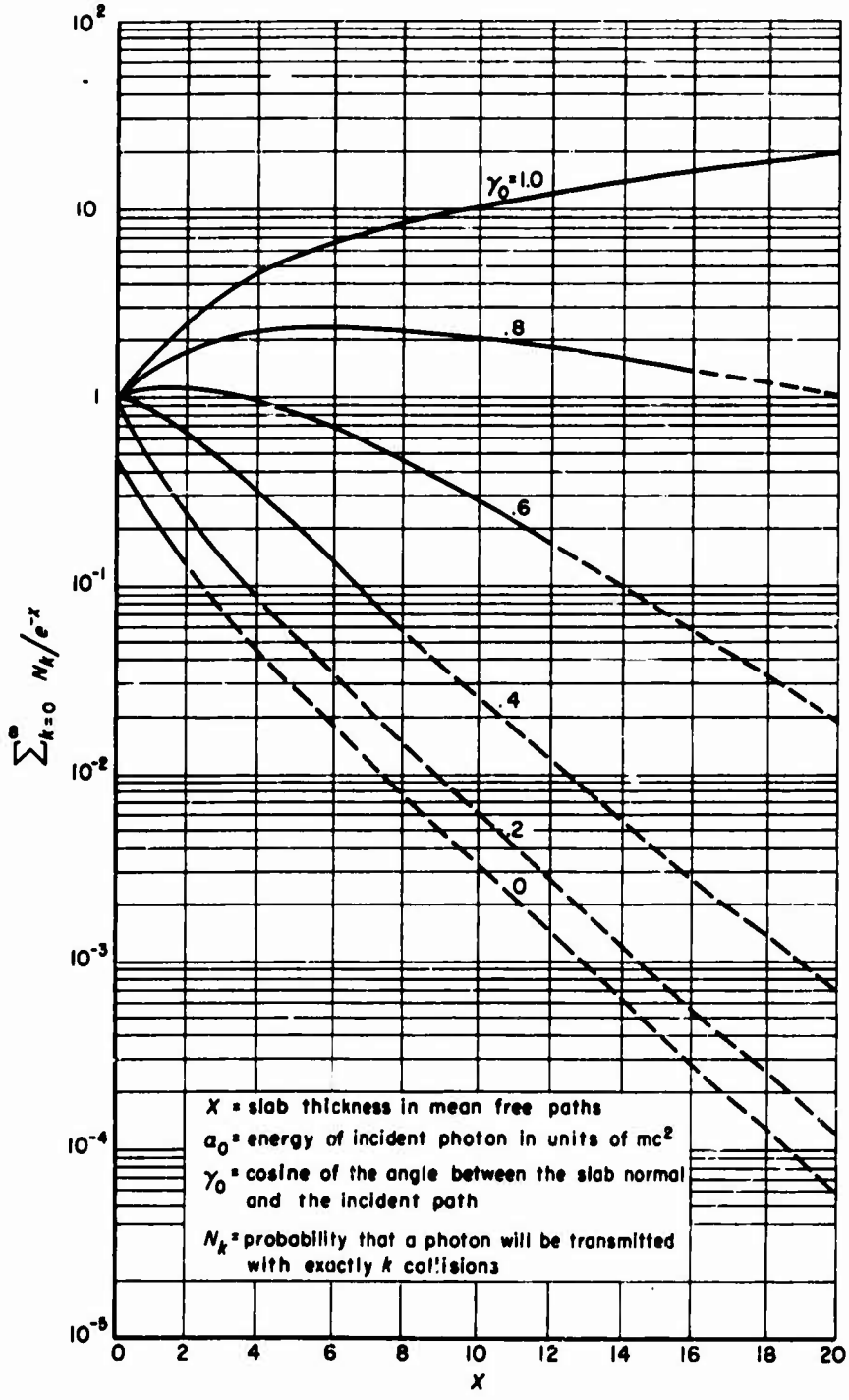

Fig. 4c—Number build-up factors for iron slabs, $\alpha_0 = 5$

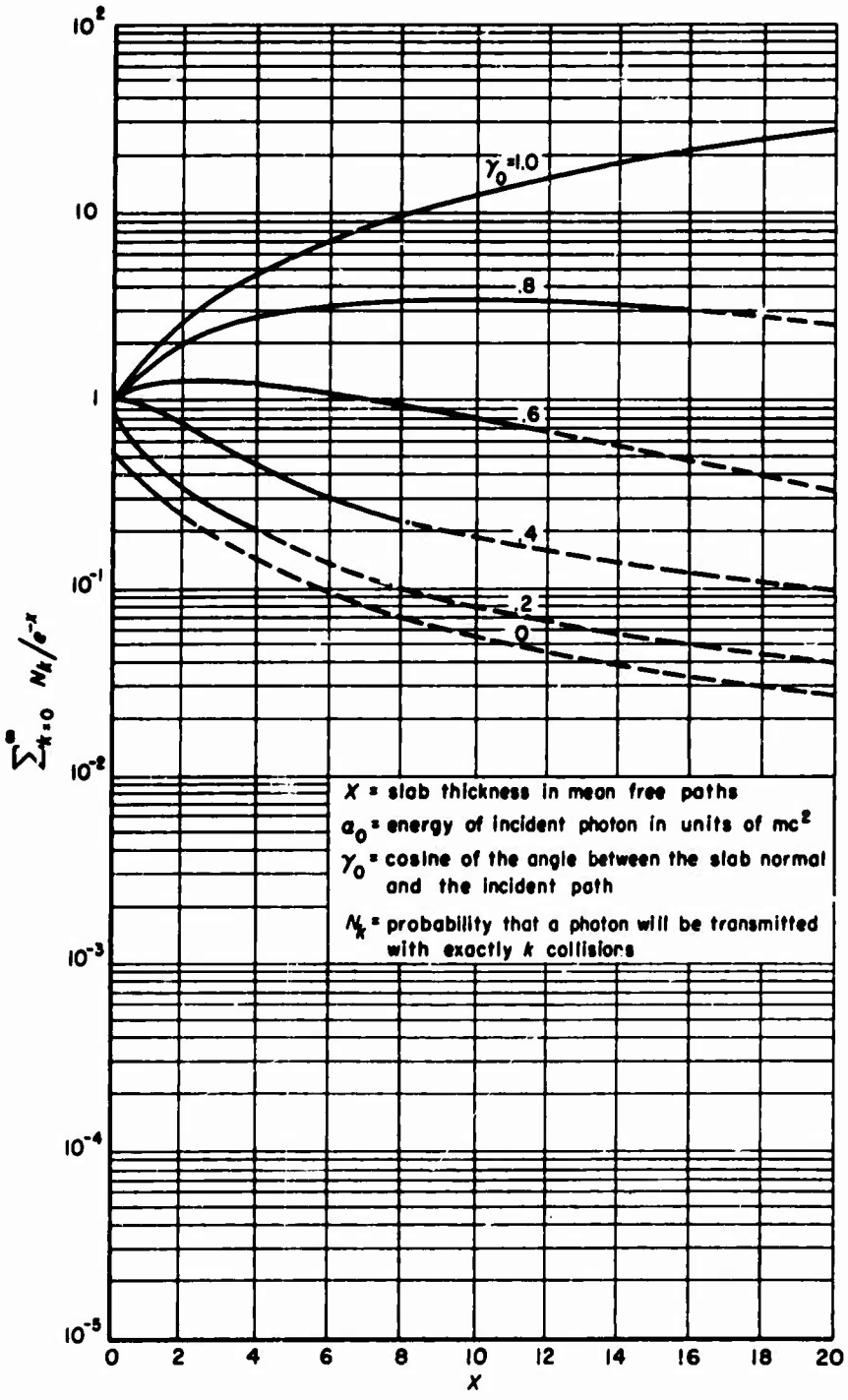

Fig. 4*d*—Number build-up factors for iron slabs, $\alpha_0 = 2.5$

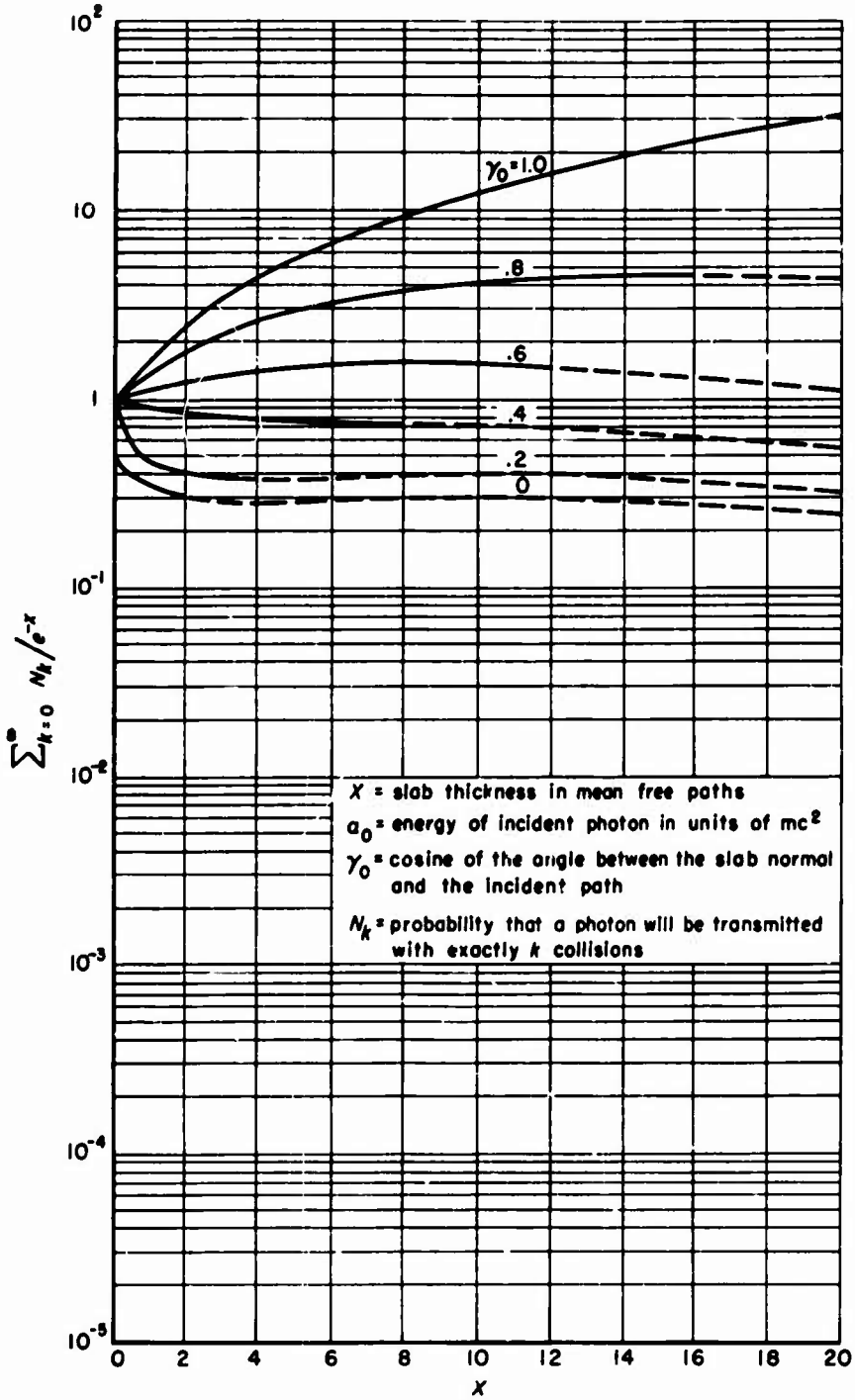

Fig. 4e—Number build-up factors for iron slabs, $\alpha_0 = 1$

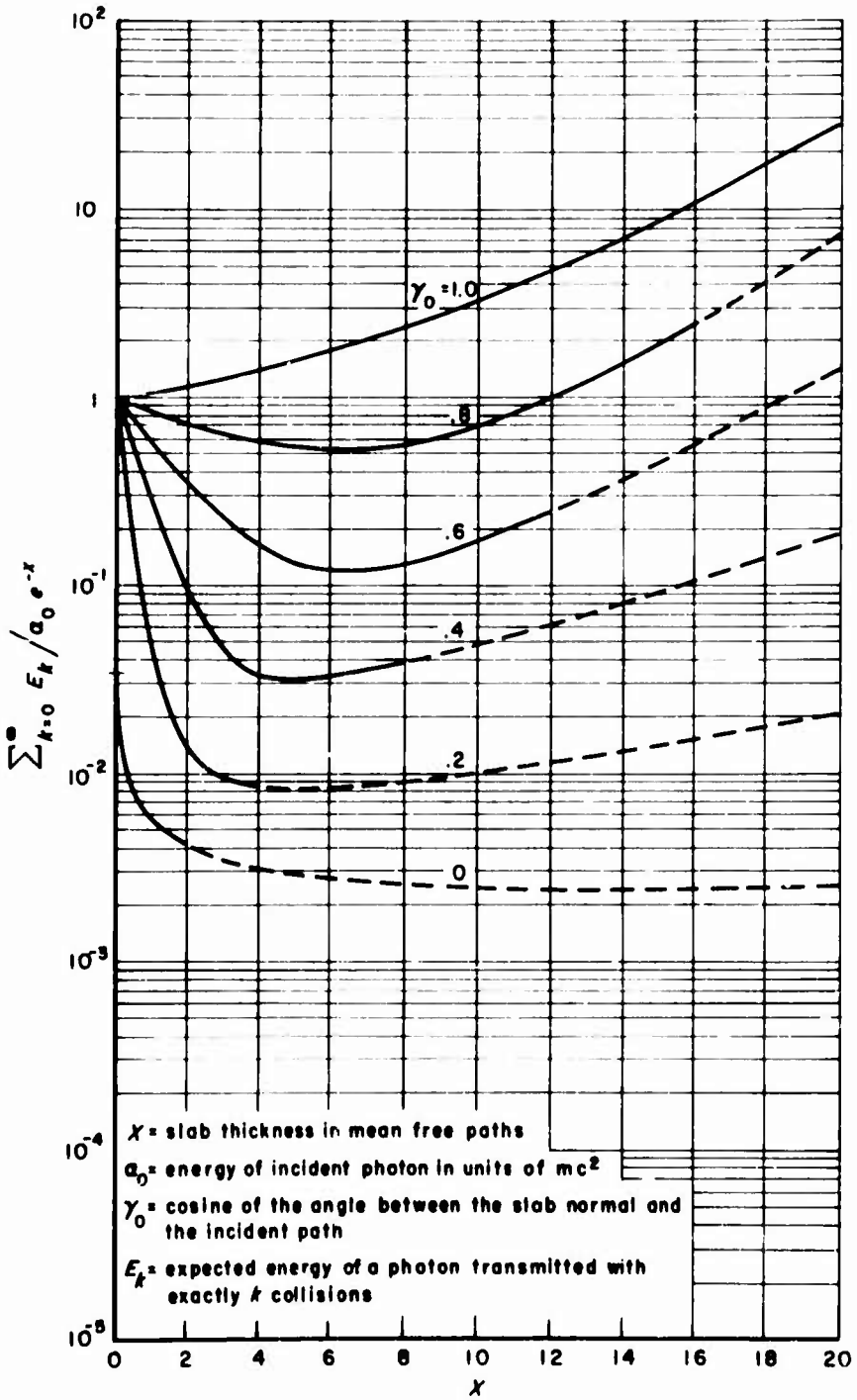

Fig. 5a—Energy build-up factors for lead slabs, $\alpha_0 = 20$

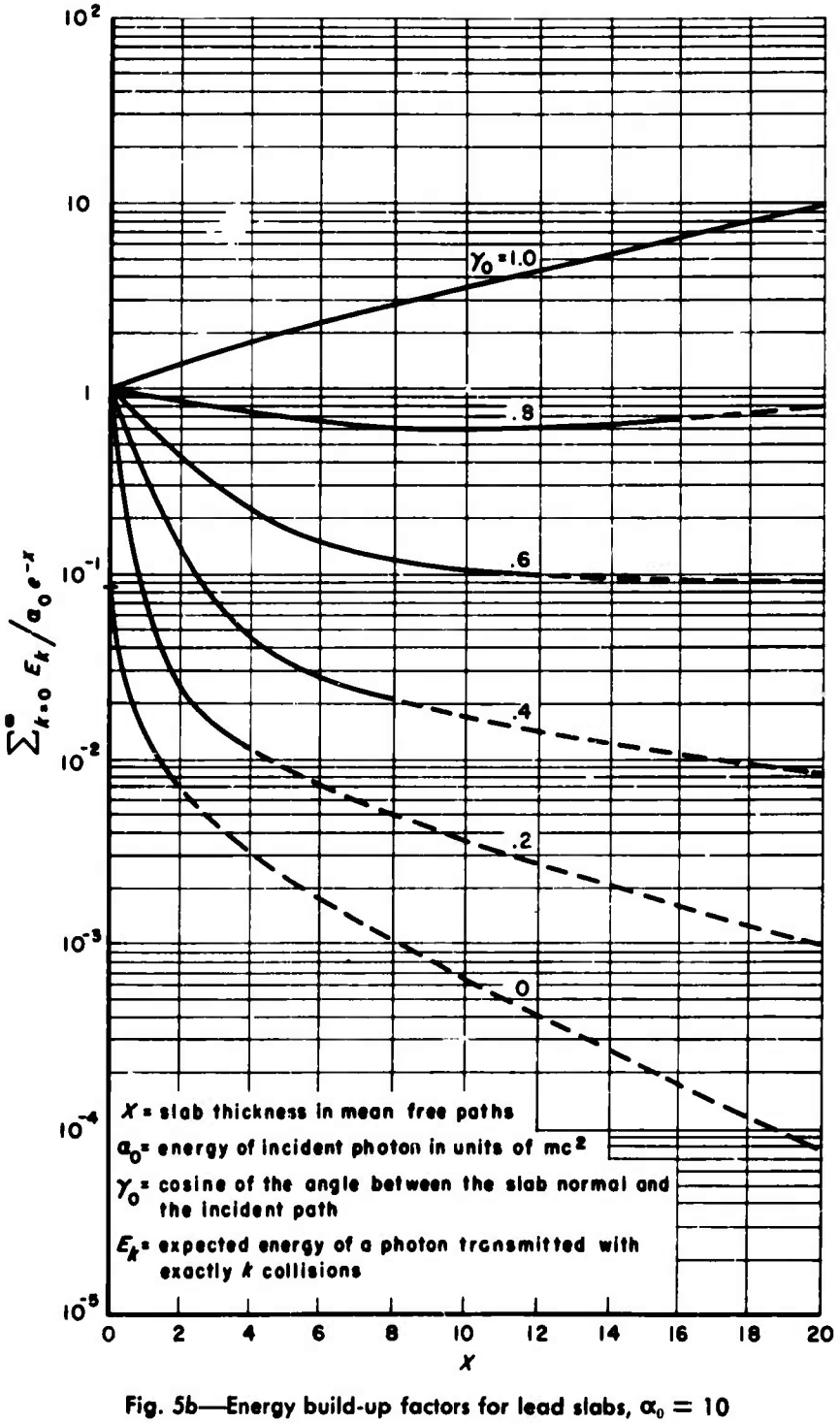

Fig. 5b—Energy build-up factors for lead slabs, $\alpha_0 = 10$

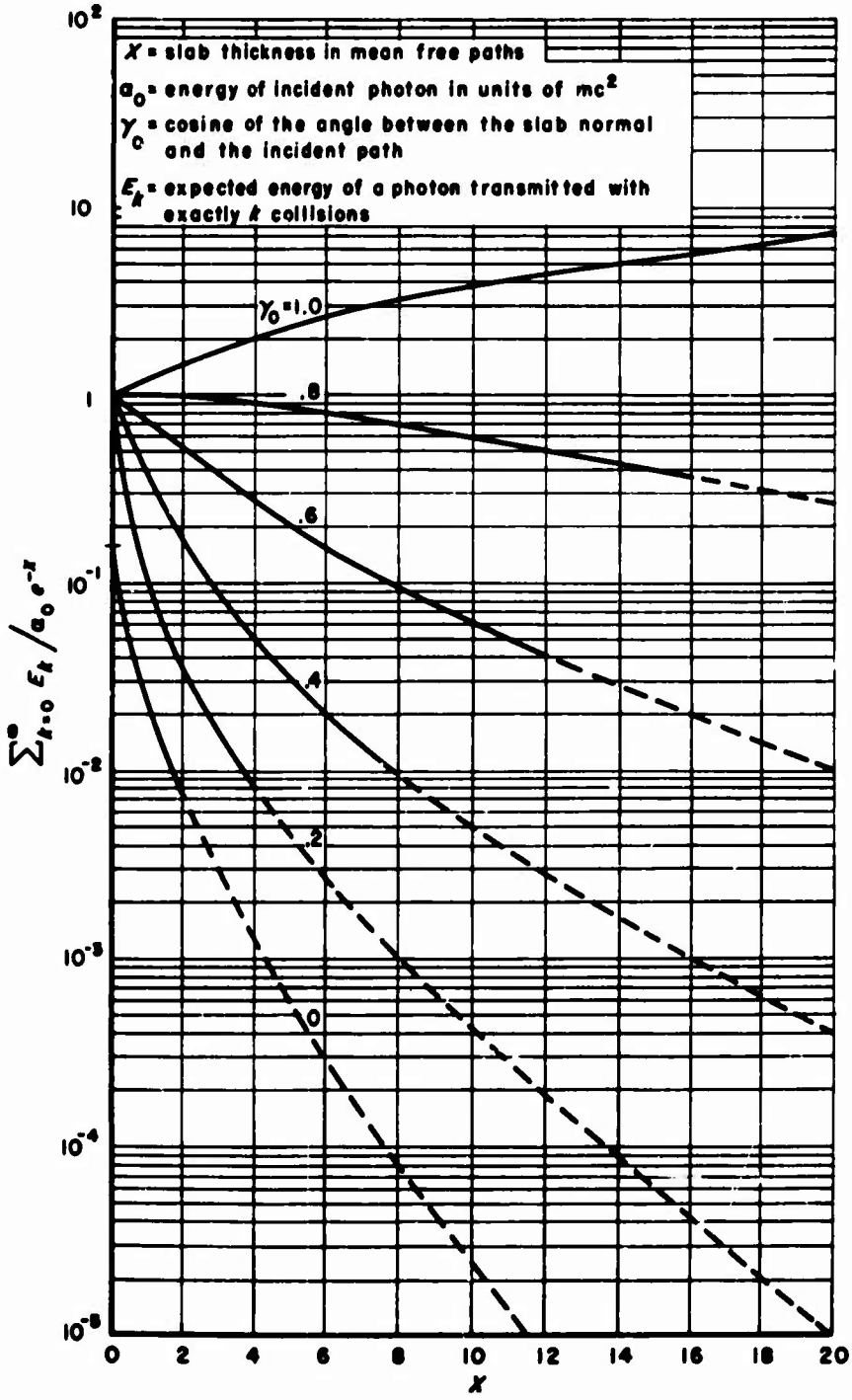

Fig. 5c—Energy build-up factors for lead slabs, $\alpha_0 = 5$

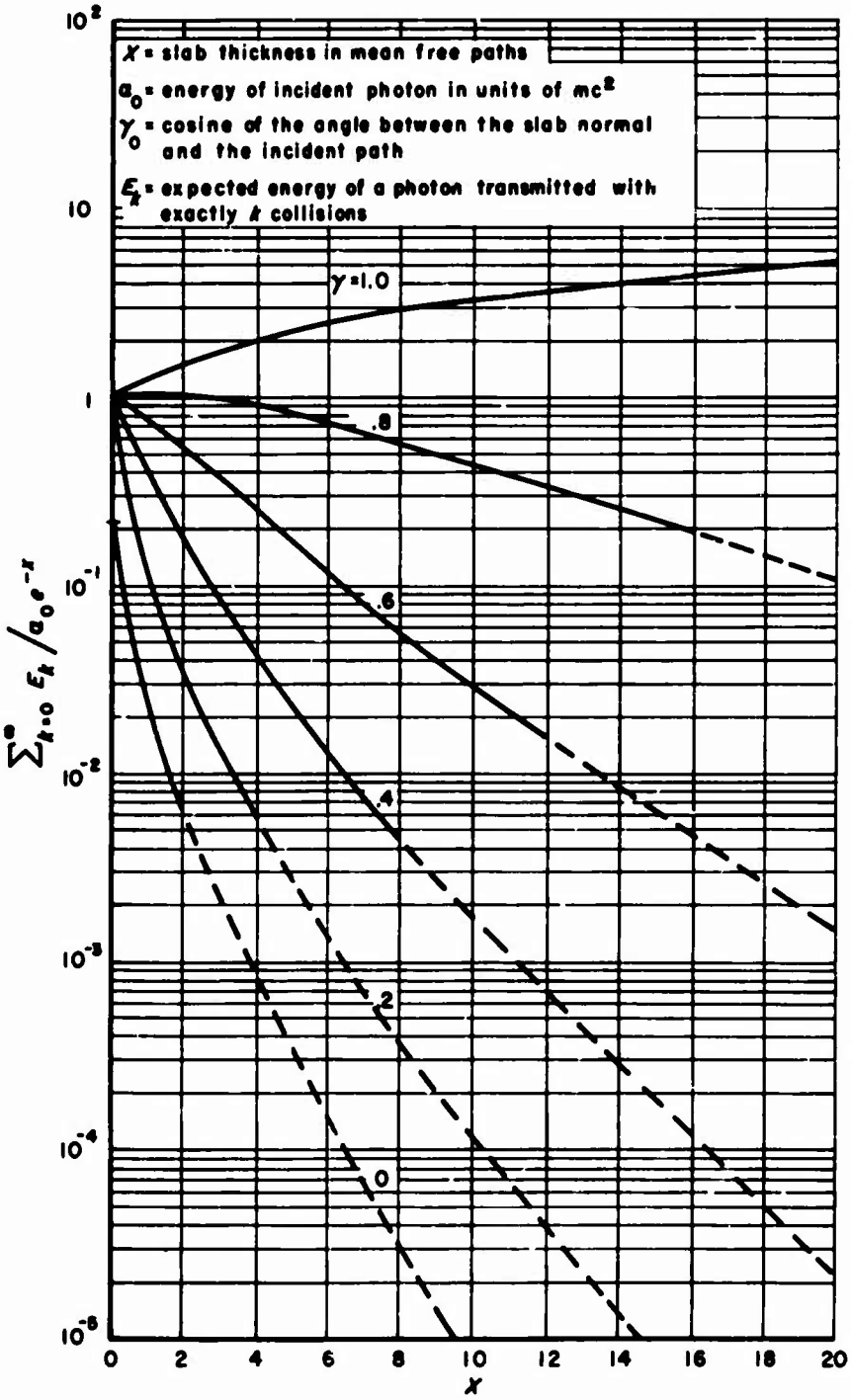

Fig. 5d—Energy build-up factors for lead slabs, $\alpha_0 = 2.5$

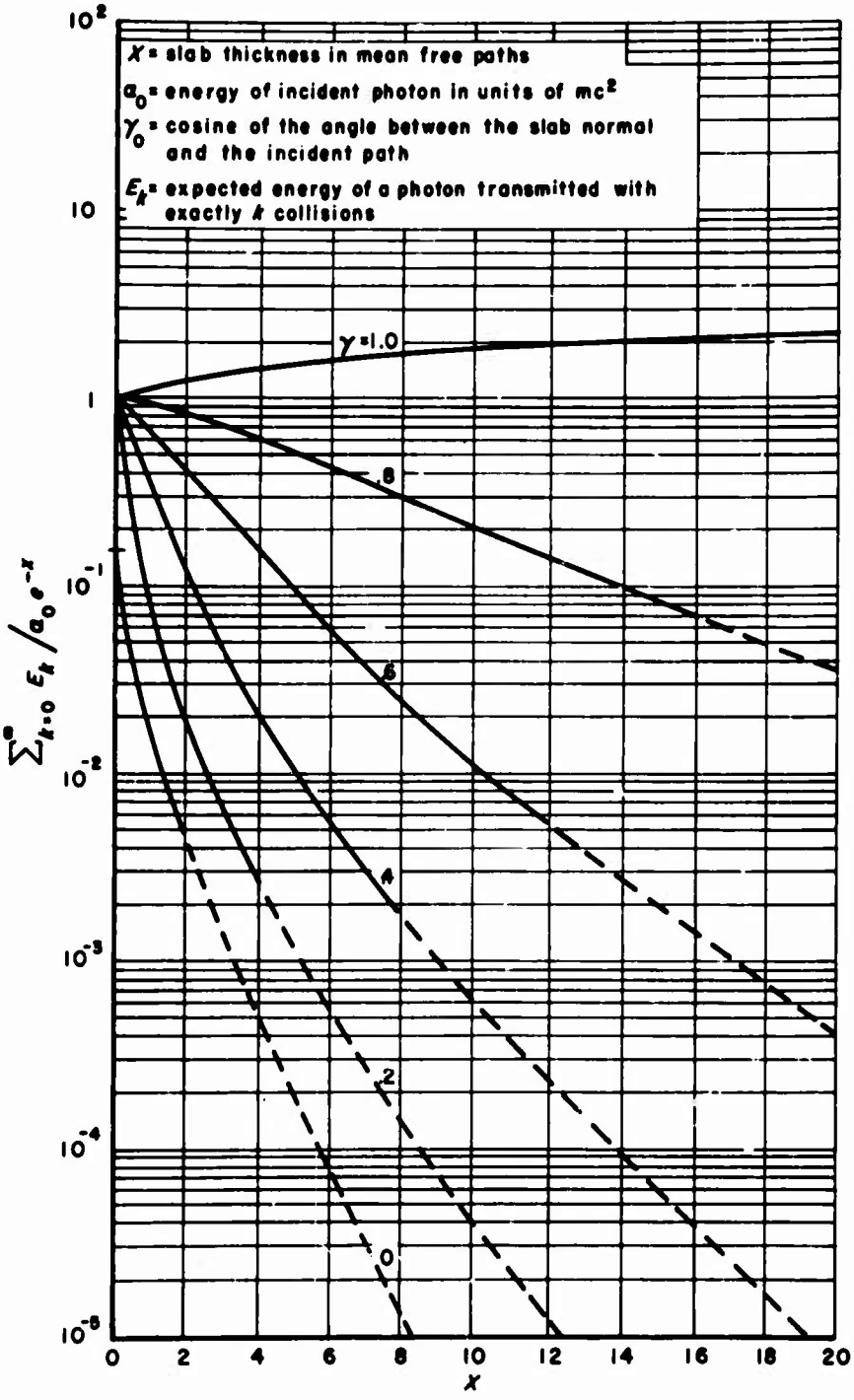

Fig. 5e—Energy build-up factors for lead slabs, $\alpha_0 = 1$

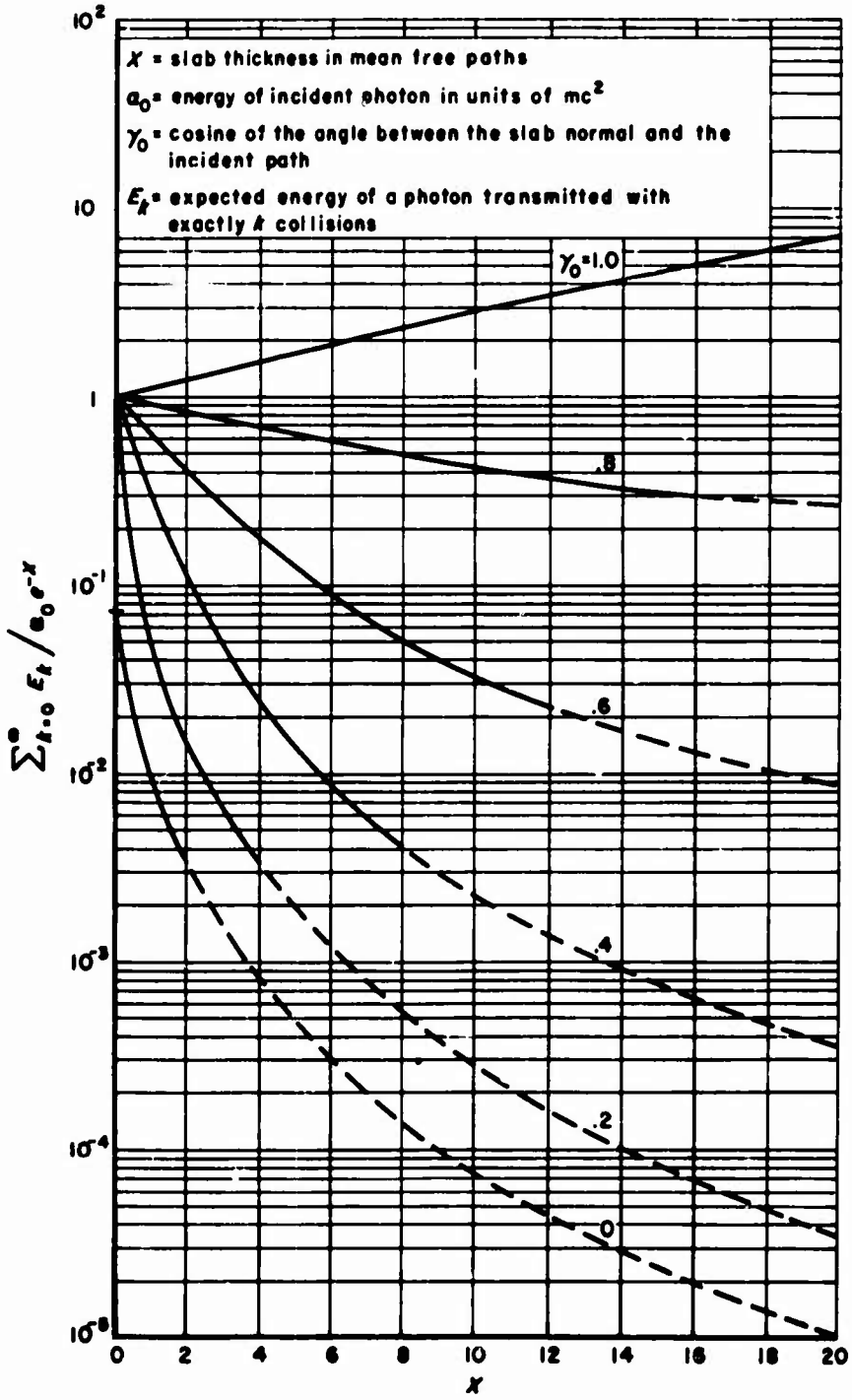

Fig. 6a—Energy build-up factors for iron slabs, $\alpha_0 = 20$

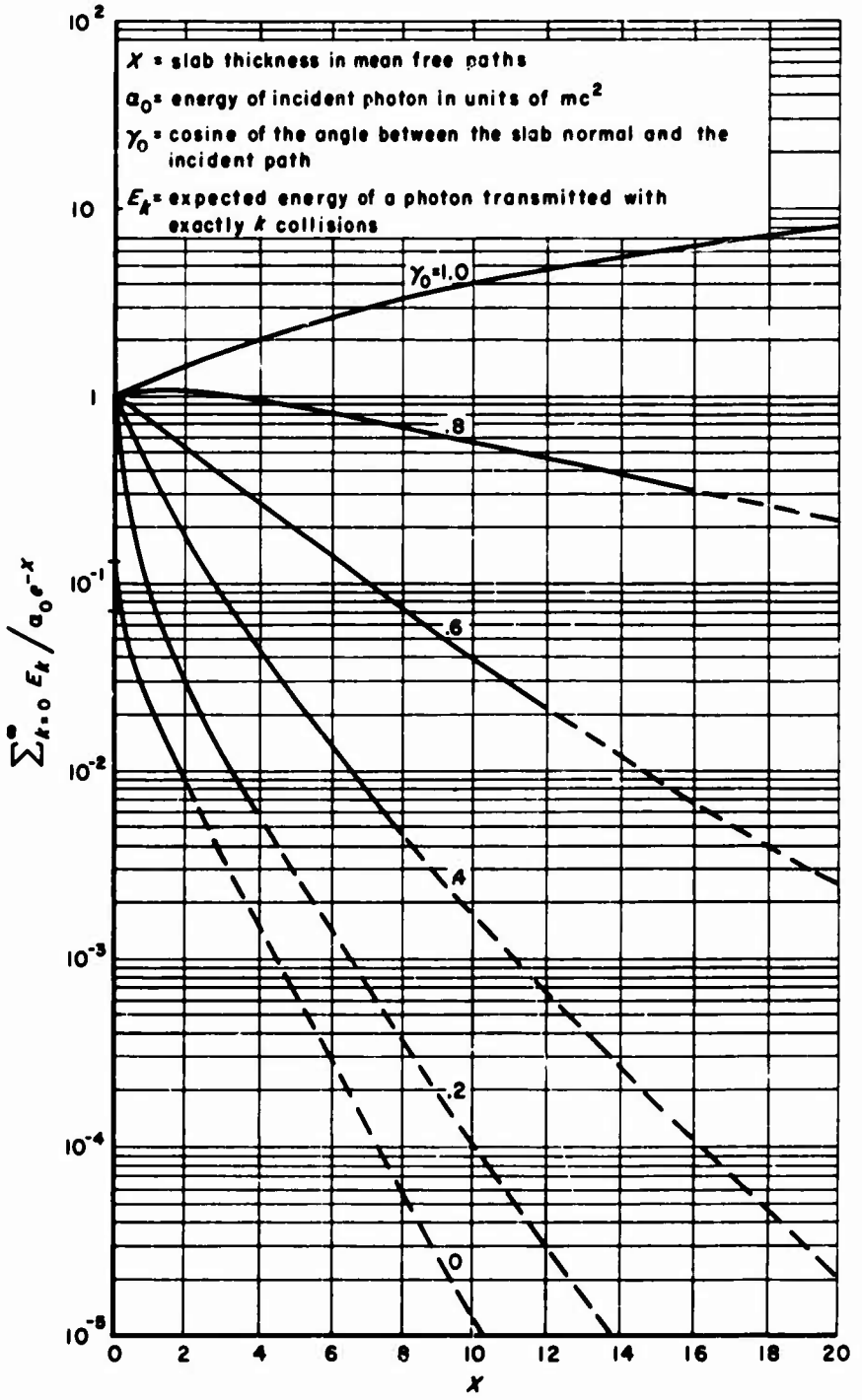

Fig. 6b—Energy build-up factors for iron slabs, $\alpha_0 = 10$

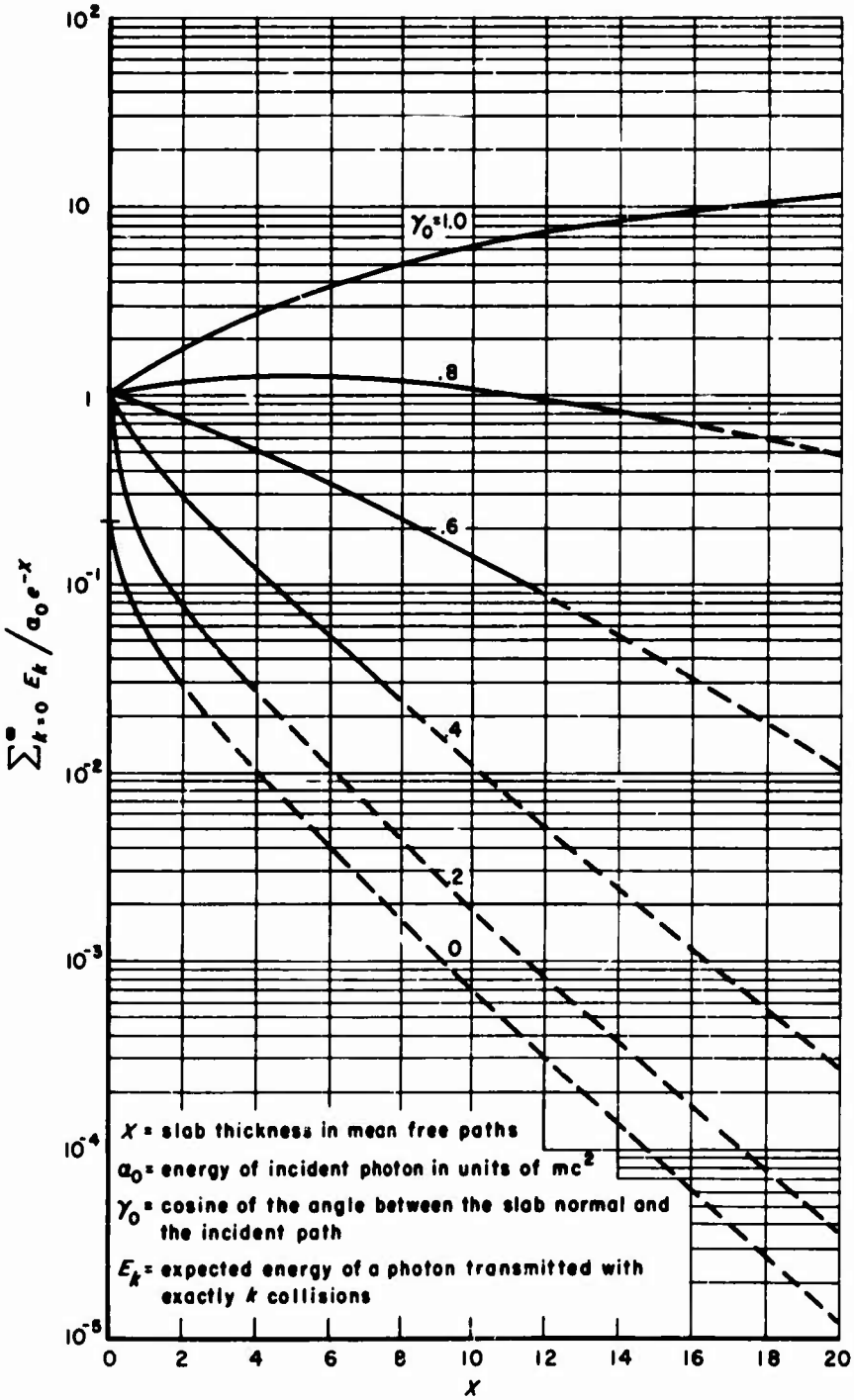

Fig. 6c—Energy build-up factors for iron slabs, $\alpha_0 = 5$

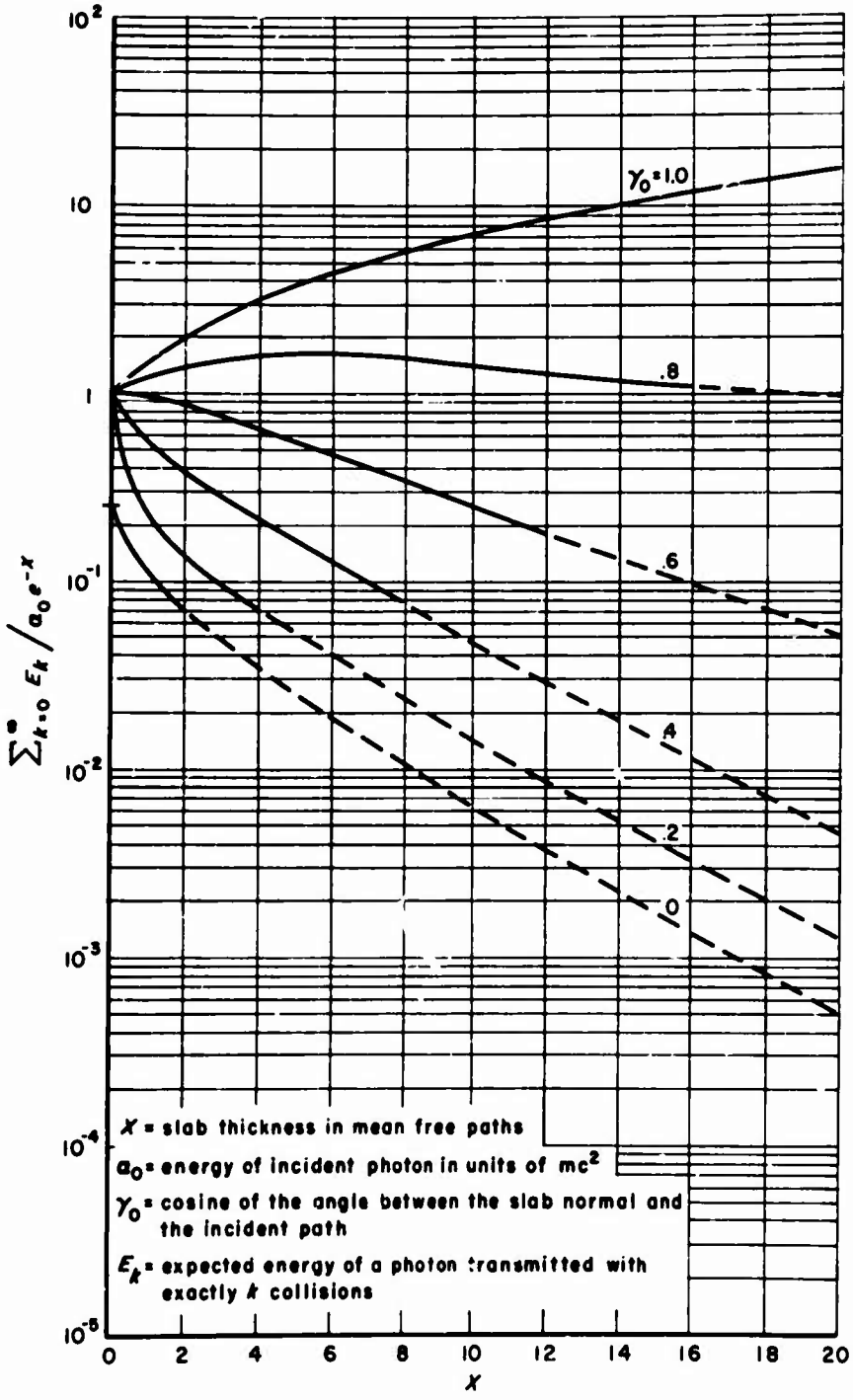

Fig. 6d—Energy build-up factors for iron slabs, $\alpha_0 = 2.5$

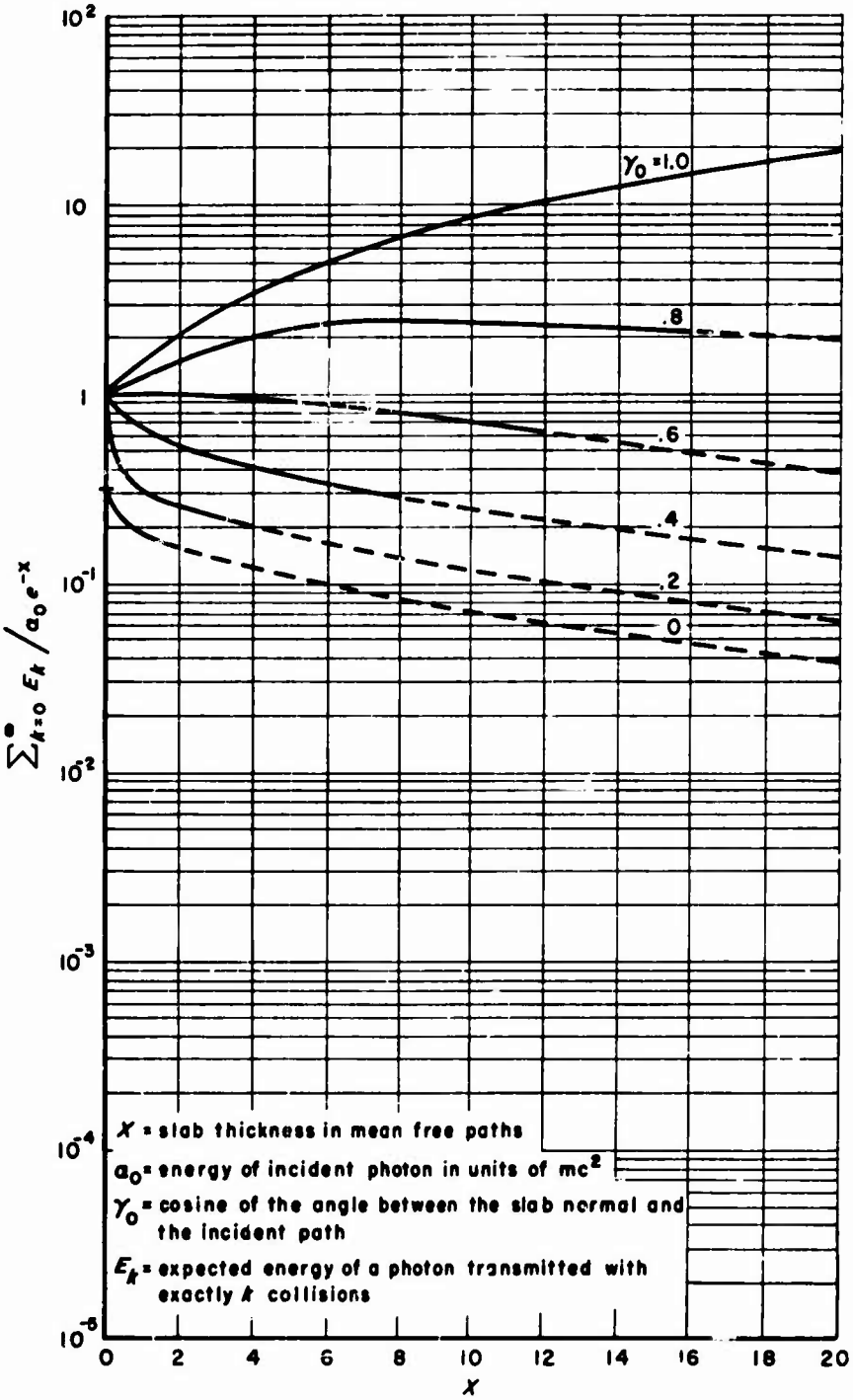

Fig. 6e—Energy build-up factors for iron slabs, $\alpha_0 = 1$

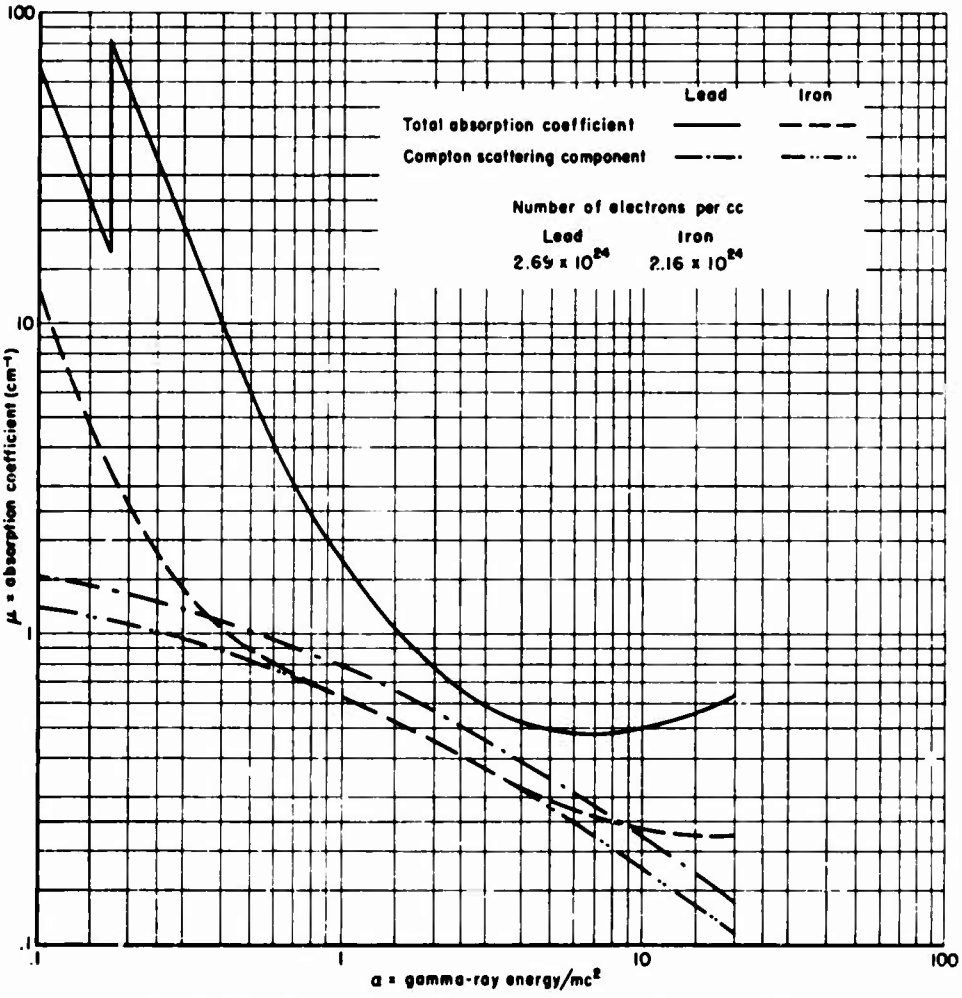

Fig. 7—The absorption coefficients for lead and iron used in the calculations of this report

III. TRANSMISSION OF PHOTONS OF 10 mc^2 AND 20 mc^2 THROUGH A SUCCESSION OF THIN SLABS OF LEAD AND OF IRON

Lengthy, intricate calculations, in the best of circumstances, tend to turn up with errors larger than are supposed possible. The reader without first-hand knowledge of the reliability of the procedures used to obtain the results given in Sec. II will no doubt welcome supporting calculations. A method which considers the transmission through thick slabs as a succession of transmissions through thin slabs seemed suitable for this purpose. Since this method and the one of the foregoing section are considerably different and therefore do not yield exactly the same information, it will be found that the preceding results have been extended as well as supported.

Description of Method

A matrix is constructed which transforms a frequency distribution incident on a thin slab into the distribution transmitted through the slab.[6] The incident and emergent distributions are functions respectively of the incident and emergent angles and energies and are represented by a grid of discrete values. In essence, the transformation matrix is the sum of three matrices which, if applied individually to the incident distribution, yield the emergent distribution for the unscattered, once-scattered, and twice-scattered photons. The slab is taken thin enough to make the contribution of photons scattered three or more times negligible; all photons scattered backwards by any collision are ignored. The thick slab is supposedly divided into a number of thin elemental slabs, and the distribution incident on the thick slab is transformed by the matrix into the distribution emerging from the first elemental slab. This emergent distribution, considered as incident on the second elemental slab, is transformed again, and so on, until the distribution emerging from the thick slab (i.e., the last elemental slab) is found.

To obtain data for comparison with those given in Sec. II, the incident distribution on the thick slab is taken as the one corresponding to an isotropic point source from which is accepted radiation within a cone of half-angle $\cos^{-1} 0.8$; the axis of the cone is normal to the slab. The choice of distribution is motivated by several considerations which need not be discussed here.[7] The source energies are 20 and 10 mc^2, and iron and lead are the slab materials. The thickness of the elemental slab is 1 mfp. The frequency distribution of the photons emerging from each elemental slab is obtained as a function of two variables: α', the energy, and γ', the cosine of the angle with the normal to the slab.

Discussion of Results

The distributions obtained are not very manageable and, in their unprocessed state, not very informative. However, representative distributions for several thicknesses are shown graphically in Figs. 8*a* through 8*g*. The source energy is 10 mc² and the material of the slab is lead. The incident distribution is a δ-function in α and it is a constant ($\neq 0$) in γ on the interval $0.8 \leq \gamma \leq 1$, zero elsewhere. The unscattered transmitted photons, therefore, have a distribution which is a δ-function in α' and which has a discontinuity at $\gamma' = 0.8$. These unscattered distributions are shown as functions of γ'. The percentage of the total transmission in unscattered transmission is given with each curve.

The distribution of scattered photons is represented by sections for fixed values of α'. The finite discontinuity in the incident distribution at $\gamma = 0.8$ shows its effect in a discontinuity in the section for $\alpha' = \alpha_0 = 10$ at $\gamma' = 0.8$, where the distribution drops to zero, and in the discontinuities in the slope of the sections for values of α' less than 10. These discontinuities appear strongly in the small thicknesses, and they disappear in the large thicknesses because their origin is in the once-scattered photons. The scattering laws for photons are such that a photon cannot pass with one collision from one energy and direction to any other arbitrarily chosen energy and direction. The distribution at, say, $\alpha' = 8$, $\gamma' = 1$ draws all its once-scattered photons from the interval $0.8 \leq \gamma \leq 1$, but the value at $\alpha' = 8$, $\gamma' = 0.6$ draws none from this interval. As γ' decreases from 1 to 0.6, there is a point at which photons would begin to be received from outside the interval $0.8 \leq \gamma \leq 1$, were there any photons there, and there is another point at which, for the first time, no photons can be received from the interval. At these points ($\gamma' = .913$ and $\gamma' = .647$) there are, understandably, discontinuities—in fact, discontinuities of infinite jump—in the slope of the sections. These discontinuities exist in every section above the lower limit of α' for one collision. Other discontinuities exist in the higher derivatives, but they are not discernible in the figures.

More informative than the distributions over α' and γ' are the marginal distributions over α'. Four quantities are of interest as functions of α': (1) the number of photons transmitted, (2) the energy transmitted, (3) the density of the photons at the rear face, and (4) the energy density at the rear face. In the case of the first two quantities, one can think of the transmission through the slab as originating either from an isotropic point source from which gamma rays are accepted in a cone of half-angle $\cos^{-1} 0.8$ or from a plane of such sources; but in the case of the last two quantities, one must suppose only a plane of sources.

The four quantities named are shown in Figs. 9*a* through 12*d* for several thicknesses of lead and of iron with source energies of 20 and 10 mc². Each of the quantities is given the same treatment. Since the unscattered photons all emerge with their incident energy, only the scattered photons give functions of α'. These functions are normalized for each thickness by dividing by the sum over all energies and over the scattered and unscattered photons. The result for each of the four quantities is a family of curves with parameter X. Figures 9*a* through 12*d* give the number of photons transmitted, the energy transmitted, the density of the photons at the rear face, and the energy density at the rear face, respectively, in the form of the ratios $N_s(\alpha', X)/N_t(X)$, $E_s(\alpha', X)/E_t(X)$,

$n_s(\alpha', X)/n_t(X)$, and $e_s(\alpha', X)/e_t(X)$, where the meaning of the new symbols introduced is clear from the choice and from the text. The percentage figure associated with each curve gives the proportion of the total contained in the scattered photons.

Most of the comment on Figs. 9*a* through 12*d* will be incidental to later discussion. However, it might be remarked here that the curves all terminate before reaching $\alpha' = 0$, because it is not feasible to make calculations down into the neighborhood of zero energy by the thin-slab method. The totals used for normalizing are from the curves as shown, without benefit of any correction. The dashed curves diverging from the solid curves in Figs. 9*c*, 9*d*, 11*c*, and 11*d* denote defects which will be discussed shortly.

The normalizing factors, or rather their reciprocals, $N_t(X)$, $E_t(X)$, $n_t(X)$, and $e_t(X)$, have the greatest interest, since they may be considered as the main goal of the calculations. These factors are shown as functions of X in Figs. 13 through 16 and are themselves normalized by the factors $1/N_i e^{-X}$, $1/E_i e^{-X}$, $c/N'_i e^{-X}$, and $c/E'_i e^{-X}$, where N_i is the number of photons, from a single point source, incident on the first elemental slab, E_i is the corresponding incident energy, c is the velocity of light, N'_i is the number of photons, from a plane of sources, incident per unit area per unit time, and E'_i is the incident energy corresponding to N'_i. Comments on these figures are confined here to the statement that the significance of the circled points in Figs. 13 and 14 will be made clear later.

Inherent Errors

Since the thin-slab method is used to provide something in the way of a check on the results obtained by summing the individual scatterings, it is well to leave as little question with regard to the accuracy of the thin-slab results as possible. The three weaknesses of the thin-slab method are (1) neglect of three or more scatterings; (2) neglect of backward scattering, both within the elemental slab and from one elemental slab to another; and (3) the presence of ample opportunity for accumulated error in the twenty iterative operations between 1 and 20 mfp.

The error due to the neglect of everything beyond the twice-scattered transmission can be assessed by examining Figs. 17*a* through 17*d*. These figures show, as a function of the photon energy, the component frequency distributions for the photons scattered by the eleventh slab. The distributions for the photons previously scattered, but unscattered by the eleventh slab, are labeled with the numeral 0. The distributions of the photons scattered once and scattered twice by the eleventh slab are respectively marked with the numerals 1 and 2, and estimates of the contributions of the third, fourth, etc., scatterings are marked with the numerals 3, 4, etc. The curves labeled with the letter *s* are the sums of the 0-, 1-, and 2-curves and are members ($X = 11$) of the families of Figs. 9*a* through 9*d*. The dashed curves diverging from the *s*-curves are estimates of the transmission from all scatterings, i.e., the sum of the curves 0, 1, 2, 3, etc.

In the case of lead, the divergences of the dashed curves from the *s*-curves are small. Since the analysis of the transmission through the eleventh elemental slab was found to be typical of the others, a thickness of 1 mfp seems sufficiently thin for the elemental slab.

In the case of iron, the neglect of the third and higher scatterings is clearly not so trivial. Even so, the damage may not be too great. In the middle energy range the divergence of the partial sums (represented by the s-curves) from the limiting sums (indicated roughly by the dashed curves) is undoubtedly large, but photoelectric absorption must bring both sums quickly to zero in the low energy range. The defection of the partial sums in the middle energy range, though large, cannot compound at an enormous rate because the middle range receives most of its photons from the high range, where, since three or more scatterings contribute negligibly, the distributions are accurate. It seems unlikely, therefore, that the total transmission of photons as calculated from the solid curves for iron is deficient by more than 10 to 30 per cent.

The error in the energy transmitted should be even smaller, not more than a few per cent at most. Figures 18*a* and 18*b*, which give the component energy distributions for iron, show this clearly.

The defect noted earlier, and indicated in Figs. 9*c*, 9*d*, 11*c*, and 11*d* by dashed curves, is the one just considered. Although the dashed curves are intended only to warn of the presence of error in the solid curves, they are certainly more nearly correct than the solid curves, and may therefore be considered as partial estimates of the true distributions. Since transmission is calculated on the basis of the solid curves, the percentage of the total in scattered photons given for each thickness is low, but perhaps not so low as one might think. One cannot, for instance, use this known error to explain why Figs. 9*a* through 9*d* show the percentage of scattered transmission to be greater for iron than for lead at 1 mfp but to be less at 20 mfp. That iron should transmit a greater percentage of scattered photons through a slab of 1-mfp thickness is to be expected, since the total absorption coefficients (Fig. 7) show that a photon has a greater probability of surviving a collision in iron than in lead. But the failure of iron to maintain the larger percentage as X increases is not conveniently explained by the neglect of three or more scatterings in the low energies. For to bring the percentage for iron up to that for lead at 20 mfp would require an error in the scattered transmission of over 1000 per cent for a source energy of 20 mc^2 and 59 per cent for a source energy of 10 mc^2. Not only is the minimum increase in the case of 20 mc^2 impossibly large, but there is also no reason why the increase should need to be so much larger for 20 mc^2 than for 10 mc^2.

The true explanation lies in the fact that the absorption coefficient for lead falls to a pronounced minimum as α decreases from 10 or 20, whereas the coefficient for iron is almost at a minimum at 20. The length of 1 mfp for the first collision, therefore, is smaller than the average for subsequent collisions in the case of iron and larger than the average, or tending to be larger, in the case of lead. The comparison on the basis of mean free paths for the first collision amounts to considering thicknesses of lead and iron which are not fundamentally equivalent. For large thicknesses, the inequality offsets the greater probability of photon survival in iron to such an extent that lead has the greater percentage of transmission in scattered photons. Another manifestation of this phenomenon is seen in Fig. 19, which gives a plot of the average energy versus X for all cases. The fact that the average energy for iron crosses that for lead for both 10 and 20 mc^2 is readily understood in the light of the preceding remarks. An explanation of the compara-

tive behavior of the build-up factors for iron and for lead in the monoangular cases of 10 and 20 mc² (Figs. 3*a*, 3*b*, 4*a*, and 4*b*) would hinge on these same considerations.

The neglect of back-scatter, which is usual in gamma-ray transmission, is more conveniently discussed in the section following. This leaves the cumulative error to be considered. The discontinuities exhibited in Fig. 8*a* by the distribution for a thickness of 1 mfp lead one to expect large error in the distribution for 2 mfp, particularly when it is known that the operation with the transformation matrix is equivalent to a numerical integration. Careful examination reveals that the discontinuities do produce errors in the calculated distributions. For the second elemental slab, the discrete values are in most cases too large, have a maximum error of about 3 per cent, and when integrated, yield a total transmission in excess of the correct value by at most 1 or 2 per cent. For large thicknesses, the steep constant-energy sections, such as those shown in Fig. 8*g*, are found to give values on the small side. Since the discontinuities tend to disappear with increasing thickness, there is a schedule of errors which should not compound powerfully, and one would not expect the distributions shown in Figs. 8*a* through 12*d* to contain large accumulated errors except possibly in the case of iron, where the neglect of the third collision has been seen to have its effect.

Comparison of Results from the Two Methods

The two quantities $N_t(X)/N_i e^{-X}$ and $E_t(X)/E_i e^{-X}$ of Figs. 13 and 14 can be considered as build-up factors for the incident distribution of the thin-slab method. Both quantities can also be calculated from the build-up factors for the δ-distributions in γ shown in Figs. 3*a*, 3*b*, 4*a*, 4*b*, 5*a*, 5*b*, 6*a*, and 6*b*. The circled points in Figs. 13 and 14, which were passed over earlier, are values calculated from the build-up factors for the δ-distributions. One would expect, in view of the preceding discussion of the accuracy of thin-slab results, that the agreement would be good except for the case of the number of photons transmitted through iron. For this case, the circled points should lie above the curve, higher when $\alpha_0 = 10$ than when $\alpha_0 = 20$. If Figs. 13 and 14 are examined carefully, it will be found that within a latitude consistent with the stated error, these expectations are realized. To be sure, the points for $X = 16$ and $X = 20$ for the iron-number-20 mc² undoubtedly should be raised so as to stand in the same relation to their comparison curve as the points at $X = 4, 8, 12$; and there are other evidences of error. If in some cases, notably iron-energy-10 mc², the deviation is larger than the 1 per cent expected at $X = 1$ or the 2 per cent at $X = 2$, the explanation almost certainly lies in the accumulation of error due to the succession of graphical and numerical steps required to pass from the transmission with the zero, one, two, and three scatterings of Tables 1 through 4 to the values of the circled points. But the deviations in the two sets of results do not indicate that there is any reason to increase the magnitude of error stated as existing for the build-up factors in Figs. 3*a* through 6*e*. In fact, in the case of lead, a rule giving errors smaller by half would stand. To be sure, these comparisons do not directly support the factors for $\alpha_0 = 5, 2.5, 1$, but the same method of extrapolation was used in all cases

and, since the method is consistent and definite over all cases, the support is considered as extending with some force to the low energies.

The similarities between flux and density are so close in Figs. 9*a* through 16 that an error in one implies the existence of a like error in the others. A case in point is found in curve (*d*) of Figs. 13 and 15. The discussion above has established that curve (*d*) for $N_t(X)/N_i e^{-X}$ in Fig. 13 should be corrected upward so as to pass closer to, if not through, the circled points. If such correction is made, one of like magnitude must also be applied to curve (*d*) for $cn_t(X)N_i' e^{-X}$ in Fig. 15.

* * *

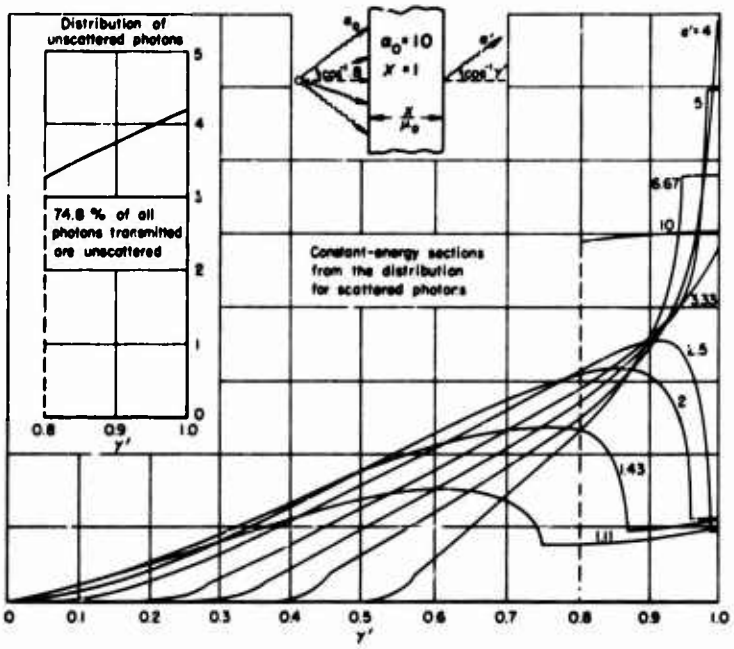

Fig. 8a—Frequency distributions for photons transmitted through lead slabs, $X = 1$

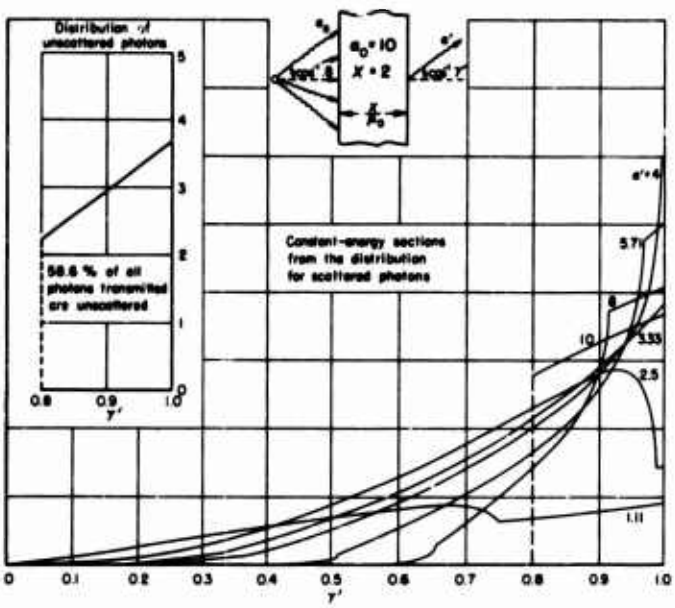

Fig. 8b—Frequency distributions for photons transmitted through lead slabs, $X = 2$

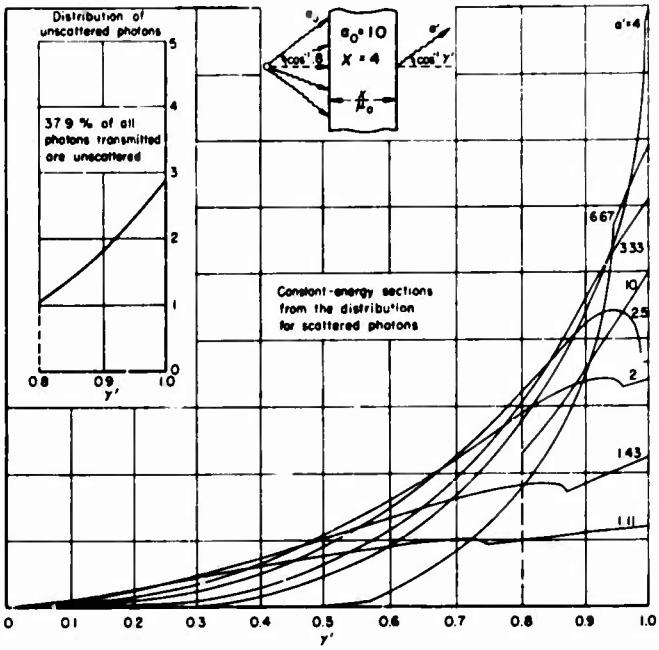

Fig. 8c—Frequency distributions for photons transmitted through lead slabs, $X = 4$

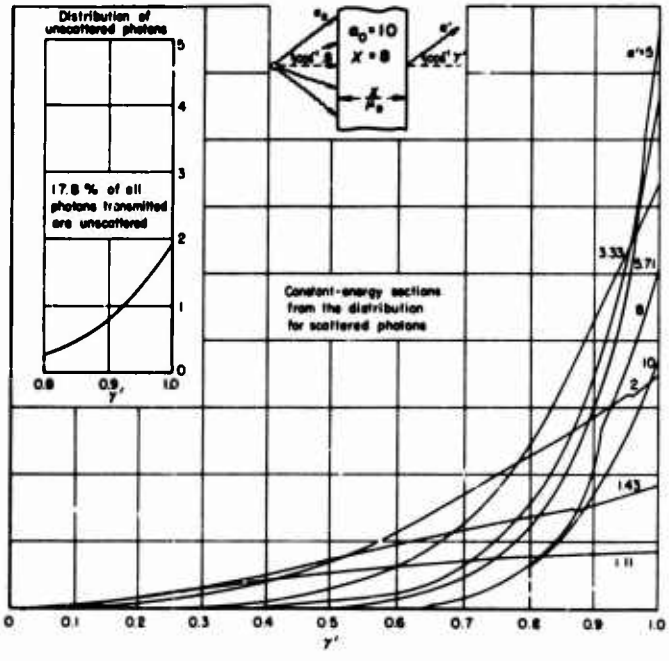

Fig. 8d—Frequency distributions for photons transmitted through lead slabs, $X = 8$

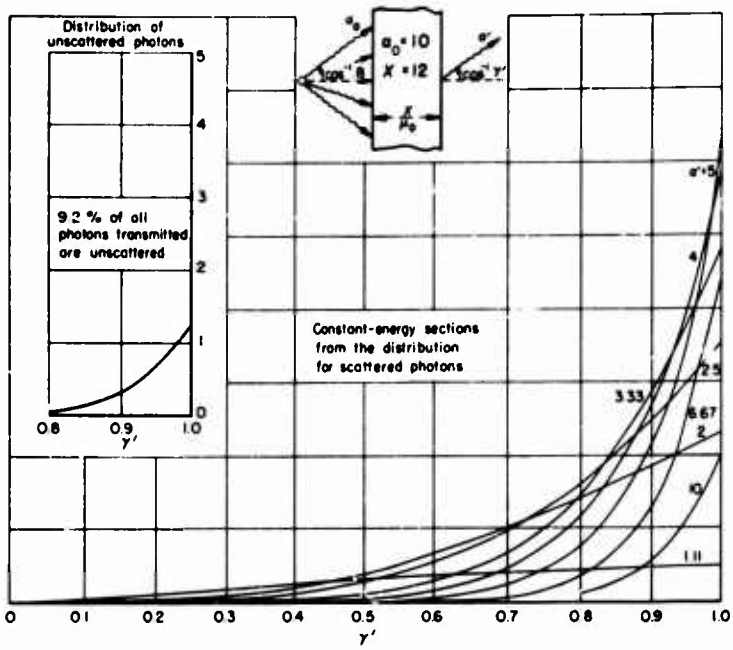

Fig. 8e—Frequency distributions for photons transmitted through lead slabs, $X = 12$

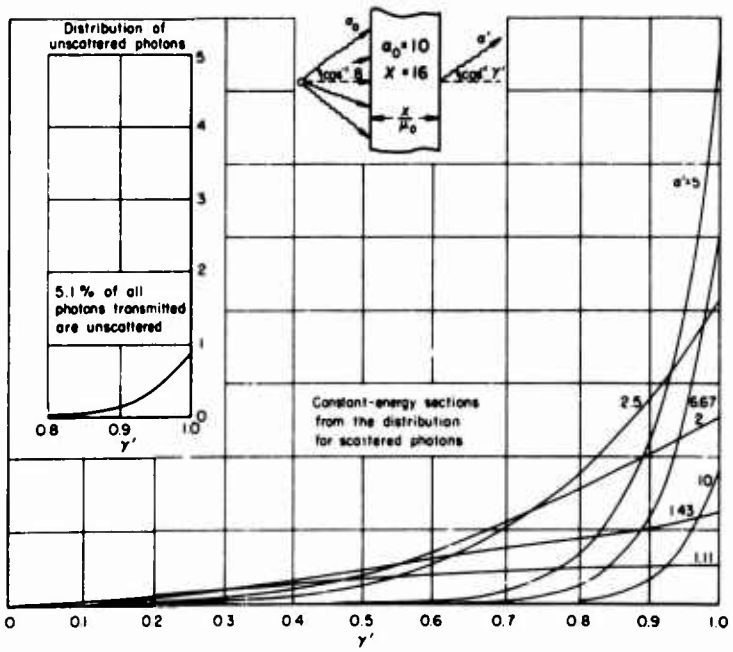

Fig. 8f—Frequency distributions for photons transmitted through lead slabs, $X = 16$

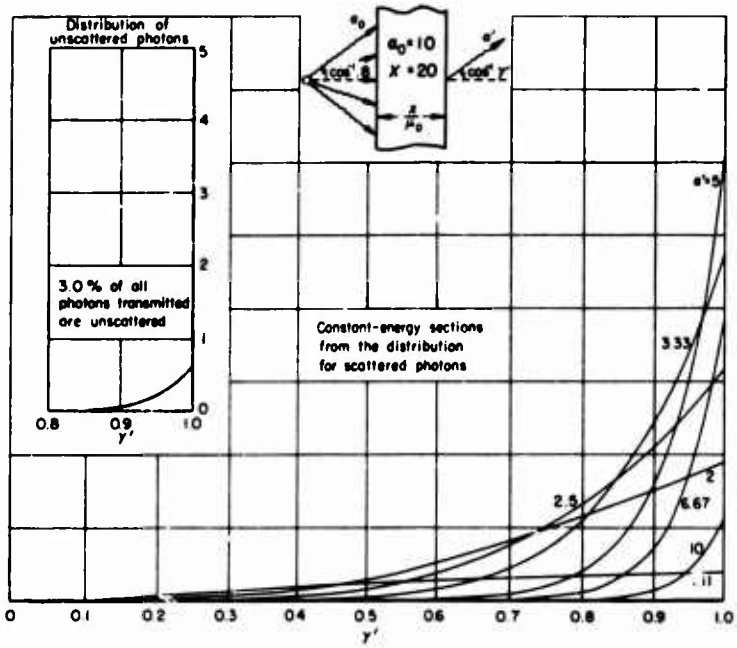

Fig. 8g—Frequency distributions for photons transmitted through lead slabs, $X = 20$

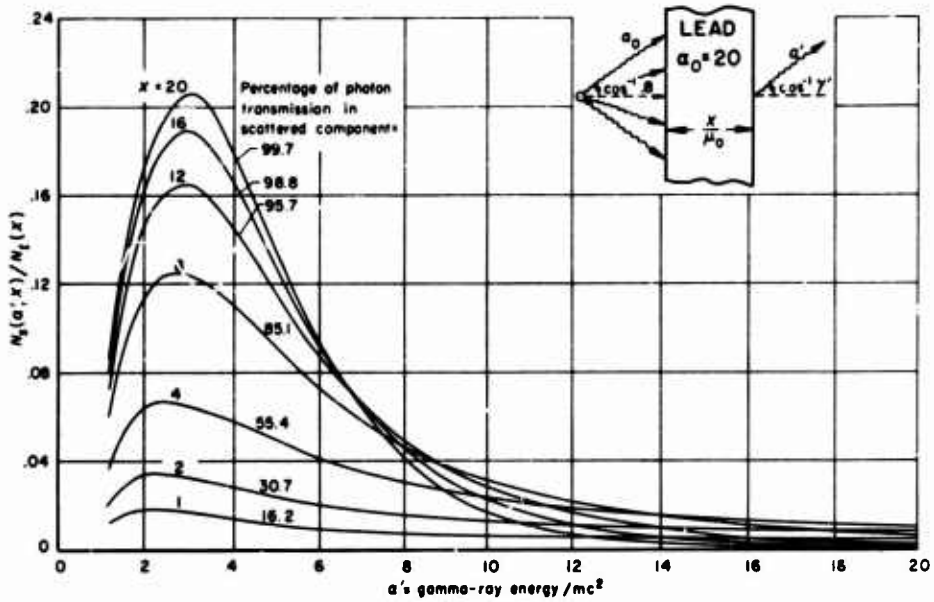

Fig. 9a—Distributions of scattered photons for several slab thicknesses, each distribution normalized by dividing by the total of all transmitted photons—lead, $\alpha_0 = 20$

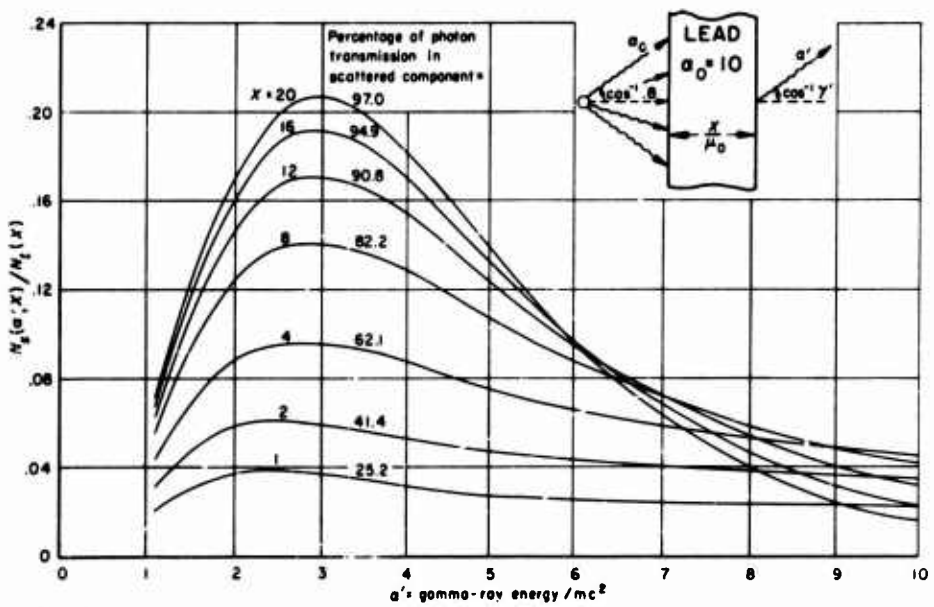

Fig. 9b—Distributions of scattered photons for several slab thicknesses, each distribution normalized by dividing by the total of all transmitted photons—lead, $\alpha_0 = 10$

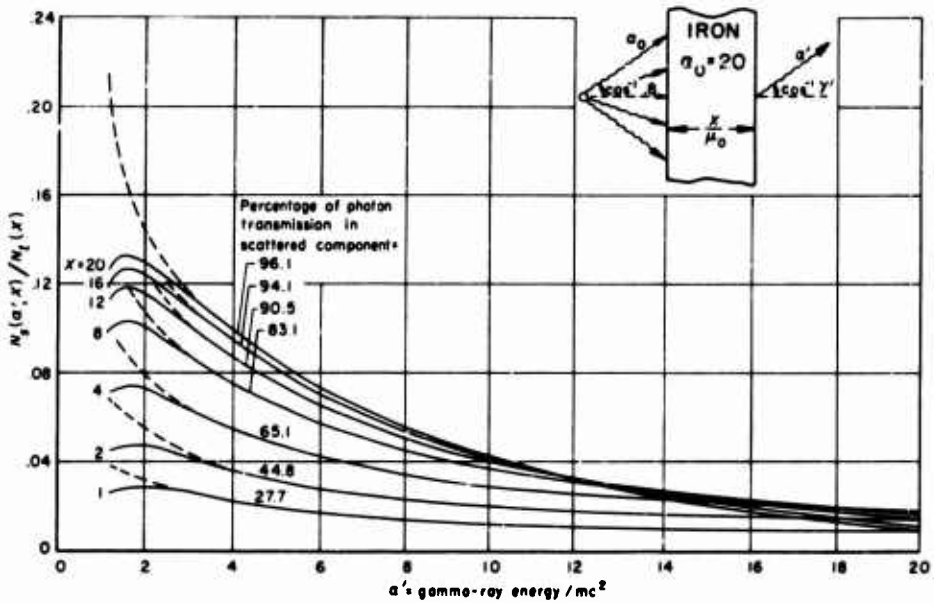

Fig. 9c—Distributions of scattered photons for several slab thicknesses, each distribution normalized by dividing by the total of all transmitted photons—iron, $\alpha_0 = 20$

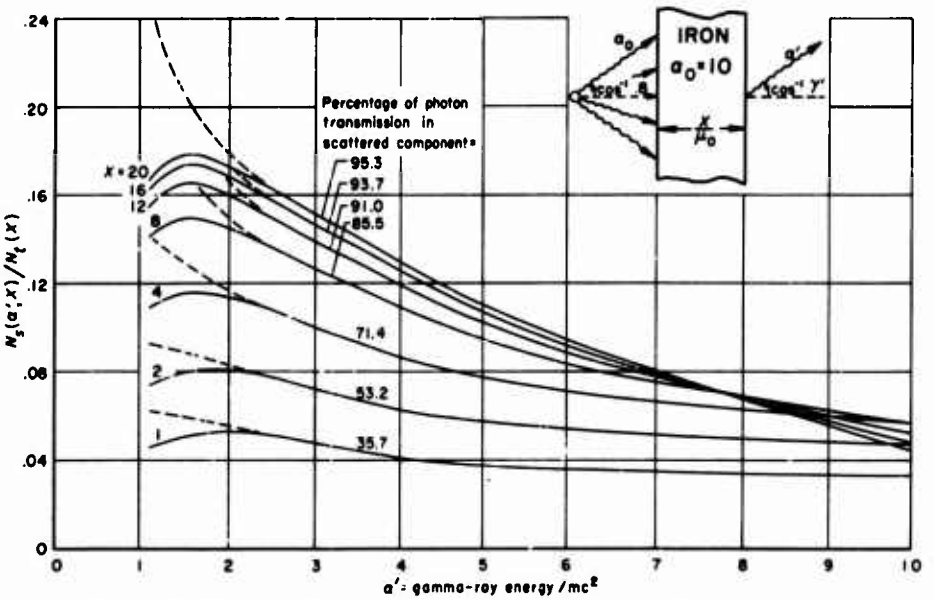

Fig. 9d—Distributions of scattered photons for several slab thicknesses, each distribution normalized by dividing by the total of all transmitted photons—iron, $\alpha_0 = 10$

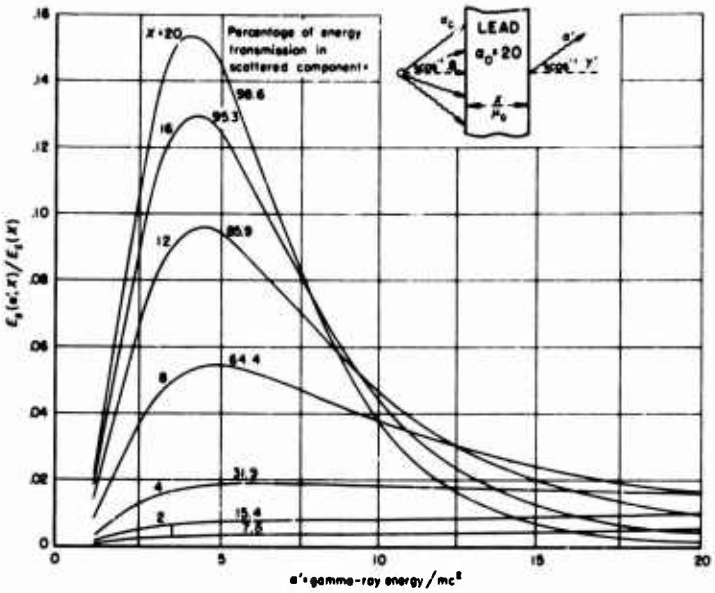

Fig. 10a—Distributions of the energy in scattered photons for several slab thicknesses, each distribution normalized by dividing by the total energy in all transmitted photons—lead, $\alpha_0 = 20$

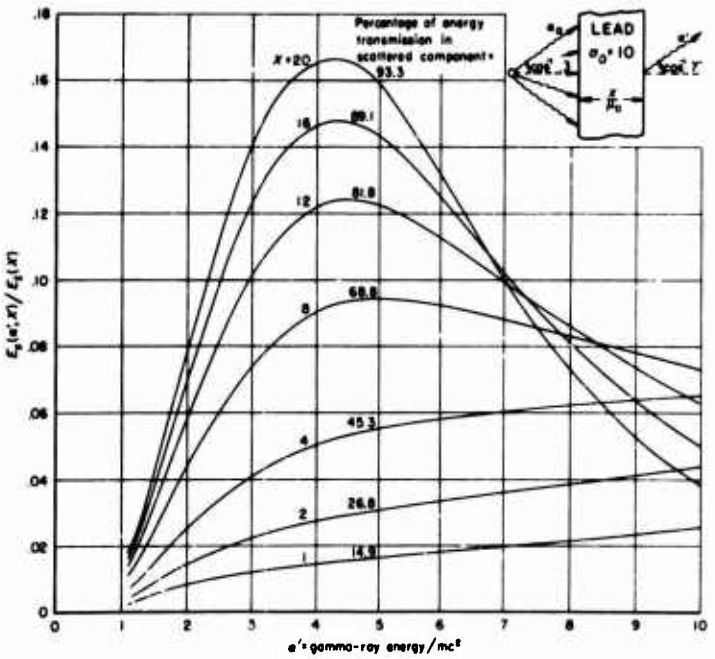

Fig. 10b—Distributions of the energy in scattered photons for several slab thicknesses, each distribution normalized by dividing by the total energy in all transmitted photons—lead, $\alpha_0 = 10$

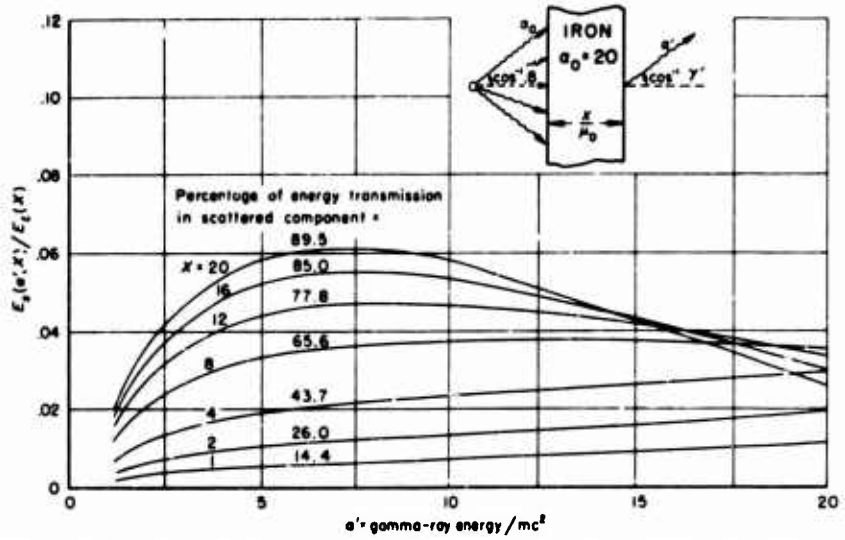

Fig. 10c—Distributions of the energy in scattered photons for several slab thicknesses, each distribution normalized by dividing by the total energy in all transmitted photons—iron, $\alpha_0 = 20$

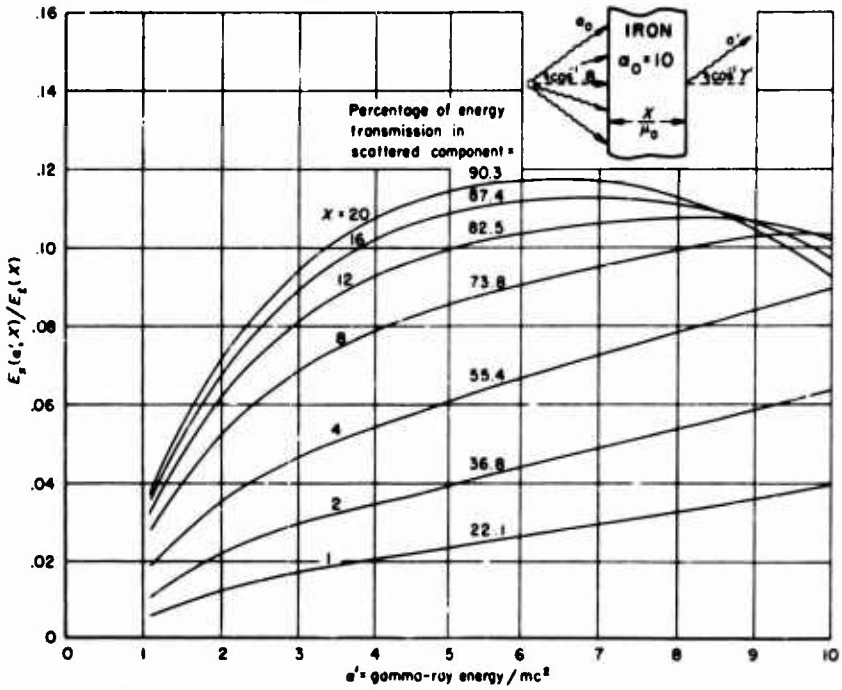

Fig. 10d—Distributions of the energy in scattered photons for several slab thicknesses, each distribution normalized by dividing the total energy in all transmitted photons—iron, $\alpha_0 = 10$

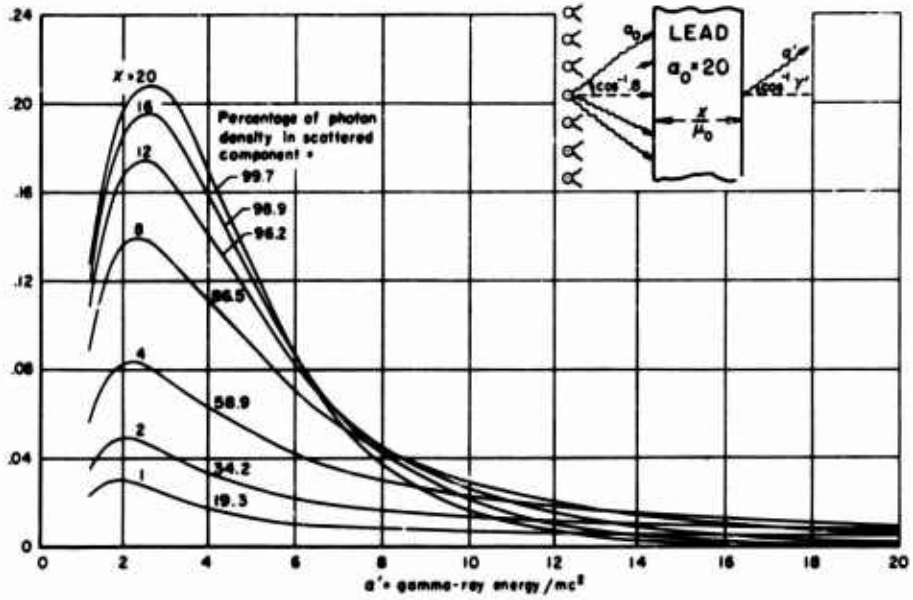

Fig. 11a—Distributions of the density of scattered photons for several slab thicknesses, each distribution normalized by dividing by the density totaled over all transmitted photons—lead, $\alpha_0 = 20$

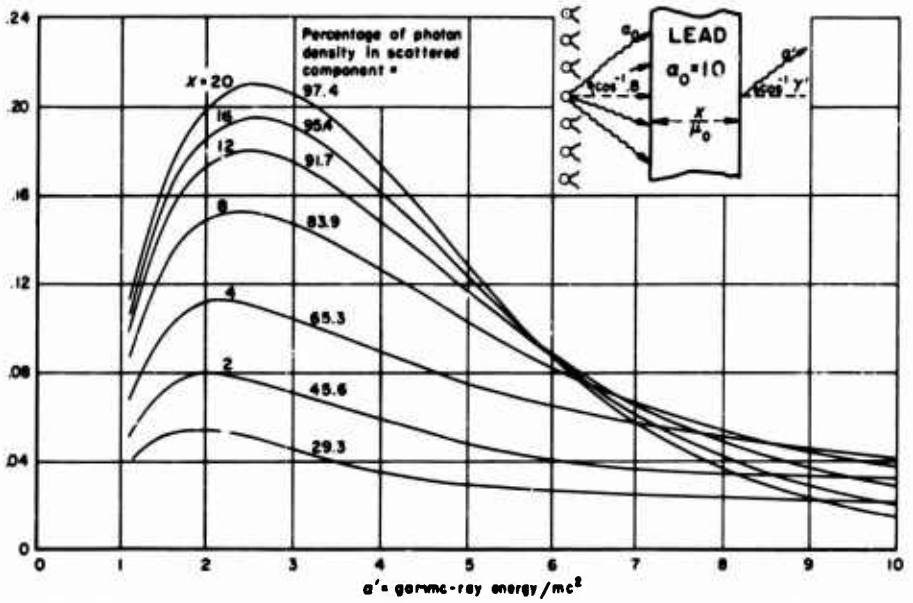

Fig. 11b—Distributions of the density of scattered photons for several slab thicknesses, each distribution normalized by dividing by the density totaled over all transmitted photons—lead, $\alpha_0 = 10$

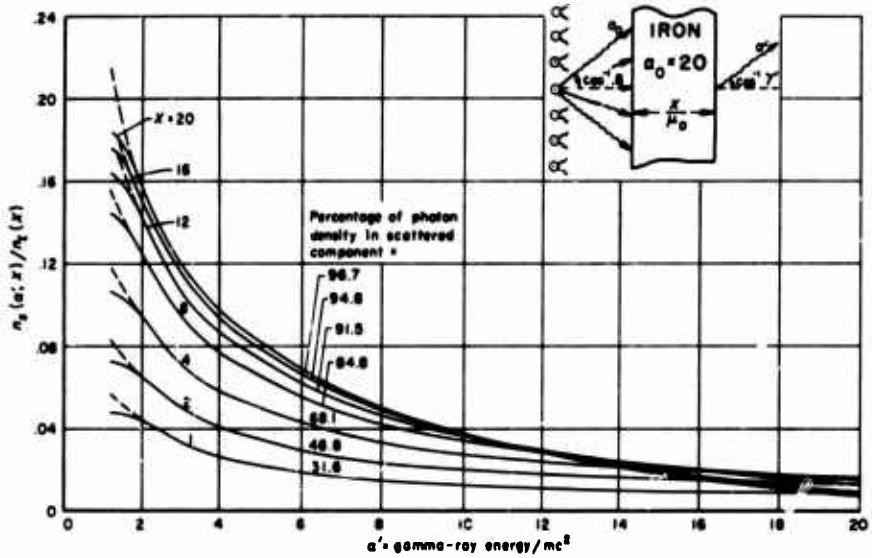

Fig. 11c—Distributions of the density of scattered photons for several slab thicknesses, each distribution normalized by dividing by the density totaled over all transmitted photons—iron, $\alpha_0 = 20$

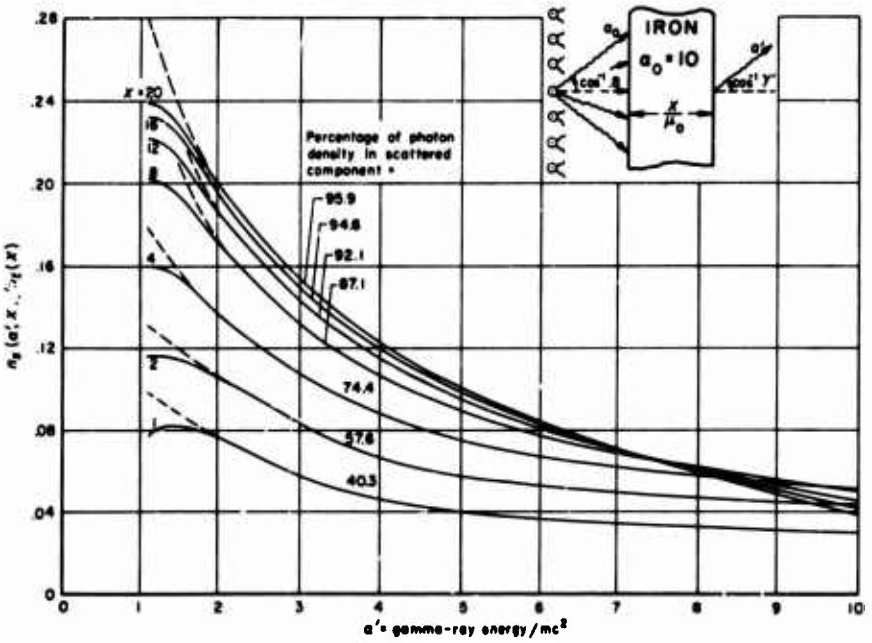

Fig. 11d—Distributions of the density of scattered photons for several slab thicknesses, each distribution normalized by dividing by the density totaled over all transmitted photons—iron, $\alpha_0 = 10$

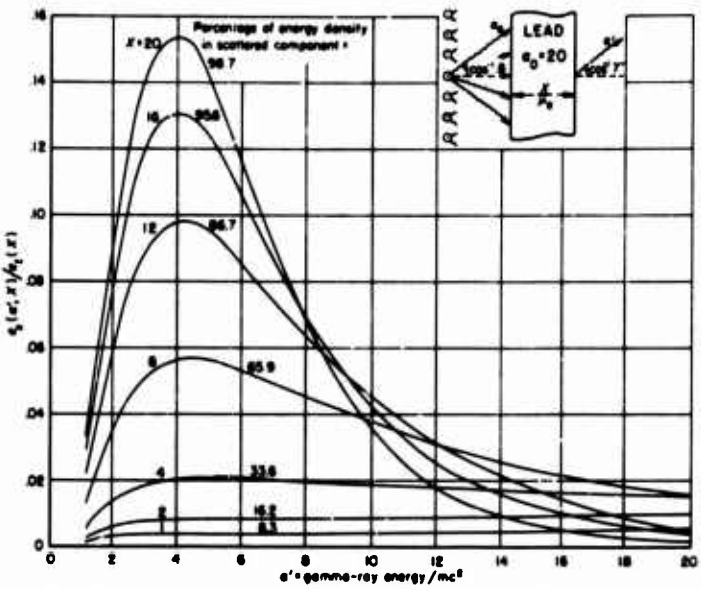

Fig. 12a—Distributions of the energy density in scattered photons for several slab thicknesses, each distribution normalized by dividing by the energy density totaled over all transmitted photons—lead, $\alpha_0 = 20$

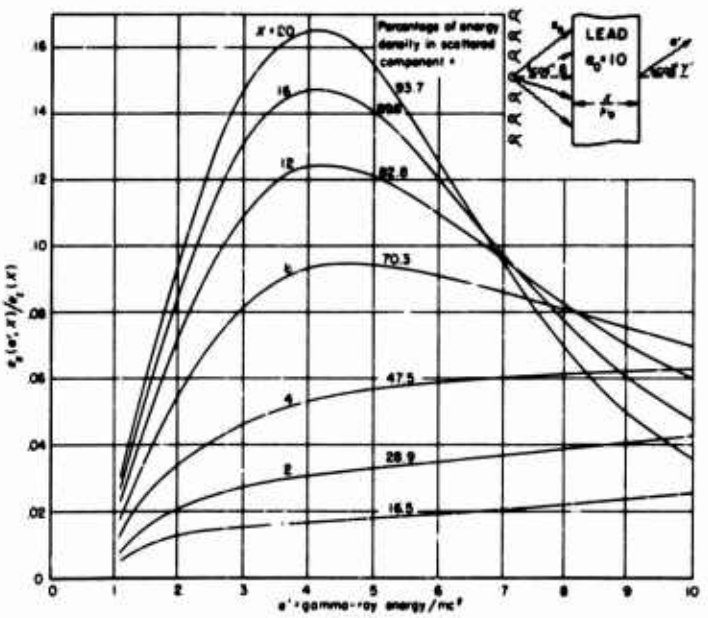

Fig. 12b—Distributions of the energy density in scattered photons for several slab thicknesses, each distribution normalized by dividing by the energy density totaled over all transmitted photons—lead, $\alpha_0 = 10$

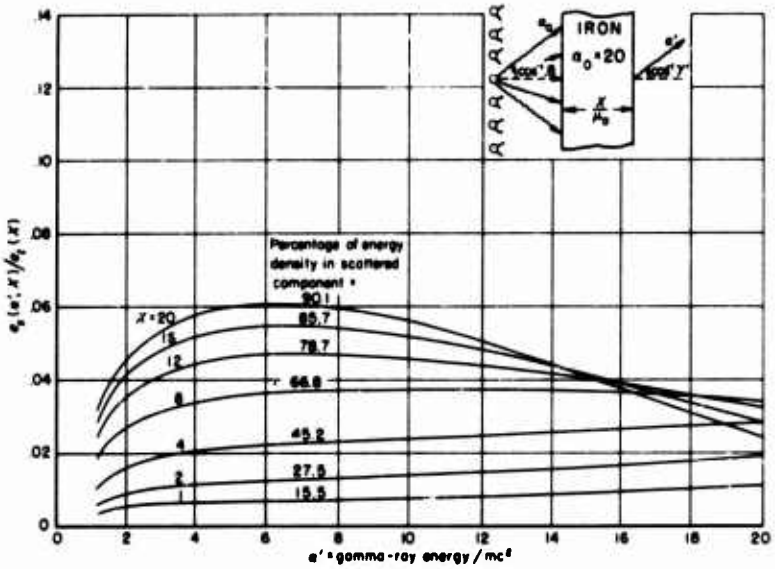

Fig. 12c—Distributions of the energy density in scattered photons for several slab thicknesses, each distribution normalized by dividing by the energy density totaled over all transmitted photons—iron, $\alpha_0 = 20$

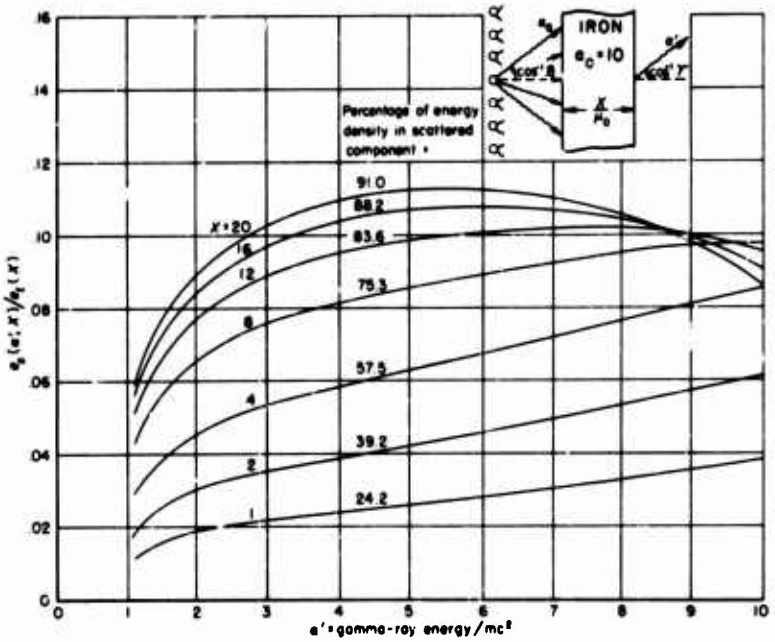

Fig. 12d—Distributions of the energy density in scattered photons for several slab thicknesses, each distribution normalized by dividing by the energy density totaled over all transmitted photons—iron, $\alpha_0 = 10$

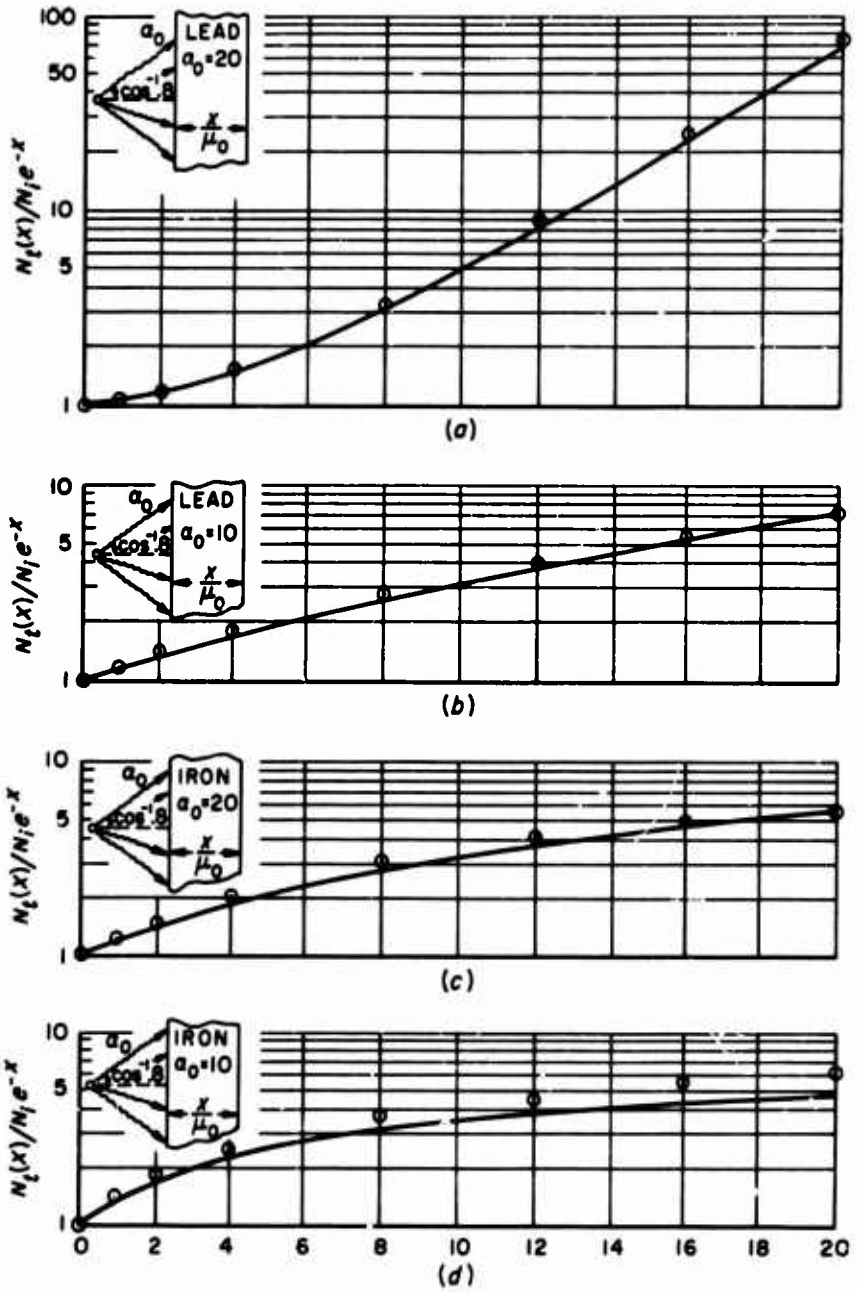

X = thickness of slab in mfp

⊙ Calculated from the results shown in Figs. 3—4

—— Calculated from the results shown in Figs. 9*a*—9*d*

Fig. 13—The ratio of the number of photons transmitted to the number incident, normalized by the factor $1/e^{-X}$

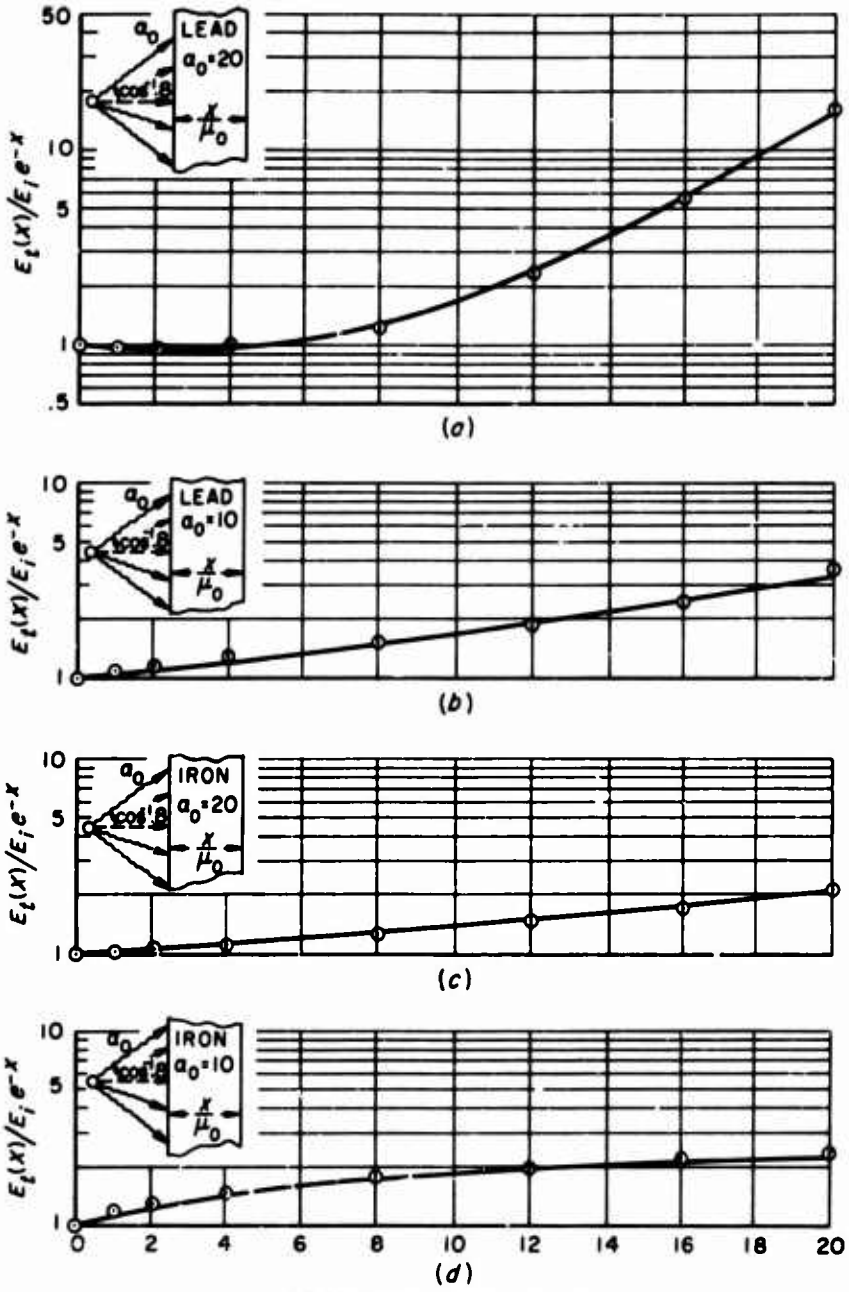

X = thickness of slab in mfp

○ Calculated from the results shown in Figs. 5—6

—— Calculated from the results shown in Figs. 10*a*—10*d*

Fig. 14—The ratio of the energy in transmitted photons to the energy in incident photons, normalized by the factor $1/e^{-X}$

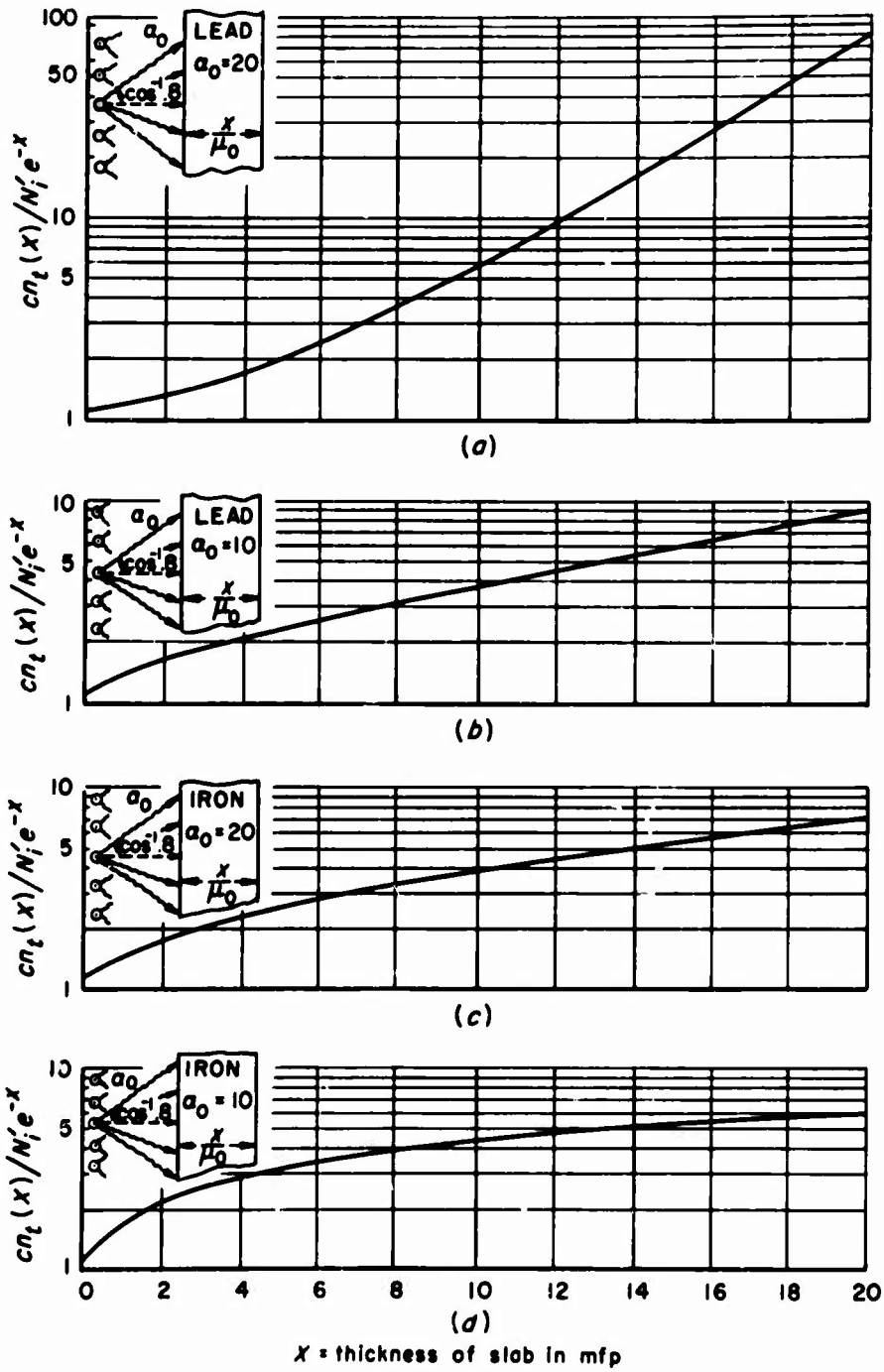

Fig. 15—The ratio of the density of transmitted photons to the number incident per unit area per unit time, normalized by the factor c/e^{-x}

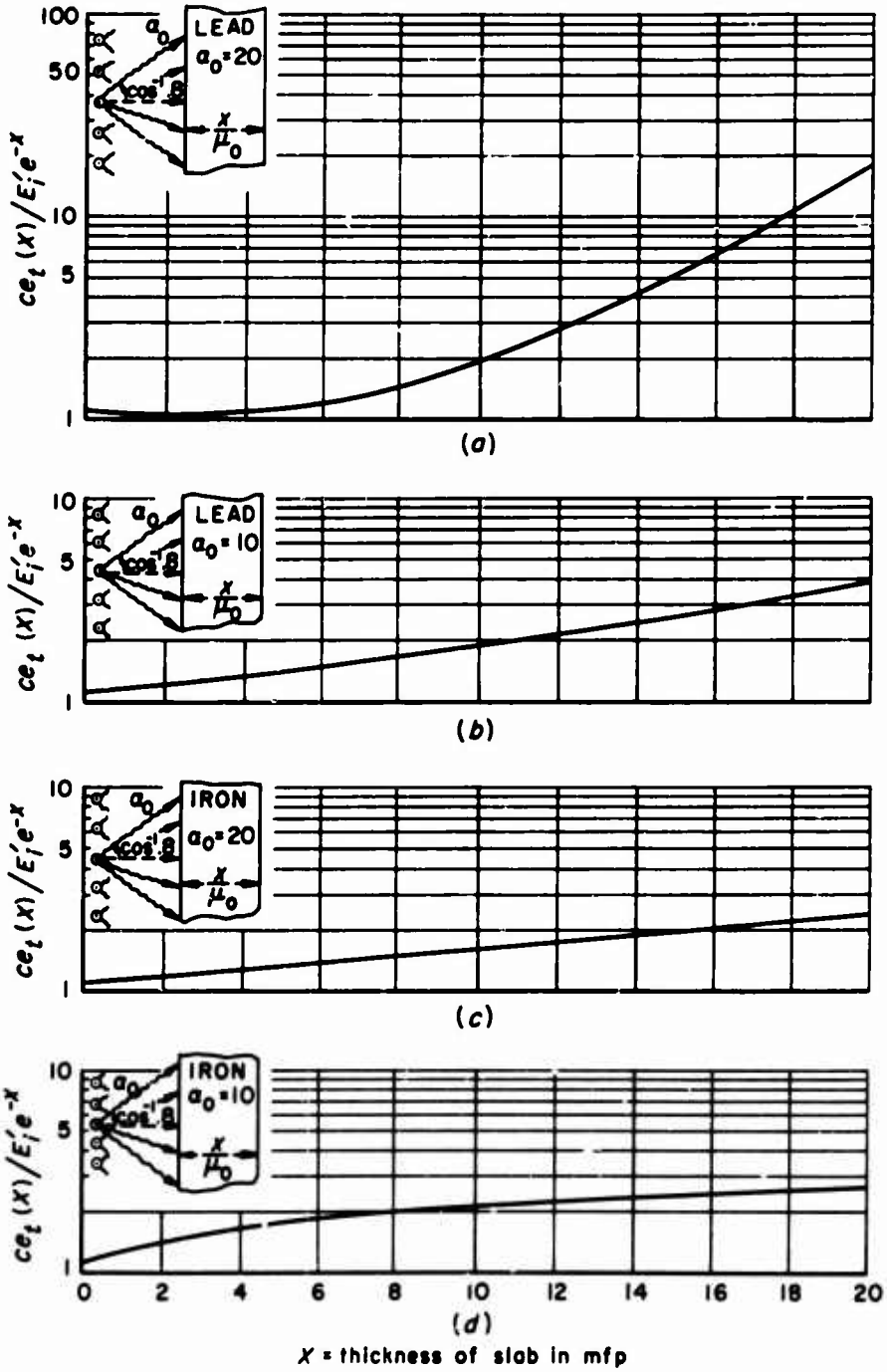

Fig. 16—The ratio of the energy density in the transmitted photons to the energy incident per unit area per unit time, normalized by the factor c/e^{-X}

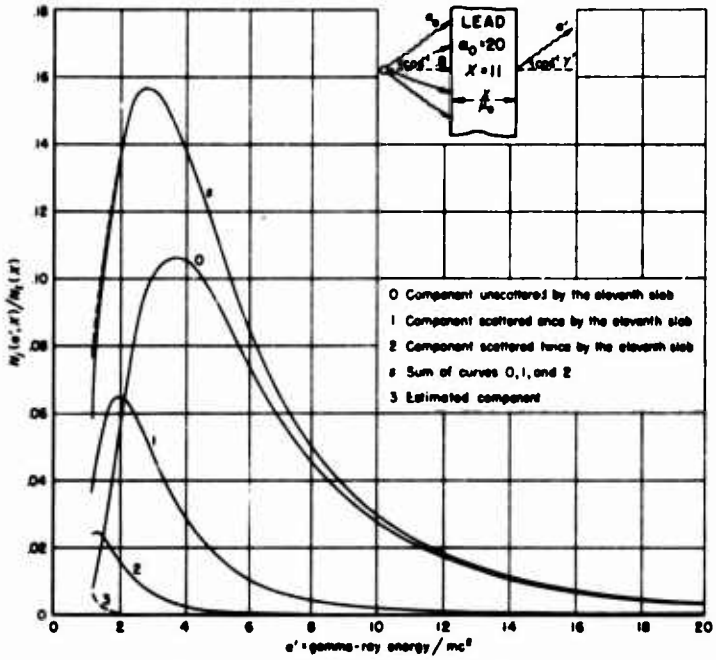

Fig. 17a—Component distributions for the eleventh elemental slab—lead, $\alpha_0 = 20$

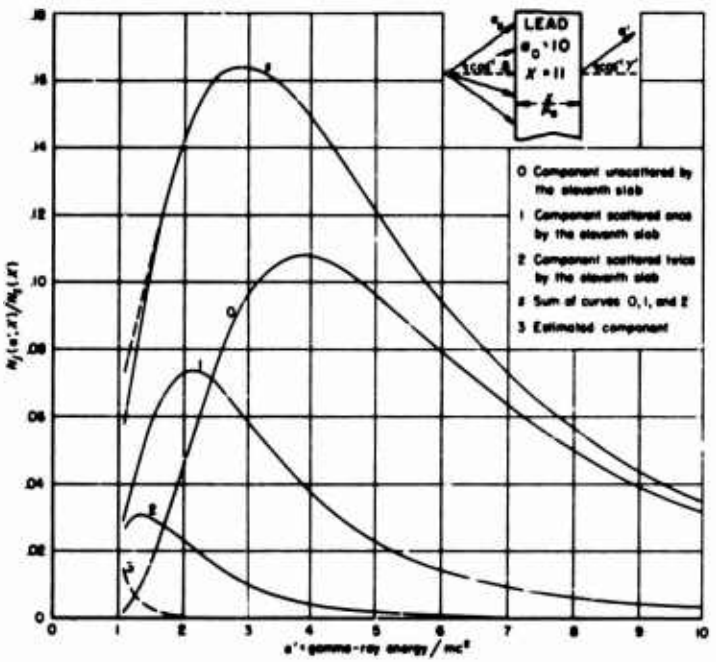

Fig. 17b—Component distributions for the eleventh elemental slab—lead, $\alpha_0 = 10$

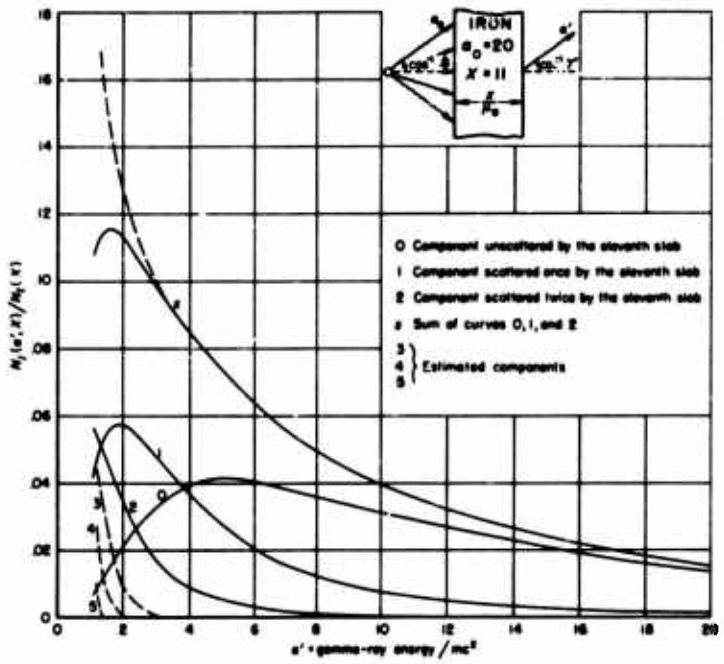

Fig. 17c—Component distributions for the eleventh elemental slab—iron, $\alpha_0 = 20$

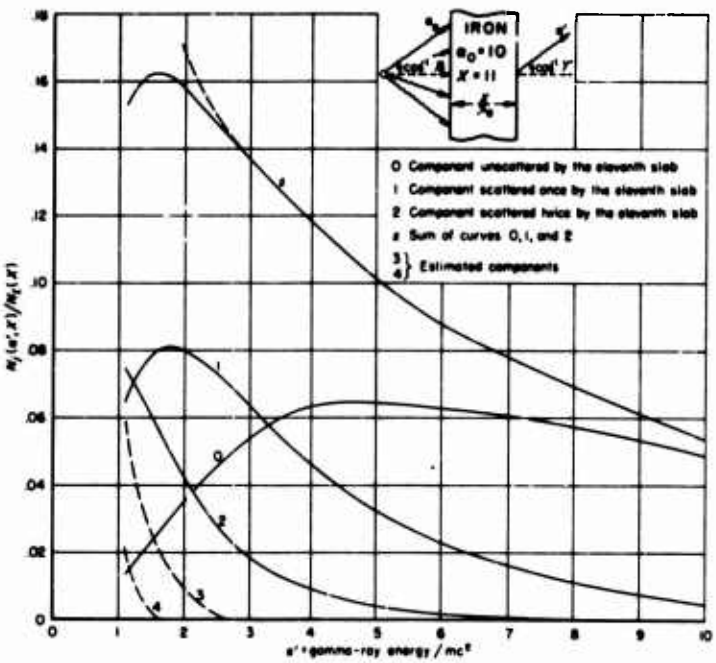

Fig. 17d—Component distributions for the eleventh elemental slab—iron, $\alpha_0 = 10$

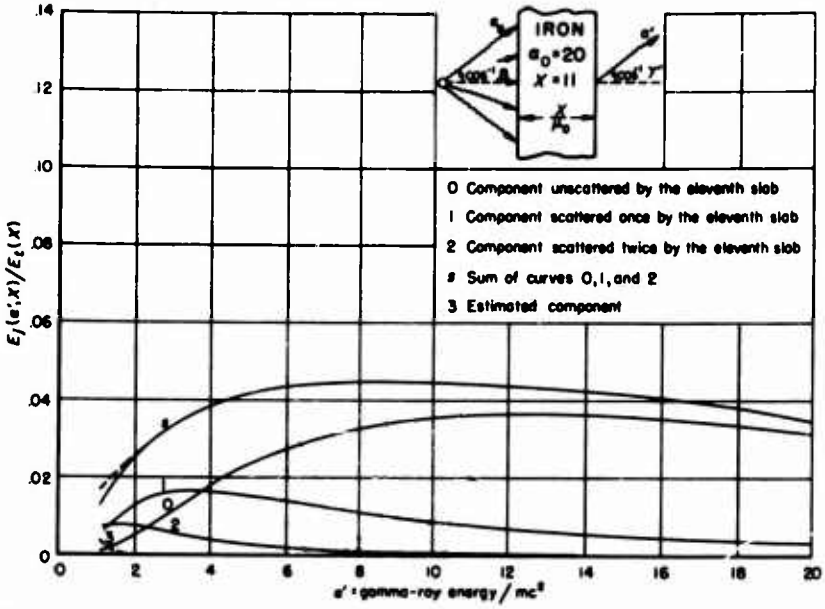

Fig. 18a—Components of the energy distribution for the eleventh elemental slab—iron, $\alpha_0 = 20$

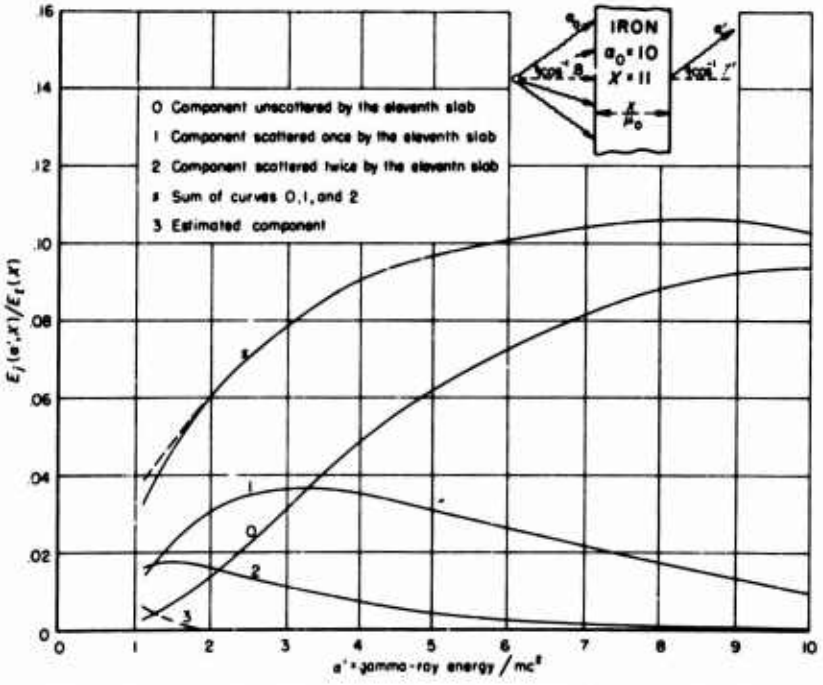

Fig. 18b—Components of the energy distribution for the eleventh elemental slab—iron, $\alpha_0 = 10$

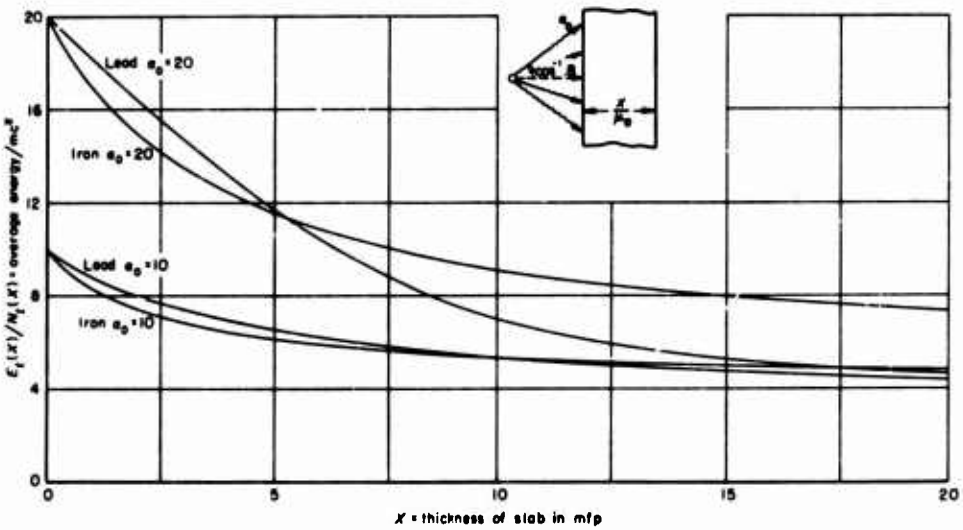

Fig. 19—Comparison of the average energy in the photons transmitted through slabs of lead and of iron

IV. TRANSMISSION IN THE ABSENCE OF ABSORPTION BY PAIR PRODUCTION AND PHOTOELECTRIC EFFECT

The Contribution of Back-scattered Radiation to Transmission

It will be recalled that photons scattered out of the forward hemisphere were ignored both in the method of thin slabs and in the method of successive scatterings. Although this neglect is intuitively acceptable, data indicating the magnitude of the quantities neglected have some interest. Table 6 gives the probabilities of transmission through, and reflection from, thin slabs of the pure Compton scatterer; transmissions and reflections for one and two collisions with all possible successions of forward and backward scatterings are tabulated for photons normally incident and of energies 10, 5, 2.5, 1, and 0.2 mc^2. The probability of transmission with a backward and a forward scattering, N_{bf}, in comparison with the probability of transmission with two forward scatterings, N_{ff}, is seen to dwindle in importance as the thickness of the slab increases. At a thickness of ½ mfp, N_{bf} is significant, running from slightly less than one-tenth of N_{ff} in the case of 10 mc^2 to about one-half in the case of 0.2 mc^2. At a thickness of 4 mfp, N_{bf} is very small except in the case of 0.2 mc^2, where it is about one-seventh of N_{ff}. The increased importance of N_{bf} for 0.2 mc^2 is of course due to the increased probability of large angles of deflection.

Backward scattering is even less important for energy transmission. This can be seen in Table 7, the energy counterpart of Table 6. Only for 0.2 mc^2 does E_{bf} attain much importance.

Tables 8 and 9 are intended to give an indication of the behavior of transmission and reflection as the angle of incidence moves away from the normal.

The importance of backward scattering to the transmission scattered k times is controlled by the relative magnitudes of k and X. If k is large, the probability of one or more backward scatterings is large. But, if X is large, the slab tends to allow transmission only to those photons which have wasted no collision in traveling backward. Hence, if X is fixed and k is allowed to increase sufficiently, nearly all the photons transmitted with k scatterings will have suffered a backward scattering. On the other hand, if k is fixed and X increases sufficiently, almost none of the transmitted photons will have suffered a backward scattering. The upshot is that one can say for a slab of any thickness that backward scattering is negligible to the k-tuply scattered transmission when k is sufficiently small, but all-important when k is sufficiently large. Whether or not backward-scattered photons form a significant part of the total transmission depends on the value of k reached before the k-tuply scattered transmission becomes negligible. In the cases of lead and iron, the evidence is that backward scattering does not have the opportunity to become important. A slab thick enough to make twice- or thrice-scattered transmission count heavily was found to be too thick for the backward-scattered component to have

significance. The rapid convergence of N_k and E_k to zero indicated that the same situation would be found to exist for transmission with a larger number of scatterings. It seems unlikely, therefore, that neglect of backward scattering can introduce large errors into the transmission results for lead or iron, or any of the heavier materials.

Comparison of kth-scattered Transmission for Lead, Iron, and the Compton Scatterer

Absorption by pair production and the photoelectric effect tends to reduce the probability of transmission. The reduction, however, does not necessarily appear in the first few scatterings. A comparison of N_1/e^{-X}, N_2/e^{-X}, $E_1/\alpha_0 e^{-X}$, and $E_2/\alpha_0 e^{-X}$ for photons normally incident on slabs of the Compton scatterer (Tables 10 and 11) with the corresponding quantities for lead and iron (Tables 1 through 4) shows that when X and α_0 are both large, the transmission values actually increase as the three materials are considered in the following order: Compton scatterer, iron, lead. This seeming paradox will be resolved in Sec. VI.

For the higher-ordered scatterings, pair production and the photoelectric effect do decrease the transmission by very significant amounts, as can easily be shown. For example, in Table 10 one finds values of N_k/e^{-X} for the Compton scatterer for $\alpha_0 = 10$ and $X = 8$, such that

$$N_0 = .000335, \qquad N_1 = .000483, \qquad N_2 = .000399.$$

The quantity N_k has reached its maximum value in the first collision. If, say, twenty terms were needed to reach an approximation to the sum of the series $\sum_{k=0}^{\infty} N_k$, a liberal estimate of the probability of transmission would not exceed .005. But no photons are lost through absorption, so that all must eventually escape. Therefore, the individual transmissions and reflections must sum to unity, and if the probability of transmission is .005, the probability of reflection is .995. The latter probability seems unreasonably large for a slab only 8-mfp thick. To get a reasonable value, the series $\sum_{k=0}^{\infty} N_k$ must converge so slowly that hundreds or thousands of terms are needed to approximate its sum. Photons on their way to being scattered hundreds or thousands of times must come into the low energy range where, in the cases of lead and iron, they are absorbed by the photoelectric effect. That the photoelectric effect is able to bring the count of terms required for lead and iron down to tens and not hundreds or thousands was proved in Sec. II by means of the quantities r_k and q_k in Table 5.

Estimates of Transmission and Reflection for Thin Slabs of the Compton Scatterer

It is clear that the method of successive scatterings must be considerably less successful for the Compton scatterer than for lead or iron. Nevertheless, for thin slabs, the results in Tables 6 and 7 can be used to obtain estimates of both transmission and reflection for normally incident photons. Estimation is aided, in the case of number, by the fact that

the probabilities of transmission and reflection must sum to unity and, in the case of energy, by the fact that $\sum_{k=0}^{\infty} E_k$ is given a degree of rapidity of convergence (compared with $\sum_{k=0}^{\infty} N_k$) by the degradation of the energy with each collision. These estimates appear in Figs. 20 through 23. Figure 20 gives the number build-up factors; Fig. 21, the estimated probabilities of reflection; Fig. 22, the energy build-up factors; and Fig. 23, the expected reflected energies. The accuracy of the estimates is uncertain, but, in the case of number, the error is believed to be about 5 per cent at $X = 4$. In the case of energy, the error may be much larger, particularly for the low incident energies, where the convergence is very slow.

Transmission Calculated by the Thin-slab Method in the Cases of Air and the Compton Scatterer

In the absence, or near absence, of photoelectric absorption in the low energies, backward scattering will become important to transmission. Therefore, the thin-slab method will not be entirely successful. It is not without profit, however, to apply this method to a light material for which absorption by pair production and photoelectric effect is small. Typical of the light materials, and of considerable interest, is air; Fig. 24 gives the total absorption coefficient assumed to hold for air.

The treatment of air parallels that of lead and of iron. The same incident distribution is used and the same quantities are calculated. Only one incident energy, 20 mc^2, is considered, however, and the thickness of the elemental slab is $\frac{2}{3}$ mfp. Figures 25, 26, 27, and 28 show, respectively, the ratios $N_s(\alpha', X)/N_t(X)$, $E_s(\alpha', X)/E_t(X)$, $n_s(\alpha', X)/n_t(X)$, and $e_s(\alpha', X)/e_t(X)$, where the normalizing factors $1/N_t(X)$, $1/E_t(X)$, $1/n_t(X)$, and $1/e_t(X)$ correspond, as in the cases of lead and iron, to the area under the terminated solid curves rather than the dashed curves. In the case of number, the differences between the two areas are very large, so that $N_t(X)$ and $n_t(X)$ far underestimate the true number of photons transmitted and the true density; but in the case of energy, the differences are presumably comparatively small, so that $E_t(X)$ and $e_t(X)$ only slightly underestimate the true energy transmitted and the true energy density. This is shown very clearly in Figs. 29 and 30, which give the components of the distribution for the sixteenth elemental slab. Figures 31, 32, 33, and 34 give, respectively, the quantities $N_t(X)/N_i e^{-X}$, $E_t(X)/E_i e^{-X}$, $cn_t(X)/N_i' e^{-X}$, and $ce_t(X)/E_i' e^{-X}$. It may seem pointless to develop $N_t(X)$ and $n_t(X)$ as though they were not known to be below the true values, but the thought is that the reader interested in estimating the true values may find it a service to have the undervalues of $N_t(X)$ and $n_t(X)$; in any event, the values given may be considered as being the true values when photons enfeebled by many collisions are disregarded.

The curves of Figs. 25 through 34 behave qualitatively as one would expect from the results for lead and iron. Trends that are apparent on considering first lead and then iron are continued to air. Backward scatter is undoubtedly more important than it was for lead or iron, but since the distribution over direction of the incident photons favors the normal, those photons which have been scattered backward at some time in their history

tend to appear in the energy range below that considered in the thin-slab method. Little change in the results of Figs. 25 through 34 would have been discernible had backward scatter been included in the calculations.

Before leaving the topic of the pure or almost pure Compton scatterer, one other calculation by the thin-slab method will be presented. In this case, the material is the pure Compton scatterer; the incident photons are of energy 10 mc^2 and are distributed over direction as in the other cases for the thin-slab method. The thickness for the elemental slab is 0.64 mfp. The computations were done early in the exploration of the possibilities of the thin-slab method and are of unknown accuracy. Of the set of figures given in each case for lead, iron, and air, only two—the distribution of the energy in scattered photons (Fig. 35) and the ratio of the energy in transmitted photons to the energy in incident photons (Fig. 36)—were thought to have value sufficient to warrant inclusion.

* * *

Table 6

PROBABILITIES OF TRANSMISSION AND REFLECTION WITH ONE AND TWO SCATTERINGS FOR PHOTONS OF 0.2 TO 10 mc^2 NORMALLY INCIDENT ON SLABS OF THE PURE COMPTON SCATTERER*

α_0	X	N_0	N_f	N_b	N_{ff}	N_{bf}	N_{bb}	N_{fb}
10	.5	.6065	.156	.0169	.0430	$.0^2305$	$.0^276$	$.0^270$
	1.	.3679	.164	.0173	.0654	$.0^2182$	$.0^288$	$.0^273$
	2.	.1353	.0947	.0173	.0525	$.0^3545$	$.0^290$	$.0^274$
	4.	.0183	.0190	.0173	.0129	$.0^4859$	$.0^3908$	$.0^2741$
5	.5	.6065	.167	.0264	.0407	$.0^254$	.011	$.0^293$
	1.	.3679	.174	.0292	.0672	$.0^235$	.015	.012
	2.	.1353	.103	.0294	.0613	$.0^385$	.016	.012
	4.	.0183	.0210	.0294	.0167	$.0^312$	.016	.012
2.5	.5	.6065	.169	.0405	.0385	$.0^278$	.015	.013
	1.	.3679	.178	.0458	.0659	$.0^266$	.020	.017
	2.	.1353	.107	.0462	.0616	$.0^218$	.022	.018
	4.	.0183	.0224	.0462	.0179	$.0^322$	.022	.018
1.0	.5	.6065	.160	.0606	.0374	.010	.018	.017
	1.	.3679	.171	.0720	.0645	.012	.028	.024
	2.	.1353	.104	.0744	.0609	$.0^252$	.032	.027
	4.	.0183	.0221	.0745	.0181	$.0^355$	.032	.027
.2	.5	.6065	.133	.0996	.0278	.013	.021	.023
	1.	.3679	.144	.119	.0531	.020	.033	.036
	2.	.1353	.0886	.128	.0516	.013	.039	.044
	4.	.0183	.0179	.130	.0152	$.0^222$	.040	.045

*N_0 = the probability of transmission without collision. In the cases of the other probabilities, the subscripts "f" and "b" indicate, respectively, a forward scattering and a backward scattering. For example, N_{bf} is the probability that a photon will be transmitted with exactly two collisions, the first resulting in a backward scattering, the second, in a forward scattering.

Table 7

EXPECTED ENERGIES OF TRANSMISSION AND REFLECTION WITH ONE AND TWO SCATTERINGS FOR PHOTONS OF 0.2 TO 10 mc^2 NORMALLY INCIDENT ON SLABS OF THE PURE COMPTON SCATTERER*

a_0	X	E_0	E_f	E_b	E_{ff}	E_{bf}	E_{bb}	E_{fb}
10	.5	6.065	.896	.0102	.111	$.0^214$	$.0^246$	$.0^242$
	1.	3.679	.966	.0103	.205	$.0^383$	$.0^248$	$.0^243$
	2.	1.353	.605	.0103	.204	$.0^326$	$.0^249$	$.0^244$
	4.	.1832	.130	.0103	.0633	$.0^3388$	$.0^249$	$.0^244$
5	.5	3.032	.522	.0153	.0691	$.0^223$	$.0^255$	$.0^243$
	1.	1.839	.565	.0164	.130	$.0^215$	$.0^272$	$.0^265$
	2.	.6765	.355	.0164	.135	$.0^344$	$.0^275$	$.0^269$
	4.	.0916	.0770	.0164	.0434	$.0^349$	$.0^276$	$.0^269$
2.5	.5	1.516	.306	.0202	.0435	$.0^230$	$.0^260$	$.0^261$
	1.	.920	.322	.0227	.0811	$.0^226$	$.0^286$	$.0^281$
	2.	.338	.202	.0232	.0835	$.0^373$	$.0^299$	$.0^291$
	4.	.0458	.0442	.0232	.0274	$.0^382$	.0101	$.0^292$
1.0	.5	.6065	.130	.0236	.0225	$.0^230$	$.0^260$	$.0^262$
	1.	.3679	.142	.0277	.0400	$.0^235$	$.0^286$	$.0^289$
	2.	.1353	.0885	.0285	.0403	$.0^214$	.011	.010
	4.	.01832	.0192	.0285	.0134	$.0^314$	.011	.010
.2	.5	.1213	.0247	.0143	$.0^2541$	$.0^215$	$.0^234$	$.0^232$
	1.	.07358	.0266	.0183	$.0^2874$	$.0^225$	$.0^251$	$.0^248$
	2.	.02706	.0164	.0195	$.0^2834$	$.0^218$	$.0^263$	$.0^258$
	4.	$.0^2366$	$.0^2342$	.0196	$.0^2269$	$.0^327$	$.0^265$	$.0^258$

*E_0 — the expected energy transmitted by unscattered photons. In the cases of the other expected energies, the subscripts "f" and "b" indicate, respectively, a forward scattering and a backward scattering. For example, E_{bf} is the expected energy in the photons transmitted with exactly two collisions, the first resulting in a backward scattering, the second, in a forward scattering.

Table 8

PROBABILITIES OF TRANSMISSION AND REFLECTION WITH ONE AND TWO SCATTERINGS FOR PHOTONS OF 2.5 mc^2 VARIOUSLY INCIDENT ON THIN SLABS OF THE PURE COMPTON SCATTERER*

γ_0	X	N_0	N_f	N_b	N_{ff}	N_{bf}
1.0	.29	.740	.132	.0338	.0226	$.0^2541$
	1.45	.234	.148	.0461	.0706	$.0^2414$
.8	.29	.695	.147	.0450	.0290	.....
	1.45	.162	.128	.0602	.0699	$.0^240$
.6	.29	.616	.168	.0642	.0373	.....
	1.45	.0887	.0986	.0834	.0651	$.0^240$
.4	.29	.484	.194	.103	.0499	.....
	1.45	.0264	.0618	.127	.0532	$.0^240$
.2	.29	.234	.230	.195	.0724	.....
	1.45	$.0^3698$	.0258	.214	.0337	$.0^23$
0	.29	0	.161	.500	.0935	0
	1.45	0	$.0^299$	.500	.0172	0

*N_0 = the probability of transmission without collision. In the cases of the other probabilities, the subscripts "*f*" and "*b*" indicate, respectively, a forward scattering and a backward scattering. For example, N_{bf} is the probability that a photon will be transmitted with exactly two collisions, the first resulting in a backward scattering, the second, in a forward scattering.

Table 9

EXPECTED ENERGIES OF TRANSMISSION AND REFLECTION WITH ONE AND TWO SCATTERINGS FOR PHOTONS OF 2.5 mc^2 VARIOUSLY INCIDENT ON THIN SLABS OF THE PURE COMPTON SCATTERER*

γ_0	X	E_0	E_f	E_b	E_{ff}	E_{bf}
1.0	.29	1.87	.225	.0173	.0229	$.0^221$
	1.45	.584	.275	.0232	.0898	$.0^215$
.8	.29	1.74	.248	.0267	.0291	.....
	1.45	.406	.231	.0351	.0873	$.0^216$
.6	.29	1.54	.277	.0456	.0386	.....
	1.45	.222	.171	.0577	.0788	$.0^217$
.4	.29	1.21	.305	.0884	.0501	.....
	1.45	.0660	.0994	.106	.0613	$.0^214$
.2	.29	.585	.334	.207	.0703	.....
	1.45	$.0^2174$	.0355	.225	.0357	$.0^38$
0	.29	0	.197	.658	.0849	0
	1.45	0	.0111	.658	.0160	0

*E_0 = the expected energy transmitted by unscattered photons. In the cases of the other expected energies, the subscripts "f" and "b" indicate, respectively, a forward scattering and a backward scattering. For example, E_{bf} is the expected energy in the photons transmitted with exactly two collisions, the first resulting in a backward scattering, the second, in a forward scattering.

Table 10

N_k/e^{-X} FOR PHOTONS OF 0.2 TO 10 mc^2 NORMALLY INCIDENT ON SLABS OF THE PURE COMPTON SCATTERER*

X	α_0	N_0/e^{-X}	N_1/e^{-X}	N_2/e^{-X}
1	10	1.00	.445	.178
	5	1.00	.473	.183
	2.5	1.00	.483	.179
	1.0	1.00	.465	.175
	.2	1.00	.390	.144
2	10	1.00	.700	.388
	5	1.00	.760	.453
	2.5	1.00	.791	.456
	1.0	1.00	.771	.450
	.2	1.00	.654	.382
4	10	1.00	1.04	.704
	5	1.00	1.15	.912
	2.5	1.00	1.22	.977
	1.0	1.00	1.20	.989
	.2	1.00	.978	.831
8	10	1.00	1.44	1.19
	5	1.00	1.63	1.62
	2.5	1.00	1.77	1.86
	1.0	1.00	1.76	1.98
	.2	1.00	1.30	1.60
12	10	1.00	1.70	1.68
	5	1.00	1.96	2.23
	2.5	1.00	2.14	2.70
	1.0	1.00	2.14	3.08
	.2	1.00	1.48	2.57
16	10	1.00	1.96	2.15
	5	1.00	2.20	2.76
	2.5	1.00	2.41	3.47
	1.0	1.00	2.43	4.24
	.2	1.00	1.66	3.63
20	10	1.00	2.22	2.53
	5	1.00	2.41	3.21
	2.5	1.00	2.64	4.16
	1.0	1.00	2.66	5.50
	.2	1.00	1.88	4.81

*X = slab thickness in mean free paths.
α_0 = energy of the incident photon in units of mc^2.
N_k = probability that a photon will be transmitted with exactly k collisions.

Table 11

$E_k/\alpha_0 e^{-X}$ FOR PHOTONS OF 0.2 TO 10 mc^2 NORMALLY INCIDENT ON SLABS OF THE PURE COMPTON SCATTERER*

X	α_0	$E_0/\alpha_0 e^{-X}$	$E_1/\alpha_0 e^{-X}$	$E_2/\alpha_0 e^{-X}$
1	10	1.00	.262	.0558
	5	1.00	.308	.0705
	2.5	1.00	.350	.0882
	1.0	1.00	.385	.109
	.2	1.00	.361	.119
2	10	1.00	.448	.150
	5	1.00	.524	.200
	2.5	1.00	.598	.247
	1.0	1.00	.653	.298
	.2	1.00	.606	.308
4	10	1.00	.713	.346
	5	1.00	.841	.473
	2.5	1.00	.964	.598
	1.0	1.00	1.04	.731
	.2	1.00	.933	.735
8	10	1.00	1.06	.660
	5	1.00	1.27	.970
	2.5	1.00	1.46	1.25
	1.0	1.00	1.57	1.58
	.2	1.00	1.36	1.51
12	10	1.00	1.31	.919
	5	1.00	1.56	1.40
	2.5	1.00	1.80	1.86
	1.0	1.00	1.93	2.36
	.2	1.00	1.67	2.21
16	10	1.00	1.54	1.21
	5	1.00	1.79	1.80
	2.5	1.00	2.06	2.48
	1.0	1.00	2.21	3.13
	.2	1.00	1.91	2.95
20	10	1.00	1.75	1.56
	5	1.00	1.98	2.18
	2.5	1.00	2.28	2.98
	1.0	1.00	2.43	3.85
	.2	1.00	2.11	3.71

*X = slab thickness in mean free paths.
α_0 = energy of incident photon in units of mc^2.
E_k = expected energy of a photon transmitted with exactly k collisions.

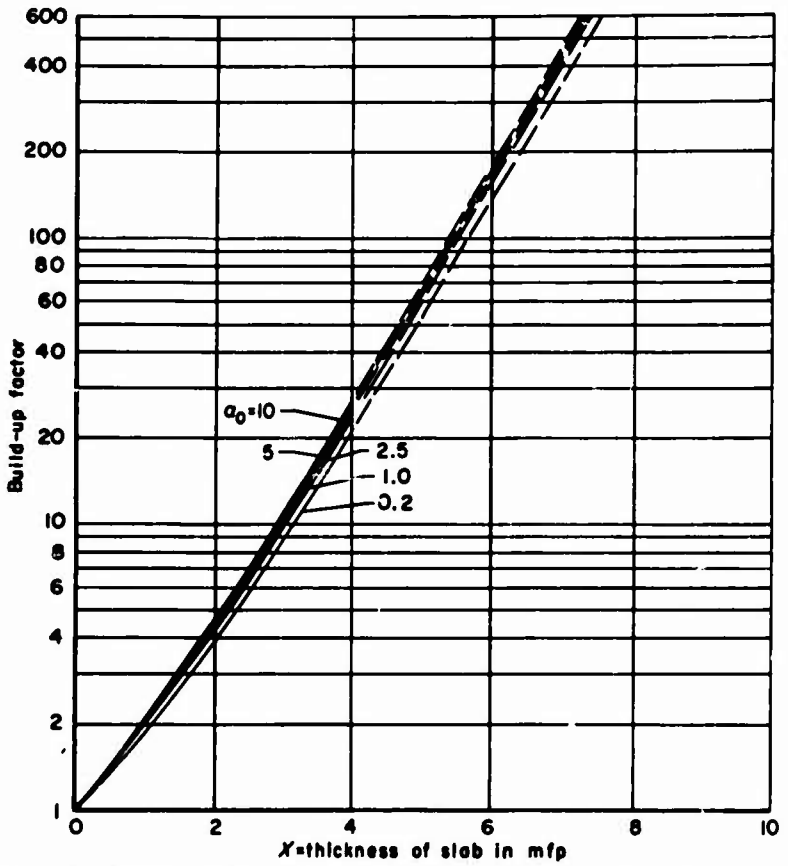

Fig. 20—Number build-up factors for photons of 0.2 to 10 mc^2 normally incident on a thin slab of the pure Compton scatterer

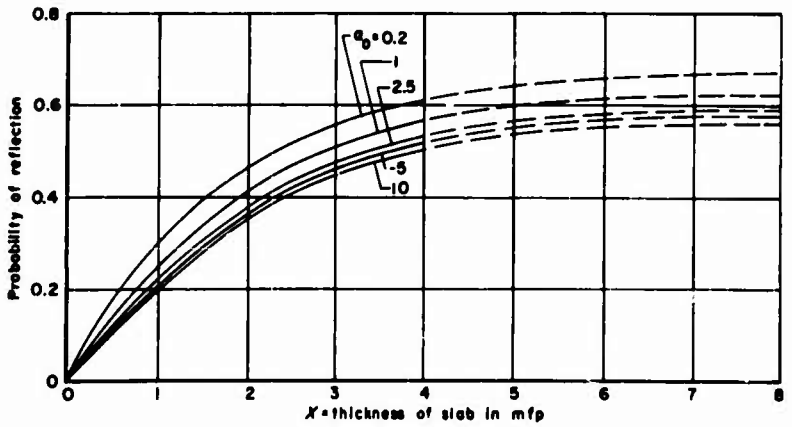

Fig. 21—Probabilities of reflection for photons of 0.2 to 10 mc^2 normally incident on a thin slab of the pure Compton scatterer

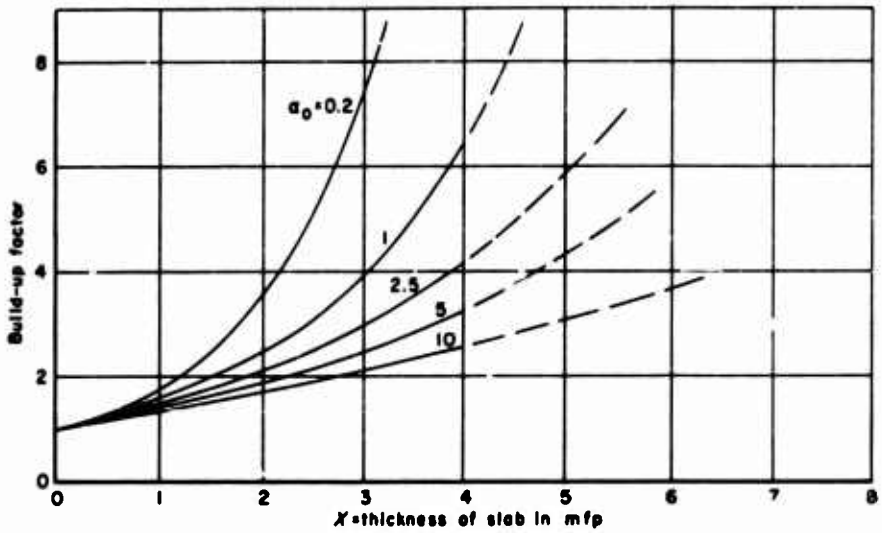

Fig. 22—Energy build-up factors for photons of 0.2 to 10 mc^2 normally incident on a thin slab of the pure Compton scatterer

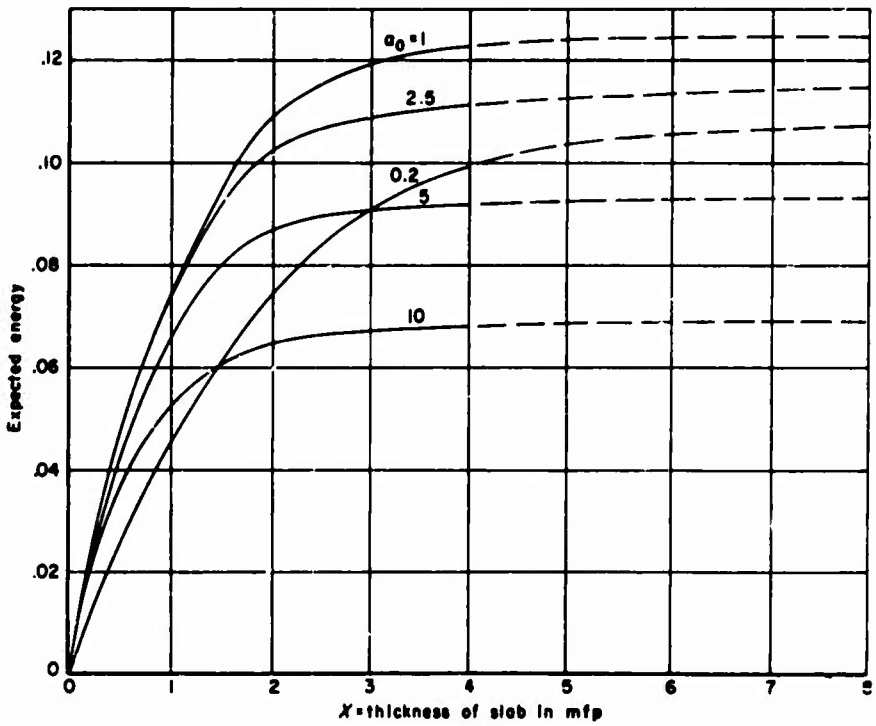

Fig. 23—Expected energies of reflection for photons of 0.2 to 10 mc^2 normally incident on a thin slab of the pure Compton scatterer

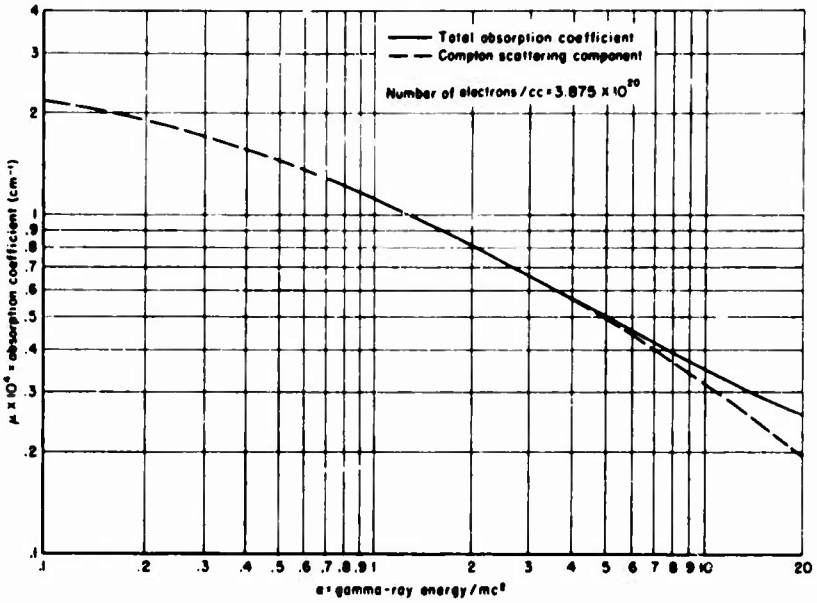

Fig. 24—Total absorption coefficient for air (taken from Ref. 9)

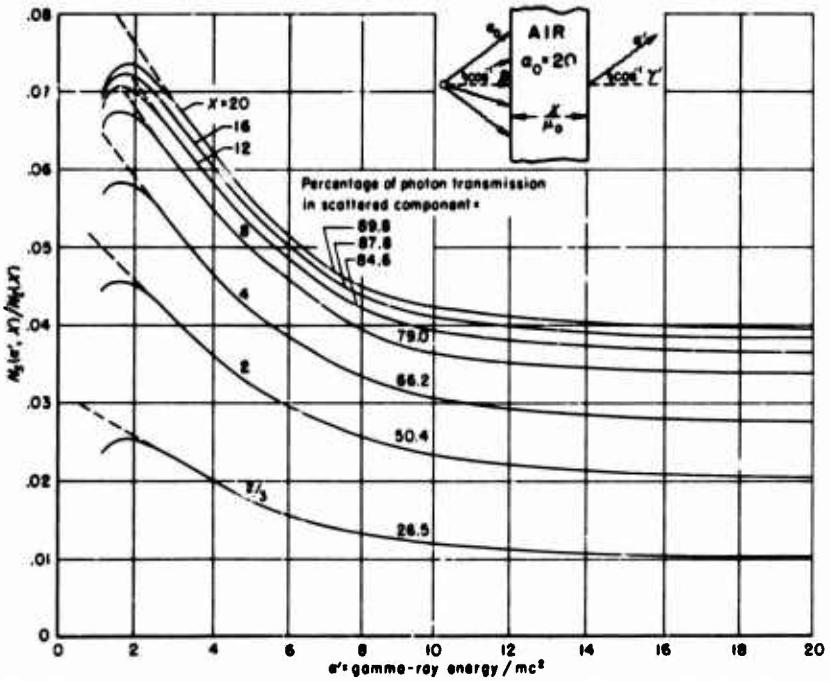

Fig. 25—Distributions of photons scattered by slabs of air, each distribution normalized by dividing by the total of all high-energy photons transmitted

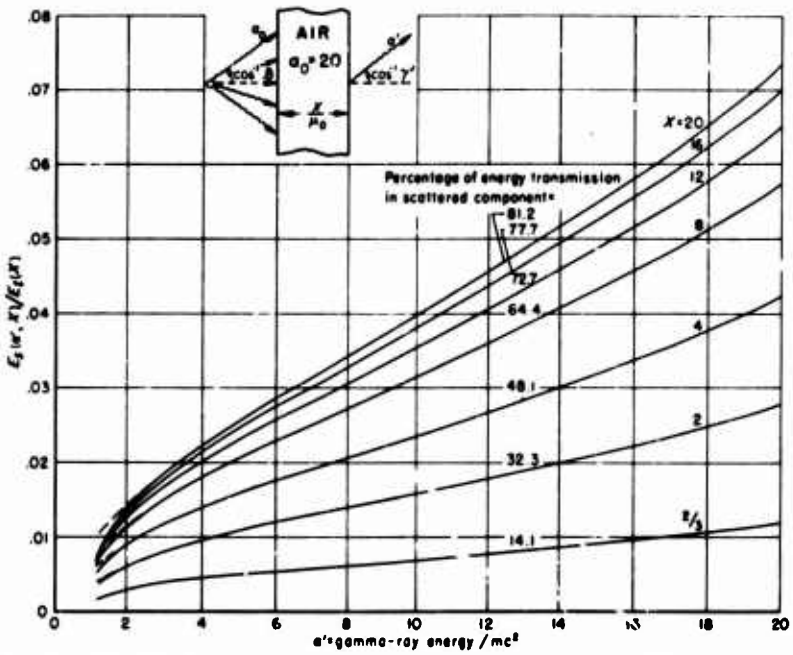

Fig. 26—Distributions of the energy in the photons scattered by slabs of air, each distribution normalized by dividing by the total energy in all transmitted photons

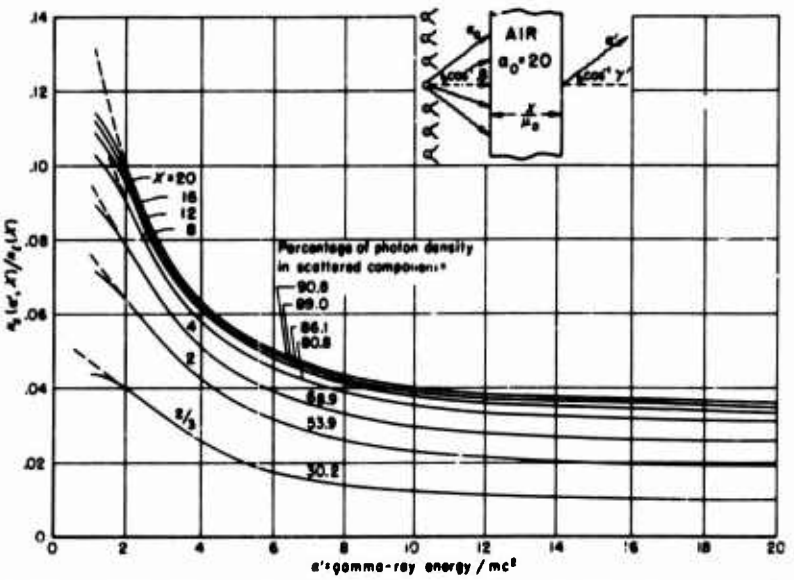

Fig. 27—Distributions of the density of the photons scattered by slabs of air, each distribution normalized by dividing by the density totaled over all high-energy photons transmitted

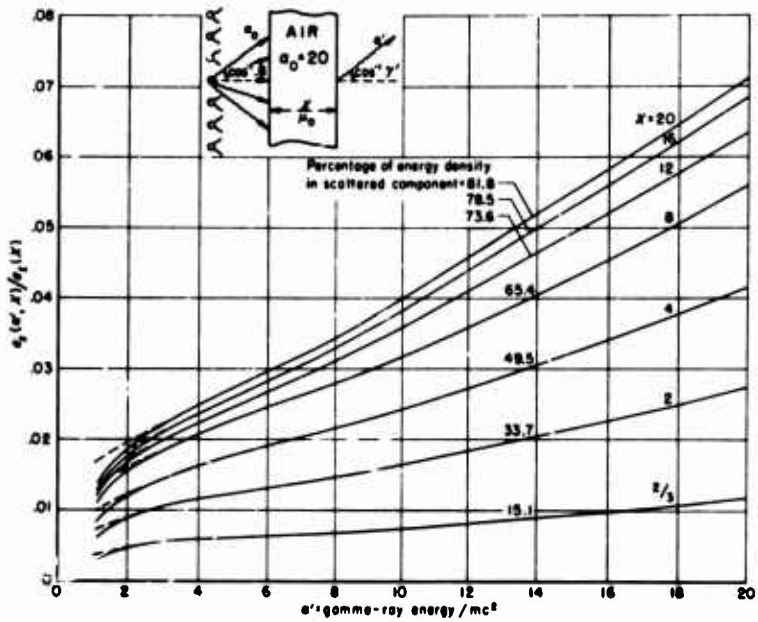

Fig. 28—Distributions of the energy density in the photons scattered by slabs of air, each distribution normalized by dividing by the energy density totaled over all transmitted photons

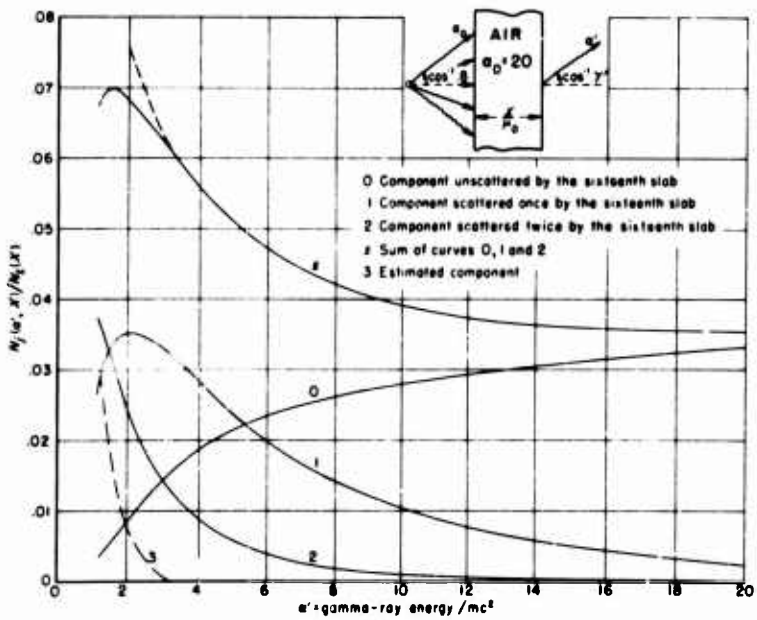

Fig. 29—Components of the distribution for the sixteenth elemental slab of air

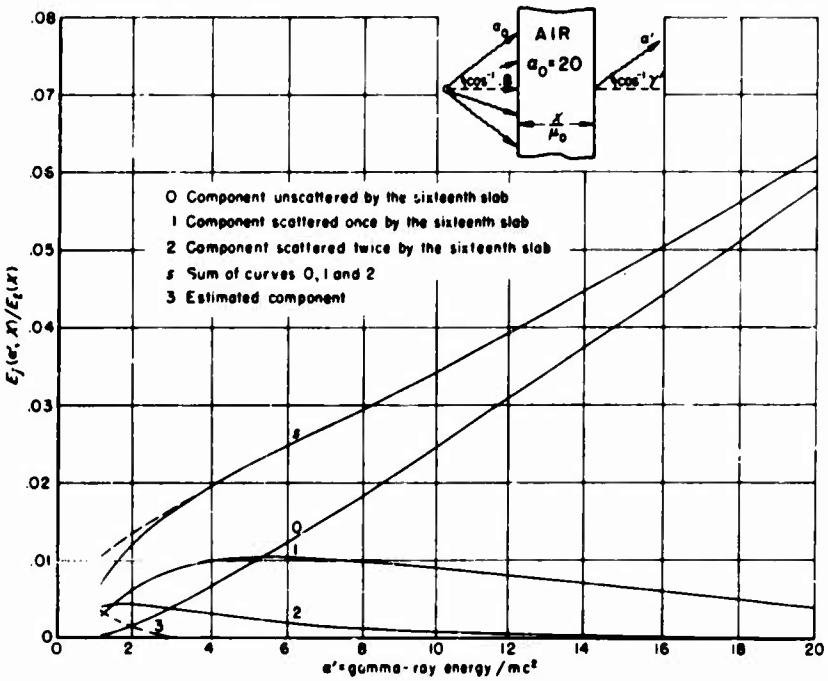

Fig. 30—Components of the energy distribution for the sixteenth elemental slab of air

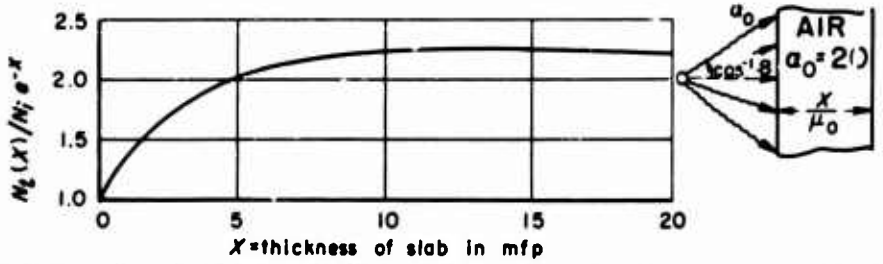

Fig. 31—The ratio for air slabs of the number of high-energy photons transmitted to the number incident, normalized by the factor $1/e^{-X}$

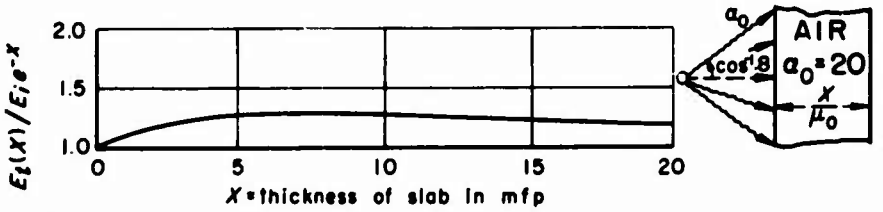

Fig. 32—The ratio for air slabs of the energy in transmitted photons to the energy in incident photons, normalized by the factor $1/e^{-X}$

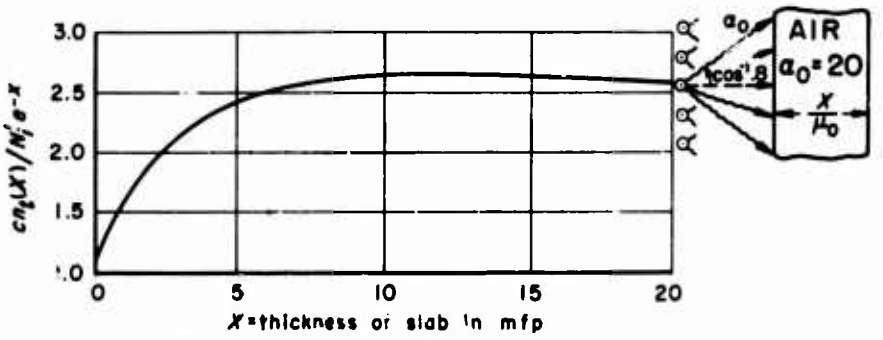

Fig. 33—The ratio for air slabs of the density of transmitted high-energy photons to the number incident per unit area per unit time, normalized by the factor c/e^{-X}

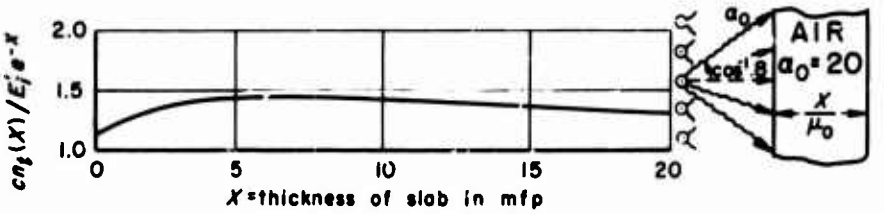

Fig. 34—The ratio for air slabs of the energy density in transmitted photons to the energy incident per unit area per unit time, normalized by the factor c/e^{-X}

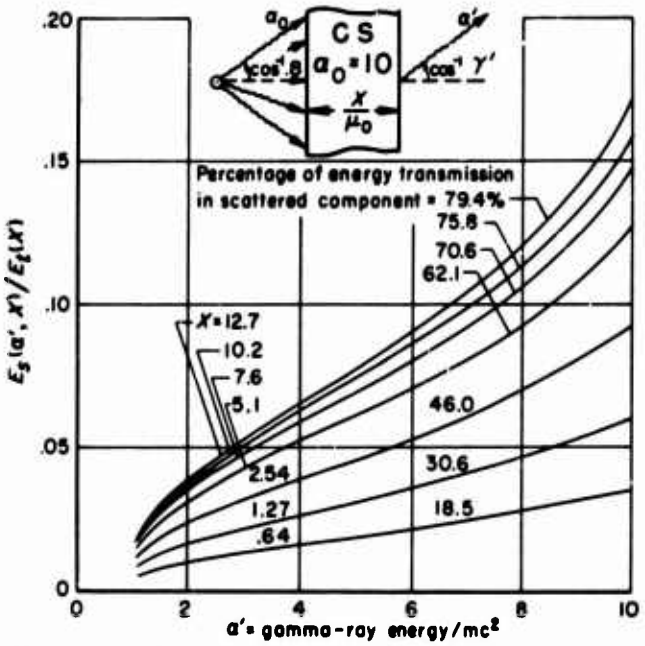

Fig. 35—Distributions of the energy in photons scattered by slabs of the pure Compton scatterer, each distribution normalized by dividing by the total energy in the transmitted photons

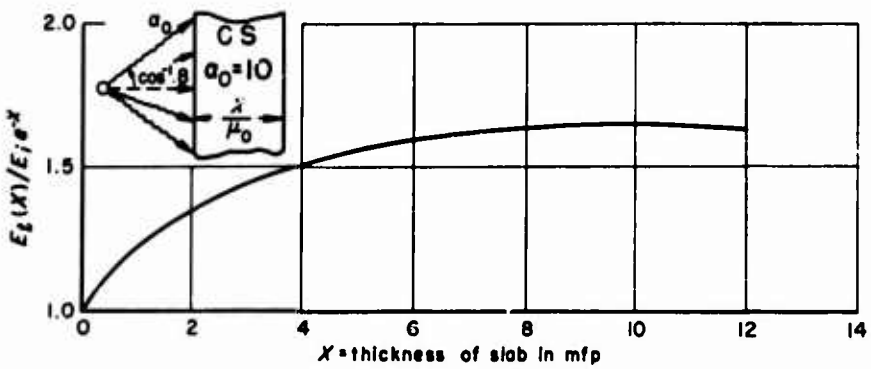

Fig. 36—The ratio for slabs of the pure Compton scatterer of the energy in transmitted photons to the energy in incident photons, normalized by the factor $1/e^{-X}$

V. TRANSMISSION OF PHOTONS OF ENERGIES LESS THAN 1 mc^2 THROUGH SLABS OF LEAD AND OF IRON

Results were presented in Sec. II for values of α_0 ranging between 1 and 20. Since α', the energy after collision, is related to α, the energy before collision, by the formula

$$\alpha' = \frac{\alpha}{1 + \alpha(1 - \cos\theta)},$$

where θ is the angle of deflection, one cannot calculate N_{k+1} at $\alpha_0 = 1$ without knowing N_k in the interval between $0.333\cdots$ and 1 mc^2. Consequently, the results given in Sec. II for $\alpha_0 = 20, 10, 5, 2.5, 1$ imply additional results at lower incident energies. These additional results were not recorded in Sec. II because they did not lie in the more or less arbitrarily selected range of interest between 1 and 20 mc^2 and because their irregularities tended to destroy the uniformity of the exposition of the first part. They do have some interest, however, so that it seems desirable to present them in a section by themselves, where the difficulties of their presentation can be minimized.

In the case of iron, no first-collision results were calculated below $\alpha_0 = 0.2$. This meant that second-collision results could be calculated to an energy no lower than $0.333\cdots$ mc^2 and third-collision results, no lower than 1 mc^2. Since only three scatterings and a lower energy limit of 1 mc^2 were contemplated, this retreat up the energy scale would have been acceptable. To calculate N_{k+1} at $\alpha_0 = 0.2$, however, it is only necessary to know N_k between the energies 0.2 and $0.1429\cdots$ mc^2. Since the variation in the functions fundamental to the calculations is not large within this narrow range, the computation of the results for the second scattering from the first and for the third from the second could, and did, proceed in the case of $\alpha_0 = 0.2$ with the help of an apparently safe extrapolation. Although the second- and third-collision results at $\alpha_0 = 0.2$ may have questionable accuracy, the spread of inaccuracy to larger values of α_0 is slow. A large error in the values of N_2 at 0.2 mc^2 causes a comparatively small error in the values of N_3 at $0.333\cdots$ mc^2, provided that N_2 is correct at the latter energy. The reason is, of course, that the interval near α_0 is by far the most important in the calculation of the transmission for an incident energy α_0.

The build-up factors for iron slabs at $\alpha_0 = 0.2$ are shown in Figs. 37 and 38. The contributions to the build-up factors of N_2/e^{-X}, N_3/e^{-X}, $E_2/\alpha_0 e^{-X}$, and $E_3/\alpha_0 e^{-X}$ are so small, because of large absorption by the photoelectric effect, that errors in their values due to the extrapolation mentioned above should not significantly affect the build-up factors. The values of N_k/e^{-X} and $E_k/\alpha_0 e^{-X}$ ($k = 1, 2, 3$) are not tabulated, but related functions F_k and G_k from which N_k/e^{-X} and $E_k/\alpha_0 e^{-X}$ can be quickly calculated are given in Sec. VI.

The treatment of lead in the low energy range does not parallel that of iron because of two marked differences in the total absorption coefficients. Figure 7 shows that the

absorption coefficient for lead has a much larger photoelectric component than that for iron and, in addition, has a discontinuity at 0.172 mc^2, where the energy reaches the limit of the K-level. So large is the absorption by the photoelectric effect for low energies that one might expect the build-up factors for normal, or nearly normal, incidence to be merely the sum of N_0/e^{-X} and N_1/e^{-X}, the latter contributing very little even for large values of X. The rapid convergence of r_k to zero in the low energy range, shown in Table 12, supports this thought. But the first-collision results in Table 13 for $\alpha_0 = 0.2$, 0.172+, 0.172−, 0.1 show that the discontinuity gives rise to values for N_1/e^{-X} very much larger than those for N_0/e^{-X}, and it is not instantly clear what to anticipate for the magnitudes of N_2/e^{-X}, N_3/e^{-X}, etc.

Let us now consider the case where $\alpha_0 = 0.172+$, $\gamma_0 = 1$, $X = 20$. Until the first collision, the photons move in a thick slab; the unscattered beam and the distribution of the points of first collision through the slab correspond to a value of $X = 20$. After the first collision the photons have a lower energy and the absorption coefficient is about one-fifth of its incident value. The probability that the photon will pass on through the slab after the first collision and the probabilities of its transmission with two or more scatterings are therefore governed more by a thickness of 4 mfp than by a thickness of 20 mfp. Because N_0 is associated with 20 mfp, N_0 is much smaller than N_1. Ordinarily, N_2 is considerably less than N_1 for a thickness of 4 mfp. In view of the rapid convergence to zero of r_k for $\alpha_0 = 0.172+$, one would expect N_2 to be not more than 10 to 20 per cent of N_1. A quick, rough calculation of N_2/e^{-X} at 20 mfp yielded the value 1350, which is less than 10 per cent of N_1/e^{-X}. It is clear then, that the probability of transmission of low-energy photons normally incident, or nearly so, on lead slabs is accurately obtained from the sum $N_0 + N_1$, with a moderate upward correction as the incident energy approaches 0.172 mc^2 from above.

Table 13 contains, in addition to N_1/e^{-X}, the corresponding number build-up factors. The factors should be accurate, since estimation has little or no role. Table 14 is the energy equivalent of Table 13.

* * *

Table 12

VALUES OF r_k and q_k FOR PHOTONS OF LOW INITIAL ENERGY IN LEAD AND IN IRON*

α_0	k	Lead		Iron	
		r_k	q_k	r_k	q_k
.2	0	1.00	.200	1.00	.200
	1	.0232	$.0^2398$	.409	.0442
	2	$.0^3934$	$.0^3140$	.129	.0121
	3	$.0^4473$	$.0^5613$	.0316	$.0^2279$
	4	$.0^5200$	$.0^6222$	$.0^2647$	$.0^3530$
.172+	0	1.0	.172		
	1	.0167	$.0^2252$		
	2	$.0^3957$	$.0^3136$		
	3	$.0^4478$	$.0^5586$		
	4	$.0^5188$	$.0^6215$		
.172--	0	1.00	.172		
	1	.0798	.0120		
	2	$.0^2458$	$.0^3648$		
	3	$.0^3229$	$.0^4280$		
	4	$.0^3900$	$.0^5103$		
.1	0	1.00	.100		
	1	.0229	$.0^2210$		
	2	$.0^3434$	$.0^4368$		
	3	$.0^5700$	$.0^6543$		
	4	$.0^7963$	$.0^8712$		

*r_k = the probability that a photon will survive its kth collision in an infinite homogeneous medium.

q_k = the expected energy of a photon surviving its kth collision in an infinite homogeneous medium.

α_0 = photon energy before the first collision in units of mc^2.

Table 13

N_1/e^{-X} AND $\sum_{k=0}^{\infty} N_k/e^{-X}$ FOR PHOTONS OF LOW ENERGY INCIDENT ON LEAD SLABS*

α_0	γ_0	X	N_1/e^{-X}	$\sum_{k=0}^{\infty} N_k/e^{-X}$	α_0	γ_0	X	N_1/e^{-X}	$\sum_{k=0}^{\infty} N_k/e^{-X}$
.2	1.0	1	.$0^2$87	1.01	.172+	1.0	1	.012	1.01
		2	.014	1.01			2	.030	1.03
		4	.021	1.02			4	.14	1.15
		8	.029	1.03			8	2.5	3.7
		12	.033	1.04			12	46.	53.
		16	.037	1.04			16	840.	930.
		20	.041	1.04			20	17000.	18000.
	.8	1	.$0^2$94	.79		.8	1	.012	.79
		2	.014	.62			2	.031	.64
		4	.020	.39			4	.12	.49
		8	.060	.20			8	1.8	2.0
		12	.30	.46			12	28.	29.
		16	2.7	6.5			16	560.	580.
		20	30.	300.			20	11000.	12000.
	.6	1	.$0^2$94	.52		.6	1	.013	.53
		2	.012	.28			2	.027	.29
		4	.020	.091			4	.096	.19
		8	.11	.13			8	1.3	1.4
		12	1.0	1.5			12	21.	22.
		16	10.	30.			16	320.	330.
	.4	1	.010	.23		.4	1	.013	.24
		2	.011	.062			2	.024	.074
		4	.020	.025			4	.075	.079
		8	.16	.19			8	.95	.98
		12	3.	3.			12	20.	21.
	.2	1	.$0^2$91	.028		.2	1	.012	.031
		2	.011	.011			2	.019	.020
		4	.022	.023			4	.057	.058
		8	.1	.1			8	.7	.8
	0	1	.$0^2$74	.$0^2$75		0	1	.$0^2$99	.010
		2	.$0^2$93	.$0^2$96			2	.015	.016
		4	.03	.03			4	.04	.05

*X = slab thickness in mean free paths.
α_0 = energy of incident photon in units of mc^2.
γ_0 = cosine of the angle between the slab normal and the incident path.
N_k = probability that a photon will be transmitted with exactly k collisions.

Table 13—continued

α_0	γ_0	X	N_1/e^{-X}	$\sum_{k=0}^{\infty} N_k/e^{-X}$	α_0	γ_0	X	N_1/e^{-X}	$\sum_{k=0}^{\infty} N_k/e^{-X}$
.172—	1.0	1	.027	1.03	.1	1.0	1	.$0^2$77	1.01
		2	.042	1.04			2	.013	1.01
		4	.063	1.07			4	.019	1.02
		8	.091	1.10			8	.027	1.03
		12	.11	1.12			12	.032	1.03
		16	.12	1.13			16	.036	1.04
		20	.13	1.14			20	.040	1.04
	.8	1	.026	.81		.8	1	.$0^2$81	.79
		2	.034	.64			2	.011	.62
		4	.034	.41			4	.011	.38
		8	.024	.16			8	.$0^2$78	.14
		12	.014	.066			12	.$0^2$52	.055
		16	.$0^2$80	.028			16	.$0^2$34	.022
		20	.$0^2$5	.012			20	.$0^2$23	.$0^2$9
	.6	1	.027	.54		.6	1	.$0^2$72	.52
		2	.025	.29			2	.$0^2$71	.27
		4	.015	.086			4	.$0^2$50	.075
		8	.$0^2$47	.010			8	.$0^2$22	.$0^2$72
		12	.$0^2$16	.$0^2$26			12	.$0^2$10	.$0^2$14
		16	.$0^3$6	.$0^2$11			16	.$0^3$5	.$0^3$6
	.4	1	.022	.25		.4	1	.$0^2$70	.23
		2	.014	.066			2	.$0^2$57	.056
		4	.$0^2$52	.$0^2$86			4	.$0^2$29	.$0^2$55
		8	.$0^2$10	.$0^2$13			8	.$0^3$70	.$0^3$75
		12	.$0^3$21	.$0^3$3			12	.$0^3$2	.$0^3$23
	.2	1	.015	.034		.2	1	.$0^2$48	.023
		2	.$0^2$63	.$0^2$75			2	.$0^2$24	.$0^2$29
		4	.$0^2$20	.$0^2$25			4	.$0^2$10	.$0^2$12
		8	.$0^3$4	.$0^3$5			8	.$0^3$4	.$0^3$4
	0	1	.$0^2$74	.$0^2$83		0	1	.$0^2$29	.$0^2$31
		2	.$0^2$30	.$0^2$36			2	.$0^2$15	.$0^2$17
		4	.$0^3$9	.$0^2$12			4	.$0^3$8	.$0^3$9

Table 14

$E_1/\alpha_0 e^{-X}$ AND $\sum_{k=0}^{\infty} E_k/\alpha_0 e^{-X}$ FOR PHOTONS OF LOW ENERGY INCIDENT ON LEAD SLABS*

α_0	γ_0	X	$E_1/\alpha_0 e^{-X}$	$\sum_{k=0}^{\infty} E_k/\alpha_0 e^{-X}$	α_0	γ_0	X	$E_1/\alpha_0 e^{-X}$	$\sum_{k=0}^{\infty} E_k/\alpha_0 e^{-X}$
2	1.0	1	.0²82	1.01	.172+	1.0	1	.010	1.01
		2	.013	1.01			2	.028	1.03
		4	.020	1.02			4	.13	1.14
		8	.028	1.03			8	2.4	3.5
		12	.033	1.03			12	41.	44.
		16	.036	1.04			16	800.	850
		20	.040	1.04			20	17000.	18000.
	.8	1	.0²87	.79		.8	1	.011	.79
		2	.013	.61			2	.028	.64
		4	.018	.39			4	.11	.48
		8	.052	.19			8	1.7	1.9
		12	.27	.36			12	28.	30.
		16	2.3	2.8			16	540.	570.
		20	23.	31.			20	13000.	14000.
	.6	1	.0²89	.52		.6	1	.011	.52
		2	.011	.28			2	.024	.29
		4	.017	.088			4	.084	.16
		8	.091	.11			8	1.2	1.3
		12	.87	1.0			12	17.	17.
		16	11.	14.			16	240.	260.
	.4	1	.0²87	.23		.4	1	.011	.23
		2	.010	.060			2	.020	.071
		4	.017	.021			4	.057	.071
		8	.15	.18			8	.85	.89
		12	3.1	4.			12	16.	17.
	.2	1	.0²77	.026		.2	1	.011	.029
		2	.0²83	.010			2	.017	.017
		4	.018	.022			4	.050	.051
		8	.25	.9			8	.6	.8
	0	1	.0²60	.0²68		0	1	.0²84	.0²85
		2	.0²75	.0²93			2	.0²23	.0²23
		4	.021	.03			4	.04	.04

*X = slab thickness in mean free paths.
α_0 = energy of incident photon in units of mc^2.
γ_0 = cosine of the angle between the slab normal and the incident path.
E_k = expected energy of a photon transmitted with exactly k collisions.

Table 14—continued

α_0	γ_0	X	$E_1/\alpha_0 e^{-X}$	$\sum_{k=0}^{\infty} E_k/\alpha_0 e^{-X}$	α_0	γ_0	X	$E_1/\alpha_0 e^{-X}$	$\sum_{k=0}^{\infty} E_k/\alpha_0 e^{-X}$
.172—	1.0	1	.024	1.03	.1	1.0	1	.$0^2$75	1.01
		2	.040	1.04			2	.012	1.01
		4	.061	1.06			4	.019	1.02
		8	.087	1.09			8	.026	1.03
		12	.10	1.11			12	.032	1.03
		16	.12	1.12			16	.035	1.04
		20	.13	1.13			20	.039	1.04
	.8	1	.025	.80		.8	1	.$0^2$74	.79
		2	.032	.64			2	.010	.62
		4	.033	.40			4	.011	.38
		8	.023	.16			8	.$0^2$81	.14
		12	.013	.064			12	.$0^2$51	.055
		16	.$0^2$78	.027			16	.$0^2$34	.022
		20	.$0^2$5	.012			20	.$0^2$22	.$0^2$9
	.6	1	.025	.54		.6	1	.$0^2$69	.52
		2	.023	.29			2	.$0^2$70	.27
		4	.013	.084			4	.$0^2$48	.074
		8	.$0^2$42	.010			8	.$0^2$21	.$0^2$70
		12	.$0^2$15	.$0^2$21			.2	.$0^3$97	.$0^2$14
		16	.$0^3$7	.$0^3$9			16	.$0^3$5	.$0^3$6
	.4	1	.019	.24		.4	1	.$0^2$68	.23
		2	.013	.064			2	.$0^2$55	.055
		4	.$0^2$46	.$0^2$77			4	.$0^2$27	.$0^2$53
		8	.$0^3$88	.$0^2$10			8	.$0^3$67	.$0^3$71
		12	.$0^3$2	.$0^3$3			12	.$0^3$2	.$0^3$2
	.2	1	.013	.032		.2	1	.$0^2$43	.023
		2	.$0^2$55	.$0^2$64			2	.$0^2$23	.$0^2$27
		4	.$0^2$15	.$0^2$18			4	.$0^2$10	.$0^2$10
		8	.$0^3$18	.$0^3$4			8	.$0^3$2	.$0^3$3
	0	1	.$0^2$63	.$0^2$69		0	1	.$0^2$27	.$0^2$27
		2	.$0^2$25	.$0^2$29			2	.$0^2$14	.$0^2$15
		4	.$0^3$8	.$0^2$1			4	.$0^3$5	.$0^3$6

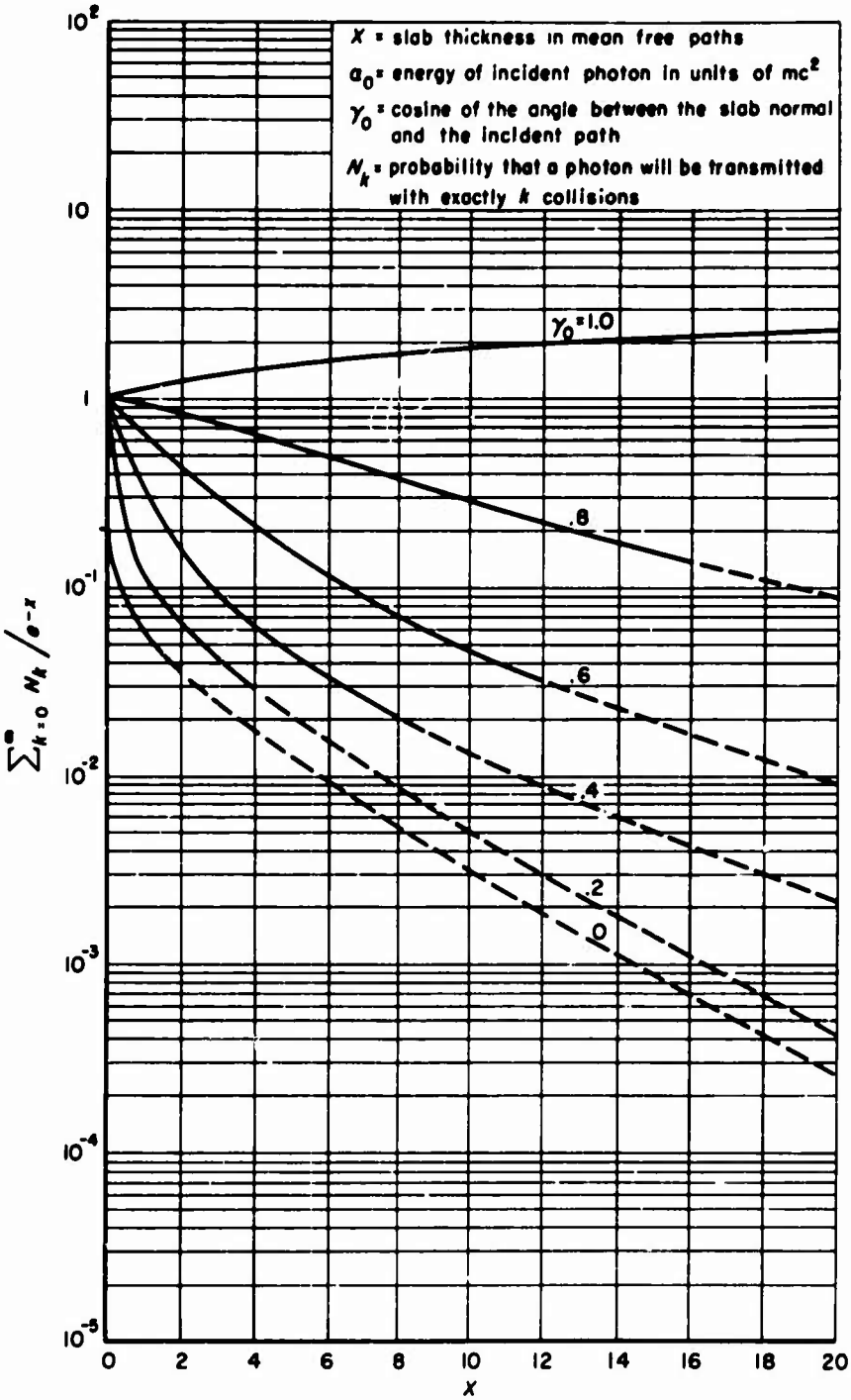

Fig. 37—Number build-up factors for iron slabs, $\alpha_0 = 0.2$

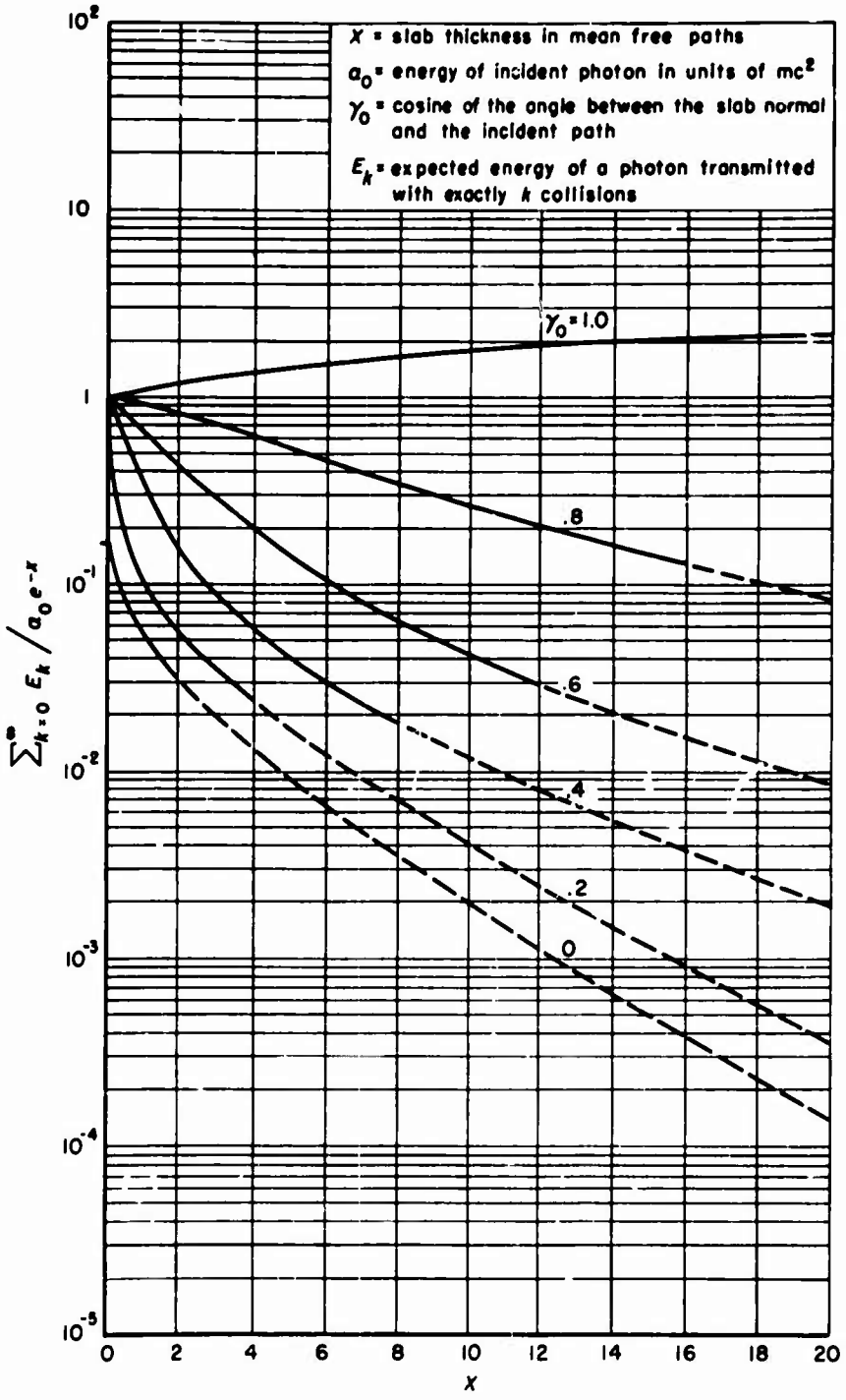

Fig. 38—Energy build-up factors for iron slabs, $\alpha_0 = 0.2$

VI. TRANSMISSION THROUGH SLABS OF AN ARBITRARY MATERIAL

A study of the dependence of gamma-ray transmission on the total absorption coefficient may be expected to extend the results for lead and for iron so as to give fair estimates for other materials. Some success is certain, since many materials have absorption coefficients not markedly different from those for lead and for iron.

Preliminary Discussion and Formulas

The study can best begin with a brief discussion of the total absorption coefficient. For the purposes of this section, the total absorption coefficient for an elemental material is conveniently written in the form

$$\mu = \nu\left(\sigma_{kn} + \frac{\sigma_{pp}}{Z} + \frac{\sigma_{pe}}{Z}\right),$$

where Z is the atomic number, σ_{kn} is the cross section per electron for Compton (or Klein-Nishina) scattering, and σ_{pp} and σ_{pe} are, respectively, the cross sections per atom for pair production and the photoelectric effect. The cross section σ_{kn} does not depend on the material, but σ_{pp} and σ_{pe} do, σ_{pp} being approximately proportional to Z^2 and σ_{pe} being roughly proportional to Z^5. Variation in the total absorption coefficient, therefore, comes from the variation in the electron density ν and the quantity $(\sigma_{pp}/Z + \sigma_{pe}/Z)$. The discussion below will attempt to determine qualitatively how changes in ν and $(\sigma_{pp}/Z + \sigma_{pe}/Z)$ affect transmission.

First, however, it is necessary to develop suitable forms for expressing N_k and E_k. The formula derived in Sec. II for the method of successive collisions becomes, for $k = 1$,

$$dN_1 = e^{-\mu_0 s} \cdot \mu_0\, ds \cdot \frac{\nu\, d\sigma}{\mu_0} \cdot N_0,$$

where

$$N_0 = e^{-(a-\gamma_0 s)\mu_1/\gamma_1},$$

and where μ_1 and γ_1 are, respectively, the values after the first collision for the absorption coefficient and the direction cosine. The integration with respect to s on the interval $(0, a/\gamma_0)$ yields

$$dN_1 = \nu e^{-\mu_1 a/\gamma_1} \frac{e^{-(\mu_0 - \mu_1\gamma_0/\gamma_1)a/\gamma_0} - 1}{\frac{\mu_1\gamma_0}{\gamma_1} - \mu_0}\, d\sigma.$$

Of the several forms possible for this result, the most useful was found to be

$$N_1 = KXe^{-X}\frac{e^{(1-1/\gamma_0)X}}{\gamma_0}\int_{\sigma_1}\frac{1-e^{-\zeta X/\gamma_0}}{\frac{\zeta X}{\gamma_0}}\frac{d\sigma}{r^2}$$

$$= KXe^{-X}F_1(X, \alpha_0, \gamma_0),$$

where

$$K = \frac{\nu r^2}{\mu_0} = \frac{r^2}{\left[\sigma_{kn} + \frac{\sigma_{pp}}{Z} + \frac{\sigma_{pe}}{Z}\right]_0},$$

$$\zeta = \frac{\mu_1\gamma_0}{\mu_0\gamma_1} - 1,$$

and where details of the two-dimensional integration implicit in the differential $d\sigma$ are of no interest for present purposes. This form for N_1, although of somewhat artificial appearance, evolved more or less naturally as the answer to certain needs, and it serves here to introduce into the discussion the parameters X and K and the functional F_1.

The parameter K is seen from its definition to be directly associated with absorption by pair production and the photoelectric effect. An increase in the quantity $(\sigma_{pp}/Z + \sigma_{pe}/Z)$ causes a decrease in K. Since photons do not survive absorption by pair production or the photoelectric effect, K is an index of photon destruction in the first collision. This, however, is incidental; a better index is the probability of surviving the first collision, $[\sigma_{kn}]_0/[\sigma_{kn} + (\sigma_{pp}/Z + \sigma_{pe}/Z)]_0$.

The quantity F_1 also is associated with absorption by pair production and the photoelectric effect, although not so directly as K. The formula for F_1 shows that a change from one material to another affects F_1 only through the function μ/μ_0. But μ/μ_0 is independent of electron density and therefore is identical for two Compton scatterers. Hence F_1 varies from one material to another only because larger or smaller components of pair production and the photoelectric effect appear in the total absorption coefficient.

To study further the dependence of F_1 on μ_1/μ_0, it is better to consider μ not as a function of the energy α in units of mc^2, but as a function of β, the reciprocal of α. In fact, throughout these calculations, β in most cases is a more suitable variable than α. Since the energy of a photon never increases with a collision, the function μ/μ_0 is needed only for the values of $\beta > \beta_0 = 1/\alpha_0$. Typical curves for μ/μ_0 are shown in Fig. 39; all the curves must have the value unity at $\beta = \beta_0$ and all must sooner or later rise as β increases. The function $[(1 - e^{-\zeta X/\gamma_0})/(\zeta X/\gamma_0)]$ governing F_1 shows that the more rapidly μ/μ_0 increases with β, the smaller the value of F_1. It can be seen from Fig. 39 that F_1 for molybdenum ($\alpha_0 = 20$) must lie between F_1's value for lead and for iron, that F_1 for copper is slightly larger than F_1 for iron, and so on. Clearly, an estimate of F_1 for other materials can be obtained by comparing one function μ/μ_0 with another.

Most of the development and discussion for F_1 can be duplicated for a general

function, F_k, defined by the relation

$$N_k = \frac{(KX)^k}{k!} e^{-X} F_k,$$

where F_k can readily be reduced to a multiple integral of a function of $2k$ variables.[8] This function of $2k$ variables is well represented in form and behavior by the case of $k = 1$ above. Like F_1, F_k (for $k > 1$) decreases as the average slope of μ/μ_0 increases, and like F_1, fair estimates of F_2 and F_3 can be obtained by comparing the function μ/μ_0 for the material under consideration with the same function for lead and for iron.

One is now in a position to see how ν and $(\sigma_{pp}/Z + \sigma_{pe}/Z)$ affect the build-up factor, which in terms of the F_k's becomes

$$\sum_{k=0}^{\infty} \frac{(KX)^k}{k!} F_k.$$

The question of the effect of electron density on transmission is disposed of by remarking that ν appears only in the dimensionless parameter X. The build-up factor, for example, is not affected by a change in ν, provided that the build-up factor is expressed as a function of X.

Absorption by pair production and the photoelectric effect is not handled so easily. There are two cases to consider: One is associated with pair production in the high energy range where the photoelectric effect is negligible; the other is associated with the photoelectric effect in the low energy range where pair production vanishes.

The cross section for pair production falls monotonically as β increases, and vanishes at $\beta = 0.5$, the reciprocal of the threshold energy for pair production. Therefore, pair production decreases the slope of μ/μ_0 and increases F_k. In fact, for heavy materials such as lead, σ_{pp}/Z is so large that in the range $\beta < 0.5$ its negative slope overcomes the positive slope of σ_{kn}. In such cases, μ/μ_0, for $\alpha_0 = 10, 20$, falls and stays below unity on a fairly large range of β before beginning to rise monotonically. This behavior leads to large F_k's (see the formula in the case of F_1), which tend to slow the convergence of the series for total transmission. But the large value of $[\sigma_{pp}/Z]_0$ associated with large F_k gives K a small value which tends to hasten the convergence. To see whether K^k or F_k is the more powerful, the results for lead and iron, $\alpha_0 = 20$, $\gamma_0 = 1$, in Tables 1 and 2 can be referred to. For $X = 1, 2, 4$, the tables show N_3/e^{-X}, N_4/e^{-X}, and N_5/e^{-X} to be smaller for lead than for iron; for $X = 8$, only N_5/e^{-X} is smaller; and for $X = 12, 16, 20$, the order is reversed for all three values. Since lead has a much greater proportion of pair production in its total absorption coefficient than iron, this case ($\alpha_0 = 20$, $\gamma_0 = 1$) indicates that K^k is the more powerful for thin slabs and F_k is the more powerful for thick slabs. However, the series for the total transmission must converge for all thicknesses. Hence, even for thick slabs, F_k dominates N_k/e^{-X} only for the first few values of k. Thus one is led to the conclusion that for high incident energies an increase in pair production always hastens the convergence of N_k to zero, although in the case of thick slabs a more rapid rise of N_k to a greater maximum may precede the appearance of the increased rate of convergence.

In the case of the photoelectric effect, K^k and F_k do not act one against the other. Since σ_{pe} is a monotonic increasing function of β, σ_{pe}/Z added to σ_{kn} increases the slope of μ/μ_0, and therefore decreases F_k as well as K. The result of increased photoelectric effect is always an increase, beginning immediately with N_1, in the rate of convergence of N_k to zero.

If one writes

$$\frac{E_k}{\alpha_0} = \frac{(KX)^k}{k!} e^{-X} G_k,$$

essentially all that has been done and said with regard to N_k and F_k applies almost unchanged to E_k/α_0 and G_k.

Fundamental Data

All the above discussion is in accordance with one's intuitive understanding. Since photons do not survive absorption by pair production and the photoelectric effect, one expects that an increase in the $(\sigma_{pp}/Z + \sigma_{pe}/Z)$ component will cause an increase in the rate of convergence of N_k. In the case of pair production, the delay with respect to k in the onset of the increased rate of convergence for thick slabs may not be foreseen, although even this may be anticipated by an intuitive consideration of mean-free-path lengths. The purpose of the discussion of K^k and F_k, however, is not to establish the intuitively obvious, but to prepare the ground for some quantitative results which make possible estimates of the transmission through slabs of materials other than iron or lead.

Most of the quantitative information supplementing the preceding qualitative results is supplied by Figs. 40*a* through 56. Figures 40*a* through 42*e* give F_1, F_2, and F_3 for lead and iron, $\alpha_0 = 20, 10, 5, 2.5, 1$, and Figs. 43*a* through 45*e* give G_1, G_2, and G_3. Figures 46*a*, 46*b*, and 46*c* show F_k and G_k $(k = 1, 2, 3)$ for iron, $\alpha_0 = 0.2$. The usefulness of Figs. 40*a* through 46*c* is increased by Figs. 47 through 56, which present the results of a partial study of the ideal case where μ/μ_0, as a function of β, is a straight line of slope λ. The dependence of F_1 and G_1 on λ for $\gamma_0 = 1$ is shown in Figs. 47 and 49 as a function of the parameter $(1 + \lambda)X$. Unfortunately, this parameter, which is easily shown to be a suitable argument for F_1 and G_1 when $\gamma_0 = 1$, is not valid for F_2 and G_2, so that in Figs. 48*a* through 48*e* and 50*a* through 50*e*, the dependence of F_2 and G_2 on λ must be given by an extensive set of curves. Figures 51 through 56 are intended to give an indication of the behavior of F_1 and G_1 when $\gamma_0 \neq 1$.

Estimates of the Build-up Factor for an Arbitrary Material

Figures 40*a* through 56 may be considered as giving a brief presentation of the accumulated experience with the method of successive scatterings. One may reasonably expect to extract from this experience useful information on the transmission of gamma rays through slabs of almost any material. It is clear that fair estimates of the trans-

mission with one, two, and three scatterings are possible and these estimates, in turn, can be expected to yield at least rough values for the build up factor. So much is estimation a matter of predilection and circumstance that to stop at this point and let the user develop, according to his needs and views, his own schemes and methods of estimation would probably be best. Nevertheless, a few useful aids to estimation and the rough estimates of the build-up factors for the elemental materials will be presented for the case of normal incidence.

Almost any method of arriving at an estimate for a particular material will depend on the choice of an average λ to correspond to the function μ/μ_0. Figures 57*a* through 57*e* should help in making the selection. They show μ/μ_0 for lead, iron, and the pure Compton scatterer, $\alpha_0 = 20, 10, 5, 2.5, 1$. For each incident energy, twelve vertical lines (four for the pure Compton scatterer, except when $\alpha_0 = 20$; four for iron; and four for lead) are marked with the symbols F_1, F_2, G_1, and G_2. On each line, points are tagged with numbers representing a value of X. These points determine the straight-line equivalents of μ/μ_0 according as F_1, F_2, G_1, or G_2 ($\gamma_0 = 1$) is the criterion.

Examination of Figs. 57*a* through 57*e* shows that the average slope has a definite pattern of behavior. Photons of high energy tend to be important to the transmission, more for large X than small, more for the first scattering than the second, and more for energy than number. Consequently, the straight-line equivalent is governed by the portion of μ/μ_0 near β_0, more for large X than small, more for the first scattering than the second, and more for energy than number. A good example of this ordering is seen in the case of lead, $\alpha_0 = 10$, where μ/μ_0 has enough concavity upward to make the phenomenon described strongly manifest.

In the case of lead, $\alpha_0 = 20$ (Fig. 57*a*), the concavity of μ/μ_0 is so great that a straight-line equivalent does not exist except for small thicknesses. Cadmium, the heaviest material for which the average slope exists for any appreciable thickness, takes the place of lead, although only the straight-line equivalents corresponding to F_1 and G_1 are given. To give some indication of the behavior of F_1 and G_1 for materials heavier than cadmium, the values of F_1 and G_1 for cadmium, tantalum, and lead are tabulated in the lower right-hand corner of Fig. 57*a*.

In some cases the errors in F_1, F_2, G_1, and G_2 and the sensitivity of the process determining the straight-line equivalent are such that a behavior was found just opposite to that expected. When it was obvious that the behavior exhibited was impossible, consistency was forced in whatever manner seemed to do the least violence to the data. In so doing, it became evident that Tables 1 through 4 were liberally sprinkled with errors less than 5 per cent, but contained few, if any, of the order of 10 per cent. This is not at all surprising in view of the fact that considerable effort was made to keep out gross errors, but many opportunities existed for small errors to creep in.

The first four terms of the infinite series for the build-up factor for an arbitrary material can be obtained with considerable ease and fair accuracy in the case of $\gamma_0 = 1$ if Figs. 40*a* through 56 are used. Attention then turns to a way of estimating the remainder of the series with comparable ease and accuracy.

Suppose that photons of the same energy and direction are incident upon two slabs of the same thickness in mean free paths, but of different materials. If the series for the two

build-up factors converge to different values, as they presumably will, the cause must lie in the fact that absorption by pair production and the photoelectric effect appears in different proportions in the two total absorption coefficients. Realizing this, one may think to attempt to correlate the remainder of the series with the amount of absorption by pair production and the photoelectric effect. The difficulty with this approach lies in defining a variable which suitably measures "destructive" absorption and is also easily evaluated for each material.

However, for the rough correlation contemplated, there is no need to be too exacting. A quantity such as

$$\frac{1}{b}\int_{\beta_0}^{\beta_0+b} \frac{\left(\frac{\sigma_{pp}}{Z}+\frac{\sigma_{pe}}{Z}\right)}{\sigma_{kn}+\left(\frac{\sigma_{pp}}{Z}+\frac{\sigma_{pe}}{Z}\right)}\,d\beta$$

is undoubtedly adequate since, if b is properly chosen, it measures destructive absorption in a region of significance. It therefore might be used for the correlation, but when examined, it turns out to be so nearly a linear function of Z that Z itself, by virtue of its greater convenience, becomes the better choice.

When an attempt was made to fix the preceding concept in a working scheme, it was found, as is usually the case, that some modification of the original idea served better. It turned out to be more convenient, and almost as accurate, to let the remainder begin with N_2/e^{-X} rather than with N_4/e^{-X}, and to correlate with Z for constant N_1/e^{-X} rather than for constant X. Since N_1/e^{-X} and the build-up factor tend to rise and fall together, the correlation for constant N_1/e^{-X} is as accurate as, if not more accurate than, that for constant X. Some loss of accuracy results from including N_2/e^{-X} and N_3/e^{-X} in the remainder, but investigation showed that the accuracy gained by estimating N_2/e^{-X} and N_3/e^{-X} separately hardly warranted the extra work.

The correlation of $\sum_{k=2}^{\infty} N_k/e^{-X}$ with Z for constant N_1/e^{-X} is given in Fig. 58. The curves are determined by only two points, $Z = 26$ and $Z = 82$, except when N_1/e^{-X} is small. Since $(\sigma_{pp}/Z + \sigma_{pe}/Z)$ vanishes with Z, $Z = 0$ corresponds here to the pure Compton scatterer. For small values of N_1/e^{-X}, the estimates of the build-up factor for the Compton scatterer provide a point at $Z = 0$. Two and three points certainly constitute the minimum number for any degree of accuracy, but it must be remembered that the remainder is a monotonic decreasing function of Z with a presumably monotonic derivative. Such being the case, inaccuracies in the curves due to an insufficient number of determining points can hardly be large according to the standards of shielding calculations.

With Figs. 57*a* through 57*e* and 58 in hand, one can easily estimate the build-up factors for slabs of those materials for which the total absorption coefficient is available. In accordance with the principles by which Figs. 57*a* through 57*e* and 58 were constructed, the total absorption coefficients given in Ref. 9 for carbon, aluminum, molybdenum, cadmium, tantalum, and uranium were used to obtain build-up factors. These build-up factors with the factors for lead, iron, and the Compton scatterer were plotted against Z for constant parameter X. The resultant figures (Figs. 59*a* through 59*e*) contain,

with some exceptions, estimates of the build-up factor for photons normally incident on slabs of thickness 1, 2, 4, 8, 12, 16, and 20 mfp for all elemental materials.

Reliability of Estimates

When one comes to considering the accuracy of the build-up factors given in Figs. 59*a* through 59*e*, one must first remember that the estimates can be no better than those for lead and for iron. The question is, Is the process of estimation such as to increase this inherent error? The sources of additional error lie in the choice of the average slope of μ, μ_0 and in the manner in which the curves of Fig. 58 are drawn. Errors due to the latter source are seen to be enormous when Z is small, but negligible compared with the inherent error when Z is large, say, greater than 26. As long as the monotonic character of the curves is retained, only relatively small changes in the readings for $Z > 26$ can result. Much more important is the error due to an incorrect average slope. If μ/μ_0 departs far from linearity, as it does for large Z and large α_0, the average slope is not easy to determine. For $\alpha_0 = 10, 20$, the values of N_1/e^{-X} were determined by direct calculation; for all other incident energies, a straight-line equivalent was used. Errors of as much as 5 per cent appeared in N_1/e^{-X} from an incorrect estimate of the average slope. Errors of this magnitude in N_1/e^{-X} seemed to translate into errors in the build-up factor of about one half the inherent error. In other words, it is necessary to suppose that, for $Z > 26$, the errors in the build-up factors of Figs. 59*a* through 59*e* are about half again those stated in Sec. II for the build-up factors for lead and iron slabs. This would mean an error approximately proportional to X and reaching about 30 per cent at $X = 20$.

Whatever the accuracy of the build-up factors of Figs. 59*a* through 59*e* may be, the behavior, in the large, is certainly correct as shown. For $\alpha_0 = 1, 2.5$, the build-up factor for large X is a rapidly decreasing, monotonic function of Z. For $\alpha_0 = 5$, the build-up factor is still a monotonic decreasing function, but it is not so rapidly decreasing, particularly in the middle range of Z. A slight sinuosity, noticeable in the case of 5 mc², develops into a pronounced minimum and maximum by the time α_0 has reached 10 and becomes so large at $\alpha_0 = 20$ that the maxima for $X = 16$ and $X = 20$ are off the scale of the figure. The explanation for this whole pattern of behavior is implicit in the previous discussion of the effect of absorption by pair production and the photoelectric effect. For the low energies of 1 and 2.5 mc², photoelectric absorption controls the magnitude of the build-up factor. As Z increases, the photoelectric absorption increases and the build-up factor decreases rapidly. The inflections noticed in the case of 5 mc² mark the appearance of the effect of absorption by pair production. The very large values of N_k/e^{-X} for the first values of k in the cases of 10 and 20 mc² cause the build-up factors to be so large that a minimum appears in the middle range of Z. However, as Z increases past the middle range, the diminishing effect of destructive absorption again takes control and a maximum is formed.

On examining the curves in the neighborhood of $Z = 0$, one notices the steepness at zero, particularly as the incident energy increases. One may feel that more steepness at $Z = 10$ and less at $Z = 0$ would be correct. Since the region of greatest error is that

of small Z, this feeling may be justified. However, a small amount of absorption acting through a decreased K can diminish greatly the sum of a slowly converging series In any case, the data seemed not to permit a less precipitous descent from the value at zero.

Another phenomenon in the small Z range, which may catch the eye as a possible irregularity, is the existence, when X is large and Z is near zero, of values of the build-up factor which are larger for 1 mc² than for 2.5 mc². If one happens to remember that the build-up factors for the Compton scatterer for small X, given in Fig. 20, increase with α_0, one may again suspect the existence of an error.

Since the curves of Figs. 59*a* through 59*e* for large X and small Z depend entirely on the build-up factors for iron, the source of the error, if the error exists, must be found in the factors for iron. Figures 4*d* and 4*e* show that the iron build-up factor for 1 mc² is slightly less than that for 2.5 mc² when X is small, but larger when X is large, reaching, at $X = 20$, a value some 15 per cent above the value for 2.5 mc². The appearance of the total absorption coefficient for iron does not seem to support this behavior of the build-up factors relative to each other. Figure 7 shows that the total absorption coefficient for iron is almost entirely Klein-Nishina scattering between 2.5 and 1 mc²; at about 1 mc² the total absorption coefficient begins, as α decreases, to rise very rapidly above its Klein-Nishina component. Since a photon of energy 1 mc² is at the beginning of the region of large photoelectric absorption, one might well think that photoelectric absorption would surely reduce the build-up factor for 1 mc² at $X = 20$ far below that for 2.5 mc² and that, consequently, a very large error, much larger than 20 per cent, must exist in one or the other of the build-up factors.

The total absorption coefficient, when plotted against α, as in Fig. 7, is somewhat misleading with regard to the effect of photoelectric absorption on the build-up factors. Figures 57*d* and 57*e*, which show μ/μ_0 versus $\beta - \beta_0$, give a more accurate concept of the effect of photoelectric absorption because the abscissa $\beta - \beta_0$ provides a better scale than does α for comparison of the energy degradation at different energies. These figures show that when β is in the range near β_0, the divergence of the function μ/μ_0 for iron from that for the Compton scatterer is not much greater for 1 mc² than it is for 2.5 mc². This means that photoelectric absorption will act to reduce N_k/e^{-X} for the first values of k with out little more strength in the case of 1 mc² than in the case of 2.5 mc². Support of this last statement is found in Table 2, where approximately identical values of both N_1/e^{-X} and N_2/e^{-X} appear for the two energies at the same values of X. These values, incidentally, can be verified with fair accuracy by the method of straight-line equivalents. Since N_1/e^{-X} and N_2/e^{-X} are nearly identical, the build-up factor for 1 mc² cannot be much smaller than that for 2.5 mc². Consequently, there is no great reason to suppose that an error at $X = 20$ is larger than the 20 per cent stated in Sec. II.

While comparing values of N_k/e^{-X} in Table 2, one notices that, at $X = 20$, N_3/e^{-X} has a value for 1 mc² some 8 per cent above its value for 2.5 mc². This undoubtedly explains why the estimate of the build-up factor for 1 mc² exceeded that for 2.5 mc² by 15 per cent, but it is difficult to believe, in the face of the fact that Table 5 shows the convergence of r_k to be more rapid for 1 mc² than for 2.5 mc², that on the third scattering the transmission for 1 mc² can exceed that for 2.5 mc² by this much. It is easier to believe that the difference in N_3/e^{-X} for the two energies is the consequence of

error and that the observed behavior of the build-up factors for large X, although not proof of error larger than that stated in Sec. II, is nevertheless evidence of error.

This conclusion, however, must be accepted with reservation. In Table 10, which gives the values of N_1/e^{-X} and N_2/e^{-X} for the pure Compton scatterer, one finds that N_1/e^{-X} at $X = 20$ has nearly the same value for both 1 and 2.5 mc^2, but that the value of N_2/e^{-X} for 1 mc^2 exceeds the value for 2.5 mc^2 by about 30 per cent. If a similar inequality holds for N_3/e^{-X}, as seems likely, then the 8 per cent inequality observed in the case of iron may not be an error at all. If the 8 per cent inequality in N_3/e^{-X} is not an error, then the 15 per cent inequality in the build-up factor, in all probability, is not an error.

The preceding comparison of the transmission for 1 and 2.5 mc^2 in the case of iron raises the question of how transmission depends on α_0 in general. The answer can best be formulated in terms of the pure Compton scatterer, since this fictitious material, considered on the basis of total absorption coefficient, is the most general, or at any rate the most fundamental, material.

Suppose that two beams, monoenergetic but of different energies, are normally incident, first one and then the other, on a slab of the pure Compton scatterer; then α_0 is the only variable that differs in the two cases. This difference appears in the calculations in two ways: (1) as a difference in the distribution of the angular deflection and (2) as a difference in the function μ/μ_0.

Since large angles of deflection become more probable as the incident energy diminishes,* one expects N_f, the probability of transmission with one collision, to decrease and expects N_b, the probability of reflection with one collision, to increase as α_0 decreases. This will certainly be true, unless the decrease in average slope of μ/μ_0 produces a sufficiently powerful countereffect. The slope of μ/μ_0 can act only through F_1 in the case of transmission and through a function very like F_1 in the case of reflection. The formula for F_1 shows that as X decreases to zero, the effect of the average slope of μ/μ_0 disappears. It follows that the expected decrease in N_f and the expected increase in N_b surely occur for thin slabs. This has already been observed in the data of Table 6, although it will be noticed that even a slab of thickness 0.5 mfp is not thin enough to cause N_f to decrease with α_0 when α_0 is large. It also follows that the build-up factor for very thin slabs will decrease as α_0 decreases. This too has been observed, in this instance in the build-up factors of Fig. 20.

As slab thickness increases, the average slope of μ/μ_0 begins to act powerfully, so that in suitable data one should be able to see evidence of its effect. The rise and fall of N_f and N_{ff} in Table 6 and of N_1/e^{-X} and N_2/e^{-X} ($N_1 = N_f$, $N_2 = N_{ff}$) in Table 10 as α_0 ranges between 10 and 0.2 is evidence of more than one cause of variation. In fact, if $\alpha_0 = 0.2$ had not been included in Table 10, N_1/e^{-X} and N_2/e^{-X} for thick slabs would have appeared to be monotonic decreasing functions of α_0 and therefore would have seemed to be governed almost entirely by the average slope. Hence, to the extent that transmission is controlled by photons which have experienced only forward scatterings, the effect of the average slope is to reverse, when X is sufficiently large, the relative

* See Ref. 10, Fig. 7, or Ref. 4, Table II.

positions of the curves for the build-up factors of Fig. 20.

However, photons which have experienced one or more backward scatterings are a large component of the transmission through even moderately thick slabs of the pure Compton scatterer. Therefore the curves of Fig. 20, if determined for large values of X, will presumably not cross one over the other as X increases but, since photons in a long passage of many collisions tend to lose all "memory" of their incident energy, will approach each other asymptotically.

The discussion of the number build-up factor for an arbitrary material can be duplicated for energy with a few appropriate and obvious changes. Figure 60 gives the correlation of $\sum_{k=2}^{\infty} E_k/\alpha_0 e^{-X}$ with Z for constant $E_1/\alpha_0 e^{-X}$; Figs. 61*a* through 61*e* give the estimated energy build-up factors for slabs of an arbitrary material.

* * *

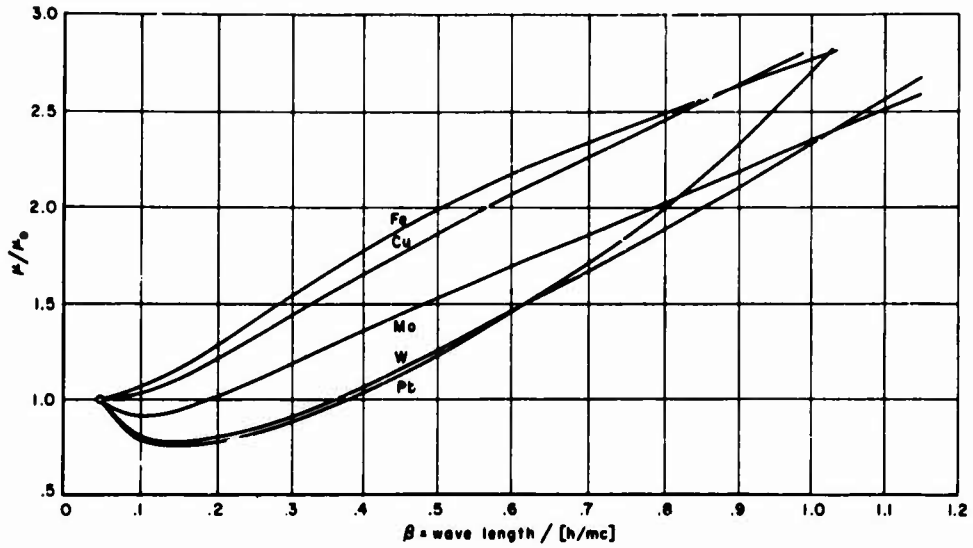

Fig. 39—μ/μ_0 vs β for several materials, $\alpha_0 = 20$

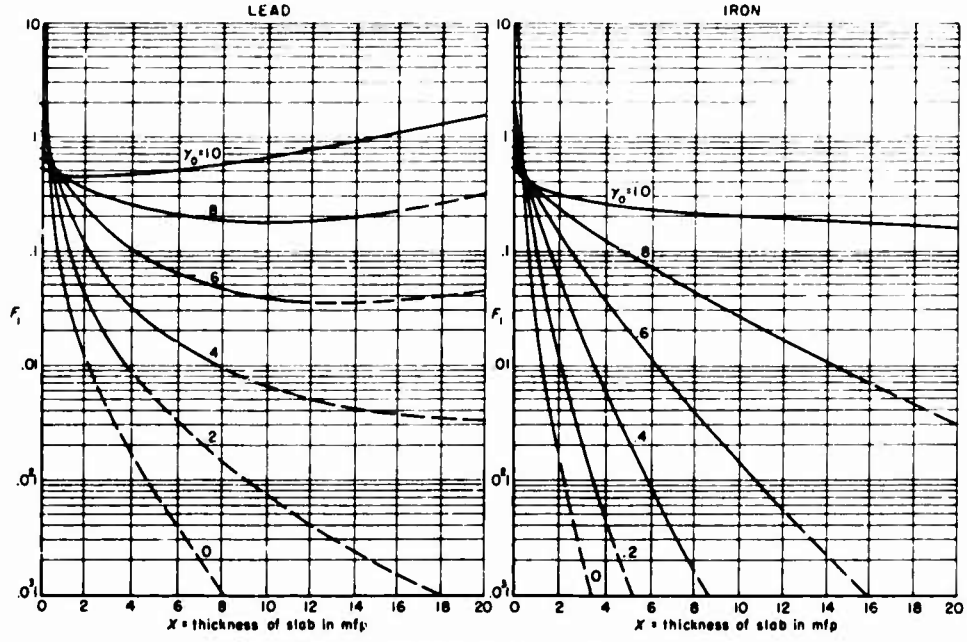

Fig. 40a—F_1 vs X for lead and iron, $\alpha_0 = 20$

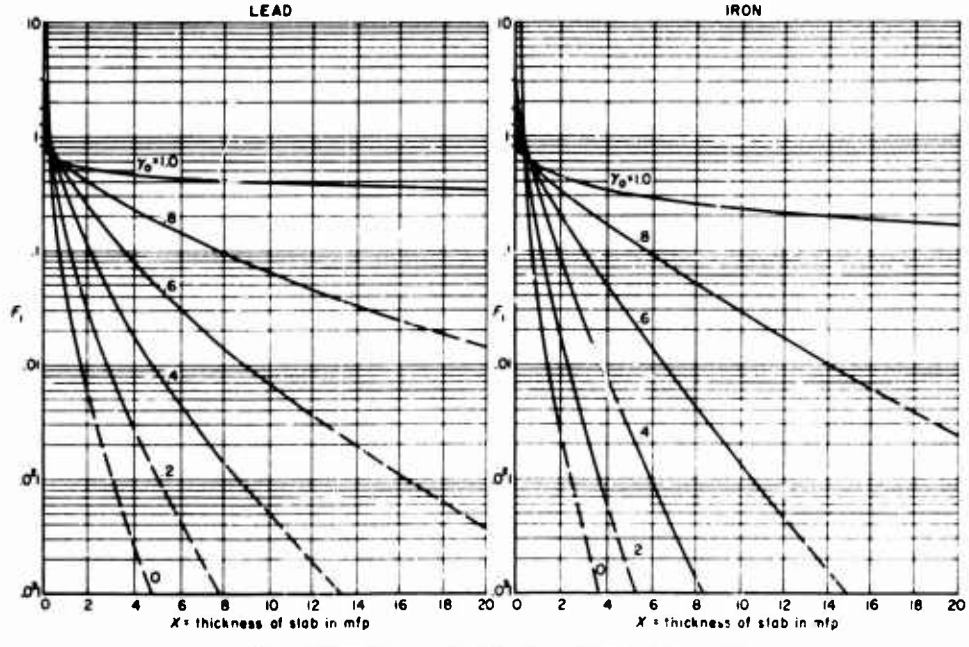

Fig. 40b—F_1 vs X for lead and iron, $\alpha_0 = 10$

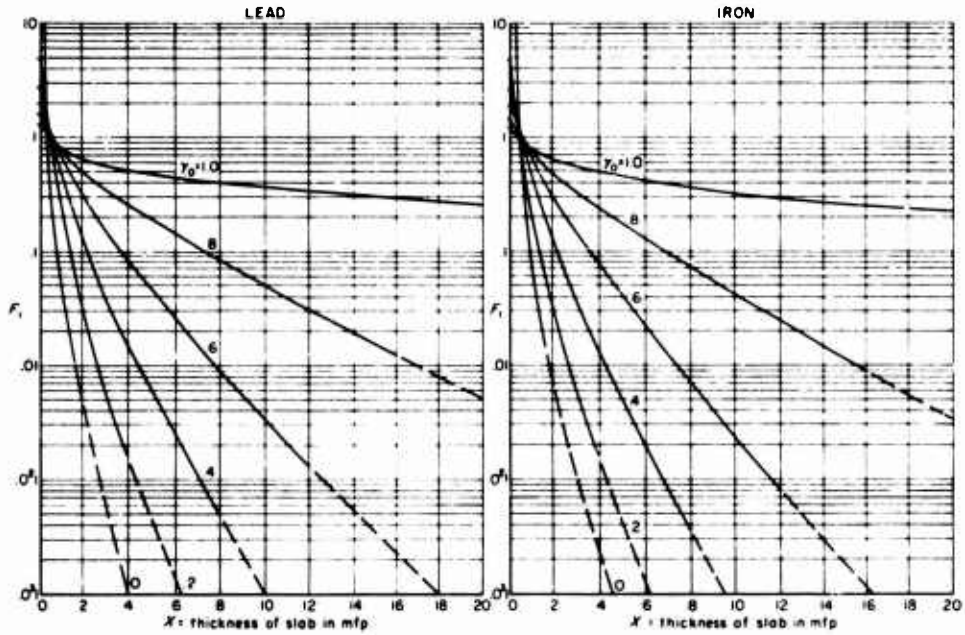

Fig. 40c—F_1 vs X for lead and iron, $\alpha_0 = 5$

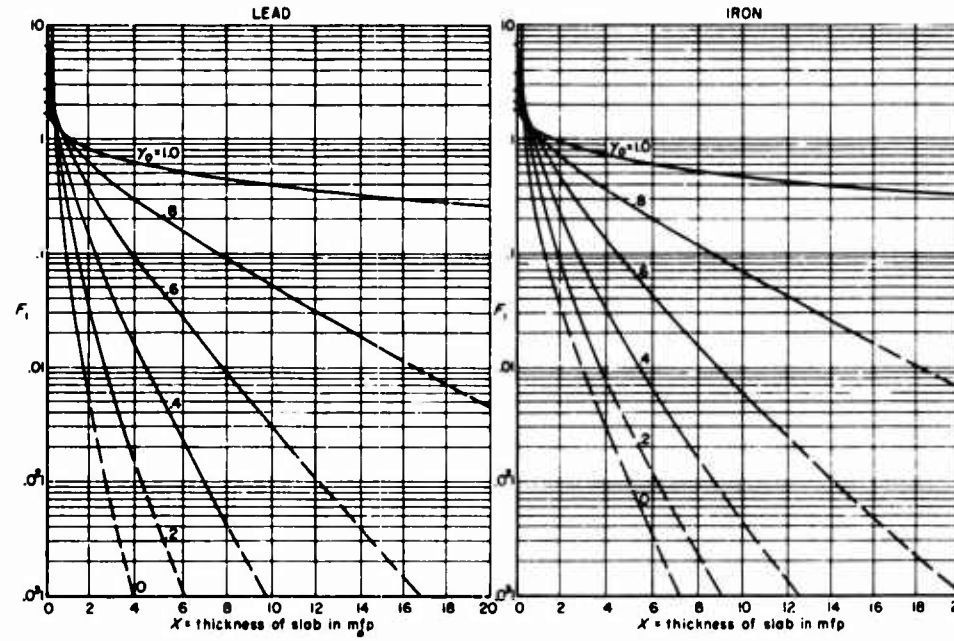

Fig. 40d—F_1 vs X for lead and iron, $\alpha_0 = 2.5$

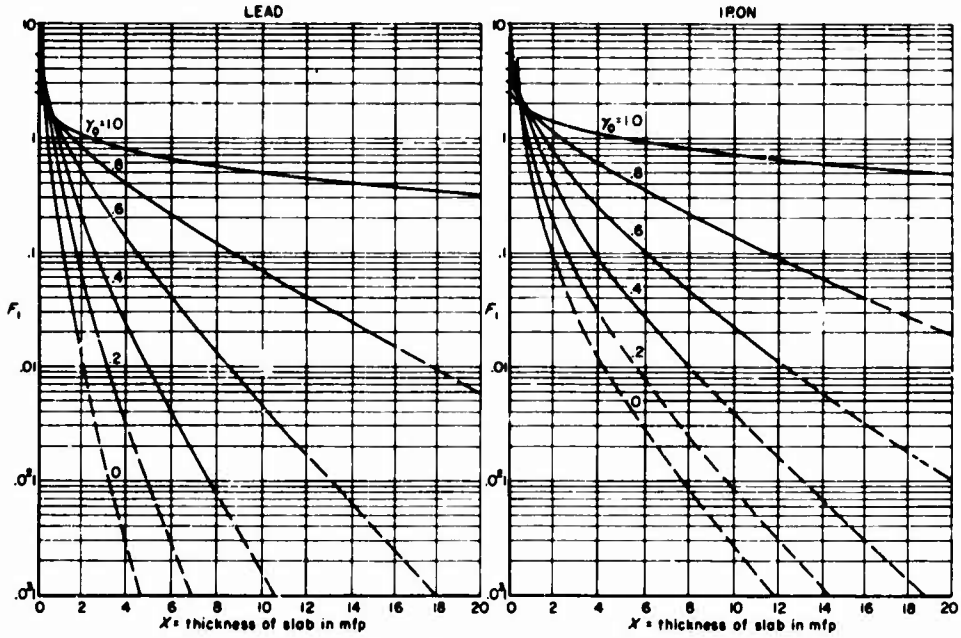

Fig. 40e—F_1 vs X for lead and iron, $\alpha_0 = 1$

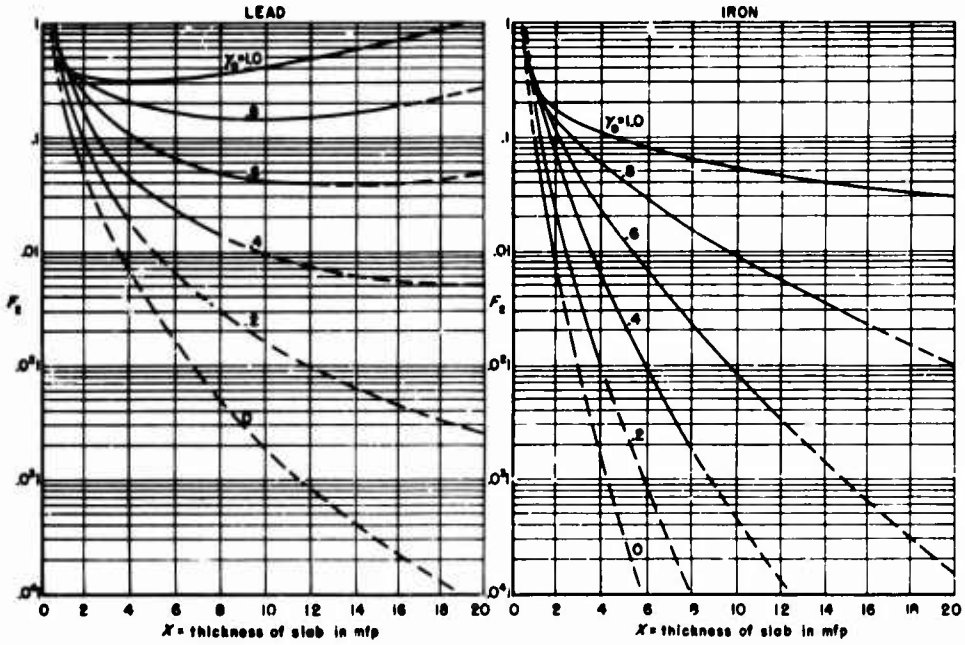

Fig. 41a—F_2 vs X for lead and iron, $\alpha_0 = 20$

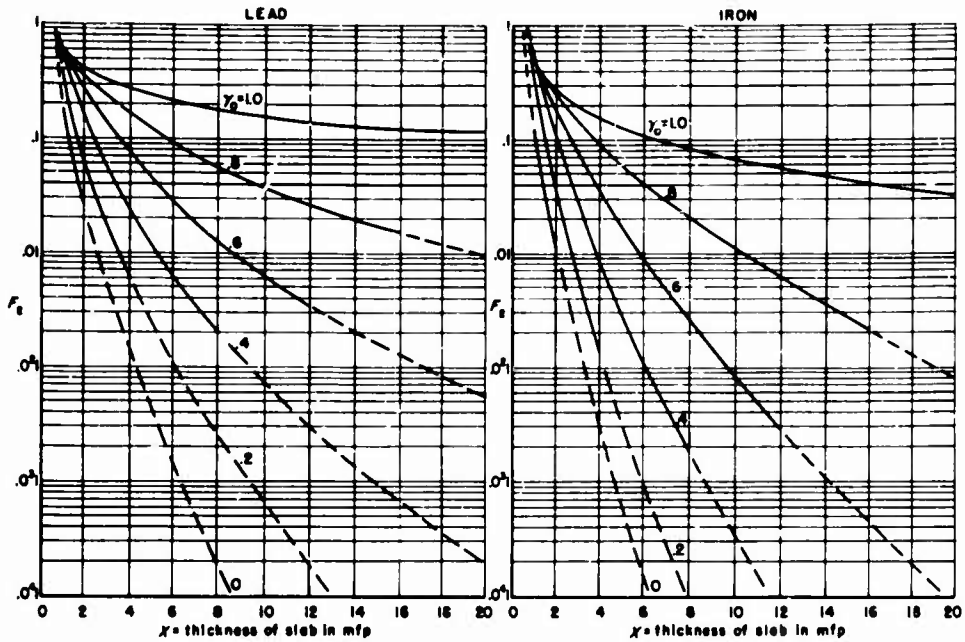

Fig. 41b—F_2 vs X for lead and iron, $\alpha_0 = 10$

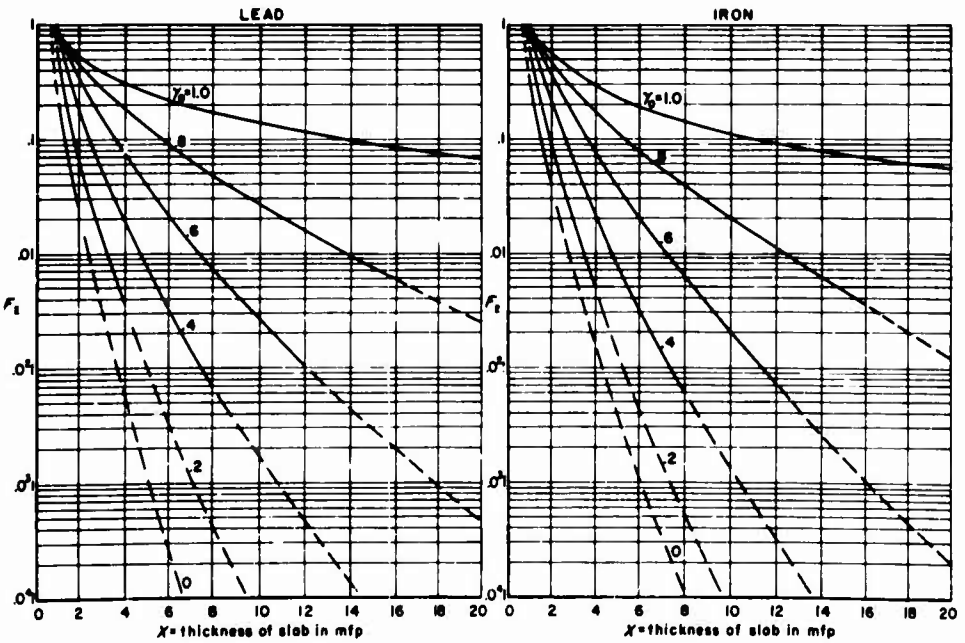

Fig. 41c—F_2 vs X for lead and iron, $\alpha_0 = 5$

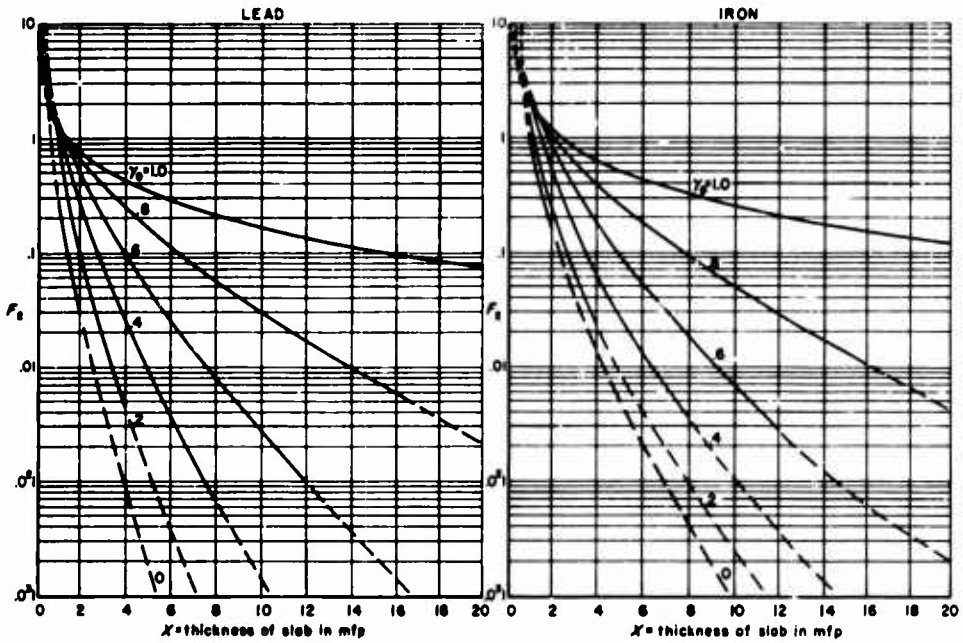

Fig. 41d—F_2 vs X for lead and iron, $\alpha_0 = 2.5$

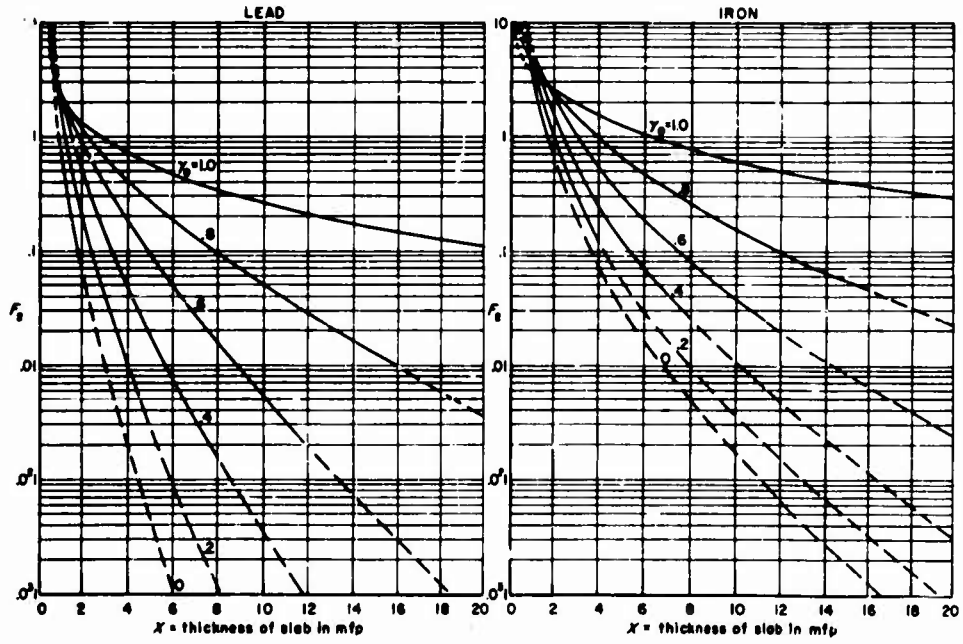

Fig. 41e—F_2 vs X for lead and iron, $\alpha_0 = 1$

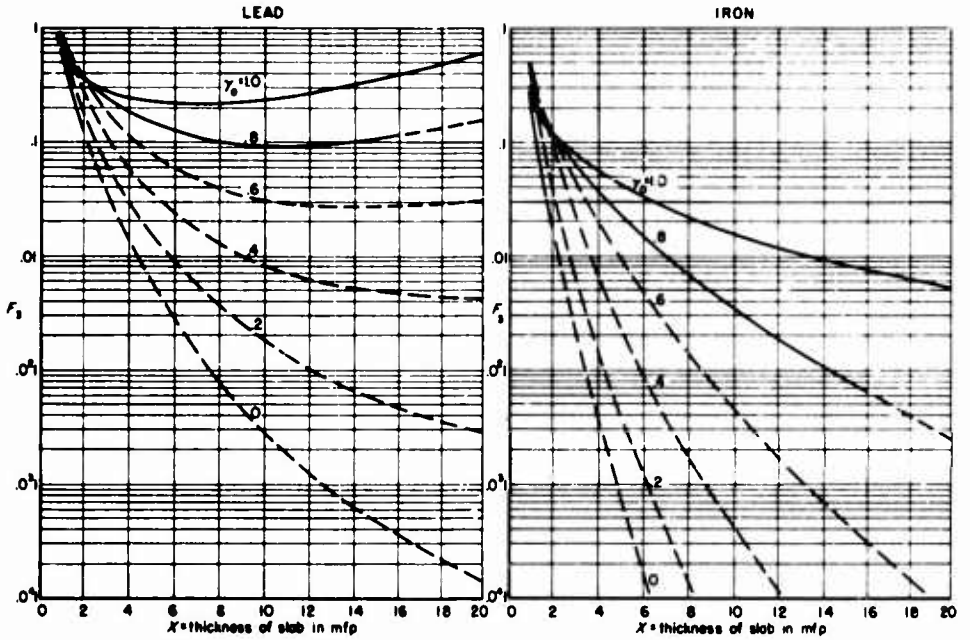

Fig. 42a—F_3 vs X for lead and iron, $\alpha_0 = 20$

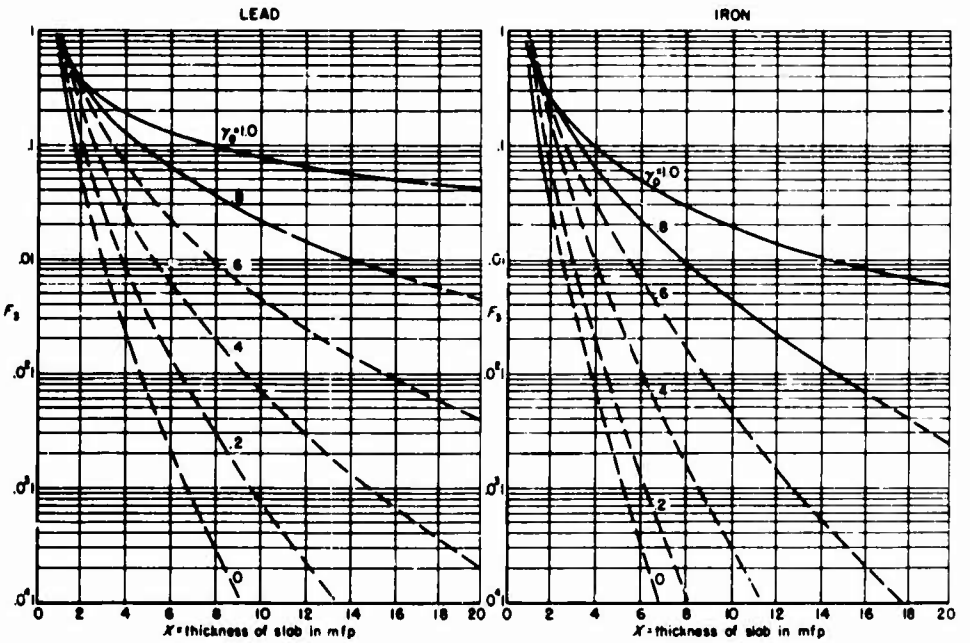

Fig. 42b—F_3 vs X for lead and iron, $\alpha_0 = 10$

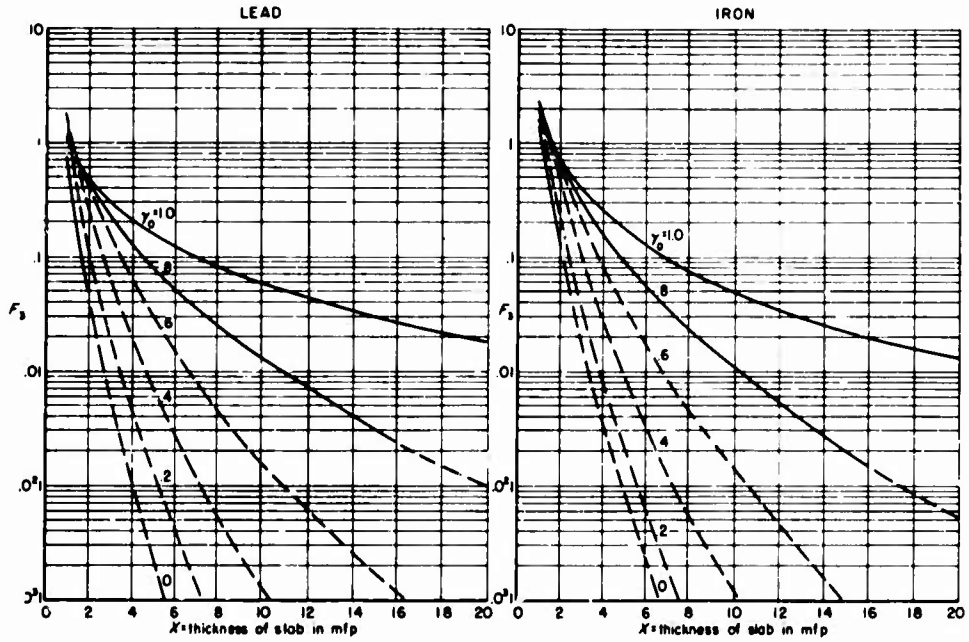

Fig. 42c—F_3 vs X for lead and iron, $\alpha_0 = 5$

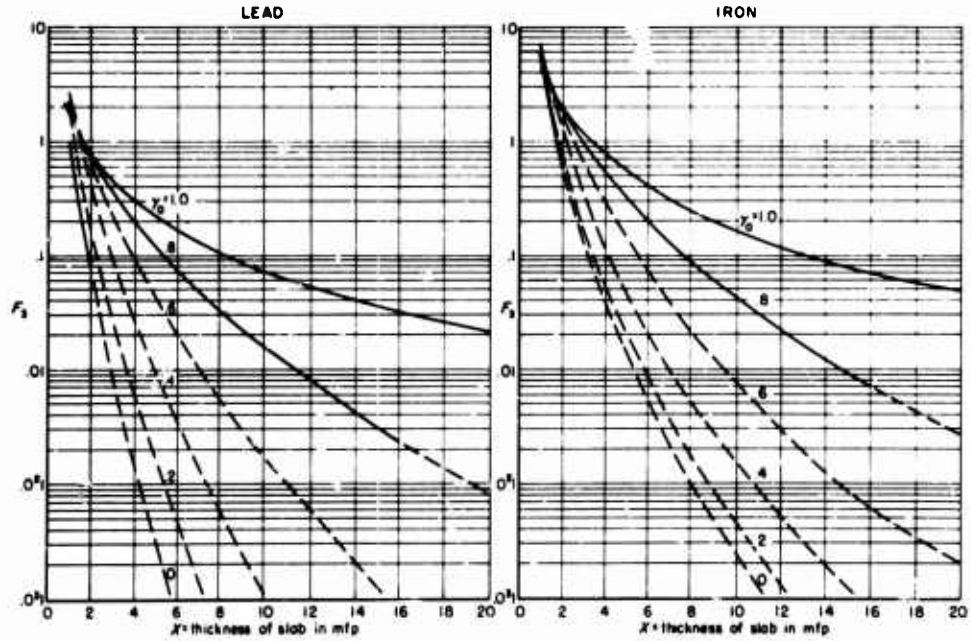

Fig. 42d—F_3 vs X for lead and iron, $\alpha_0 = 2.5$

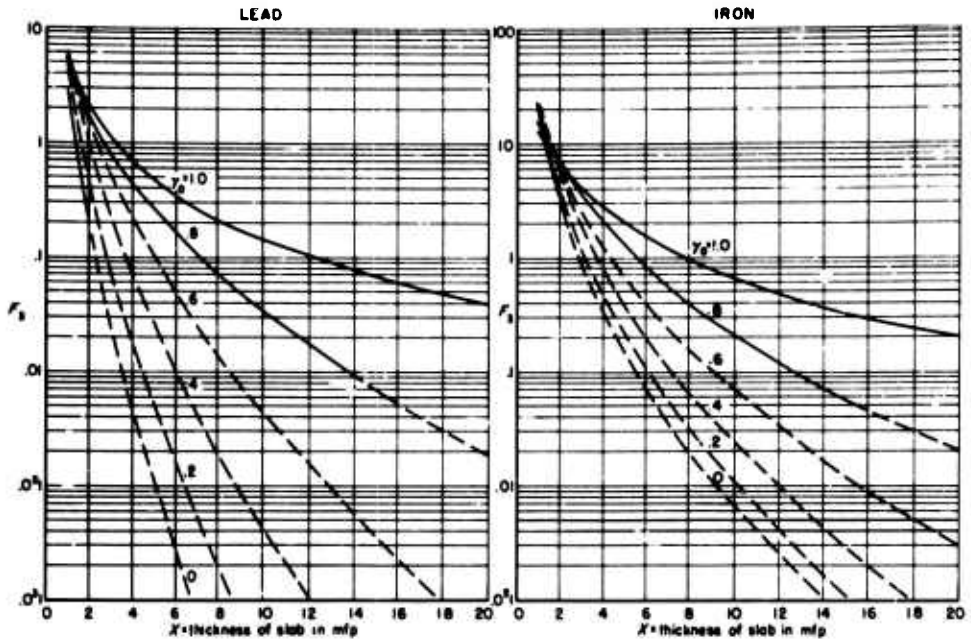

Fig. 42e—F_3 vs X for lead and iron, $\alpha_0 = 1$

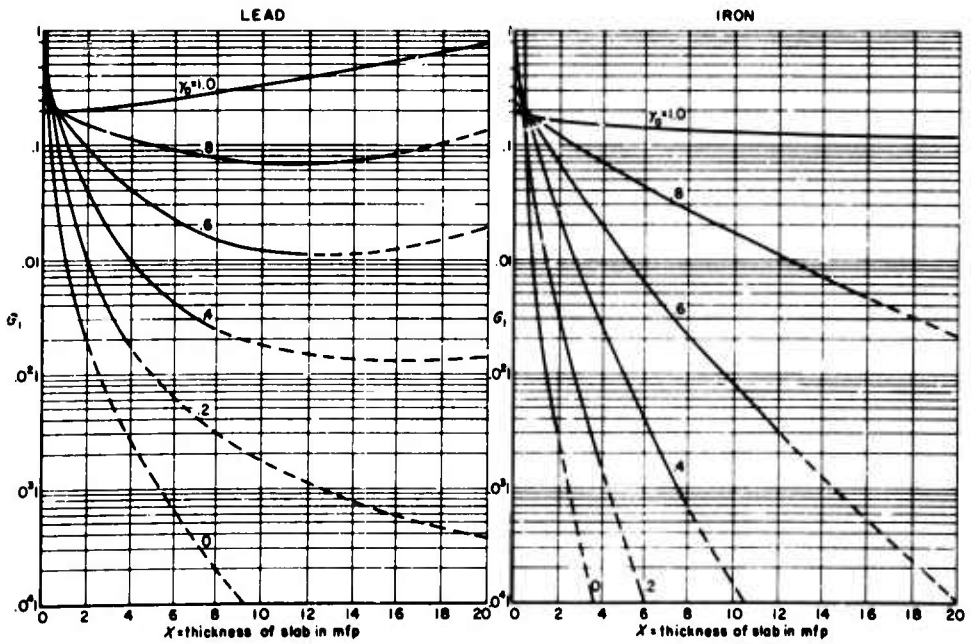

Fig. 43a—G_1 vs X for lead and iron, $\alpha_0 = 20$

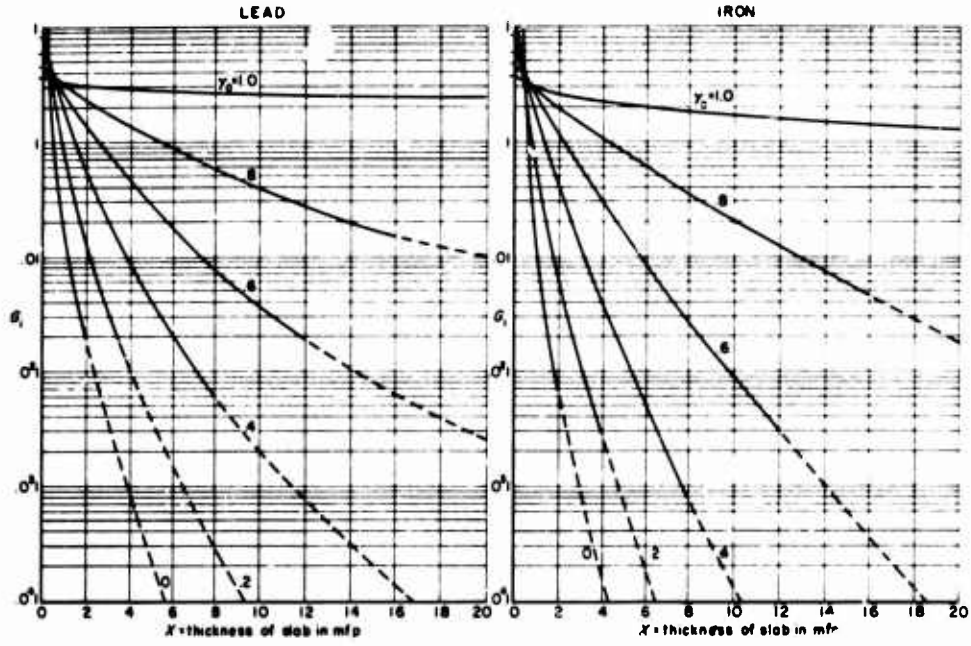

Fig. 43b—G_1 vs X for lead and iron, $\alpha_0 = 10$

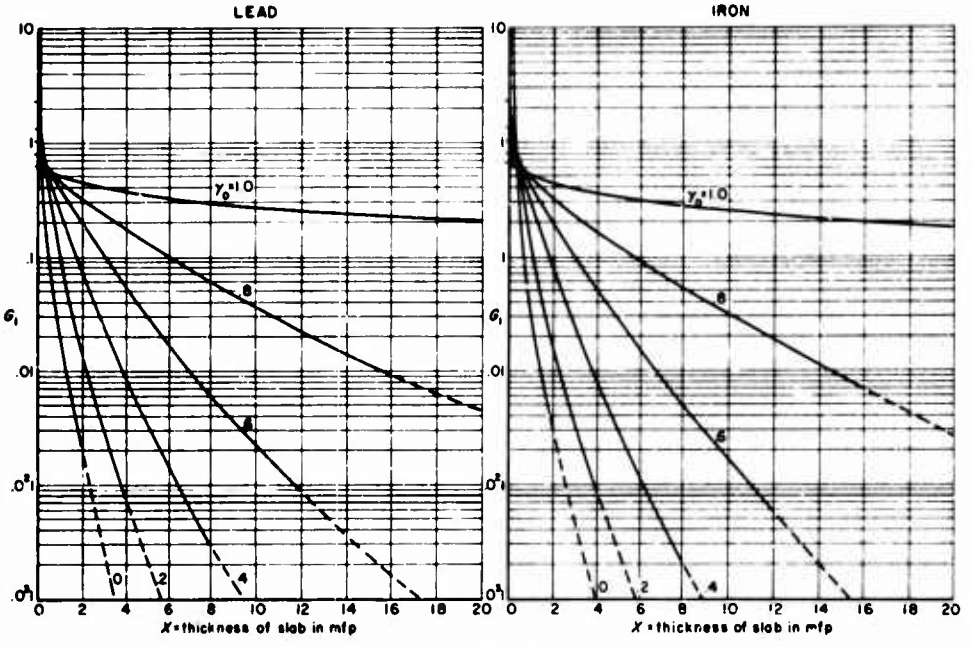

Fig. 43c—G_1 vs X for lead and iron, $\alpha_0 = 5$

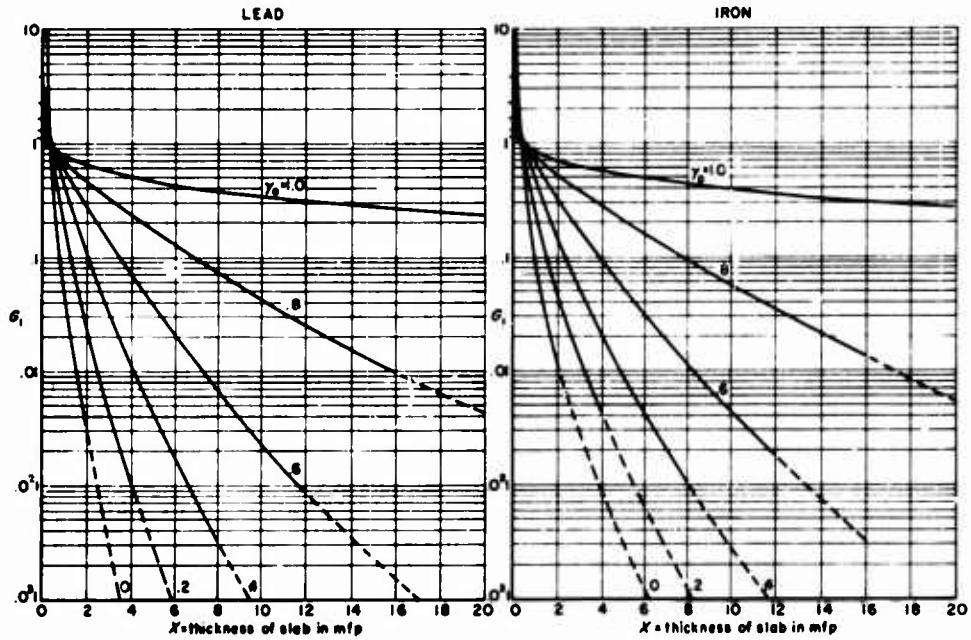

Fig. 43d—G_1 vs X for lead and iron, $\alpha_0 = 2.5$

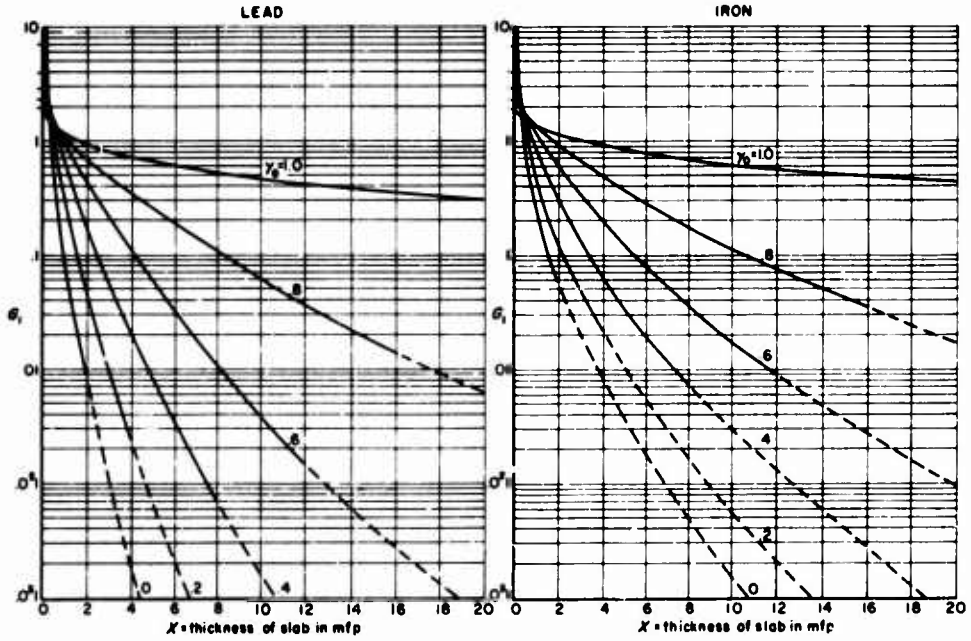

Fig. 43e—G_1 vs X for lead and iron, $\alpha_0 = 1$

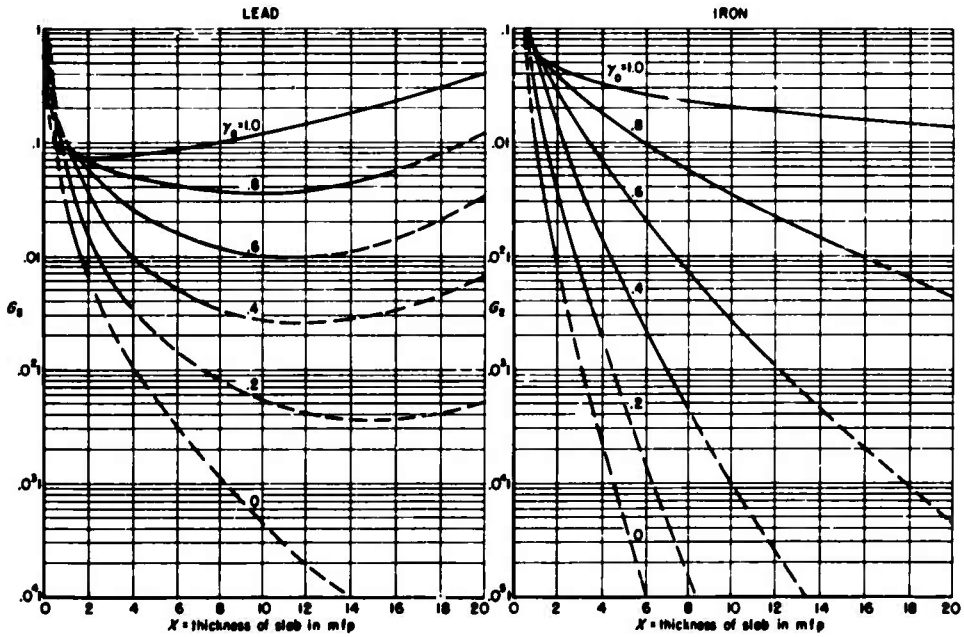

Fig. 44a—G_2 vs X for lead and iron, $\alpha_0 = 20$

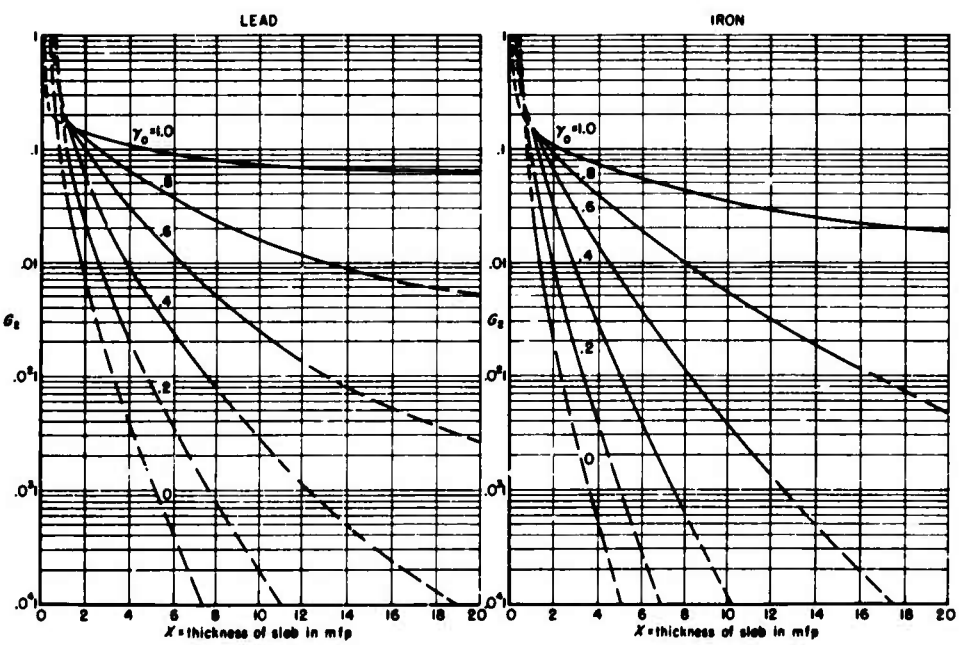

Fig. 44b—G_2 vs X for lead and iron, $\alpha_0 = 10$

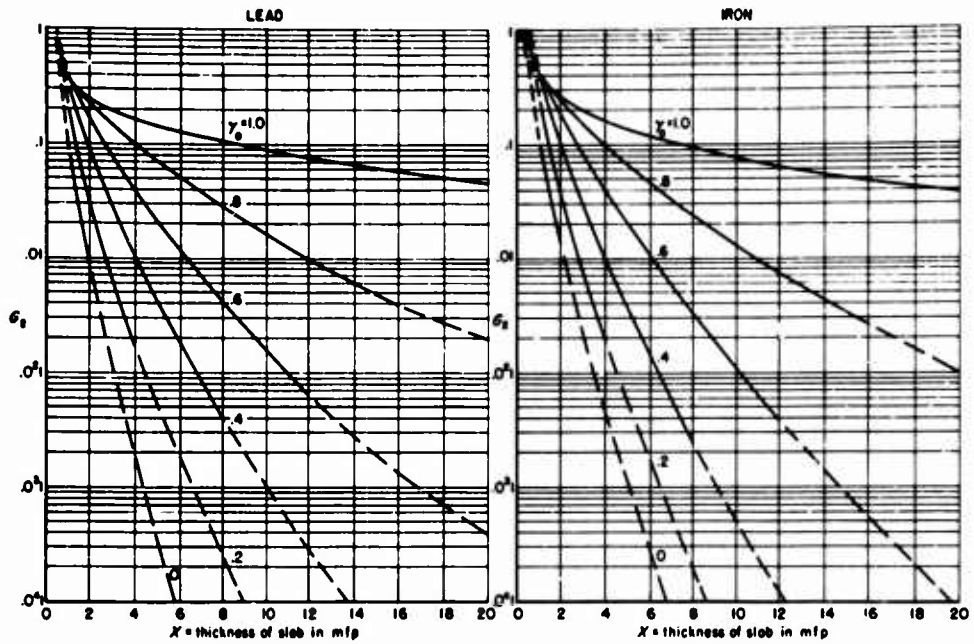

Fig. 44c—G_2 vs X for lead and iron, $\alpha_0 = 5$

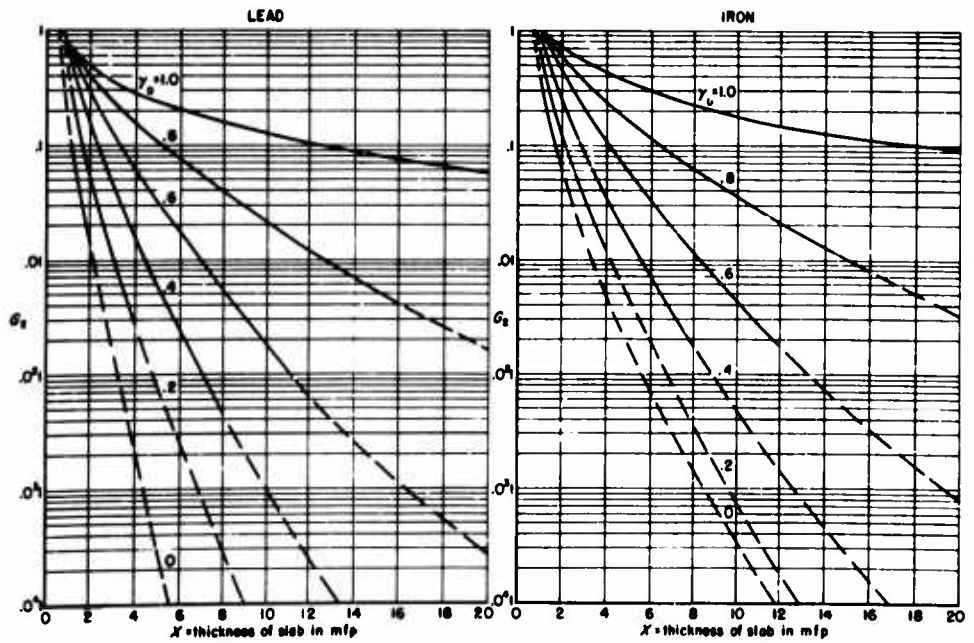

Fig. 44d—G_2 vs X for lead and iron, $\alpha_0 = 2.5$

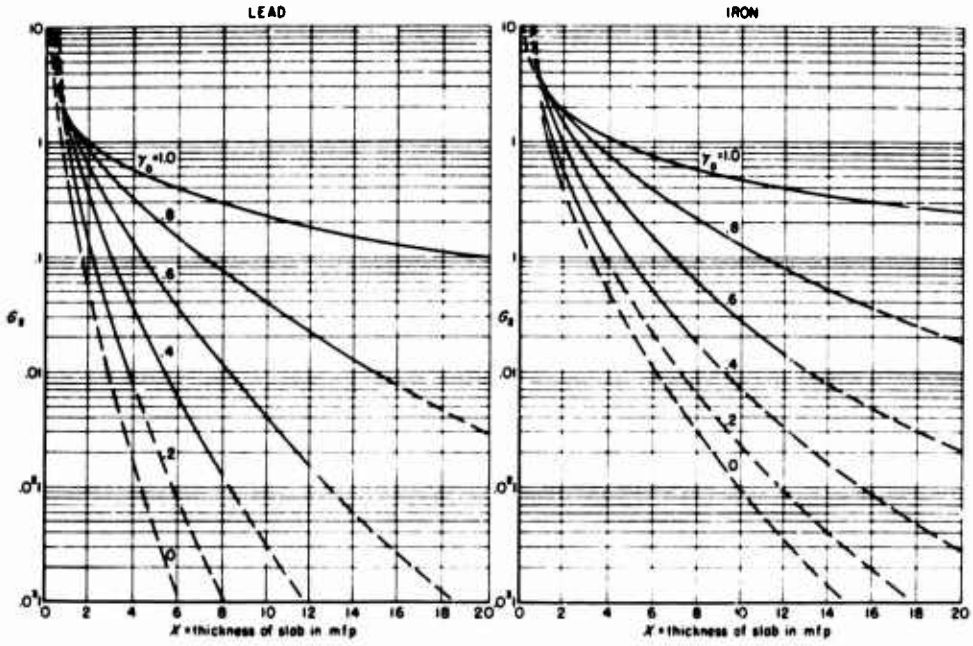

Fig. 44e—G_2 vs X for lead and iron, $\alpha_0 = 1$

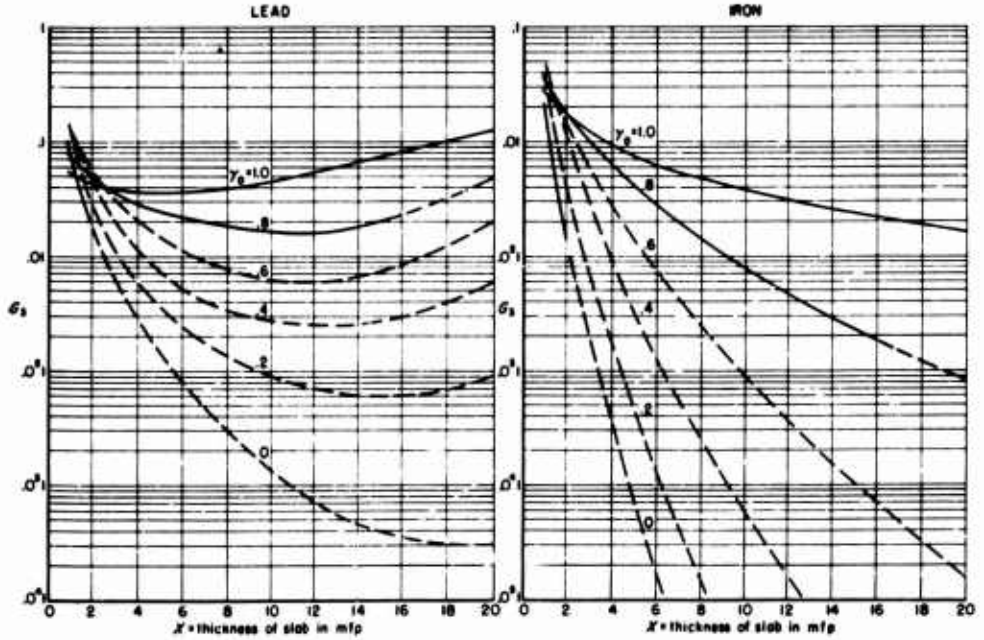

Fig. 45a—G_2 vs X for lead and iron, $\alpha_0 = 20$

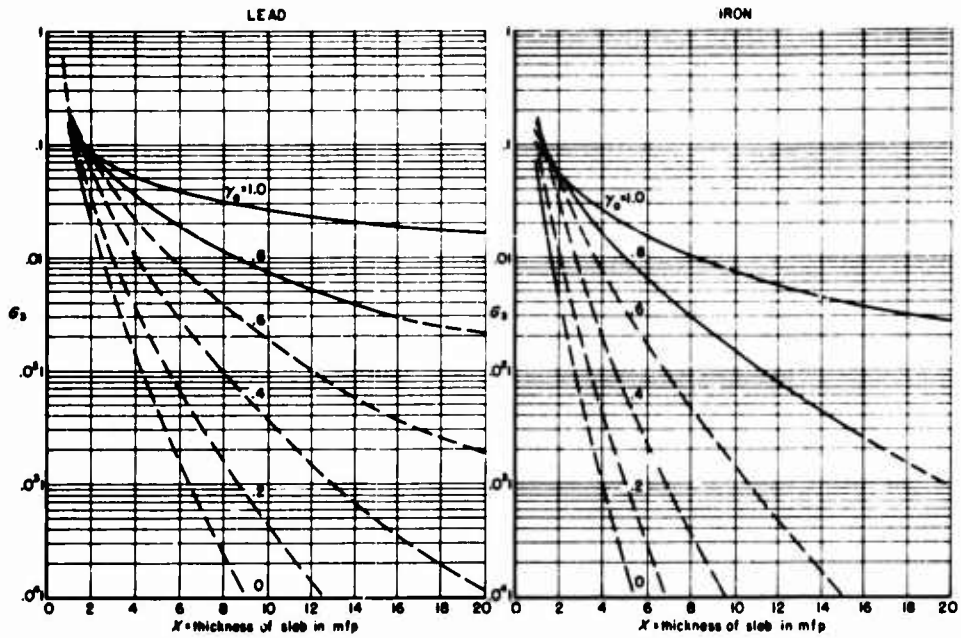

Fig. 45b—G_3 vs X for lead and iron, $\alpha_0 = 10$

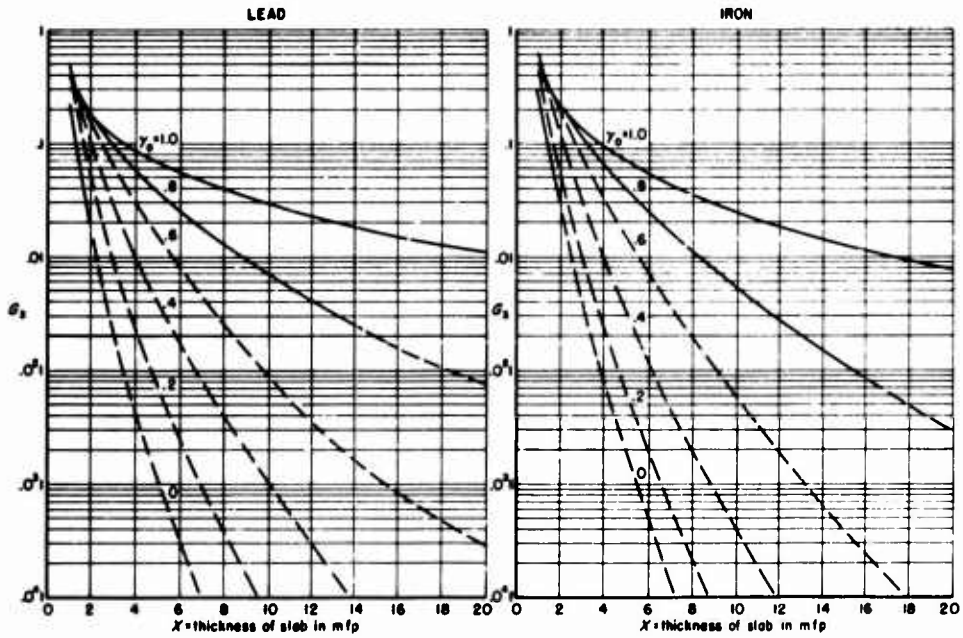

Fig. 45c—G_3 vs X for lead and iron, $\alpha_0 = 5$

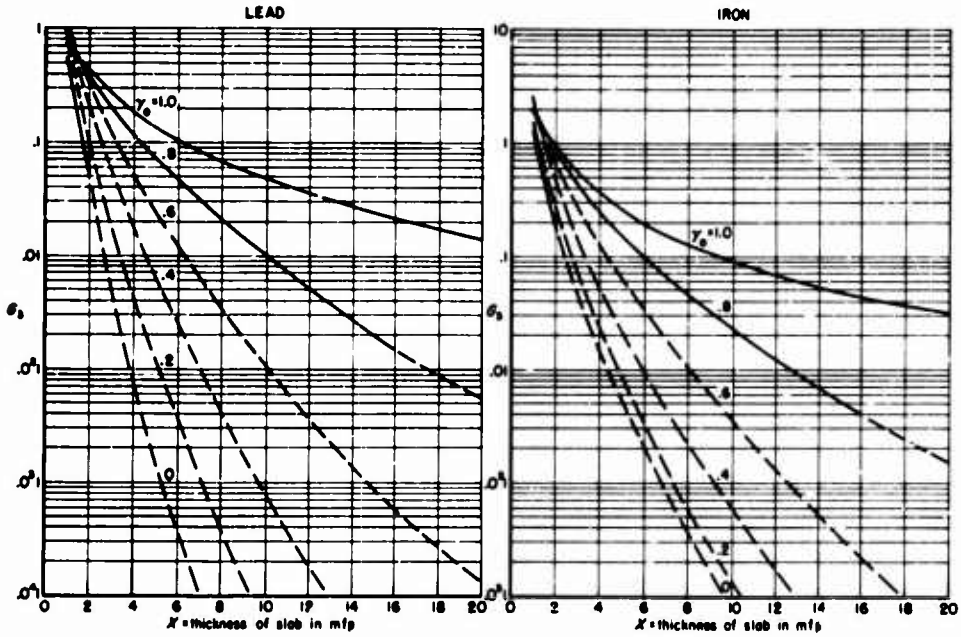

Fig. 45d—G_3 vs X for lead and iron, $\alpha_0 = 2.5$

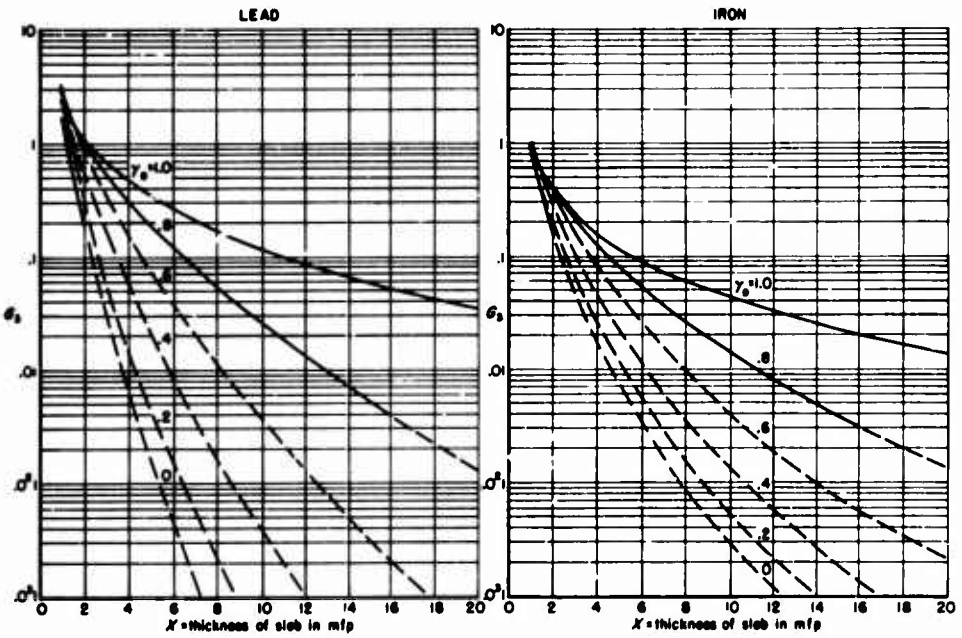

Fig. 45e—G_3 vs X for lead and iron, $\alpha_0 = 1$

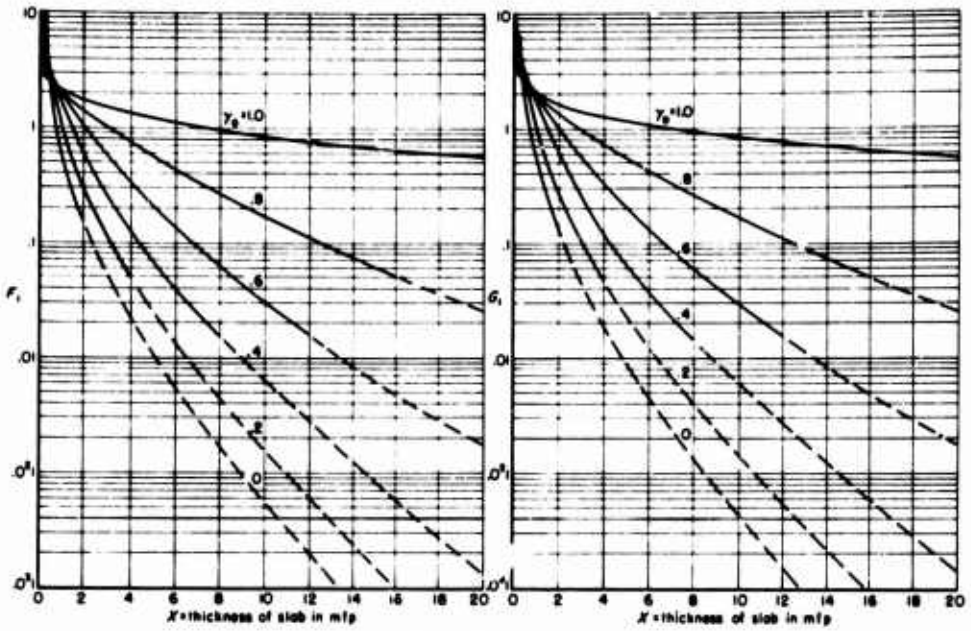

Fig. 46a—F_k and G_k vs X for iron, $\alpha_0 = 0.2$ ($k = 1$)

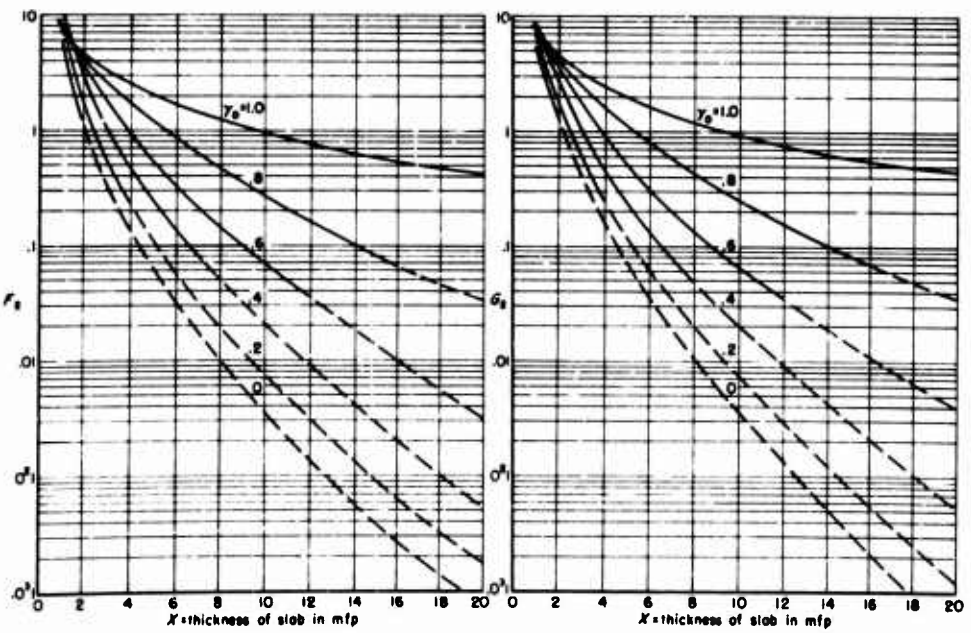

Fig. 46b—F_k and G_k vs X for iron, $\alpha_0 = 0.2$ ($k = 2$)

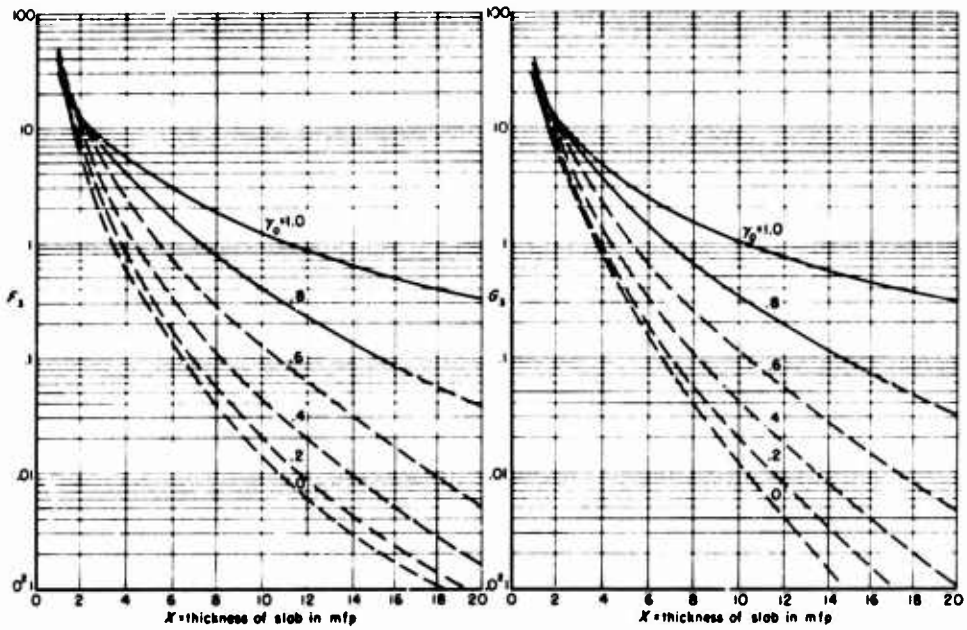

Fig. 46c—F_k and G_k vs X for iron, $\alpha_0 = 0.2$ ($k = 3$)

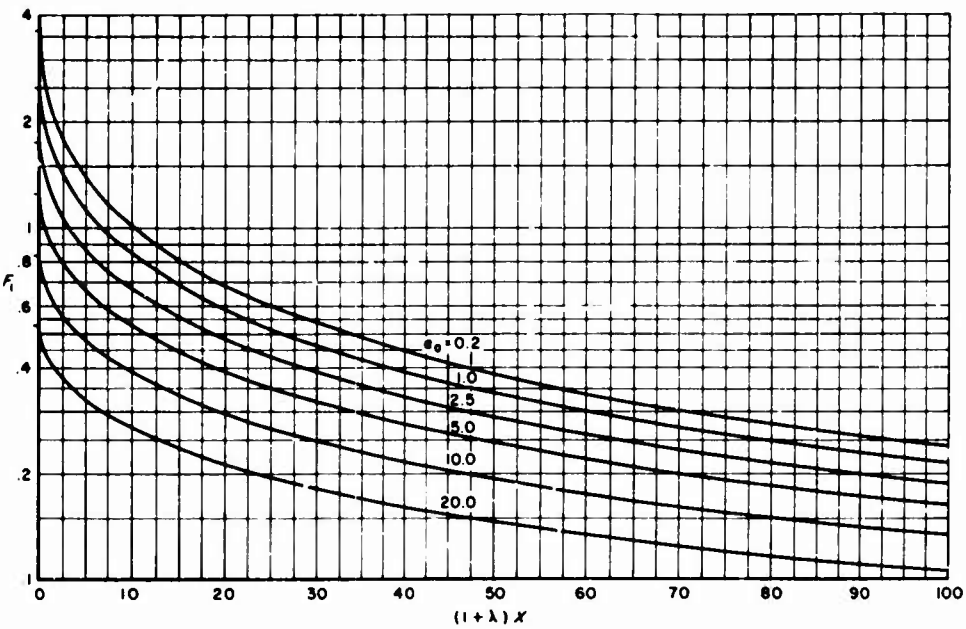

Fig. 47—F_1 vs $(1 + \lambda)X$ for $\gamma_0 = 1$

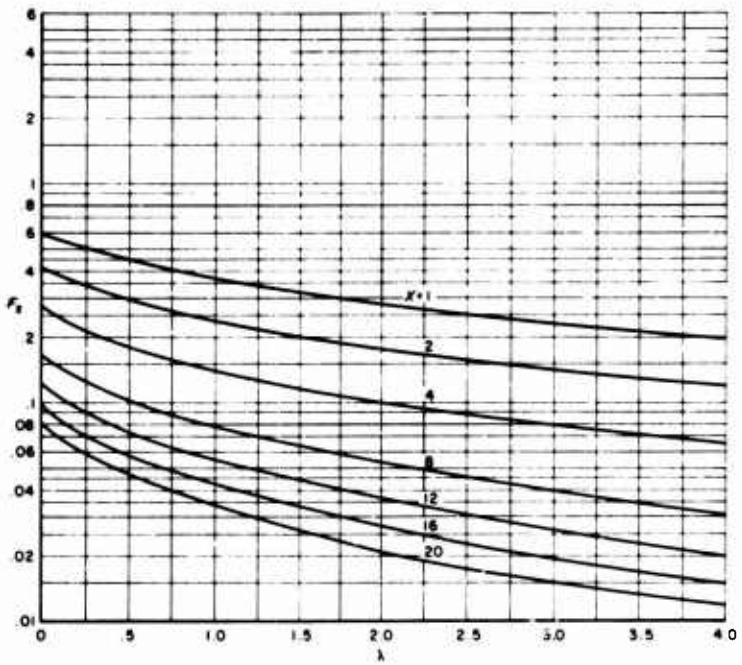

Fig. 48a—F_2 vs λ for $\gamma_0 = 1$, $\alpha_0 = 20$

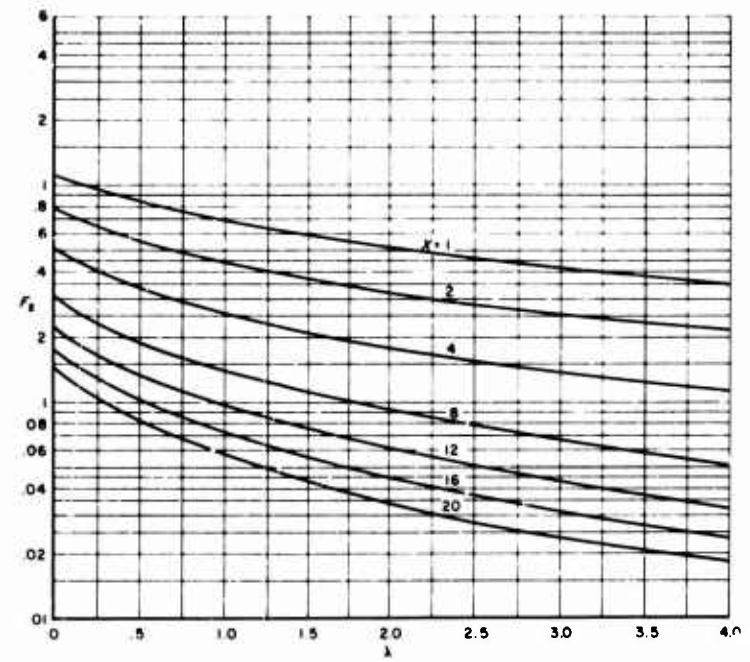

Fig. 48b—F_2 vs λ for $\gamma_0 = 1$, $\alpha_0 = 10$

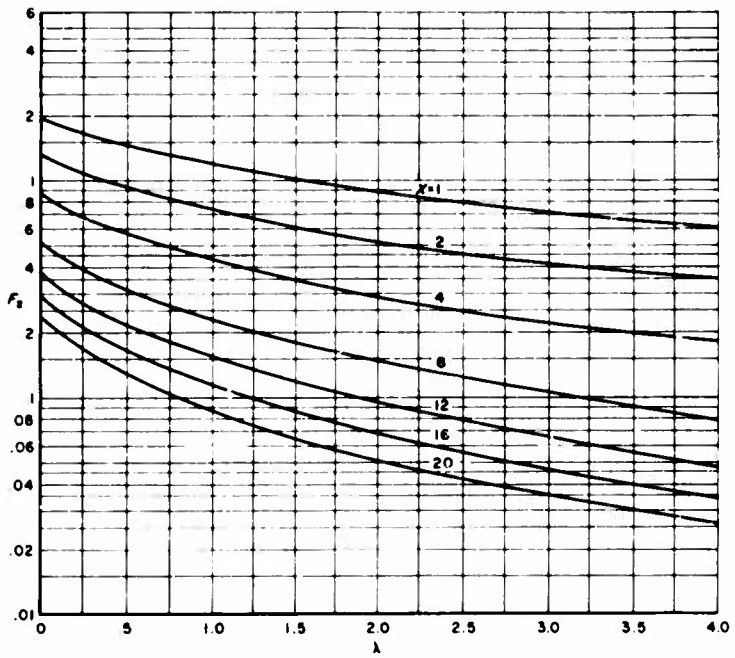

Fig. 48c—F_2 vs λ for $\gamma_0 = 1$, $\alpha_0 = 5$

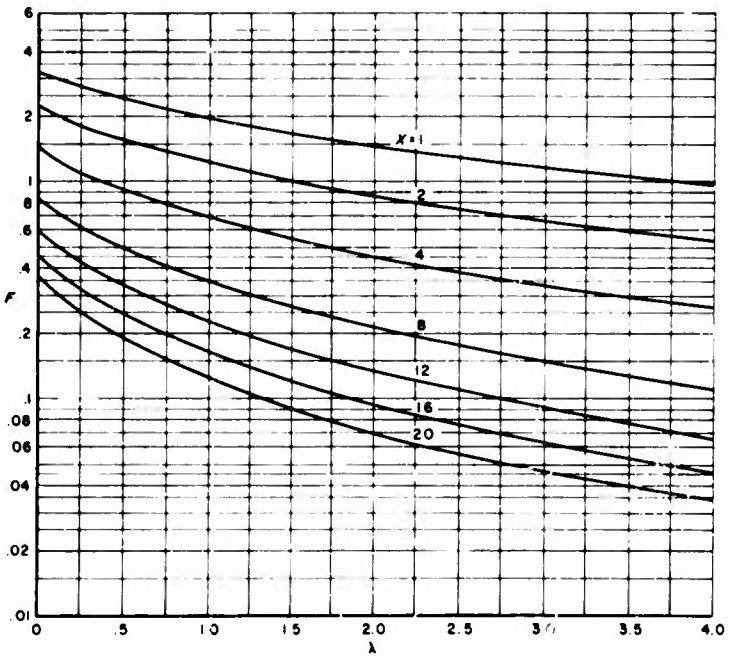

Fig. 48d—F_2 vs λ for $\gamma_0 = 1$, $\alpha = 2.5$

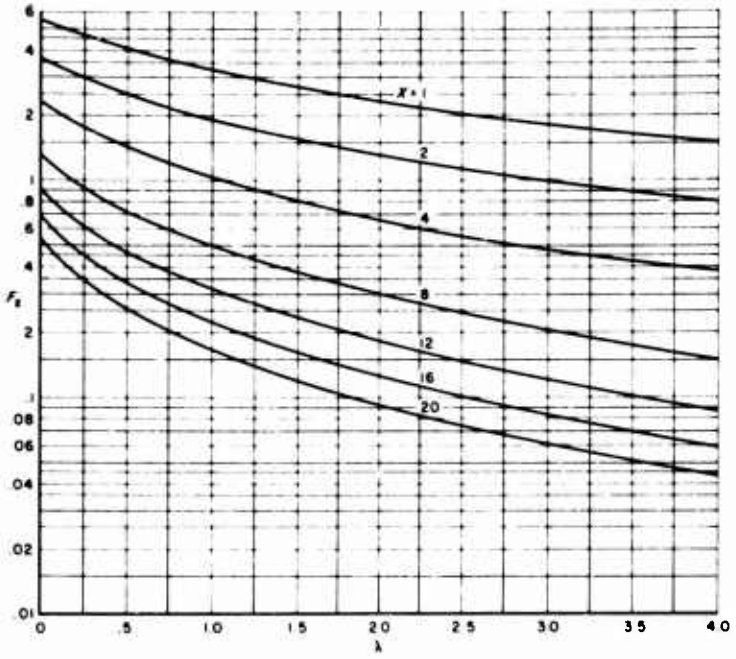

Fig. 48e—F_2 vs λ for $\gamma_0 = 1$, $\alpha_0 = 1$

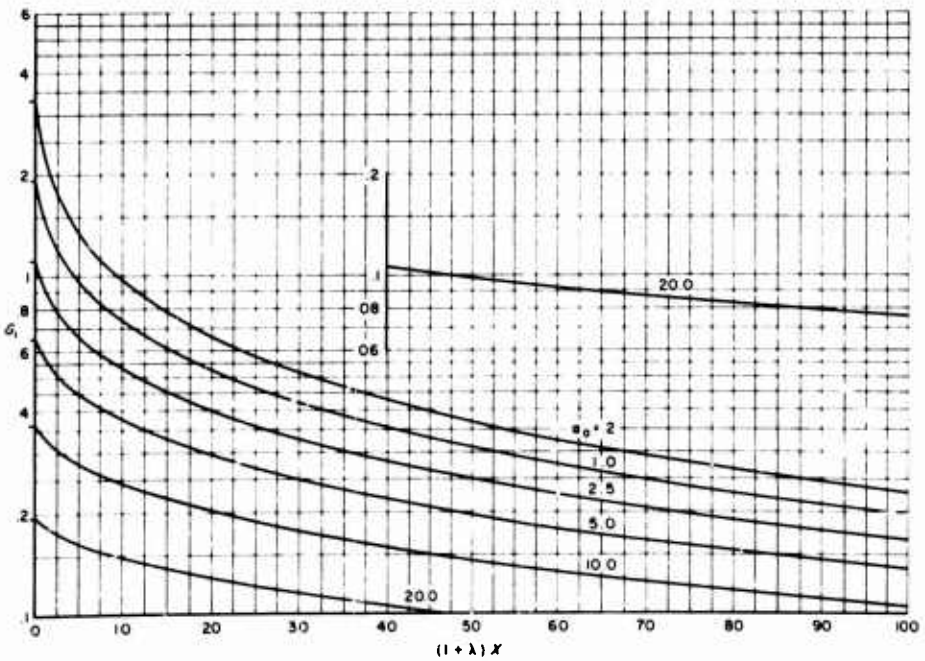

Fig. 49—G_1 vs $(1 + \lambda)X$ for $\gamma_0 = 1$

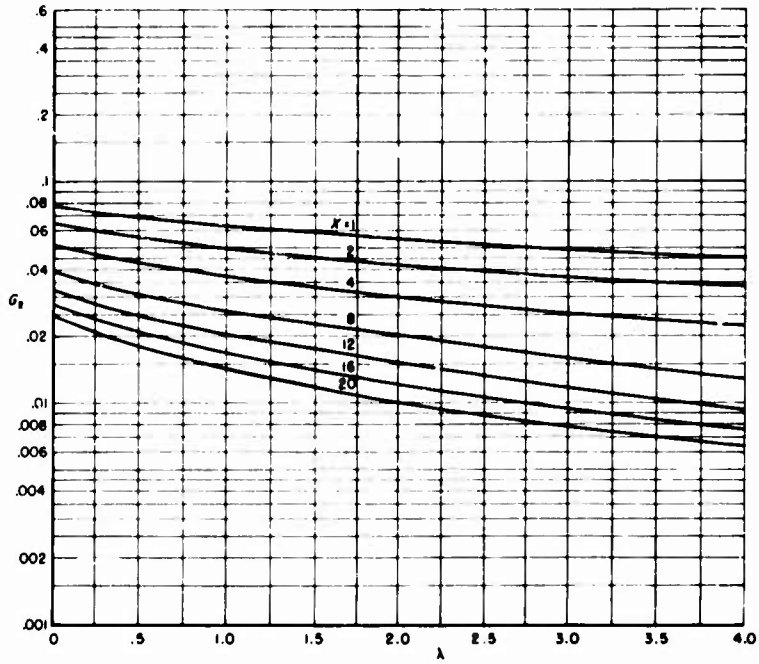

Fig. 50a—G_2 vs λ for $\gamma_0 = 1$, $\alpha_0 = 20$

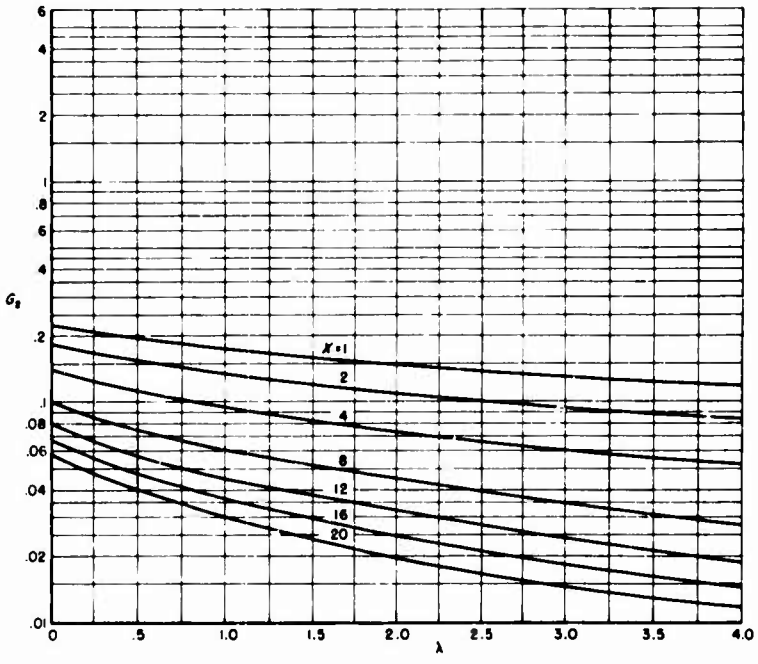

Fig. 50b—G_2 vs λ for $\gamma_0 = 1$, $\alpha_0 = 10$

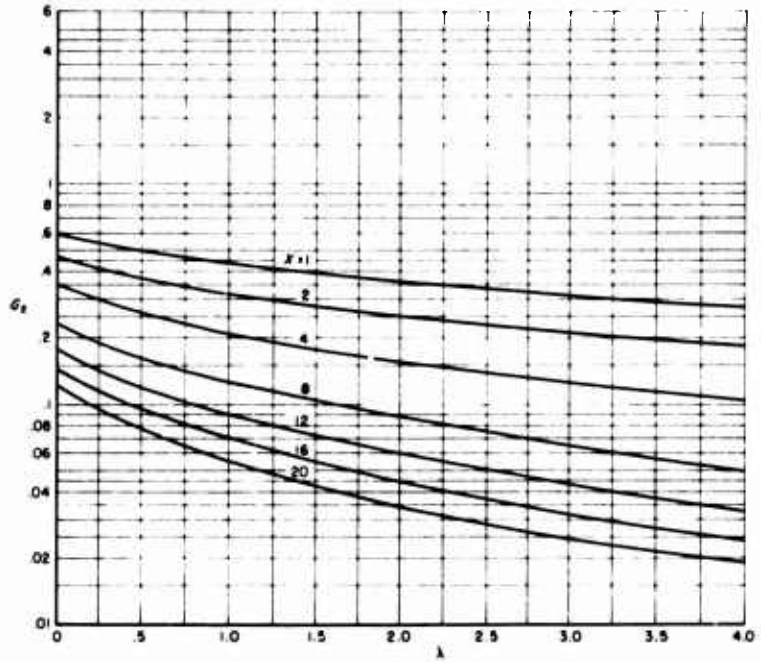

Fig. 50c—G_2 vs λ for $\gamma_0 = 1$, $\alpha_0 = 5$

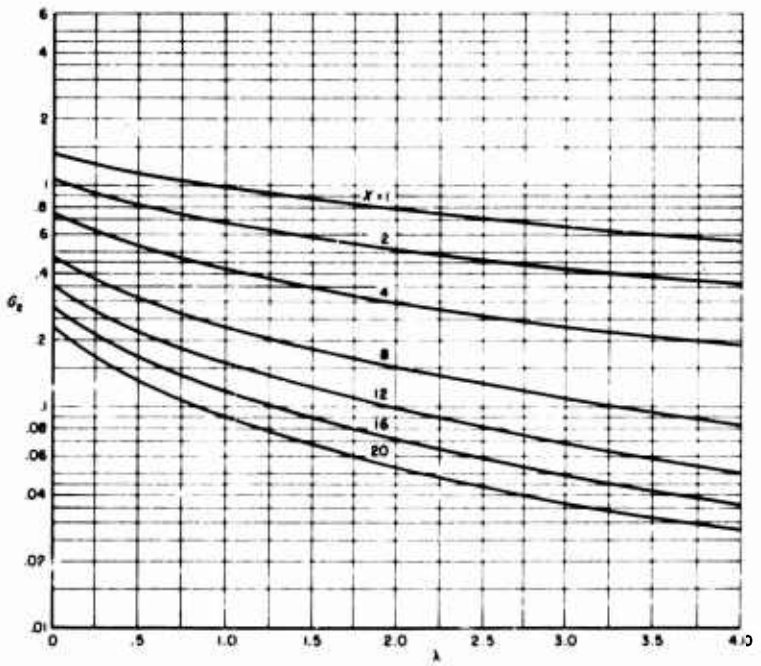

Fig. 50d—G_2 vs λ for $\gamma_0 = 1$, $\alpha_0 = 2.5$

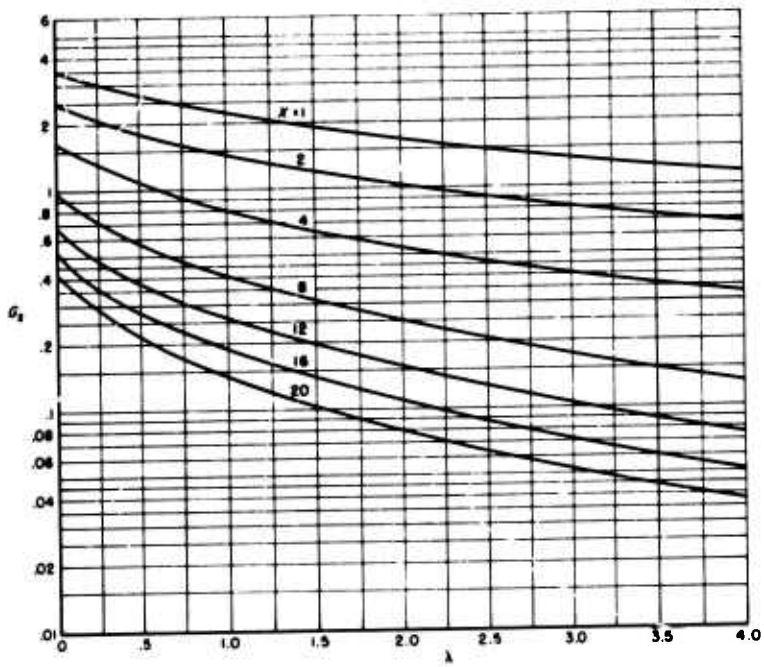

Fig. 50e—G_2 vs λ for $\gamma_0 = 1$, $\alpha_0 = 1$

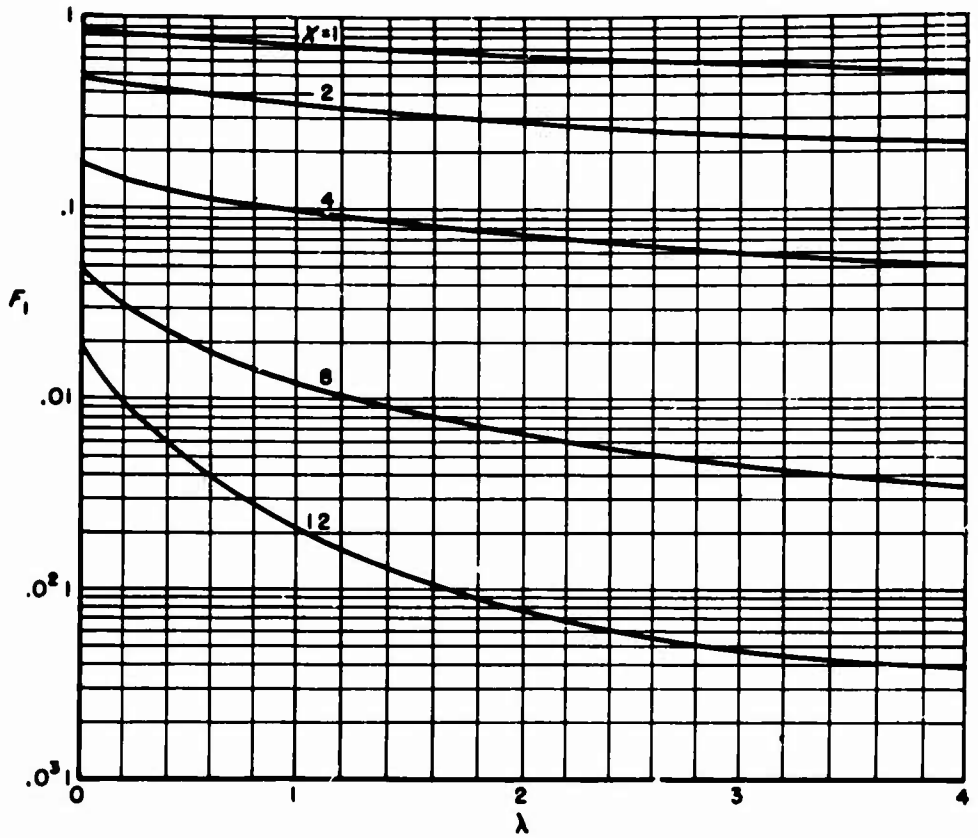

Fig. 51—F_1 vs λ for $\alpha_0 = 5$, $\gamma_0 = 0.6$

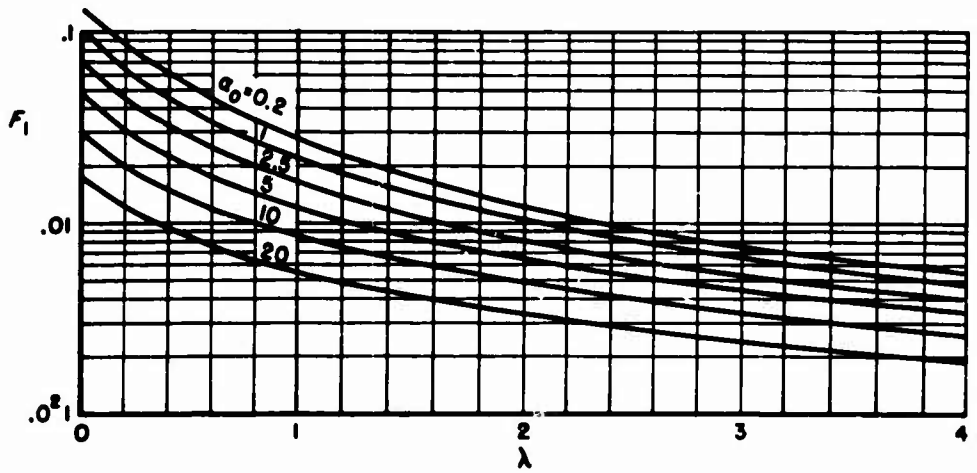

Fig. 52—F_1 vs λ for $\gamma_0 = 0.6$, $X = 8$

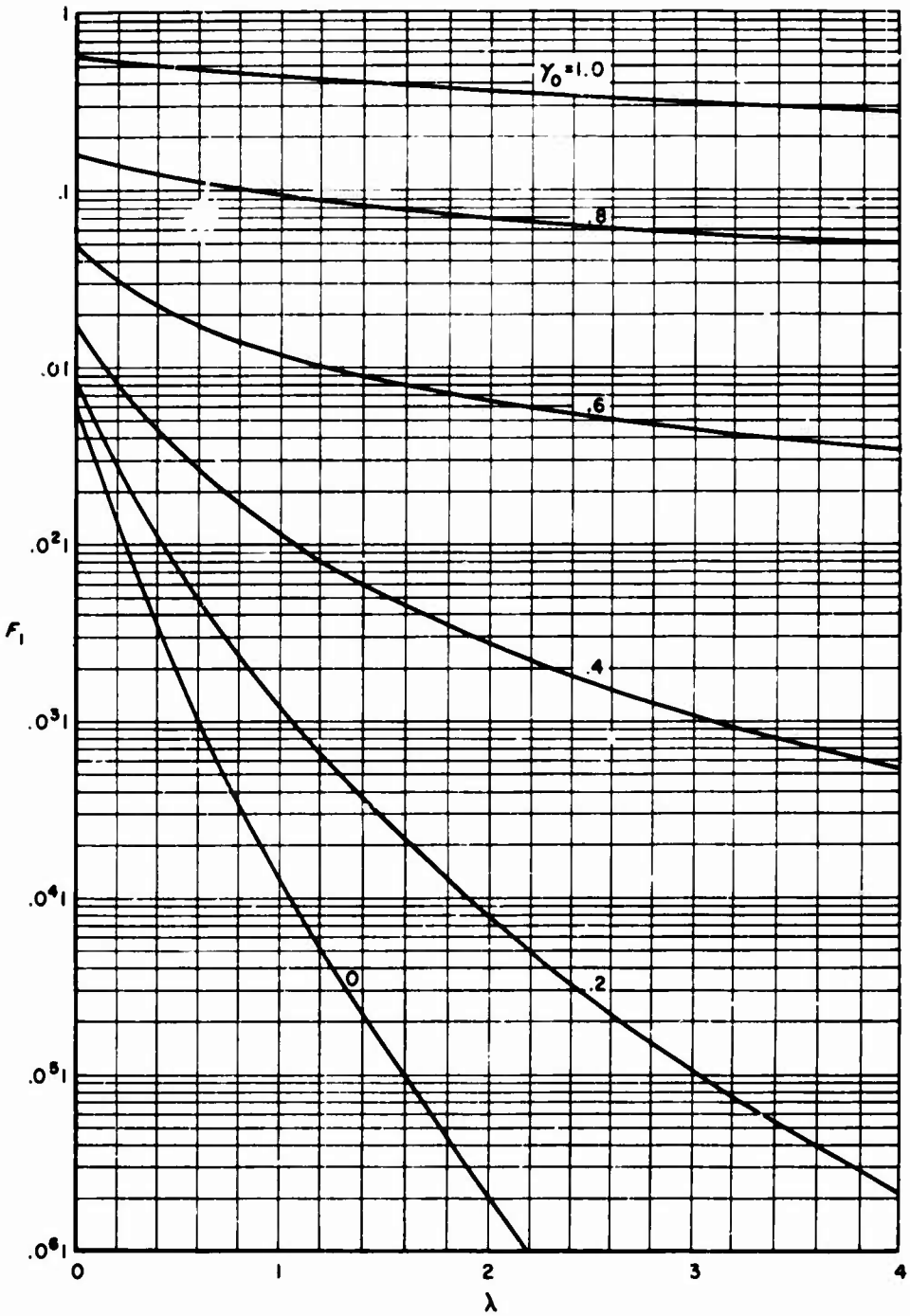

Fig. 53—F_1 vs λ for $\alpha_0 = 5$, $X = 8$

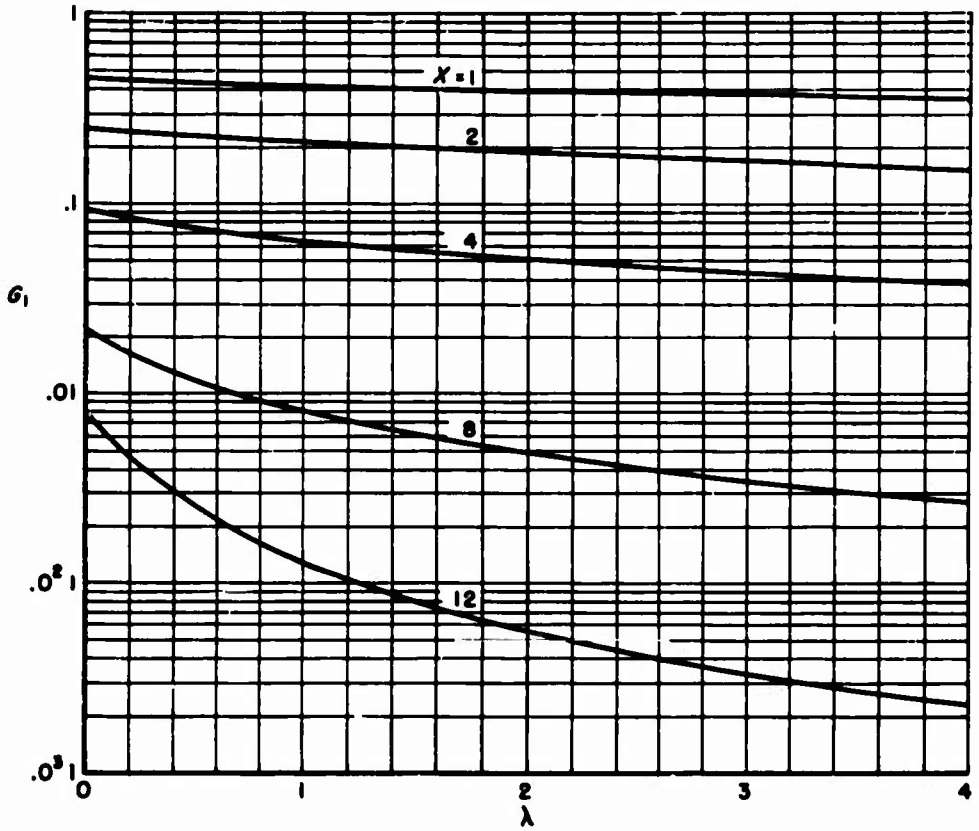

Fig. 54—G_1 vs λ for $\alpha_0 = 5$, $\gamma_0 = 0.6$

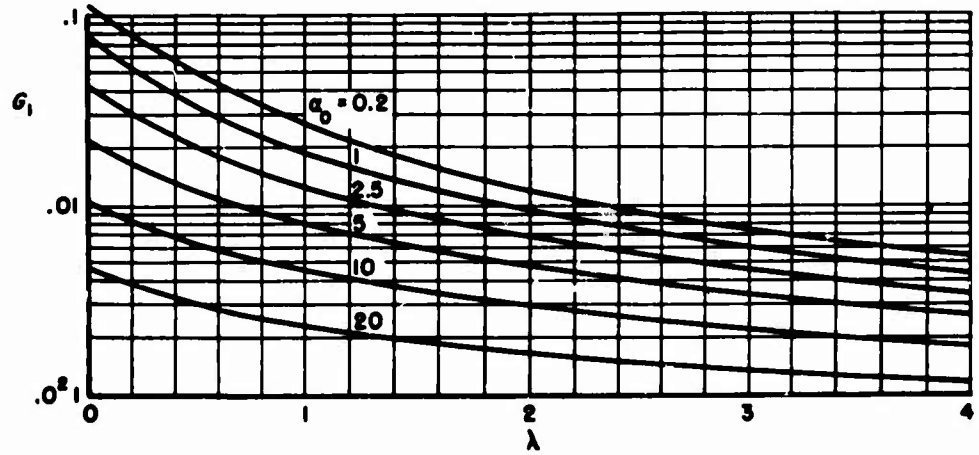

Fig. 55—G_1 vs λ for $\gamma_0 = 0.6$, $X = 8$

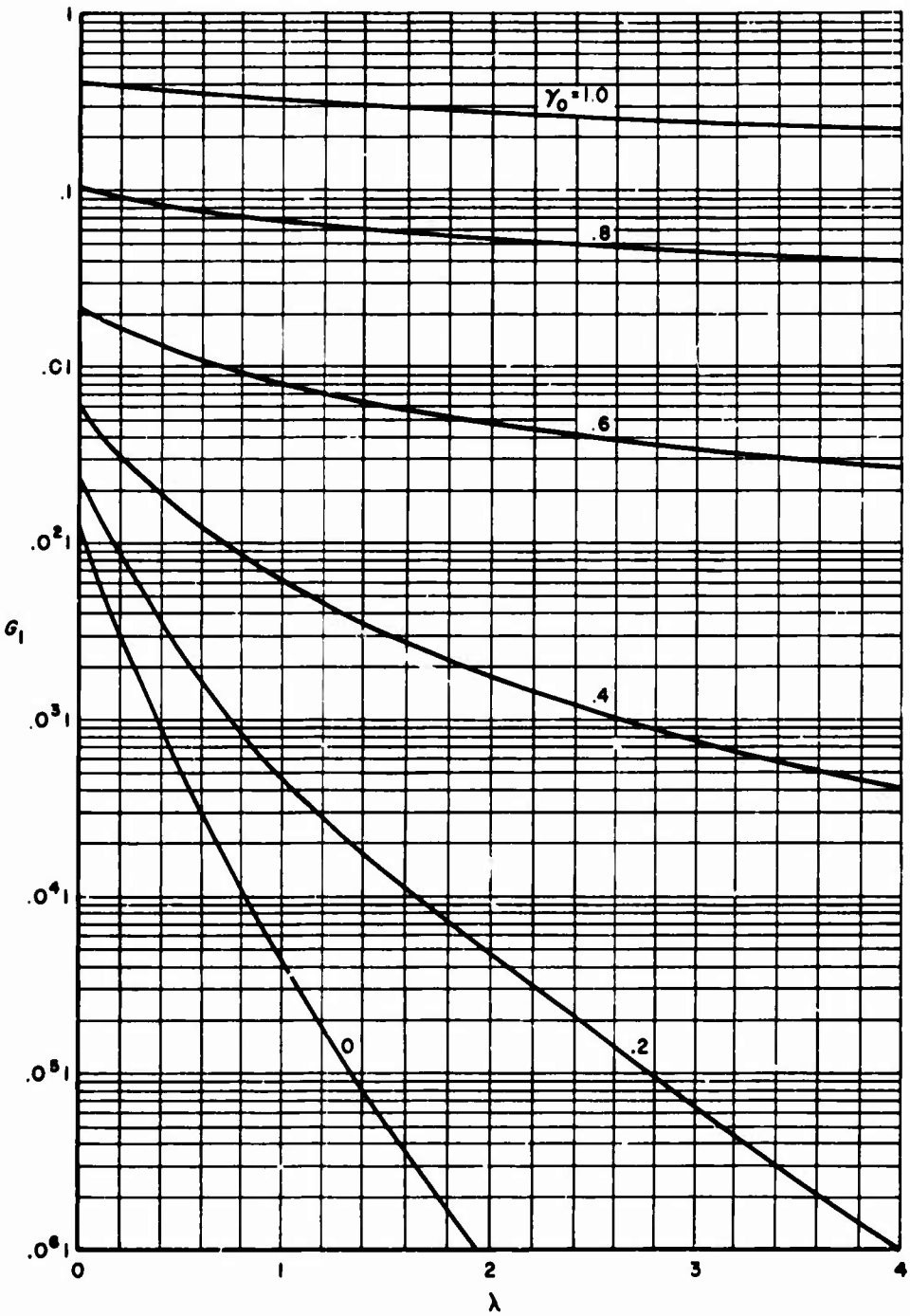

Fig. 56—G_1 vs λ for $\alpha_0 = 5$, $X = 8$

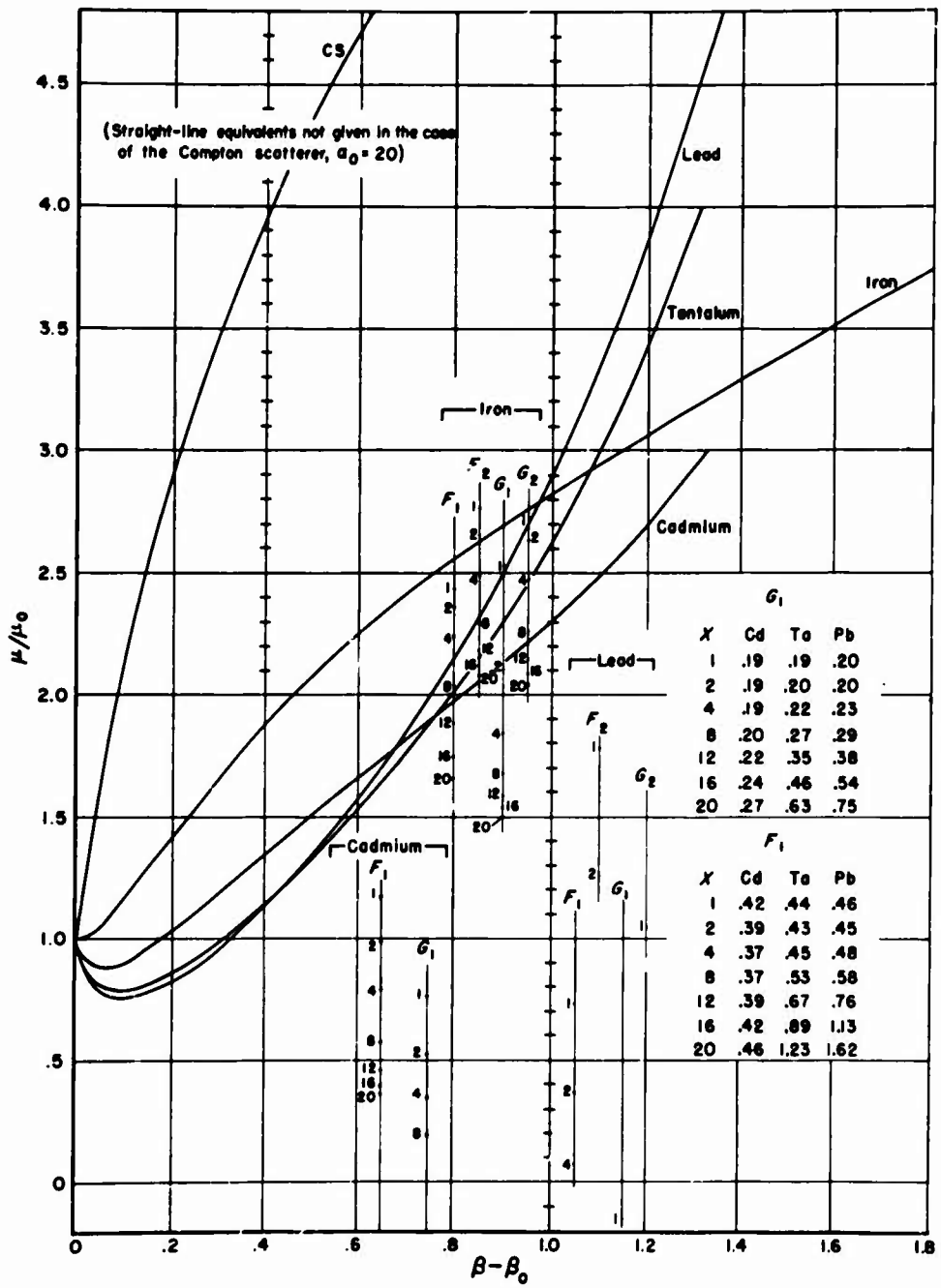

Fig. 57a—Straight-line equivalents of μ/μ_0 for lead, iron, and the pure Compton scatterer, $\alpha_0 = 20$

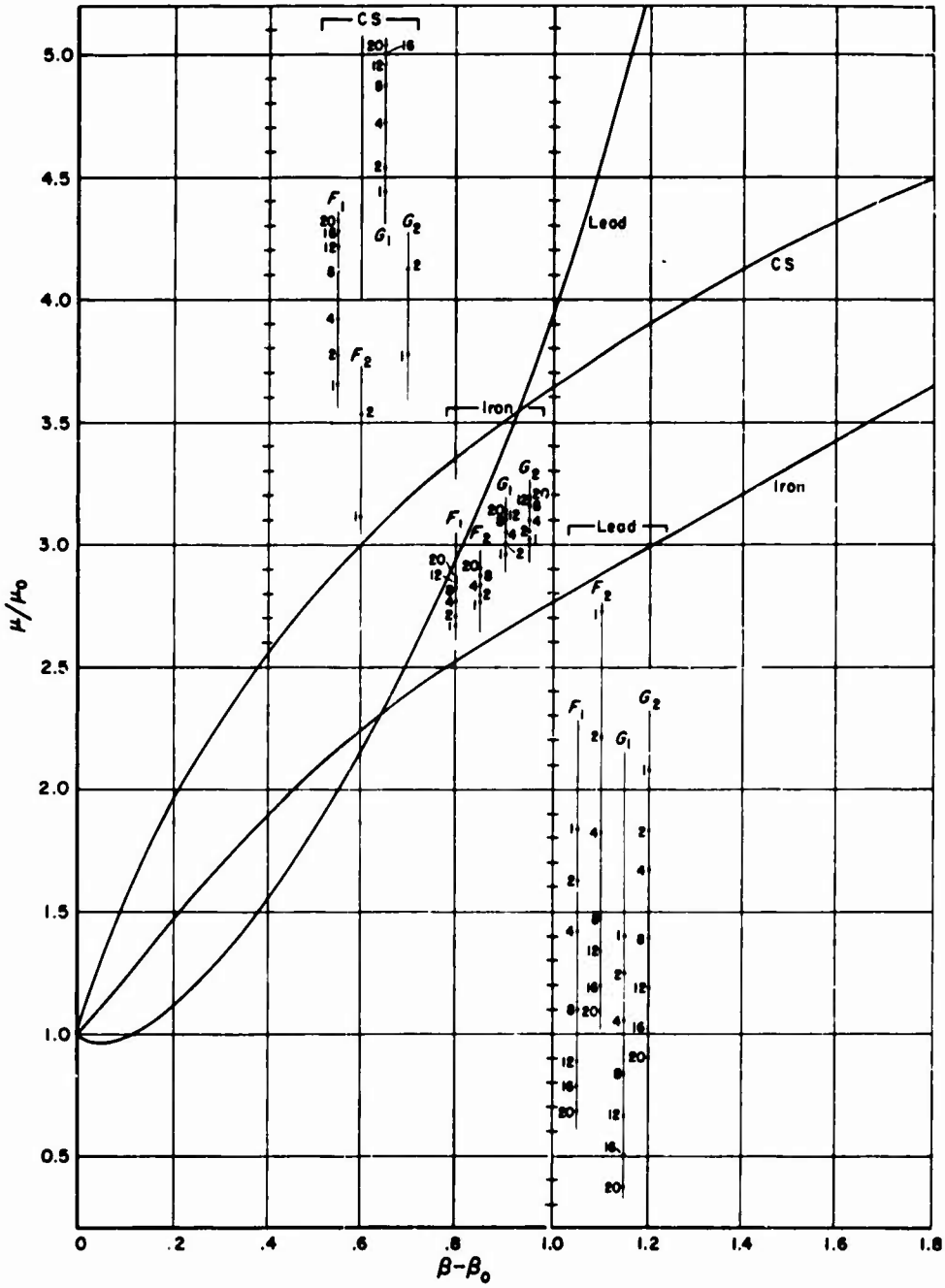

Fig. 57b—Straight-line equivalents of μ/μ_0 for lead, iron, and the pure Compton scatterer, $\alpha_0 = 10$

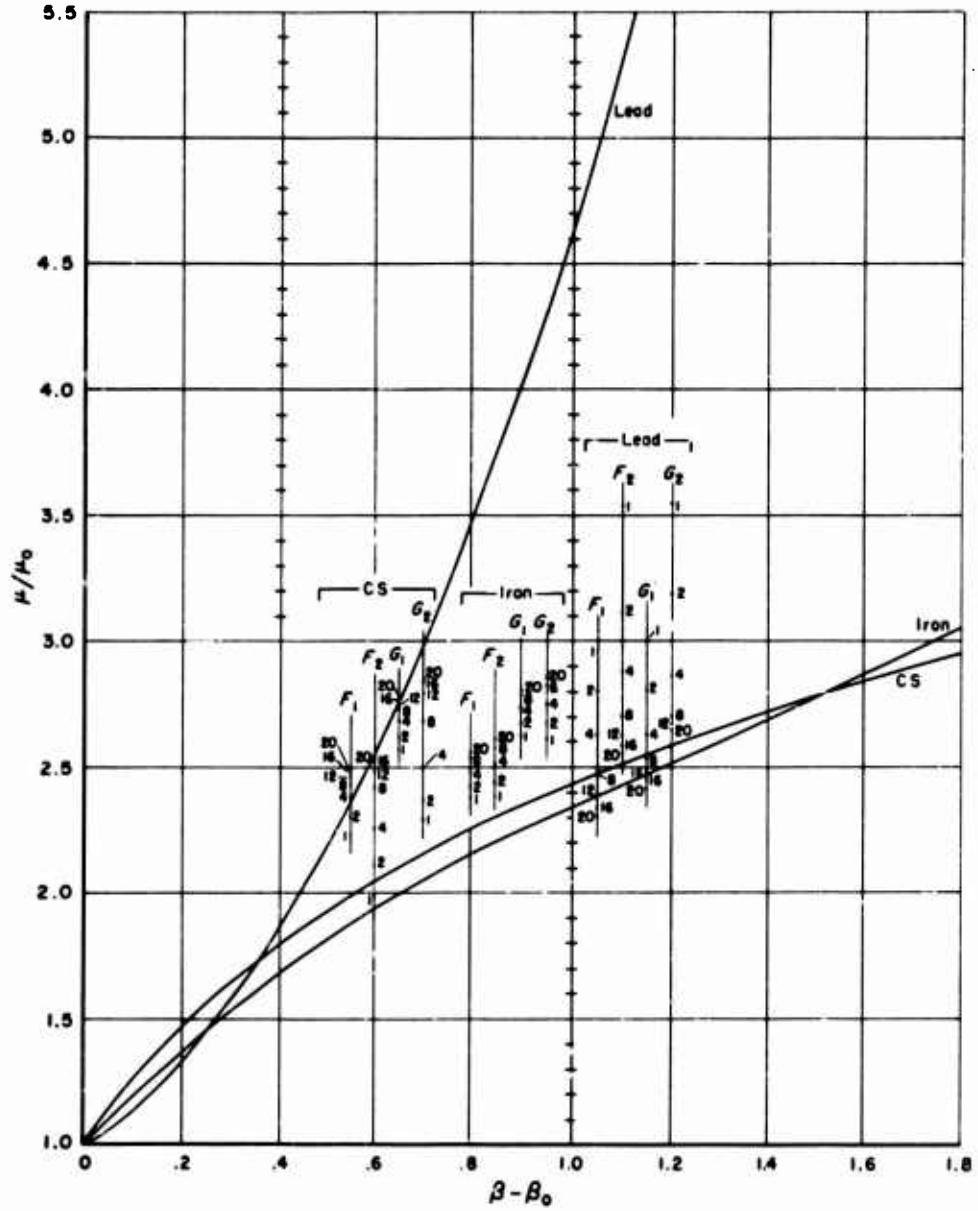

Fig. 57c—Straight-line equivalents of μ/μ_0 for lead, iron, and the pure Compton scatterer, $\alpha_0 = 5$

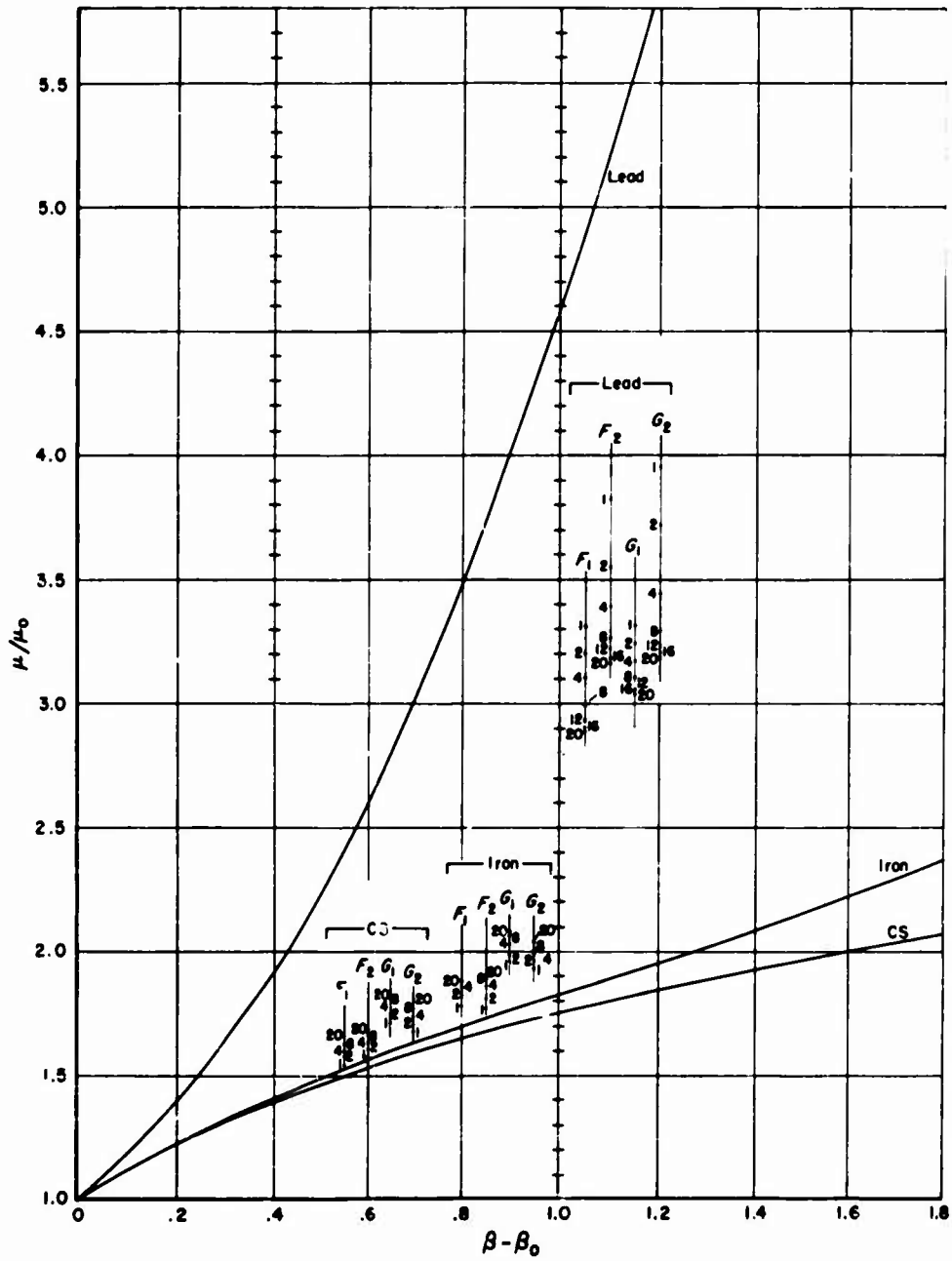

Fig. 57d—Straight-line equivalents of μ/μ_0 for lead, iron, and the pure Compton scatterer, $\alpha_0 = 2.5$

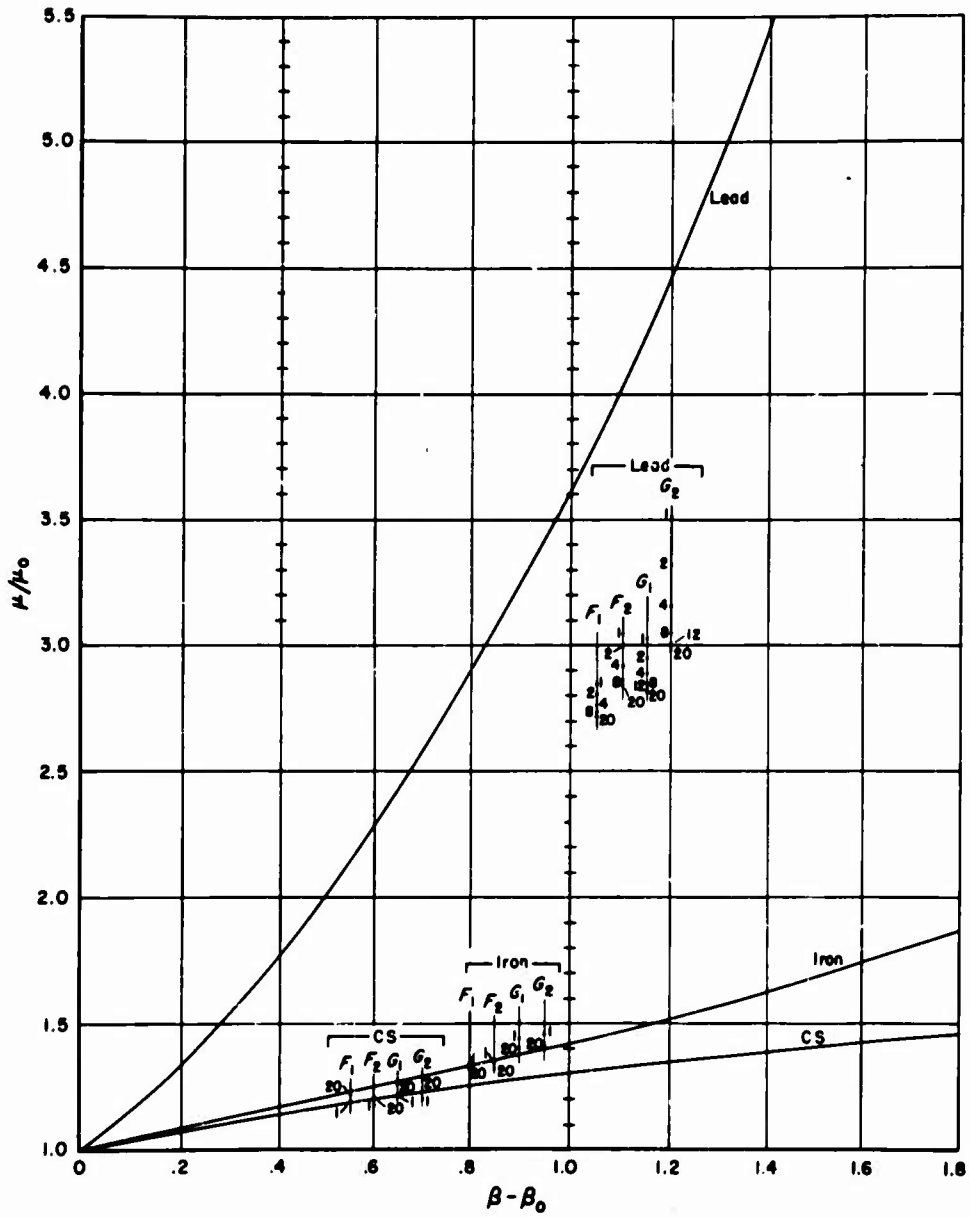

Fig. 57e—Straight-line equivalents of μ/μ_0 for lead, iron, and the pure Compton scatterer, $\alpha_0 = 1$

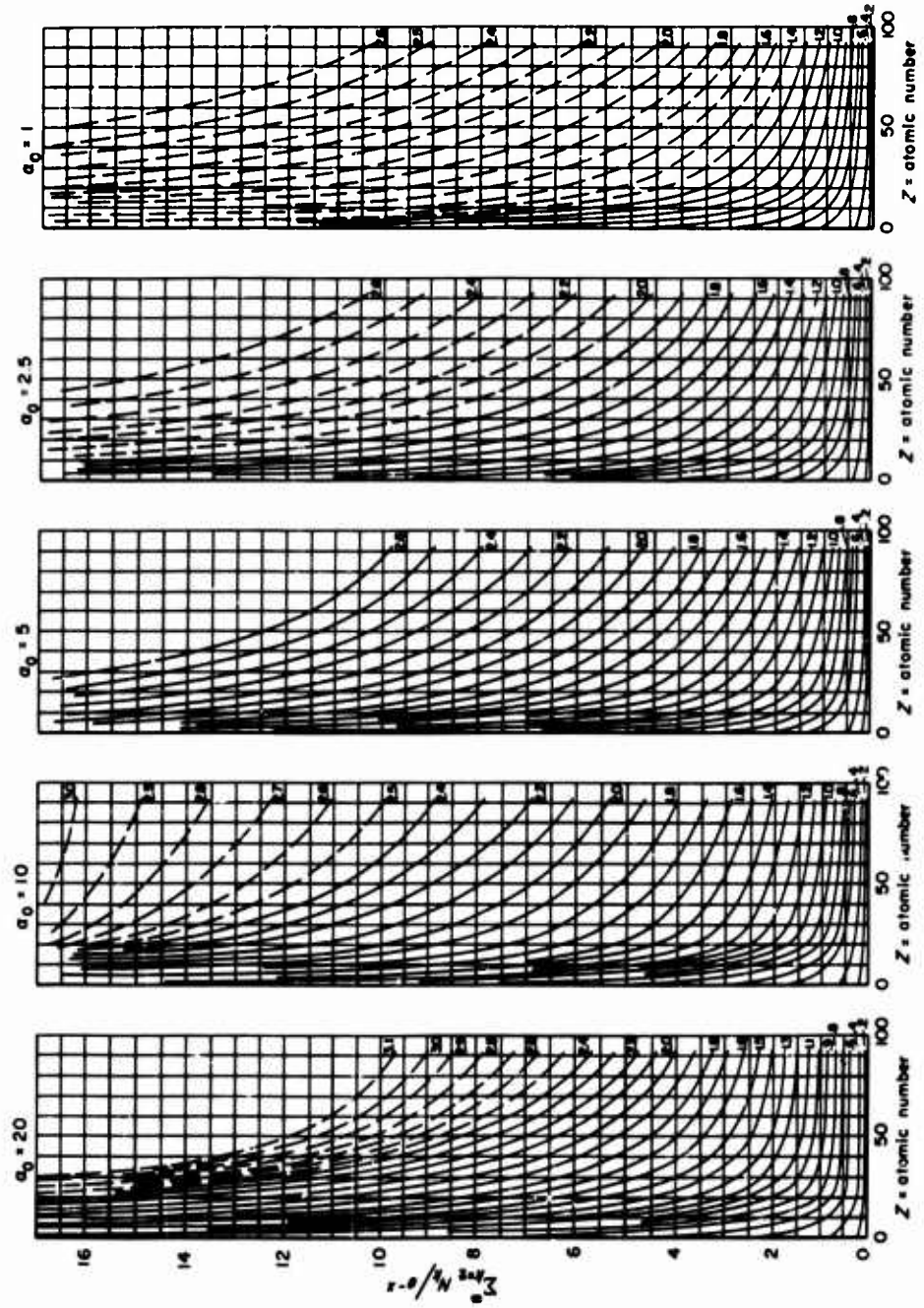

Fig. 58—$\sum_{k=2}^{\infty} N_k/e^{-X}$ vs Z with N_1/e^{-X} as a constant parameter, $\gamma_0 = 1$

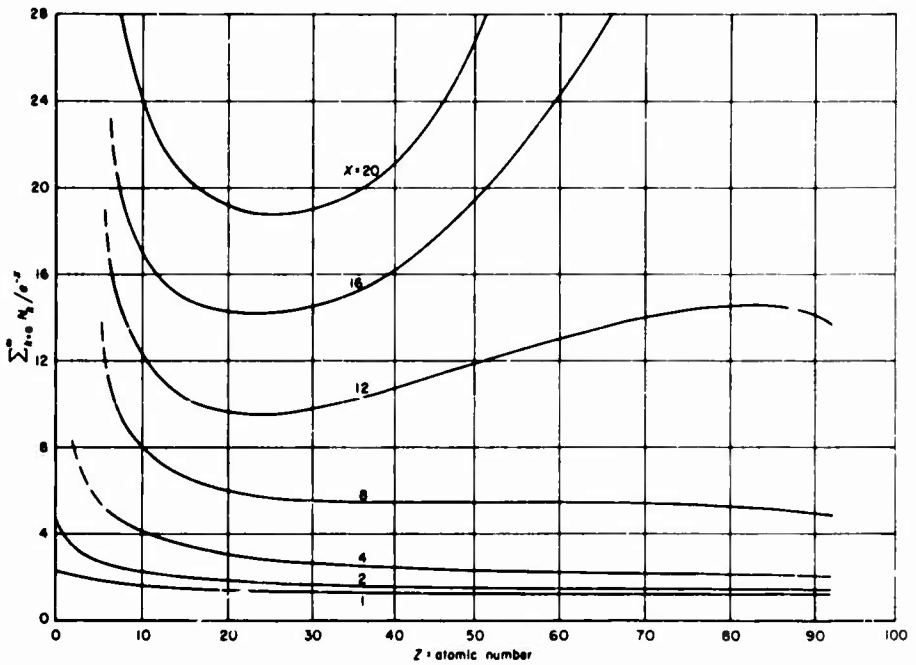

Fig. 59a—Number build-up factor vs atomic number, $\gamma_0 = 1$, $\alpha_0 = 20$

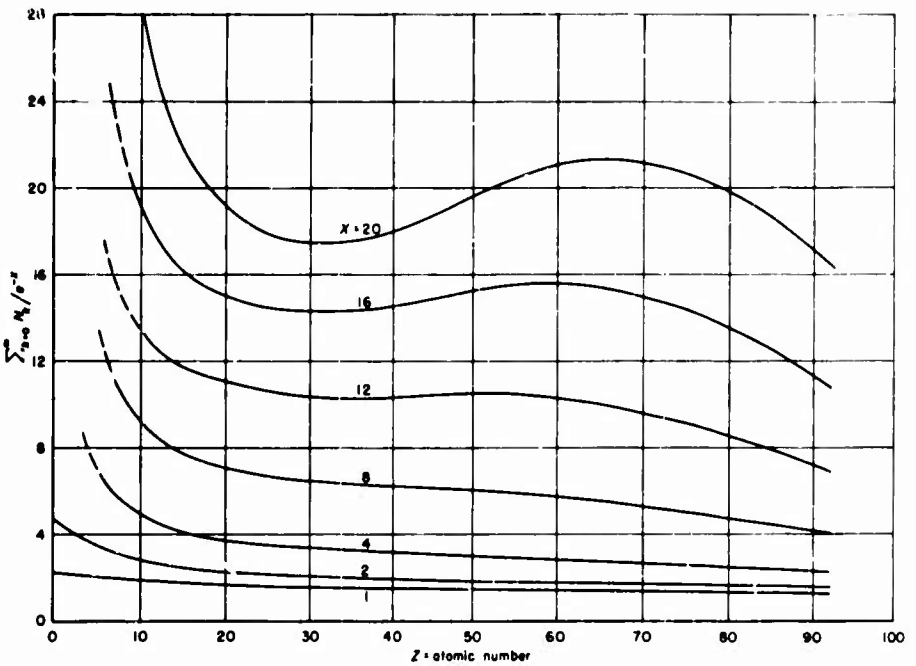

Fig. 59b—Number build-up factor vs atomic number, $\gamma_0 = 1$, $\alpha_0 = 10$

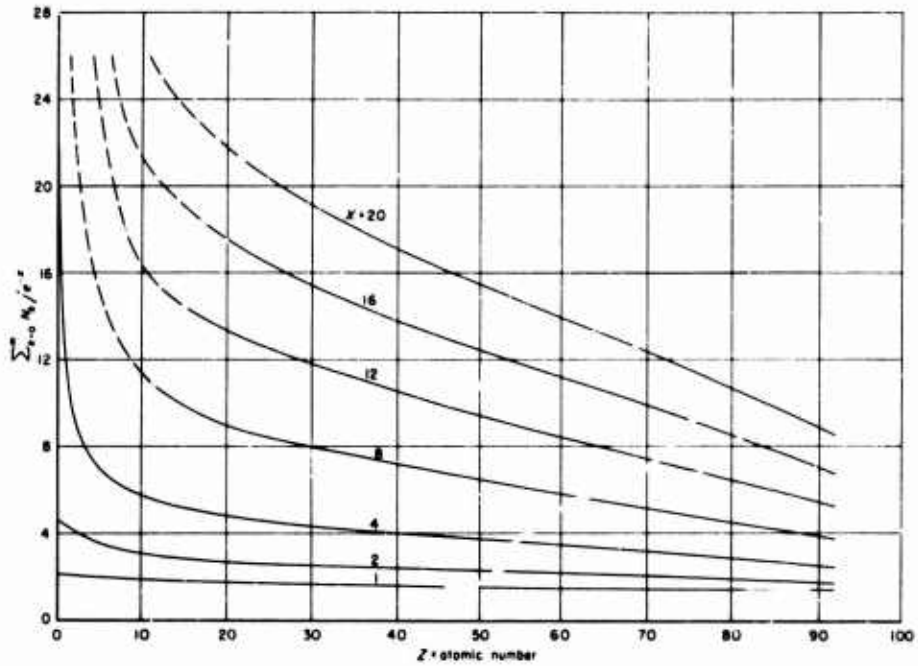

Fig. 59c—Number build-up factor vs atomic number, $\gamma_0 = 1$, $\alpha_0 = 5$

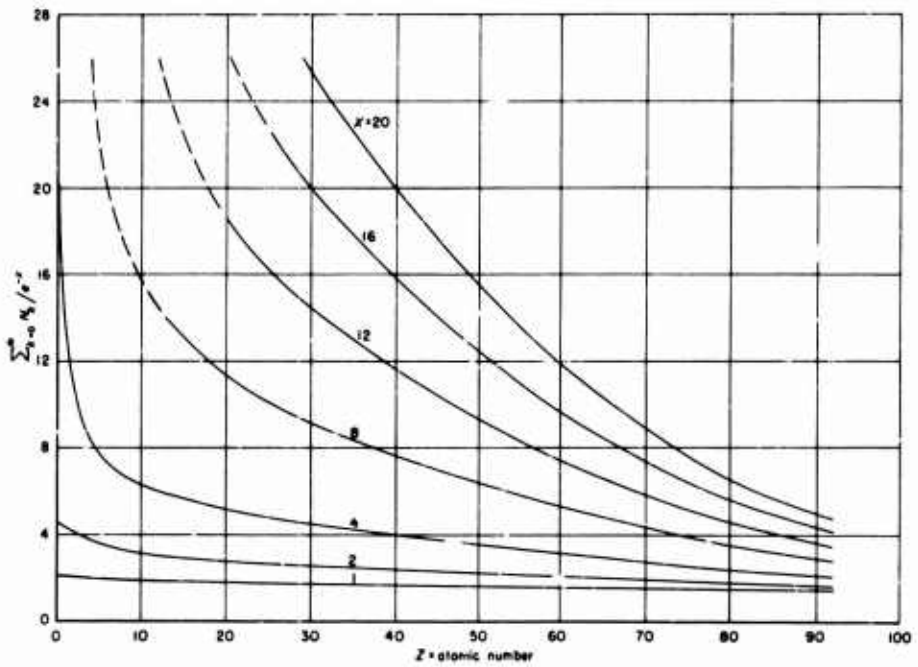

Fig. 59d—Number build-up factor vs atomic number, $\gamma_0 = 1$, $\alpha_0 = 2.5$

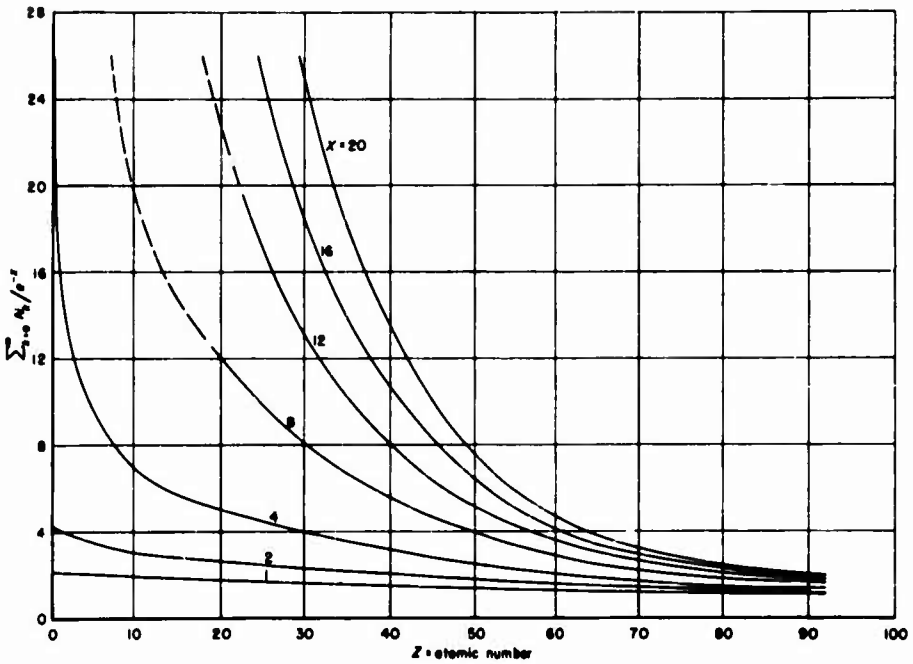

Fig. 59e—Number build-up factor vs atomic number, $\gamma_0 = 1$, $\alpha_0 = 1$

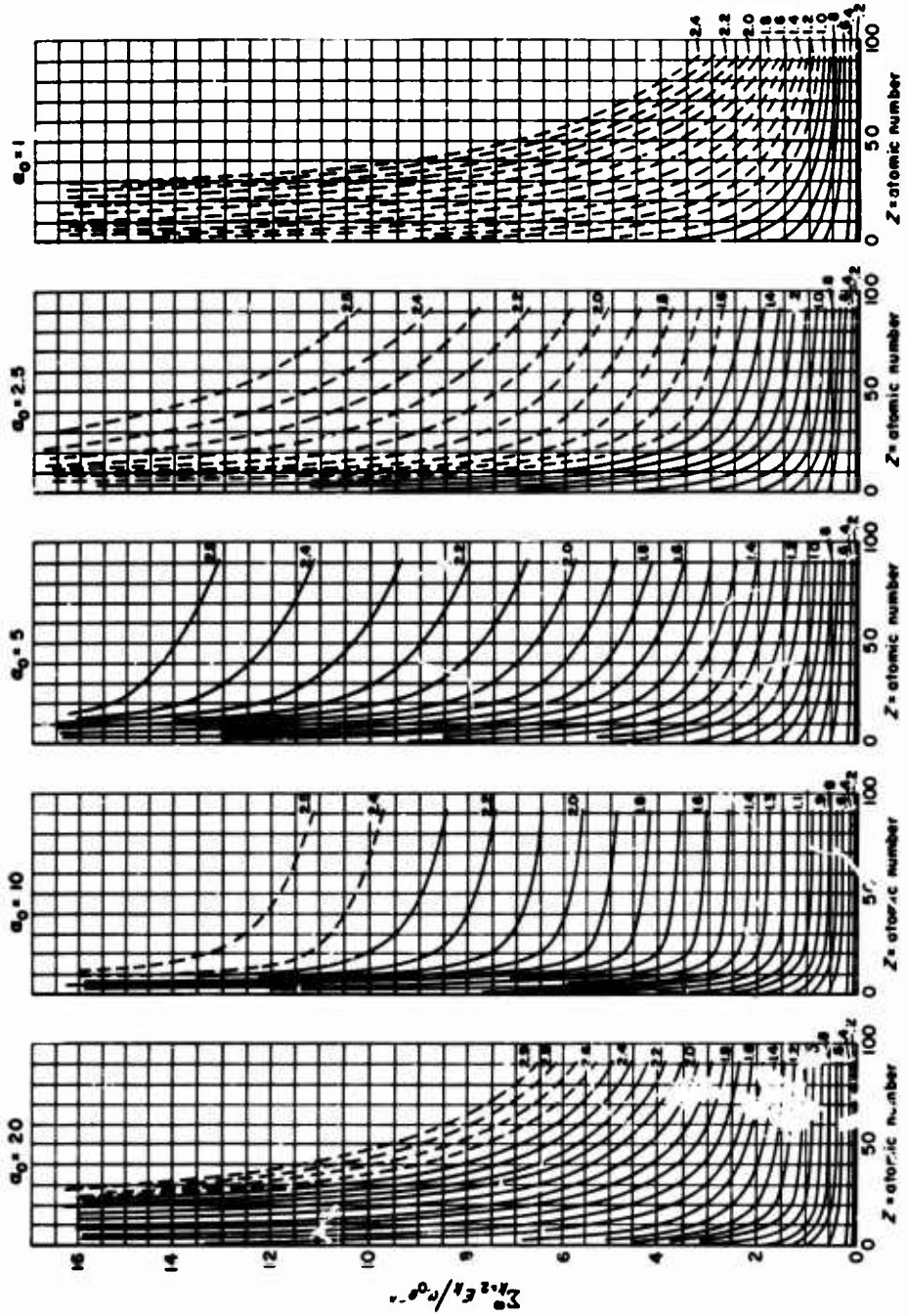

Fig. 60—$\sum_{k=2}^{\infty} E_k/\alpha_0 e^{-Z}$ vs Z with $E_1/\alpha_0 e^{-Z}$ as a constant parameter, $\gamma_0 = 1$

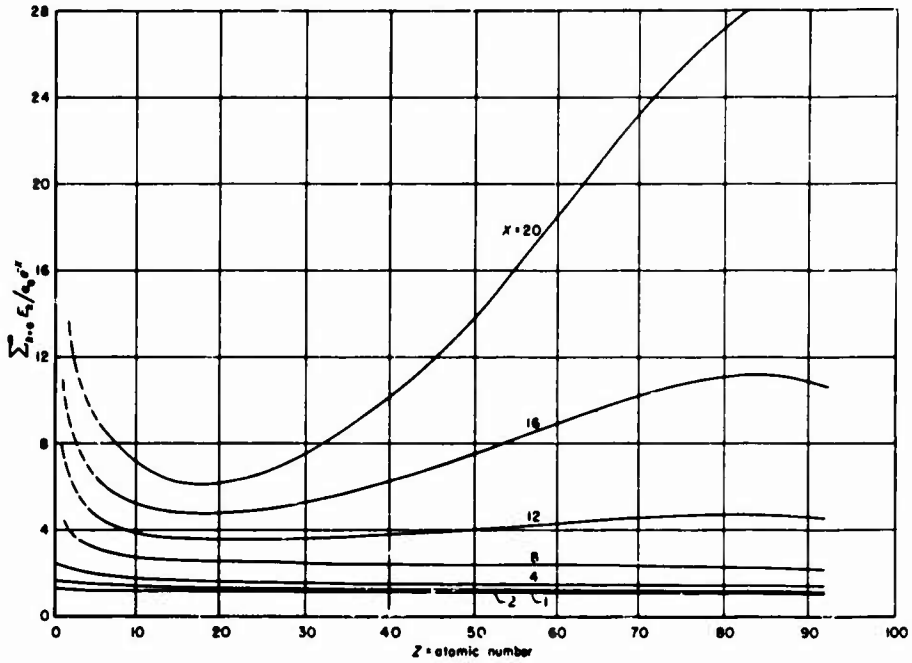

Fig. 61a—Energy build-up factor vs atomic number, $\gamma_0 = 1$, $\alpha_0 = 20$

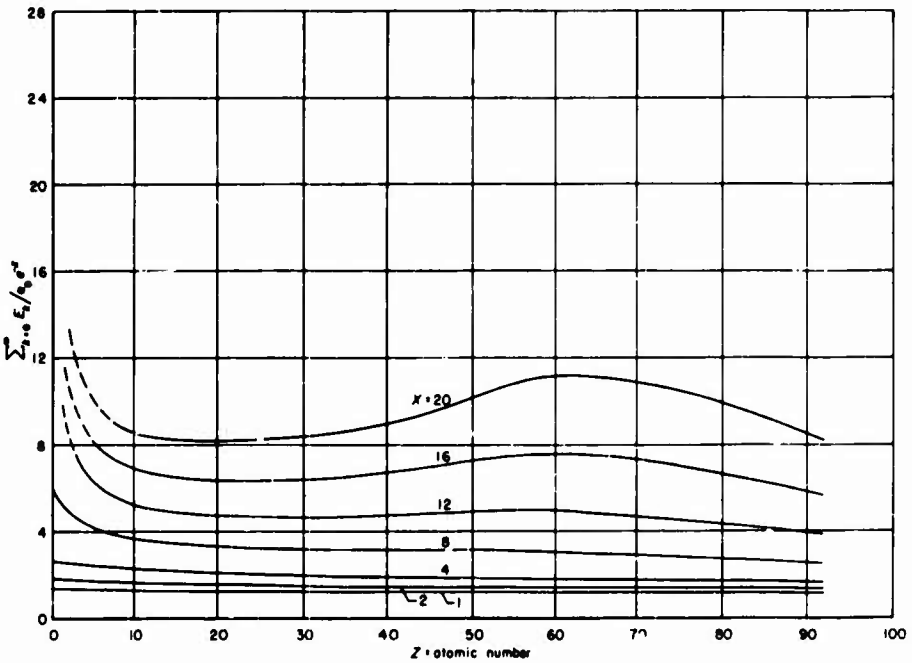

Fig. 61b—Energy build-up factor vs atomic number, $\gamma_0 = 1$, $\alpha_0 = 10$

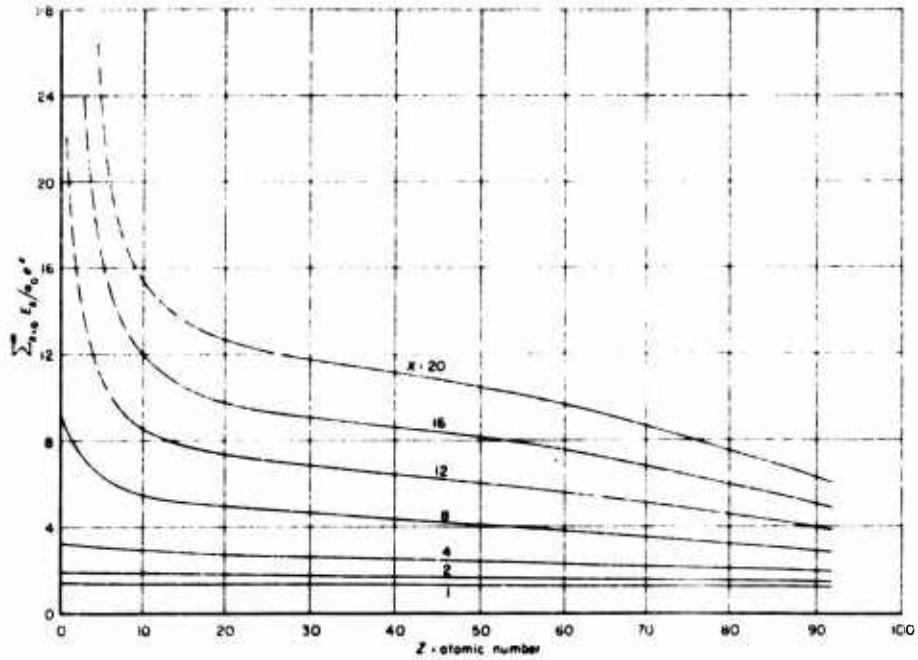

Fig. 61c—Energy build-up factor vs atomic number, $\gamma_0 = 1$, $\alpha_0 = 5$

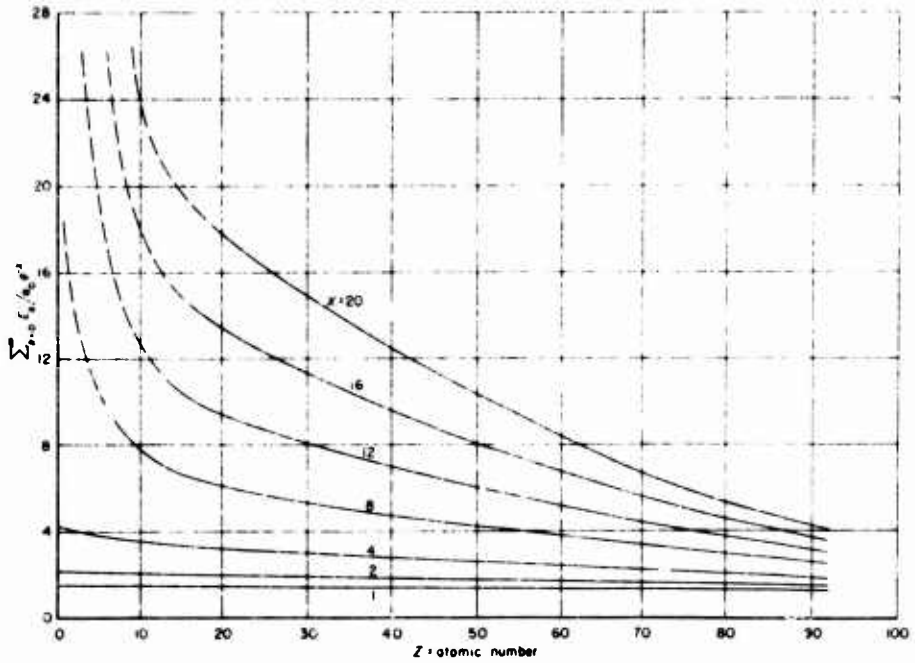

Fig. 61d—Energy build-up factor vs atomic number, $\gamma_0 = 1$, $\alpha_0 = 2.5$

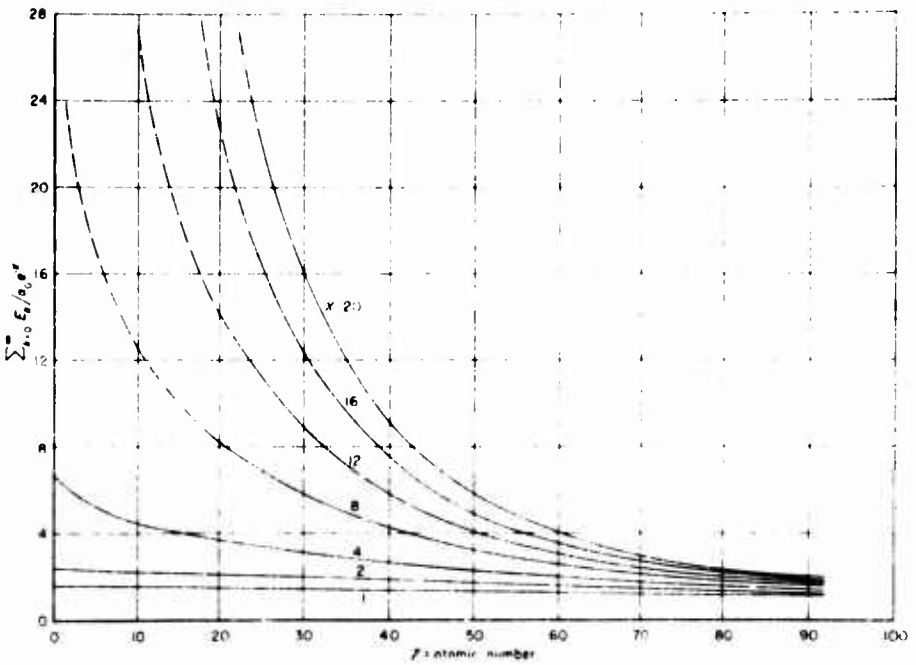

Fig. 61e—Energy build-up factor vs atomic number, $\gamma_0 = 1$, $\alpha_0 = 1$

VII. OTHER GEOMETRIES

If one knows the density of photons due to an isotropic point source in an infinite homogeneous medium, then by superposition one obtains the density arising from any configuration of point sources. In particular, if $p(r)$ is the density at the distance r from a point source of unit strength, the density $pl(x)$ at a distance x from a source plane of unit strength per unit area is readily found to be

$$pl(x) = \int_x^\infty 2\pi r\, p(r)\, dr.$$

Or again, if $l(y)$ is the density at a distance y from a line source of unit strength per unit length, then

$$l(y) = \int_y^\infty \frac{2r\, p(r)\, dr}{\sqrt{r^2 - y^2}}.$$

It is the intention here to apply these relations to the densities which were calculated in Sec. III and which were displayed graphically in Figs. 15 and 16.

It will be recognized at once that the relation between $pl(x)$ and $p(r)$ does not hold for the densities calculated in Sec. III, since the densities were obtained there for a finite slab and a plane of nonisotropic sources. Nevertheless, it may be possible to bring the integral relations to bear, if certain allowances are made.

The incident distribution of Sec. III corresponds to a sheet of isotropic sources from which only those gamma rays in a cone of half-angle $\cos^{-1}0.8$ are accepted. The densities calculated, therefore, are smaller than would have been obtained had the full isotropic source been used. For large slab thickness, the density contribution of those photons whose angle of incidence exceeds $\cos^{-1}0.8$ is certainly small, so that beyond some thickness the density for the plane of isotropic sources can be considered as equal to the density calculated for the plane of nonisotropic sources. To get some indication of where the two densities might be expected to become nearly equal, one turns to Figs. 8*a* through 8*g*, which give the distribution of the transmitted photons for several slab thicknesses. One finds in these figures that the discontinuities in the transmitted distribution caused by not using the full isotropic source have nearly disappeared at a thickness of 12 mfp. It seems reasonable, therefore, to assume that the two densities will have become approximately equal at about this thickness.

For thin slabs, the density corresponding to a plane of isotropic sources can be determined with fair accuracy from a calculation of the density of photons unscattered and once scattered. Suppose a calculation of this density, which is not a large task, is made for a thickness of 1 mfp. Then one has available for determining the density at the rear face

of a slab of thickness X, when a sheet of isotropic sources lies in the front face, a value for $X = 1$ and the approximate values for $X > 12$. By drawing a curve passing through the point at $X = 1$ and gradually approaching coincidence with the density curve calculated for the plane of nonisotropic sources, one should obtain a reasonably accurate curve of the density corresponding to a plane of isotropic sources.

This estimate, which is for a finite slab, must be converted to a like result for the infinite homogeneous medium. Clearly the density at a distance X from the source plane in an infinite homogeneous medium is greater than the density at the rear face of a slab of thickness X. But the difference is composed entirely of photons which have experienced at least one backward scattering. One would expect, therefore, in the case of the heavier materials such as iron and lead, that the absorption by the photoelectric effect would make the difference small. The difference in the density at $X = 1$ was found to be about 10 per cent. The important cause of the difference is those photons which pass through the slab without a collision but which are reflected back with one collision by the infinite medium. It seems likely that the difference would decrease percentagewise as X increases. For with increasing values of X, the difference must be composed more and more of reflected photons which have experienced several collisions at low energies. The probability of a photon's surviving several collisions in the low energy range is small.

The uppermost curve of the three curves displayed in Figs. 62*a* through 62*d* gives the photon density (normalized by the factor c/e^{-X}, where c is the velocity of light) at a distance X from a plane of isotropic sources in an infinite medium. The materials are lead and iron and the energies of the emitted photons are 20 and 10 mc^2. In each of these four cases, the plane of isotropic sources is assumed to be emitting one photon per square centimeter per unit time. The photon densities are estimated in accordance with the preceding remarks. That is to say, the curve given is determined from an estimate of the densities at $X = 1$ and $X > 12$. At $X = 1$, the 10 per cent increase in the density for the infinite medium over the finite slab is taken, but as X increases to about 12 or 16, the difference is allowed to dwindle to zero. This is equivalent to assuming that beyond $X = 12$ the density for the plane of isotropic sources in the infinite medium becomes identical with the density for the nonisotropic plane of sources and the finite slab.

The lowermost curve of the three curves presented in Figs. 62*a* through 62*d* is obtained from the corresponding uppermost curve by means of the integral relation between $pl(x)$ and $p(r)$, given at the beginning of this section. Specifically, the lowest curve gives the photon density (normalized by the factor c/e^{-R}) at the distance R (in mean free paths) from a point source which emits in an infinite homogeneous medium one photon per unit time.

The middle curve is the photon density (normalized by the factor c/e^{-Y}) at a distance Y (in mean free paths) from a line source which emits in an infinite homogeneous medium one photon per centimeter per unit time. This curve is derived from the lowest curve by means of the integral relation between $l(y)$ and $p(r)$.

Figures 63*a* through 63*d* are identical with Figs. 62*a* through 62*d*, except that the quantity under consideration is the energy density and the normalization factor contains $1/\alpha_0$.

The three curves forming a set are consistent.* So if it is assumed that the density for the plane source is accurate, then the densities for the line source and the point source are also accurate. Whether or not the density for the plane source is reasonably accurate is difficult to say. It would seem that the errors, though possibly large, should be small enough to allow the set of three densities given to retain some interest. To be sure, the density corresponding to the point source is obtained by a numerical evaluation of a derivative, so that the error associated with the plane source is likely to be aggravated in the passage from plane source to point source, but if the assumptions under which the key density is obtained are not altogether erroneous, the error in the derived densities should not be serious in terms of practical attenuation calculations. In any case the relative position of one curve to another has interest as an indication of the effect of geometry even if the absolute position is judged to be too much in error to have value.

* Not only are the three curves of a set consistent with respect to the two integral relations stated, but also $pl(x)$ and $l(y)$ satisfy the relation

$$pl(x) = \int_x^\infty \frac{2y\, l(y)\, dy}{\sqrt{y^2 - x^2}} .$$

* * *

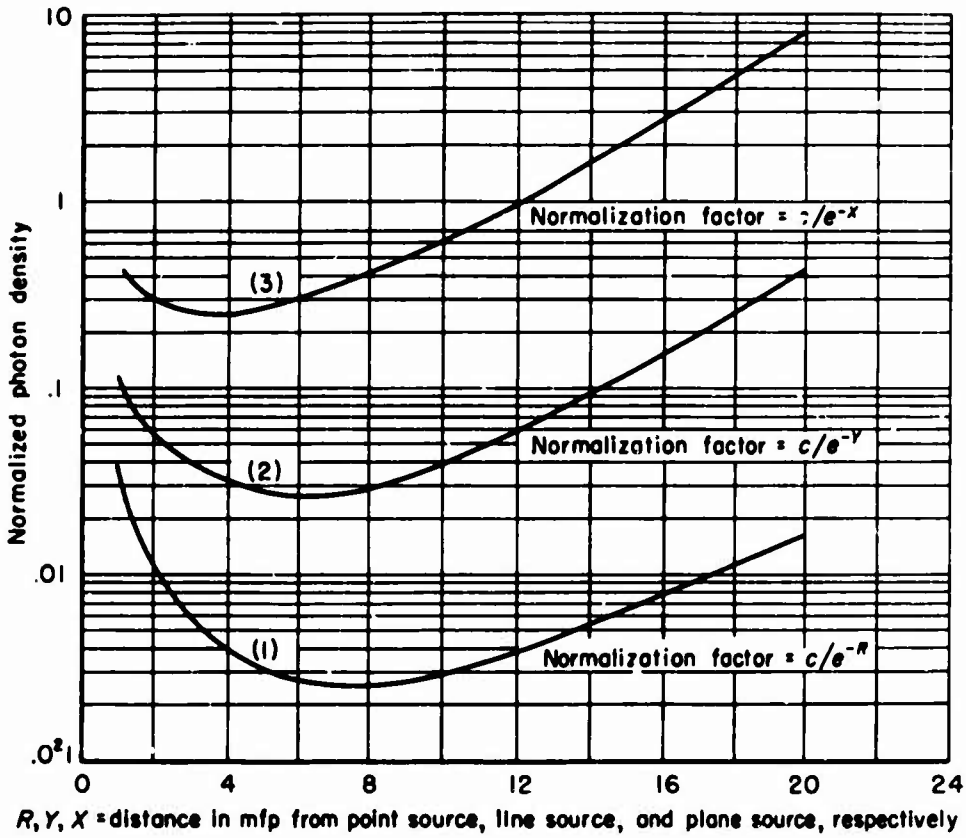

Fig. 62a—Comparison of photon densities for three source configurations in an infinite homogeneous medium—lead, $\alpha_0 = 20$

The three source configurations are (1) point source of unit strength, (2) line source of unit strength per centimeter, and (3) plane source of unit strength per square centimeter. (A source of unit strength is defined here as a source emitting one photon per unit time.)

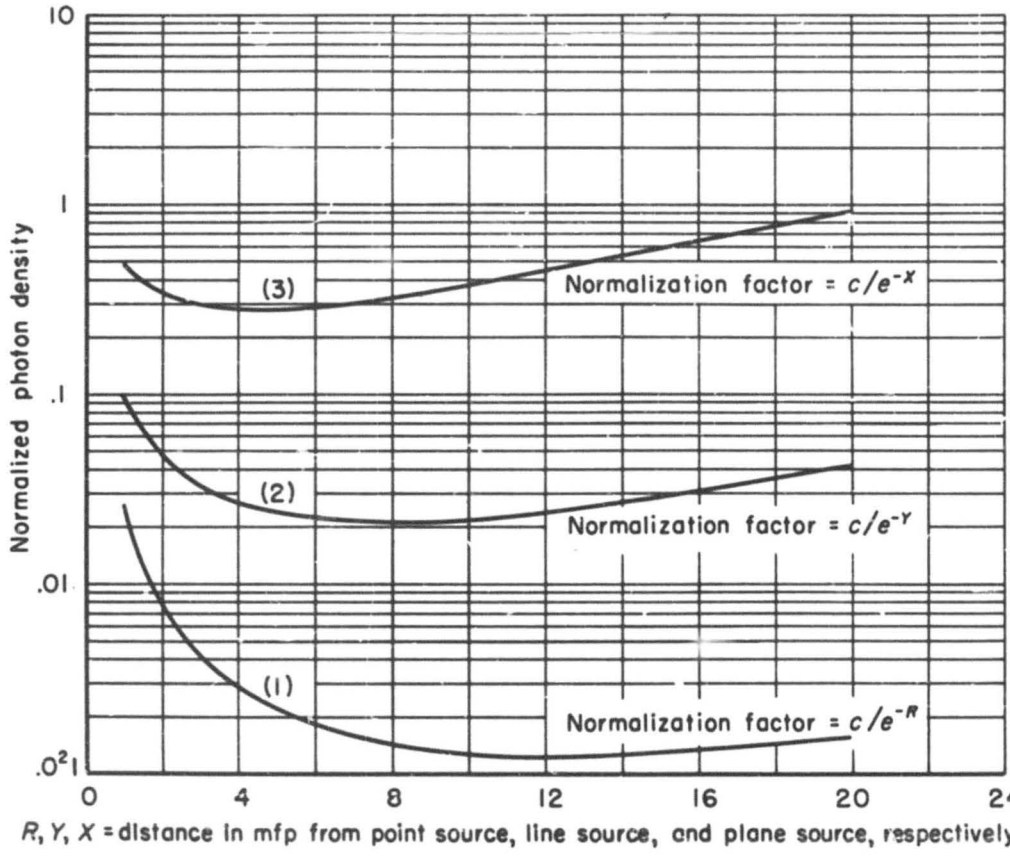

Fig. 62b—Comparison of photon densities for three source configurations in an infinite homogeneous medium—lead, $\alpha_0 = 10$

The three source configurations are (1) point source of unit strength, (2) line source of unit strength per centimeter, and (3) plane source of unit strength per square centimeter. (A source of unit strength is defined here as a source emitting one photon per unit time.)

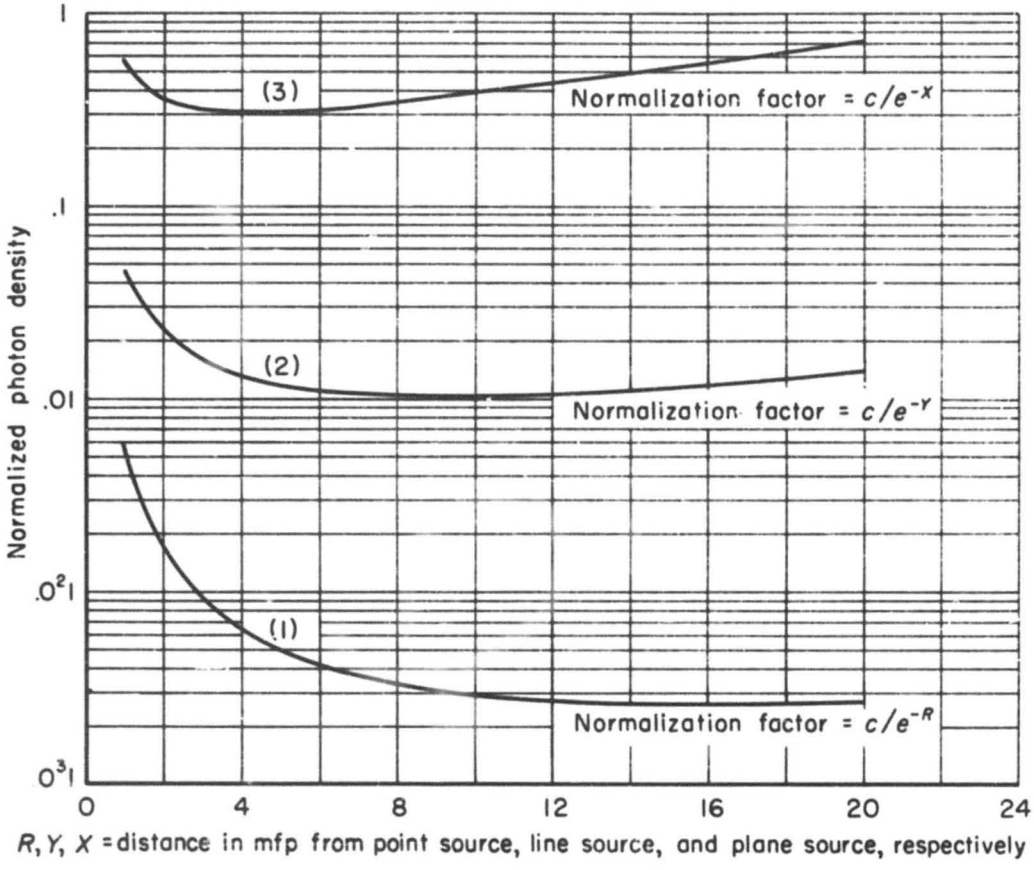

Fig. 62c—Comparison of photon densities for three source configurations in an infinite homogeneous medium—iron, $\alpha_n = 20$

The three source configurations are (1) point source of unit strength, (2) line source of unit strength per centimeter, and (3) plane source of unit strength per square centimeter. (A source of unit strength is defined here as a source emitting one photon per unit time.)

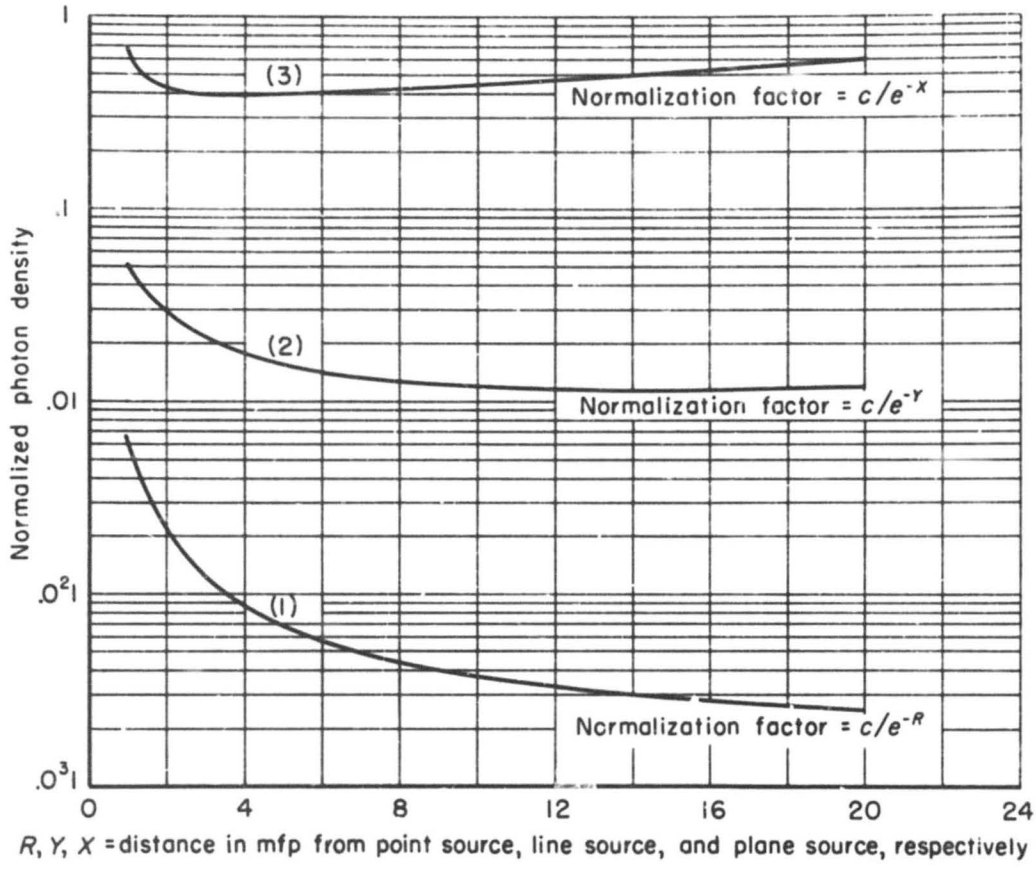

Fig. 62*d*—Comparison of photon densities for three source configurations in an infinite homogeneous medium—iron, $\alpha_0 = 10$

The three source configurations are (1) point source of unit strength, (2) line source of unit strength per centimeter, and (3) plane source of unit strength per square centimeter. (A source of unit strength is defined here as a source emitting one photon per unit time.)

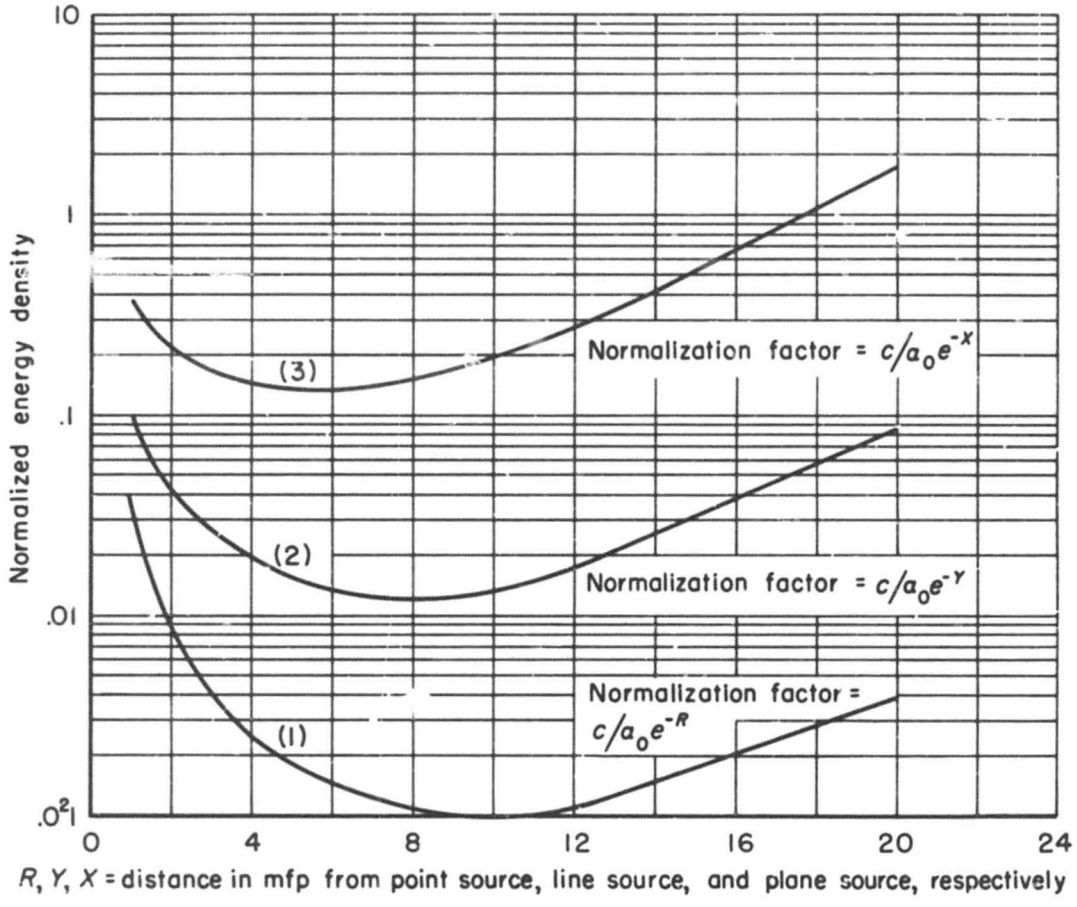

Fig. 63a—Comparison of energy densities for three source configurations in an infinite homogeneous medium—lead, $\alpha_0 = 20$

The three source configurations are (1) point source of unit strength, (2) line source of unit strength per centimeter, and (3) plane source of unit strength per square centimeter. (A source of unit strength is defined here as a source emitting one photon per unit time.)

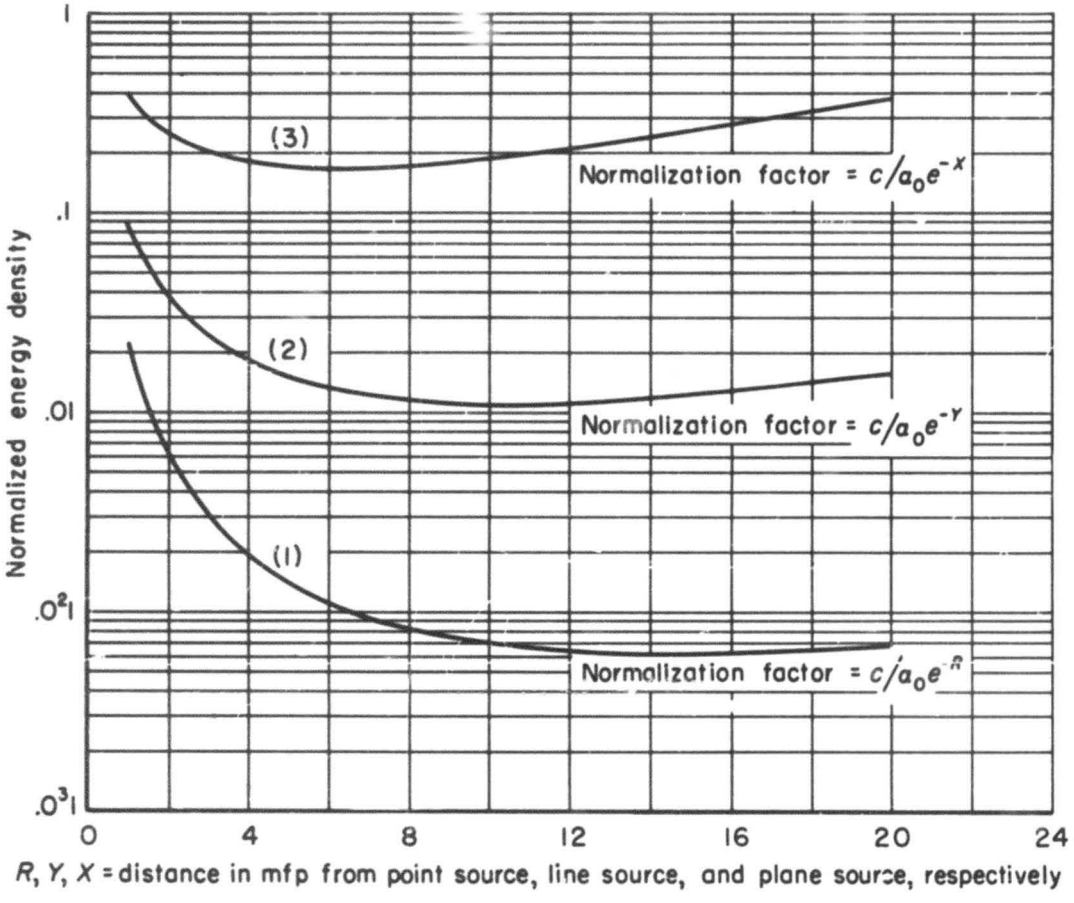

Fig. 63b—Comparison of energy densities for three source configurations in an infinite homogeneous medium—lead, $\alpha_0 = 10$

The three source configurations are (1) point source of unit strength, (2) line source of unit strength per centimeter, and (3) plane source of unit strength per square centimeter. (A source of unit strength is defined here as a source emitting one photon per unit time.)

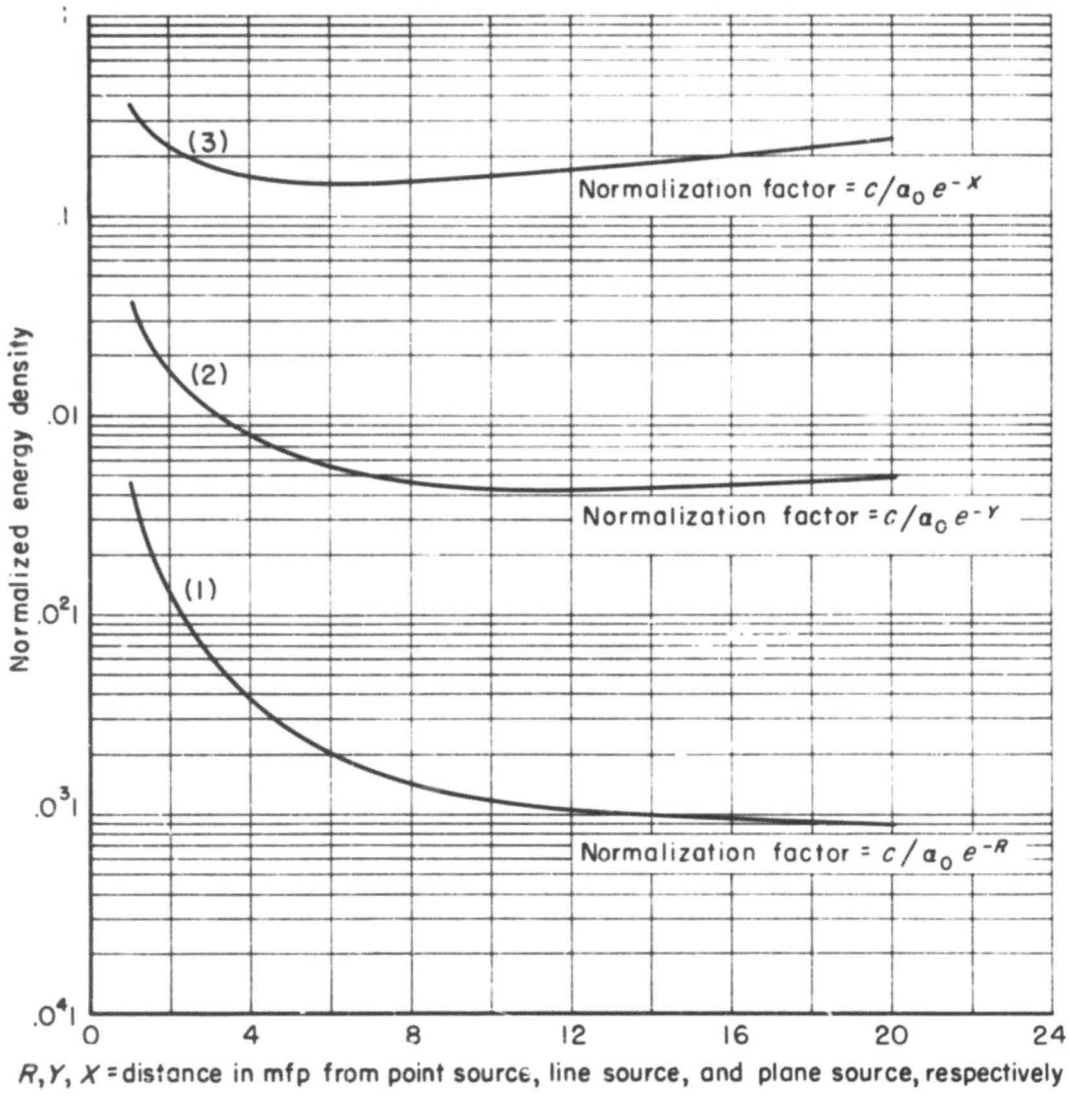

Fig. 63c—Comparison of energy densities for three source configurations in an infinite homogeneous medium—iron, $\alpha_0 = 20$

The three source configurations are (1) point source of unit strength, (2) line source of unit strength per centimeter, and (3) plane source of unit strength per square centimeter. (A source of unit strength is defined here as a source emitting one photon per unit time.)

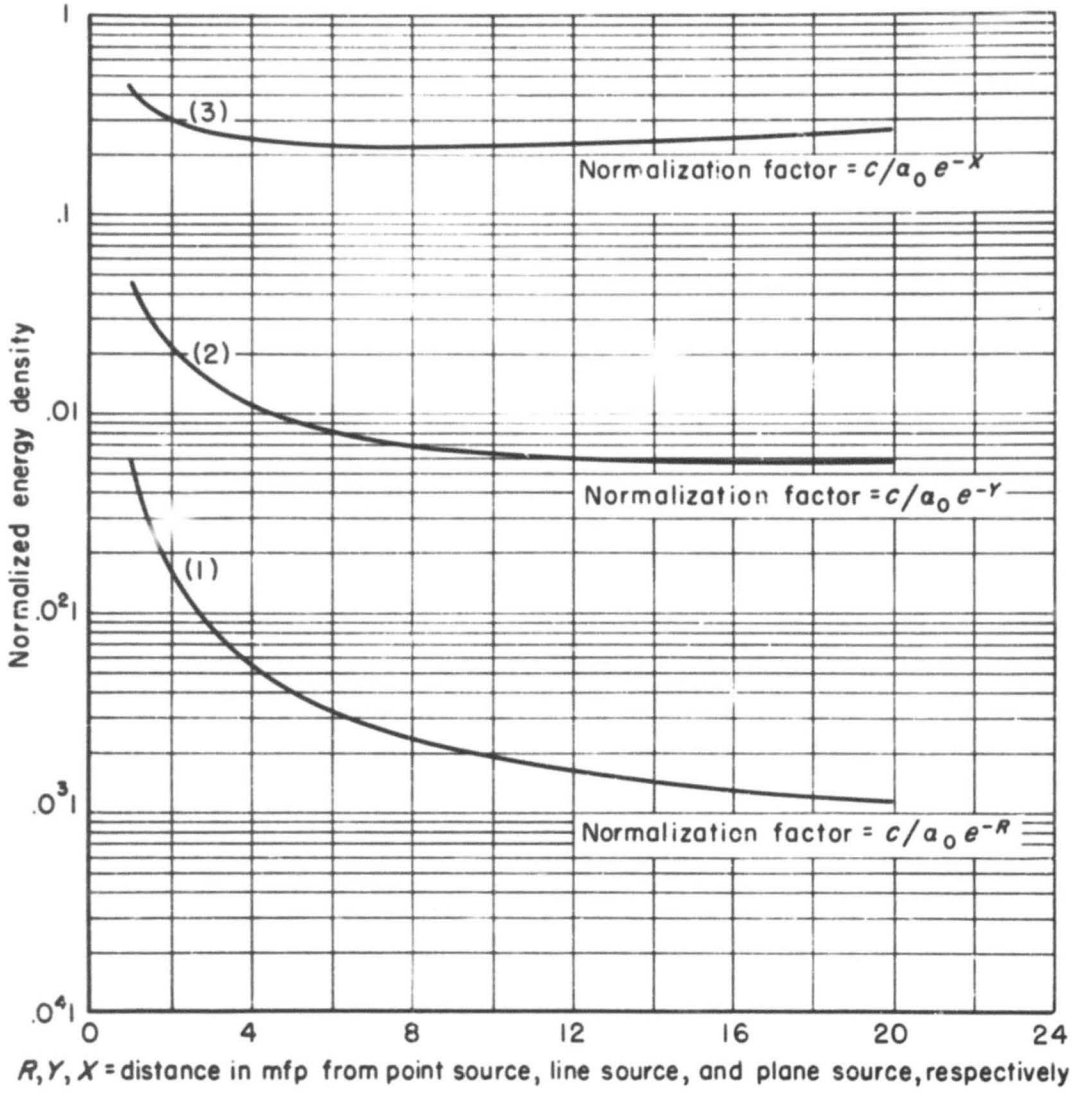

Fig. 63*d*—Comparison of energy densities for three source configurations in an infinite homogeneous medium—iron, $\alpha_0 = 10$

The three source configurations are (1) point source of unit strength, (2) line source of unit strength per centimeter, and (3) plane source of unit strength per square centimeter. (A source of unit strength is defined here as a source emitting one photon per unit time.)

VIII. COMPARISONS

Most investigations of gamma-ray transmission differ a great deal in the problem set, in the conditions assumed, or in the form of the results. As a consequence, comparison of results is very difficult. One can note that the curves given by Spencer and Fano* are very similar to those of Fig. 10*a* of this report, but the comparison is not exact and, since any existing essential differences can presumably be attributed to the difference in the incident beams, nothing much is proved. Nor can one expect to obtain much in the way of a comparison between the asymptotic formulas of Fano, Hurwitz, and Spencer† and the energy build-up factors presented here, since the latter are most accurate for small thicknesses and the former are most accurate for large thicknesses. In general, comparison is a matter of much computation leading to inconclusive results. The present results are compared here only with those unclassified results of other workers which are generally available.

The difficulties are least in the comparison of the results with Hirschfelder, Magee, and Hull,[4] and Hirschfelder and Adams.[5] The geometry and the materials are the same as those used here; even the methods are similar in that both attempt to obtain the total transmission by summing the successive transmissions with k scatterings. The device used by Hirschfelder *et al.* for expediting the calculation or the estimation of the transmission with k scatterings is an "effective angle of Klein-Nishina scattering"; i.e., an average angle of scatter is taken so that the correct transmission with one collision is obtained for Compton scattering. With this short-cut the individual transmissions are calculated successively, and presumably rapidly, to a large number of scatterings.

The comparison can appropriately begin with a pure Compton scatterer.†† For, although the methods of this report are much less effective in the absence of pair production and the photoelectric effect, Hirschfelder's use of an average angle of scatter based on Klein-Nishina scattering gives the pure Compton scatterer precedence over iron or lead. Table 15 displays side by side the transmission with one and two scatterings and the build-up factors taken from the two sets of results. The quantities I_1/A, I_2/A, and I/I_0 are identical, respectively, with the quantities E_1/α_0, E_2/α_0, and $\sum_{k=0}^{\infty} E_k/\alpha_0 e^{-X}$ of this report.

No large discrepancies should exist in the transmission with one scattering. This is seen to be the case, except in one instance: $\alpha_0 = 10$, $X = 20$. If the use of the average angle of scatter is sound, then the transmissions with two scatterings should also agree. The difference expressed in a percentage is given in the column headed "per cent difference." Except in the cases $\alpha_0 = 2, 6, 10$, $X = 1$ and in the case $\alpha_0 = 10$, $X = 10$, the percentages are not too large. The differences are, however, all of the same sign.

---

* See Ref. 11, Fig. 5.

† See Ref. 12, Table I.

†† Cave *et al.* (Ref. 1) compare their results with those of Hirschfelder *et al.* A comparison here with Hirschfelder *et al.* is therefore an indirect comparison with Cave *et al.*

This fact, more than the magnitude of the differences, is disturbing, since it indicates a uniform tendency to underestimate. This tendency, one surmises, might increase rapidly as the number of collisions increases. If this surmise is correct, it should show in the comparison of the build-up factors. Unfortunately, the greatest thickness for which $\sum_{k=0}^{\infty} E_k/\alpha_0 e^{-X}$ can be read from Fig. 22 is 4 mfp. Since even this thickness may have overstrained the resources of the method used to obtain the energy build-up factor, one cannot say which of the quantities, $\sum_{k=0}^{\infty} E_k/\alpha_0 e^{-X}$ or I/I_0, is more likely to be the cause of the large discrepancy in their values at 4 mfp. Kahn obtains by the "Monte Carlo" method* a value of about 3.3 for the build-up factor when $\alpha_0 = 2.5$, $X = 4$. His value at this thickness is certainly correct, and since Hirschfelder's value is practically identical to Kahn's, it seems that the divergence of I_k/A from the correct value does not occur. However, Kahn, in obtaining his build-up factor, discarded all photons transmitted with energy less than 0.1 mc^2. One may judge that this cannot account for the difference of some 21 per cent between his value and the value 4.2 given in Table 15 for $\sum_{k=0}^{\infty} E_k/\alpha_0 e^{-X}$; but had $E_k/\alpha_0 e^{-X}$ been discarded for those values of k for which the average energy in the photons was estimated to be less than 0.1 mc^2, then the estimated build-up factor would have been about 19 per cent smaller. It would seem, therefore, that $\sum_{k=0}^{\infty} E_k/\alpha_0 e^{-\lambda}$ is correct at $X = 4$, or if not correct, then the error is due to an overestimate of the energy transmitted in the form of photons of many collisions. This last conclusion the writer is reluctant to accept.†

Tables 16 and 17 compare, respectively, results for iron and for lead. Not much needs to be pointed out that the reader will not discover from a brief examination of the tables. Agreement, it will be noted, improves as the incident energy passes from 10 to 2 mc^2. This is just the opposite to what was found in the case of the pure Compton scatterer. Apparently when absorption by pair production and the photoelectric effect is present, the use of the effective angle of scatter causes overestimates which tend to destroy the agreement observed at high incident energies, but which tend to compensate for the underestimates noticed at low incident energies in the case of the Compton scatterer.

In the case of iron, the total absorption coefficients used in both sets of calculations are nearly identical except for a small difference in the electron density—a difference of no significance as long as thickness is expressed in mean free paths. In the case of lead, the difference in the total absorption coefficients has a little more significance. About 5 to 10 per cent of the magnitude of the differences for lead can be attributed to this difference in the total absorption coefficients.

The "straight-ahead" and "root-mean-square-angle" approximations to the transport equation of Solon and Wilkins[14] and of Solon, Wilkins, Oppenheim, and Goldstein[15] also give results relatively easy to compare. The straight-ahead approximation modifies the transport equation by assuming that the photons are not deflected from their incident direction by the Compton scattering. The root-mean-square-angle approximation moder-

---

* See Ref. 13, Fig. 4.

† This is not to say that Kahn's value is incorrect or that he is wrong in ignoring photons of energy less than 0.1 mc^2. His intent was to obtain—to use his words from a casual conversation—"the energy transmitted in 'able-bodied' photons."

ates the severity of this assumption by introducing an average angle of deviation from the incident direction. The average is so taken that the angular deviation is "... exact for those photons which have suffered at most one collision, and ... an approximation in a root mean-square sense for those photons which have experienced two or more small-angle collisions."

In this case, only the build-up factors can readily be compared. The definitions of the number and energy build-up factors used by Solon *et al.* become, in the notation of this report, $\sum_{k=1}^{\infty} N_k/e^{-\mu_0 a}$ and $\sum_{k=1}^{\infty} E_k/\alpha_0 e^{-\mu_0 a}$, except in the case of the results for the the straight-ahead approximation, where μ_0 is replaced by μ_m, the smallest value of μ for $\alpha \leq \alpha_0$. The values given by Solon *et al.* for the lead and the iron build-up factors are changed to the forms $\sum_{k=0}^{\infty} N_k/e^{-\mu_0 a}$ and $\sum_{k=0}^{\infty} E_k/\alpha_0 e^{-\mu_0 a}$, and appear in Tables 18 and 19 under the headings $1 + B_N$ and $1 + B_E$.

With a few exceptions, all the build-up factors obtained by the root-mean-square-angle approximation are less than those of this report. Although in many cases the differences are less than the error, and although some of the discrepancies are no doubt due to the total absorption coefficients used, the fact that nearly all the build-up factors obtained by the root-mean-square-angle approximation are low—in some instances less than the sum of the transmissions with zero, one, two, and three scatterings—indicates that the root-mean-square-angle approximation overcompensates for the neglect of the angular deviation in the straight-ahead approximation. One notes, however, that when conditions are such that the deviations are small, or when the transmission with at most one collision is a large part of the total transmission (conditions under which the approximation used is nearly valid), the build-up factors agree fairly well. One infers from this that the root-mean-square-angle approximation might serve very well to estimate transmission for many practical problems.

Data obtained experimentally and suitable for comparison are scarce. The experimental data most frequently referred to are those of White,[16] but they, unfortunately, do not lend themselves to comparison here because of the geometry (spherical) and the material (water). Build-up factors reported by Dixon[17] for slabs of lead and of concrete seem to provide the most suitable experimental data.

Dixon's source of gamma rays is Co^{60}, which emits two rays averaging approximately 2.5 mc^2. For photons of 2.5 mc^2 incident on a slab of lead 12-mfp thick, Fig. 5*d* of this report gives a build-up factor of 3.6, a value about 19 per cent smaller than Dixon's value of 4.5. Although this is not remarkably good agreement, it is probably as good as can be expected.

Concrete, since it is composed of elemental materials of small atomic number, provides build-up factors in a region where the methods of this report are not very successful. However, values of the build-up factor read from Fig. 61*d* for an atomic number of about 7 agree fairly well up to a thickness of 12 mfp with Dixon's build-up factors for concrete.

Perhaps it should be pointed out that the position of experimental data as arbiter of the correctness of a build-up factor is not too secure. The value of a build-up factor is only ordinarily sensitive to variations in the total absorption coefficient; on the other hand, the total transmission is exceptionally sensitive. This is, of course, due to the fact

that e^{-X} appears in the transmission, but not in the build-up factor. An error of p per cent in μ_0 causes an error of Xp per cent in $e^{-\mu_0 a}$. In the computation of a build-up factor, one is calculating directly the ratio of the total transmission to e^{-X}. In determining a build-up factor experimentally, one is dealing not with the ratio, but with the numerator and denominator separately. Hence, in the determination of a build-up factor, computation has an advantage over experiment in not having to contend with the sensitivity of e^{-X} to errors in μ_0. In the determination of transmission, computation does not have this advantage.

* * *

Table 15

COMPARISON OF TWO SETS OF RESULTS FOR SLABS OF THE PURE COMPTON SCATTERER: ONE SET OBTAINED BY THE METHOD OF "EFFECTIVE ANGLE OF KLEIN-NISHINA SCATTERING," THE OTHER BY THE METHODS OF THIS REPORT*

α_0	X	E_1/α_0	I_1/A	E_2/α_0	I_2/A	Per cent difference	α_0	X	$\sum_{k=0}^{\infty} E_k/\alpha_0 e^{-X}$	I/I_0
10	1	.0964	.0969	.0205	.0233	12	10	1	1.35	1.35
	2	.0606	.0603	.0203	.0214	5		2	1.71	1.70
	5	$.0^{2}540$	$.0^{2}547$	$.0^{2}289$	$.0^{2}310$	7		4	2.58	2.39
	10	$.0^{4}536$	$.0^{4}538$	$.0^{4}358$	$.0^{4}426$	16				
	20	$.0^{8}361$	$.0^{8}335$	$.0^{8}322$	$.0^{8}352$	9				
6	1	.108	.109	.0243	.0282	14	5	1	1.42	1.42
	2	.0685	.0681	.0253	.0263	4		2	1.90	1.87
	5	$.0^{2}627$	$.0^{2}624$	$.0^{2}373$	$.0^{2}380$	2		4	3.23	2.81
	10	$.0^{4}617$	$.0^{4}617$	$.0^{4}486$	$.0^{4}519$	6				
	20	$.0^{8}394$	$.0^{8}386$	$.0^{8}408$	$.0^{8}426$	4				
2	1	.133	.133	.0346	.0403	14	2.5	1	1.51	1.50
	2	.0838	.0836	.0353	.0385	8		2	2.12	2.05
	5	$.0^{2}755$	$.0^{2}771$	$.0^{2}552$	$.0^{2}581$	5		4	4.2	3.26
	10	$.0^{4}767$	$.0^{4}767$	$.0^{4}758$	$.0^{4}806$	6				
	20	$.0^{8}482$	$.0^{8}483$	$.0^{8}668$	$.0^{8}676$	1				

*X = slab thickness in mean free paths.
α_0 = energy of incident photons in units of mc^2.
E_k = expected energy of a photon transmitted with exactly k collisions.
I_k/A is equivalent to E_k/α_0 but is obtained by using the effective angle of Klein-Nishina scattering.
I/I_0 is equivalent to $\sum_{k=0}^{\infty} E_k/\alpha_0 e^{-X}$.

Table 16

COMPARISON OF TWO SETS OF RESULTS FOR IRON SLABS: ONE SET OBTAINED BY THE METHOD OF "EFFECTIVE ANGLE OF KLEIN-NISHINA SCATTERING," THE OTHER BY THE METHODS OF THIS REPORT*

α_0	X	E_1/α_0	I_1/A	E_2/α_0	I_2/A	E_3/α_0	I_3/A	$\sum_{k=0}^{\infty} E_k/\alpha_0 e^{-X}$	I/I_0
10	1.36	.0713	.0757	.0160	.0191	$.0^{2}334$	$.0^{2}534$	1.35	1.40
	2.72	.0320	.0351	.0119	.0136	$.0^{2}333$	$.0^{2}509$	1.75	1.86
	6.80	$.0^{2}108$	$.0^{2}122$	$.0^{3}673$	$.0^{3}833$	$.0^{3}298$	$.0^{3}465$	2.9	3.69
	13.6	$.0^{5}187$	$.0^{5}219$	$.0^{5}159$	$.0^{5}223$	$.0^{6}901$	$.0^{5}171$	5.4	8.33
	27.2	$.0^{11}35$ (?)	$.0^{11}401$	$.0^{11}38$ (?)	$.0^{11}577$	$.0^{11}38$ (?)	$.0^{11}591$	13.0 (?)	23.00
6	1.12	.0989	.101	.0228	.0263	$.0^{2}512$	$.0^{2}743$	1.39	1.42
	2.25	.0554	.0572	.0206	.0224	$.0^{2}672$	$.0^{2}854$	1.80	1.88
	5.62	$.0^{2}366$	$.0^{2}376$	$.0^{2}230$	$.0^{2}246$	$.0^{2}113$	$.0^{2}142$	3.33	3.51
	11.25	$.0^{4}199$	$.0^{4}208$	$.0^{4}178$	$.0^{4}193$	$.0^{4}115$	$.0^{4}146$	6.11	7.03
	22.50	$.0^{9}37$ (?)	$.0^{9}384$	$.0^{9}46$ (?)	$.0^{9}481$	$.0^{9}37$ (?)	$.0^{9}469$	11.19 (?)	16.5
2	1.00	.134	.131	.0368	.0384	$.0^{2}938$	.0103	1.50	1.50
	2.00	.0819	.0820	.0368	.0365	.0138	.0140	1.98	2.04
	5.01	$.0^{2}754$	$.0^{2}744$	$.0^{2}535$	$.0^{2}547$	$.0^{2}308$	$.0^{2}324$	3.90	3.89
	10.02	$.0^{4}743$	$.0^{4}730$	$.0^{4}761$	$.0^{4}747$	$.0^{4}574$	$.0^{4}596$	7.88	7.84
	20.04	$.0^{8}463$	$.0^{8}442$	$.0^{8}693$	$.0^{8}605$	$.0^{8}681$	$.0^{8}629$	18.3	18.4

*X = thickness of slab in mean free paths.
α_0 = energy of incident photons in units of mc^2.
E_k = expected energy of a photon transmitted with exactly k collisions.
I_k/A is equivalent to E_k/α_0 but is obtained by using the effective angle of Klein-Nishina scattering.
I/I_0 is equivalent to $\sum_{k=0}^{\infty} E_k/\alpha_0 e^{-X}$.

Table 17

COMPARISON OF TWO SETS OF RESULTS FOR LEAD SLABS: ONE SET OBTAINED BY THE METHOD OF "EFFECTIVE ANGLE OF KLEIN-NISHINA SCATTERING," THE OTHER BY THE METHODS OF THIS REPORT*

α_0	X	E_1/α_0	I_1/A	E_2/α_0	I_2/A	E_3/α_0	I_3/A	$\sum_{k=0}^{\infty} E_k/\alpha_0 e^{-X}$	I/I_0
10	2.14	.0336	.0440	$.0^{2}706$	.0111	$.0^{2}125$	$.0^{2}212$	1.41	1.49
	4.28	$.0^{2}741$	.0113	$.0^{2}248$	$.0^{2}497$	$.0^{3}721$	$.0^{2}147$	1.87	2.30
	10.70	$.0^{4}275$	$.0^{4}589$	$.0^{4}174$	$.0^{4}554$	$.0^{5}945$	$.0^{4}303$	3.71	8.06
	21.40	$.0^{8}115$	$.0^{8}394$	$.0^{8}141$	$.0^{8}714$	$.0^{8}107$	$.0^{8}671$	11.13	49.26
6	1.40	.0616	.0801	.0120	.0171	$.0^{2}192$	$.0^{2}25$	1.37	1.41
	2.80	.0295	.0363	$.0^{2}900$	.0122	$.0^{2}216$	$.0^{2}283$	1.72	1.85
	7.00	$.0^{3}857$	$.0^{2}116$	$.0^{3}452$	$.0^{3}724$	$.0^{3}192$	$.0^{3}308$	2.87	3.54
	14.00	$.0^{5}126$	$.0^{5}178$	$.0^{5}101$	$.0^{5}178$	$.0^{6}610$	$.0^{5}114$	5.04	7.62
	28.00	$.0^{11}14$ (?)	$.0^{11}228$	$.0^{11}19$ (?)	$.0^{11}336$	$.0^{11}18$ (?)	$.0^{11}317$	16.60 (?)	19.68
2	1.14	.0828	.0790	.0138	$.0^{2}962$	$.0^{2}162$	$.0^{3}61$	1.29	1.28
	2.28	.0441	.0396	.0108	$.0^{2}764$	$.0^{2}223$	$.0^{3}82$	1.58	1.48
	5.70	$.0^{2}251$	$.0^{2}221$	$.0^{2}102$	$.0^{3}762$	$.0^{3}321$	$.0^{3}157$	2.24	1.96
	11.45	$.0^{4}114$	$.0^{4}107$	$.0^{5}555$	$.0^{5}546$	$.0^{5}261$	$.0^{5}175$	3.18	2.71
	22.90	$.0^{9}16$ (?)	$.0^{9}160$	$.0^{9}12$ (?)	$.0^{9}117$	$.0^{10}55$ (?)	$.0^{10}547$	4.98 (?)	4.10

*X = slab thickness in mean free paths.
α_0 = energy of incident photon in units of mc^2.
E_k = expected energy of a photon transmitted with exactly k collisions.
I_k/A is equivalent to E_k/α_0 but is obtained by using the effective angle of Klein-Nishina scattering.
I/I_0 is equivalent to $\sum_{k=0}^{\infty} E_k/\alpha_0 e^{-X}$.

Table 18

COMPARISON OF THE BUILD-UP FACTORS OBTAINED BY THE "STRAIGHT-AHEAD" APPROXIMATION FOR LEAD WITH THOSE OBTAINED BY THE METHODS OF THIS REPORT*

α_0	X	$\sum_{k=0}^{\infty} N_k/e^{-X}$	$1+B_N$	$\sum_{k=0}^{\infty} E_k/\alpha_0 e^{-X}$	$1+B_E$
20	12.0	15.0	17.9	4.60	11.4
	24.1	400. (?)	328.	77. (?)	130.

*X = slab thickness in mean free paths.
α_0 = energy of incident photons in units of mc^2.
E_k = expected energy of a photon transmitted with exactly k collisions.
N_k = probability that a photon will be transmitted with exactly k collisions.
$1+B_N$ is the straight-ahead equivalent of $\sum_{k=0}^{\infty} N_k/e^{-X}$.
$1+B_E$ is the straight-ahead equivalent of $\sum_{k=0}^{\infty} E_k/\alpha_0 e^{-X}$.

Table 19

COMPARISON OF THE BUILD-UP FACTORS OBTAINED BY THE "ROOT-MEAN-SQUARE-ANGLE" APPROXIMATION FOR LEAD AND FOR IRON WITH THOSE OBTAINED BY THE METHODS OF THIS REPORT*

		Lead			
α_0	X	$\sum_{k=0}^{\infty} N_k/e^{-X}$	$1+B_N$	$\sum_{k=0}^{\infty} E_k/\alpha_0 e^{-X}$	$1+B_E$
20	11.2	11.9	11.4	4.00	8.96
	22.5	262. (?)	88.7	55. (?)	64.4
10	4	2.40	2.16	1.81	1.80
	7	3.95	3.51	2.60	2.34
	10	6.07	5.37	3.53	3.26
	20	19.6	17.16	9.70	8.73
6	4	2.69	2.41	2.02	1.85
	7	4.15	3.47	2.94	2.49
	10	5.74	4.53	3.82	3.13
	20	11.7	8.06	7.97	5.26
2	4	2.16	2.03	1.94	1.81
	7	2.69	2.54	2.58	2.23
	10	3.23	2.98	2.97	2.60
	20	5.22	4.19	4.36	3.64

*X = slab thickness in mean free paths.
α_0 = energy of incident photons in units of mc^2.
E_k = expected energy of a photon transmitted with exactly k collisions.
N_k = probability that a photon will be transmitted with exactly k collisions.
$1+B_N$ is the root-mean-square-angle equivalent of $\sum_{k=0}^{\infty} N_k/e^{-X}$.
$1+B_E$ is the root-mean-square-angle equivalent of $\sum_{k=0}^{\infty} E_k/\alpha_0 e^{-X}$.

Table 19—continued

α_0	X	Iron			
		$\sum_{k=0}^{\infty} N_k/e^{-X}$	$1 + B_N$	$\sum_{k=0}^{\infty} E_k/\alpha_0 e^{-X}$	$1 + B_E$
10	4	3.47	2.63	2.04	1.95
	7	5.70	4.12	3.00	2.80
	10	8.45	5.83	4.00	3.77
	20	17.2	13.20	8.20	7.86
6	4	4.23	2.91	2.57	2.15
	7	6.99	4.34	3.93	3.01
	10	9.40	5.76	5.77	3.87
	20	18.4	10.53	10.2	6.75
2	4	4.63	3.53	3.27	2.72
	7	8.27	5.42	5.27	4.01
	10	12.6	7.32	7.39	5.30
	20	28.8	13.64	17.2	9.59

IX. RÉSUMÉ

The attenuation of a continuous, incident distribution of photons can be obtained from a knowledge of the attenuation of δ-function distributions. The monoenergetic, monoangular beam, therefore, may be considered as the fundamental incident distribution. The most important results obtained in the preceding sections are for such beams.

Transmissions with k scatterings ($k = 0, 1, 2, 3$) were calculated by an approximate, integral recursion formula for beams discrete in energy and angle and incident on slabs of lead and of iron. The transmissions with one and with two scatterings were compared with the results obtained by means of an idealized case where the total absorption coefficient is a linear function of wave length in Compton units. Build-up factors were estimated from the transmissions with zero, one, two, and three scatterings; and in the case of the incident energies 10 and 20 mc^2, the estimates were checked against results obtained from an application of the thin-slab method to a continuous incident distribution. An attempt to assess the importance to transmission of photons which have suffered one or more backward scatterings led to estimates of the transmission through, and reflection from, thin slabs of the Compton scatterer.

These results possess a pattern of consistency which gives the writer and, it is hoped, the reader confidence in their reliability. Errors certainly exist, and the accuracy claimed is not high, but the errors seem to be isolated and not dense in their distribution. Also, it must be remembered that unless total absorption coefficients are accurately known and all circumstances are favorable, an accuracy greater than that claimed is in most instances unwarranted.

In addition to the preceding results, which are tied together in a net of mutual verification, there appeared three other sets of results standing, by comparison, more or less alone. These consisted of the set having its origin in the calculation by the method of thin slabs of the transmission through air, the set estimating transmission through a slab of arbitrary material, and the set comparing the photon and energy densities arising from point, line, and plane sources in an infinite homogeneous medium. The purpose of these three sets of results is to extend in a way obvious in each case the range of information supplied by the group of results first mentioned. The total system of results, the reader should note, is capable of giving an answer or of helping to give an answer of some kind to a good many questions on gamma-ray attenuation.

* * *

REFERENCES

1. CAVE, L., J. CORNER, AND R. H. A. LISTON, "The Scattering of Gamma-Rays in Extended Media. I. Perpendicular Incidence on a Plane Slab," *Proc. Roy. Soc.* (*London*), Ser. A, Vol. 204, 1950, pp. 223–259.
2. CORNER, J., AND R. H. A. LISTON, "The Scattering of Gamma-Rays in Extended Media. II. Back-Scattering of Gamma-Rays from a Thick Slab," *Proc. Roy. Soc.* (*London*), Ser. A, Vol. 204, 1950, pp. 323–329.
3. CORNER, J., F. A. G. DAY, AND R. E. WEIR, "The Scattering of Gamma-Rays in Extended Media. III. Problems with Spherical Symmetry," *Proc. Roy. Soc.* (*London*), Ser. A, Vol. 204, 1950, pp. 329–338.
4. HIRSCHFELDER, J. O., J. L. MAGEE, AND M. H. HULL, "The Penetration of Gamma-Radiation through Thick Layers. I. Plane Geometry, Klein-Nishina Scattering," *Phys. Rev.*, Vol. 73, 1948, pp. 852–862.
5. HIRSCHFELDER, J. O., AND E. N. ADAMS, "The Penetration of Gamma-Radiation through Thick Layers. II. Plane Geometry, Iron and Lead," *Phys. Rev.*, Vol. 73, 1948, pp. 863–868.
6. PEEBLES, GLENN H., AND MILTON S. PLESSET, "Transmission of Gamma-Rays through Large Thicknesses of Heavy Materials," *Phys. Rev.*, Vol. 81, 1951, pp. 430–439.
7. *Ibid.*, p. 437.
8. *Ibid.*, p. 433.
9. LATTER, RICHARD, AND HERMAN KAHN, *Gamma-Ray Absorption Coefficients*, The RAND Corporation, R-170, September 19, 1949
10. PLESSET, M. S., AND S. T. COHEN, *Scattering and Absorption of Gamma Rays and Neutrons*, The RAND Corporation, R-132, March 1, 1949.
11. SPENCER, LEWIS V., AND U. FANO, "Penetration and Diffusion of X-Rays. Calculation of Spatial Distributions by Polynominal Expansion," *J. Research Nat. Bur. Standards*, Vol. 46, 1951, pp. 446–456.
12. FANO, U., H. HURWITZ, JR., AND L. V. SPENCER, "Penetration and Diffusion of X-Rays. V. Effect of Small Deflections upon the Asymptotic Behavior," *Phys. Rev.*, Vol. 77, 1950, pp. 425–426.
13. KAHN, HERMAN, "Random Sampling (Monte Carlo) Techniques in Neutron Attenuation Problems—II," *Nucleonics*, Vol. 6, 1950, pp. 60–65.
14. SOLON, LEONARD R., AND J. ERNEST WILKINS, JR., *Straight-Ahead and Root-Mean-Square-Angle Calculations for 20 mc^2 γ-Rays in Lead*, Nuclear Development Associates, Inc., NYO-635, December 15, 1950.
15. SOLON, LEONARD R., J. ERNEST WILKINS, JR., ALAN OPPENHEIM, AND HERBERT GOLDSTEIN, *Gamma-Transmission in Iron, Tungsten, Lead, Uranium, and a Pure Compton Scatterer by Root-Mean-Square-Angle Calculation*, Nuclear Development Associates, Inc., NYO-637, April 5, 1951.
16. WHITE, GLADYS R., "The Penetration and Diffusion of Co^{60} Gamma-Rays in Water Using Spherical Geometry," *Phys. Rev.*, Vol. 80, 1950, pp. 154–156.
17. DIXON, W. R., "Build-up Factors for Transmission of Co^{60} Gamma-Rays through Concrete and Lead," *Phys. Rev.*, Vol. 85, 1952, pp. 498–499.